# Hydrogels composites acrylique-kaolinite pour une libération contrôlée de fertilisants azotés

Mahamat Saleh Elhadj Yacoub

**ÉCOLE DOCTORALE n° 548 « *Mer et Sciences* »**

**Laboratoire Matériaux Polymères Interfaces Environnement Marin**

**(E.A. 4323)**

# THÈSE

présentée par :

**Mahamat Saleh Yacoub ELHADJ**

soutenance prévue le : **10 décembre 2021**

pour obtenir le grade de Docteur en Chimie

spécialité : Chimie des Matériaux

# Acrylic-kaolinite composite hydrogels for controlled-release nitrogen fertilizers application

**THÈSE dirigée par :**

**M. François Xavier Perrin**, Professeur, Université de Toulon — Directeur de thèse

**JURY :**

**Mme. Maguy JABER,** Professeure, Sorbonne Université — Rapporteur

**M. Nicolas SBIRRAZZUOLI,** Professeur, Université Côte d'Azur — Rapporteur

**Mme. Cécile PAGNOUX,** Professeure, Université de Limoges — Examinateur

**M. Jean-François CHAILAN,** Professeur, Université de Toulon — Examinateur

# Acrylic-kaolinite composite hydrogels for controlled-release nitrogen fertilizers application

Mahamat Saleh Yacoub Elhadj

# REMERCIEMENTS

Cette thèse de recherche a été effectuée au laboratoire Matériaux Polymères Interfaces Environnement Marin (MAPIEM), à l'Université de Toulon campus La Garde. Elle s'est déroulée sous la direction scientifique de François Xavier Perrin, professeur d'Université de Toulon.

Je commence tout d'abord par remercier mon encadrant François Xavier Perrin qui a placé sa confiance en moi pour accomplir ce bout de travail ensemble, de m'avoir appris scientifiquement et humainement tant de chose, d'avoir contribué à mon suivi de manière très régulière durant la thèse. Merci aussi pour le temps qu'on a passé ensemble pour analyser les résultats et valoriser tout ce travail.

Je remercie également les partenaires du projet européen PROWSPER à savoir Tanta Verona Iordache, Andrei Sarbu et Arthur M.J Valente.

Mes remerciements s'adressent aussi à Jean François Chailan, notre ancien directeur du laboratoire, de m'avoir accueilli au sein de l'équipe du laboratoire, à Pascal Carrière qui était mon premier contact au sein du laboratoire.

J'adresse également mes chaleureux remerciements à mes professeurs de l'Université de Hanoï au Vietnam, à commencer par Madame Chu, et tous les amis formidables que j'ai pu me faire à Hanoï.

Merci à Fabio Ziarelli de l'Université Aix-Marseille qui a passé mes échantillons en RNM.

Je remercie Lénaïk Beleck d'avoir contribuer à ma formation sur plusieurs appareils ainsi que pour sa disponibilité et ses conseils, je remercie aussi Armand Fahs et Sophie Berlioz de m'avoir formé à l'utilisation du MEB et bien d'autres appareils au laboratoire.

Merci à Gérald Culioli, Bruno Viguier, Lucile Pelloquet, Raphaëlle Barry, Isabelle Martin, Olivier Bottzeck, pour l'aide apportée sur les différents équipements (RMN, lyophilisateur, DMA, machine de traction, analyses thermiques). Merci aux autres membres permanents et non permanents de MAPIEM que je ne cite pas, notamment pour tous ces bons moments passés autour d'une galette des rois, d'une raclette ou d'un barbecue.

Un grand merci à toute l'équipe du SIM, en particulier Mélanie Wolfs, Edwige Joliff, Jean-Michel Robert, vous m'avez aidé dans l'utilisation de plusieurs équipements et de leurs conseils et disponibilté.

Mes remerciements vont également vers les membres du laboratoire MIO en particulier Sebastien, Gael, Amonda de m'avoir formé sur l'appareil d'analyse élémentaire et le broyeur à billes.

Je remercie tous les thésards du labo MAPIEM en particulier Laure Gevaux, Réné William, Bénoit Paix, Isis Castro pour les soirées Games of Thrones et les soirées de jeux de société ainsi qu'Anthony Grard, Monica Campos pour les soirées de bowling, Alexandre, Manar, Linh.

Tous mes sincères remerciements à l'amour de ma vie Mastoura, ma femme qui est à mes côtés dans les moments difficiles de la thèse ainsi que les moments de joie et à mon fils Abdelhamid qui illumine notre vie de bonheur et ma fille Fatma qui vient d'arriver au monde et qui apporte sérénité et joie, je vous aime de tout mon cœur ma petite famille.

Je remercie de tout cœur mon père Mahamat Saleh Yacoub et ma mère Arafa Ahmat Daoud de m'avoir soutenue et permis d'accomplir mes études de la maternelle jusqu'aujourd'hui. Sans vous je ne serai jamais arriver à ce stade d'études. Encore une fois, Maman merci pour tout ce que tu as fait et continue de faire pour moi et merci Baba d'avoir cru en moi dans tous mes projets personnels.

Chaleureuses encouragements à mon frère Abdelhamid en qui je crois de toutes mes forces et à mes sœurs Koubra, Achta, Noura, Zahra, Rawda, Akhayé sans oublier mes autres frères Mahamat Issakha, Ali et Ahmat.

Je remercie mon ami et confident Dr Omar Abakar Adam de m'avoir conseillé et soutenu tout le long de ces années ainsi Tidjani Ahmat Annadif. Sans oublier tous les amis du Mans, Mariam Moussa, Issakha Adam Daoud et feu Dr Moustapha Idriss.

Je dédie cette thèse de doctorat à toute ma famille au sens large, en particulier à mon père Dr Mahamat Saleh Yacoub, mes oncles Cheick Abdoulaye Yacoub Sabre, Yaya Yacoub Sabre, à mon beau père Habib Daoud et au professeur Ali Dabye.

# VALORIZATION OF THE PHD WORK

## Scientific papers

M-S.Yacoub Elhadj, F.Xavier Perrin, « Influencing parameters of mechanochemical intercalation of kaolinite with urea », Applied Clay Science 213 (2021) 106250;
https://doi.org/10.1016/j.clay.2021.106250

## Oral presentations

Elhadj Yacoub M.S, Perrin F.X « Polymères superabsorbants pour application en agriculture »
*15èmes journées du Groupe Français des Polymères – section méditerranée,* Montpellier, 16 March 2018.

Elhadj Yacoub M.S, Perrin F.X « Superabsorbent polymers for application in agriculture » *IX Journées Franco-Italiennes de Chimie,* Gênes, 17 Avril 2018.

Elhadj Yacoub M.S, Perrin F.X « Hydrogel-clay hybrid materials for nutrient retention » *workshop waterwork* Toulon, 25 June 2019.

Elhadj Yacoub M.S, Perrin F.X « Hybrid hydrogel-clay materials for slow release of fertilizer in the field of Agriculture » *9ès journée de la jeune recherche de l'Université de Toulon Doctoriades* Toulon, 18 October 2019.

Elhadj Yacoub M.S, Perrin F.X « Kaolinite as a carrier for controlled release of urea nutrient » *workshop waterwork* Bucharest, 2 March 2020.

# ACRONYMS AND SYMBOLS

| | |
|---|---|
| Polymers | |
| PAA | Poly(acrylic acid) |
| PAAm | Poly(acrylamide) |
| P(AA-co-Am) | Poly(acrylic acid-co-acrylamide) |
| PDMS | Poly(dimethylsiloxane) |
| Others compound | |
| AA | Acrylic Acid |
| Am | Acrylamide |
| APS | Ammonium persulfate |
| DAEE | 2-[2-(dimethylamino)ethoxy]ethanol |
| DMSO | dimethylsulfoxide |
| K | Kaolin |
| Kaol | Kaolinite |
| Kaol-U | Kaolinite-urea complex |
| KGa-1b | Kaolin (low-defect) from Georgia, USA |
| MBA | N,N' Methylene-bis-acrylamide |
| MeOH | Methanol |
| NaOH | Sodium Hydroxide |
| TEMED | N, N, N', N'-tetramethylenediamine |
| U | Urea |
| Characterization techniques | |
| DSC | Differential scanning calorimetry |
| TGA | Thermogravimetric analysis |
| SEM | Scanning electron microscopy |
| FTIR-ATR | Fourier-transform infrared Attenuated Total Reflectance |
| NMR | Nuclear magnetic resonance |
| XRD | X-Ray diffraction |
| CHNS | Elemental analysis |
| Other Acronyms | |

| | |
|---|---|
| α | Degree of intercalation |
| I | Relative intensity (in XRD diffractograms) |
| HI | Hinckley crystallinity index for kaolinites |
| MAS-NMR | Solid state nuclear magnetic resonance - magic angle spinning method |
| Q | Swelling ratio |
| $Q_{eq}$ | Swelling ratio at equilibrium |
| WR | Water retention |
| SRFs | Slow Release of Fertilizers |
| CRFs | Controlled Release of Fertilizers |

Symbols

| | |
|---|---|
| $A_{abs}$ | Absorbance |
| D | Diffusion coefficient |
| $\Delta H_m$ | Enthalpy of melting |
| E' | Elastic modulus |
| G' | Storage modulus |
| G'' | Loss modulus |
| F | Force |
| tan δ | Dissipation factor |
| $T_g$ | Glass transition temperature |
| $t_R$ | Reaction time |
| λ | Wavelength |

# TABLE OF CONTENTS

# General Introduction

# General Introduction

Plants need light, heat, mechanical support, air, water and nutrients for growth, which can be assisted by other substances like herbicides, insecticides, and fungicides (i.e. pesticides). These are called growth factors. The level of growth cannot be greater than that allowed by the most limiting growth factor. Although water is fundamental for growth, plant nutrients and pesticides are the following most likely limiting factors. However, plant nutrients and pesticides affect soil and water quality during the process! How?

First of all, although nutrients contained in fertilizers and manures are present in both organic and inorganic forms, plants can only use the inorganic nutrients. Eventually, organic forms of nutrients are converted into inorganic ones for the plant growth. Most commonly, excess fertilizer or manure is applied to avoid nutrient loss by runoffs or just the need to create a nutrient-rich environment, for instance, in sandy-soils. Many inorganic nutrients are easily dissolved in soil water and can be quickly transported to surface or ground water, by leaching, and thereafter converted to inorganic forms available for use by algae and aquatic plants. However, there are enough natural sources of nutrients to allow these plants to grow; and the additional nutrients from fertilizers and manure usually lead to excessive growth of plants and algae, called *bloom*. This process produces compounds which are toxic to livestock, and which decrease the quality of bathing waters, and that of surface water bodies. Most importantly, such uncontrolled growth of aquatic flora can lead to fish-kills, because an excess of algae needs greater quantities of oxygen, depleting the amount available to sustain aquatic life. Sustainable agriculture requires that soil and water quality be maintained; some farm practices have the potential to cause environmental harm, which may affect rural and urban areas alike. Many of the potential negative impacts of farming can be greatly reduced by the use of the Best Management Practices BMP. These are agricultural practices that reflect current knowledge about conserving soil and water without sacrificing productivity.

Similar considerations apply to pesticides. In agriculture, a large quantity of pesticides (over 2 million tons per year) is used globally, and their presence in surface water bodies is reaching alarming concentration values, near 1 µg/L. Most commonly encountered pesticides are the herbicide atrazine, the fungicide vinclozolin, the insecticide dichlor-diphenyl-trichloretane (DDT), and the biocide tributyltin (TBT). In some European countries the use of the above-mentioned pesticides is prohibited due to their proven neurological and health effects upon humans and animals. Nevertheless, the absence of efficient control measures and of awareness programs leads to their continuing. In addition, the population is exposed to these chemicals because they eat fruits, vegetables and grains imported from countries that are still using these pesticides (without a judicious management plan to overcome

their accumulation in plants) or because they remain in the environment for long periods of time. These toxic pesticides can bio-accumulate in soil and in different water bodies, as well, reaching dangerous levels in the food chain.

ProWsper was an experimental and demonstrative research project conducted in partnership with four Institutions from three European countries (ICECHIM and ICPA from Romania, University of Toulon laboratory MAPIEM from France and University of Coimbra from Portugal) that face these common problems. The main objective of the project referred to developing original, sustainable, and cost-effective solutions/products for protecting underground water and soil against nutrient and pesticide pollution while ensuring the well-balanced growth of plants (particularly, for greenhouses and small crop cultures). Therefore, this project practically developed protective composite layers (as end-products) as shown in Figure 1. Applying such solutions/products during the fruit/vegetable growth cycles, reduces pollution and provides humid- and nutrient-stable environment for plant growth.

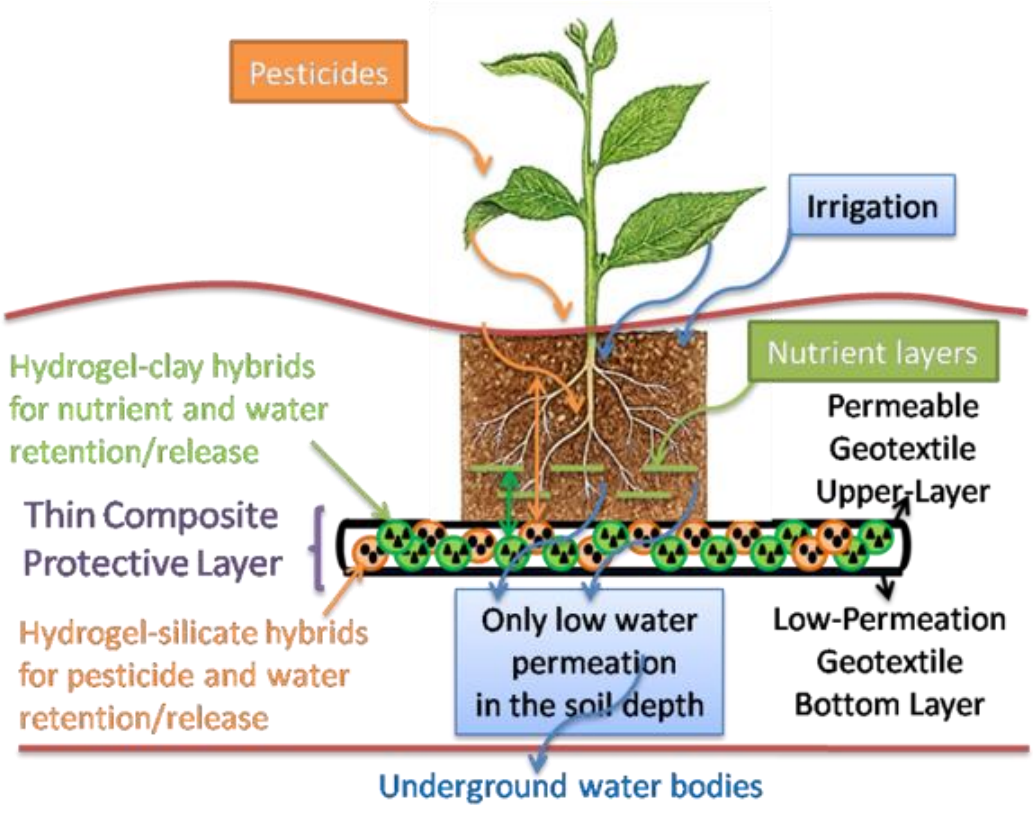


*Figure 1. Concept of ProWsper project.*

Several reviews report the different strategies for the preparation of slow/controlled release fertilizers (SRFs, CRFs) (Shaviv and Mikkelsen, 1993; Shaviv, 2001; Bajpai et al., 2008; Azeem et al., 2014; Pereira et al., 2015; Caccavo et al., 2018; Fu et al., 2018; Kuśtrowski et al., 2018; Ramli, 2019; Lawrencia et al.,

2021). Controlled or slow release fertilizers can be generally classified into four main categories (Figure 2): matrix-based fertilizers, coated-based fertilizers, low solubility inorganic fertilizers and chemically bonded N- fertilizers (Shaviv, 2001). Matrix-based formulations formed the largest category of SRFs due to their simple fabrication. The fertilizer is dispersed in a polymer matrix (hydrophilic or hydrophobic) and diffuses through pores in the carrier phase. Coated-based fertilizers are the second main category of SRFs, in which the fertilizer is surrounded by an inorganic or organic coating material. A third category of SRFs is low solubility inorganic fertilizers which include compounds with the general formula $MeNH_4PO_4$ $xH_2O$, where Me is a divalent cation (Mg, Fe, Zn, Mn), and N-P-K fertilizers, prepared by mixing potassium, phosphate and ammonium salts. A last category is chemically bonded N- fertilizers. The most common chemically bonded fertilizers used for SRFs are urea-formaldehyde (UF) and isobutylidenediurea (IBDU).

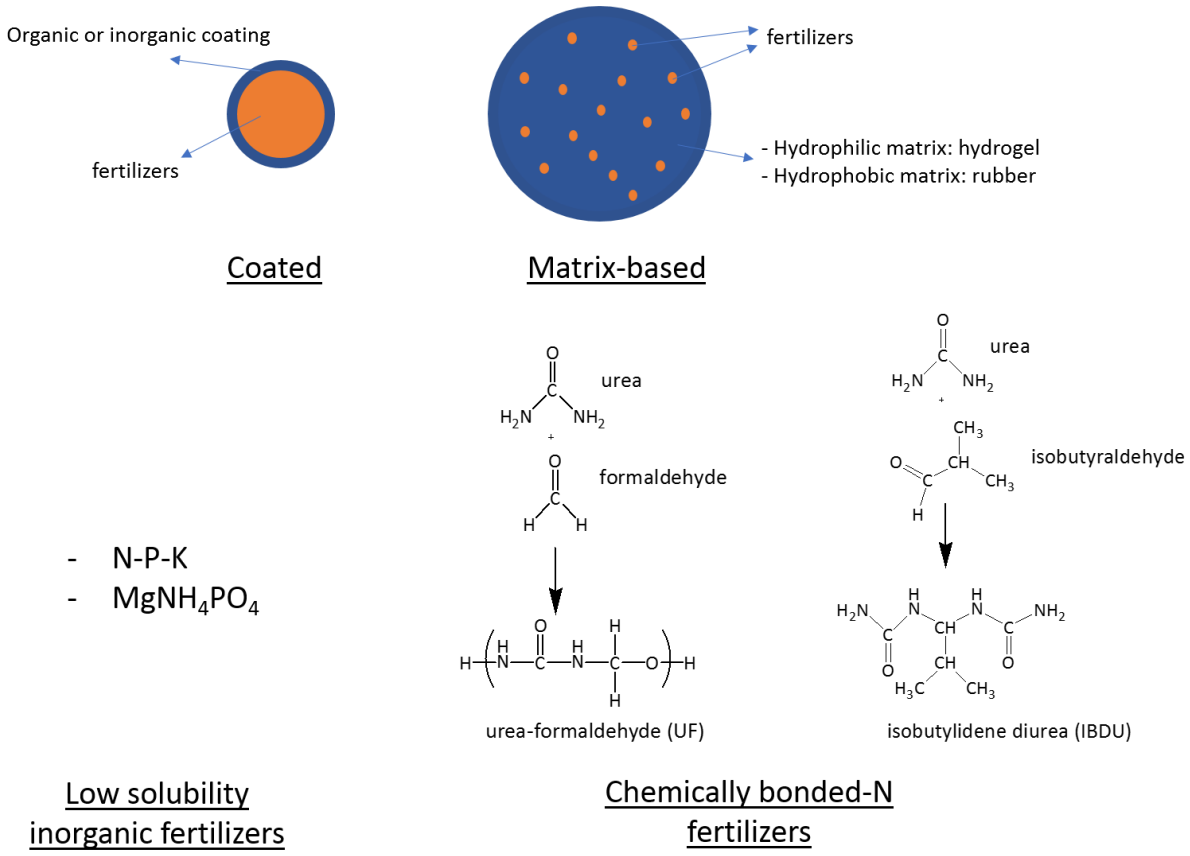


*Figure 2. Examples of slow/controlled release fertilizers systems (part of the image is taken from (Guo et al., 2018)).*

The thesis work carried out at the MAPIEM laboratory focused on matrix-based fertilizers based on kaolinite-hydrogel-urea composite materials. In the following, we will define each of the constituent elements of the composites prepared in this work.

Hydrogels are three-dimensional networks of hydrophilic polymers with ability to absorb very large amounts of water or biological fluid, without dissolving and without losing their structure (Fumihiko Tanaka, 2011; Ullah et al., 2015). This three-dimensional network is formed by the crosslinking of polymer chains, by covalent bonds (chemical crosslinking) or by physical bonds (hydrogen, ionic or hydrophobic bonds). Chemically crosslinked gels can be obtained by radical polymerization of low molecular weight monomers in the presence of crosslinking agents. Obviously, the degree of crosslinking of a polymer is controlled by the amount of crosslinking agent present in the copolymerization and the monomer conversion. Smaller amounts of crosslinking agent and decreased final conversion result in both less crosslinked material. Most importantly, not all crosslinking agent bonds react to form crosslinks. Potential crosslinking is lost due to intramolecular cyclization reactions, where both ends of the crosslinking agent react in the same growing polymer chain, forming a loop structure, as shown in Figure 3.

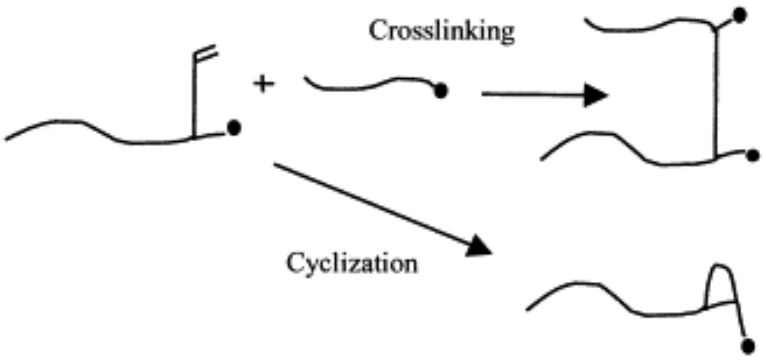


*Figure 3. Cyclisation vs crosslinking during polymerization of a monomer in presence of a crosslinking agent , (Elliott et al., 2004)*

The high-water absorption is partly provided by the presence of hydrophilic groups in their structure, such as hydroxyl (OH), carboxylic (COOH), amide (CONH or $CONH_2$) or sulfonic ($SO_3H$) groups. The proportion of water inside the hydrogel structure is characterized by three interdependent parameters, namely the volume fraction of polymer in the swollen state, the average molar mass between crosslinking points as well as the mesh size network.

There are different ways to classify hydrogels depending on whether it is based on their origin, structure or properties (Figure 4).

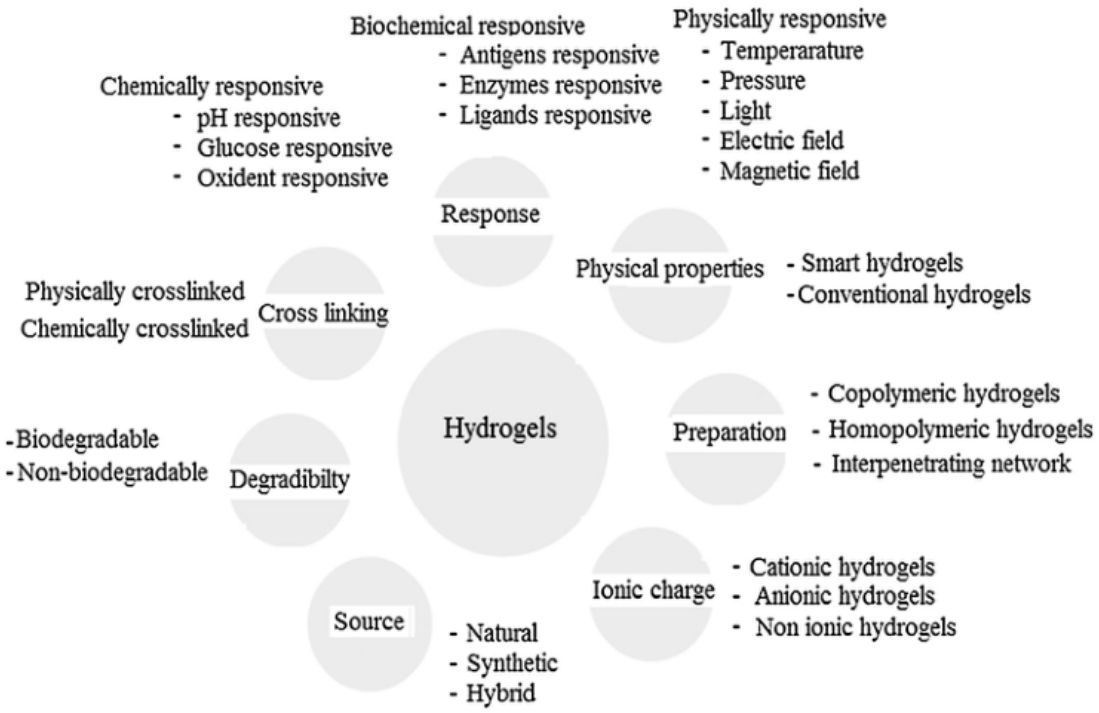


*Figure 4. Classification of hydrogels based on their origin, structure or property, (Ullah et al., 2015).*

Scientists have devoted a lot of energy to the development of hydrogels for their vast applications such as biodegradable materials, drug delivery applications (Bajpai et al., 2007; Wu et al., 2008), tissue engineering (Lee and Mooney, 2001; Khan et al., 2009), sensors (Lee and Braun, 2003; Sorber et al., 2008), contact lenses (Katsoulos et al., 2009) or agriculture applications (Akelah, 2013; Demitri et al., 2013; Guilherme et al., 2015; Behera and Mahanwar, 2019; Głowińska et al., 2019). Synthetic hydrogels are most often prepared by crosslinking poly(ethylene glycol) (Nagahama et al., 2008), poly(vinyl alcohol) (Paranhos et al., 2007), poly(N-isopropylacrylamide) (Bokias et al., 1998; Garay et al., 2000; Hirashima et al., 2004; Ma et al., 2007; Chang et al., 2011), poly(acrylamide) (Liang and Liu, 2007; Cândido et al., 2012; Zhang et al., 2016) and poly(acrylic acid) (Adnadjevic and Jovanovic, 2008; Liang et al., 2009; Cheng et al., 2018).

The large quantity of water that composes hydrogels give them properties similar to those of living tissues, and therefore makes them very interesting for biomedical applications (release of drugs into a well-defined target). They can also be used as water tank and thus allow better water management. Parvathy and Jyothi, (2014) indicated that hydrogels are potential candidates to be applied as an alternative to combat global climate change because they can improve the soil properties, mainly in conditions of reduced moisture availability.

Besides, the structure of hydrogels allows molecules of different sizes to diffuse in or out of the network. The rate and mechanisms of diffusion can be controlled by altering factors such as polymer composition, crosslink density and crystallinity.

Kaolins are white, friable and refractory clays, composed mainly of kaolinite of formula $Al_2Si_2O_5(OH)_4$ (Figure 5) from the silicate group, subgroup of the phyllosilicates. Originally discovered in China, they are the basis for the manufacture of porcelain, but are also used in the paper industry, medicine, into the catalyst-units in cars and cosmetics.

Kaolinite is a hydrated alumina silicate built by combining tetrahedral and octahedral sheets in equal proportions, the minerals are called 1:1 clay minerals, constituting one of the main clay minerals and forming the essential element of kaolin (Gardolinski et al., 2000; Detellier and Letaief, 2013).

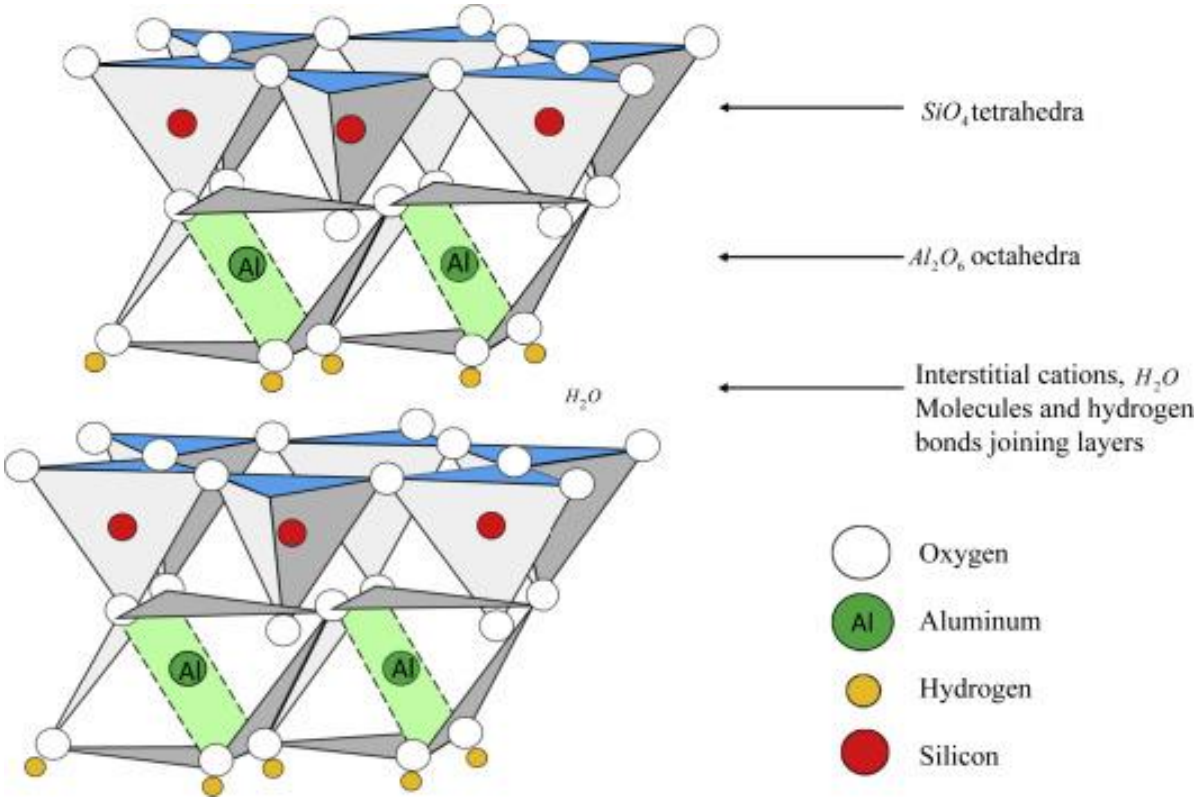


*Figure 5. Structure of kaolinite. (Kotal and Bhowmick, 2015).*

Fertilizers are inorganic or organic materials with high analytical value and definite composition which can supply nutrients and trace elements, usually applied to the soil to encourage the growth of crops. For example, nitrogenous fertilizers (urea, $CO(NH_2)_2$, ammonium sulfate, $(NH_4)_2SO_4$) or potassium fertilizers (potassium chloride, KCl). In this work, urea was used as a fertilizer. It has been widely used due to its high nitrogen content and easy application, in dry granular form or as aqueous solution. When urea is added in the soil, it is first hydrolyzed to ammonium by urease enzymes (Equation 1). Then, the ammonium is oxidized to nitrate by the nitrification process (Equation

2 and 3). Depending on the soil composition (clay content), pH and temperature, ammonium can be converted to ammonia which is lost to the atmosphere. When applied at high rates, urea fertilizer can inhibit soil microorganisms due to ammonia toxicity and increases in ionic strength (Eno et al., 1955; Omar and Ismail, 1999). The loss of nitrogen through volatilization of ammonia to the atmosphere is the main problem responsible for the low efficiency of urea applied to the soil with up to 80% loss of applied nitrogen.

$$CO(NH_2)_2 + 3H_2O \xrightarrow{\text{urease}} 2NH_4^+ + HCO_3^- + OH^- \quad \text{Eq. 1}$$

$$NH_4^+ + 3/2\ O_2 \longrightarrow NO_2^- + 2H^+ + H_2O \quad \text{Eq. 2}$$

$$NO_2^- + 1/2\ O_2 \longrightarrow NO_3^- \quad \text{Eq. 3}$$

This work was divided into four chapters. It is noted that the chapters are independent of each other and have their own experimental part.

In **Chapter 1** the clay compound, kaolinite-urea are prepared by mechanochemically intercalation of urea into kaolinite layers. Effect of ball milling time, of mass % urea (fertilizers) and kaolinite (clay) are investigated and discussed by using XRD, FTIR, DTG-DSC and SEM as characterization of materials.

The **Chapter 2** focus on the synthesis of poly(acrylic acid)-urea hydrogels by two different methods. In the first method, the polymerization has been carried out in presence of urea while in the second method urea was loaded after polymerization by imbibition of the hydrogel in an urea solution. The effect of the crosslinker content, neutralization degree and acrylamide comonomer content will be studied by measuring the swelling capacity, the water retention capacity and the release rate of urea in water. On the other hand, the structure of the hydrogels will be explored by $^{1}H$ and $^{13}C$ NMR spectroscopy and by FTIR spectroscopy. Tensile tests have also been performed to determine the mechanical properties of the hydrogel materials.

The preparation and properties of kaolinite-hydrogel composite materials is reported in **Chapter 3**. Urea was incorporated along with the other ingredients but either in free form or as kaolinite-urea intercalate. The effect of kaolinite on the water absorption and retention properties will be investigated. The release kinetics of urea in water is reported for all the prepared composite materials.

A new method for the preparation of kaolinite-poly(acrylamide) hydrogels without organic crosslinker agent is presented in **Chapter 4**. The preparation method is based on the grafting of 2-[2-(dimethylamino)ethoxy]ethanol on the interlayer surface of kaolinite. The functionalized kaolinite will

be characterized by XRD, elemental analysis, FTIR and DTG-DSC analysis. The swelling behavior and mechanical properties of the hydrogels have been investigated.

In the end, the main results of this PhD work will be resumed in the conclusion and some perspectives will be presented.

# References


Adnadjevic, B., Jovanovic, J., 2008. Novel approach in investigation of the poly(acrylic acid) hydrogel swelling kinetics in water. J. Appl. Polym. Sci. 107, 3579–3587. https://doi.org/10.1002/app.27451

Akelah, A., 2013. Polymers in the Controlled Release of Agrochemicals, in: Functionalized Polymeric Materials in Agriculture and the Food Industry. Springer, Boston, MA, pp. 133–192. https://doi.org/10.1007/978-1-4614-7061-8_3

Azeem, B., KuShaari, K., Man, Z.B., Basit, A., Thanh, T.H., 2014. Review on materials & methods to produce controlled release coated urea fertilizer. Journal of Controlled Release 181, 11–21. https://doi.org/10.1016/j.jconrel.2014.02.020

Bajpai, A.K., Shukla, S.K., Bhanu, S., Kankane, S., 2008. Responsive polymers in controlled drug delivery. Progress in Polymer Science 33, 1088–1118. https://doi.org/10.1016/j.progpolymsci.2008.07.005

Bajpai, J., Mishra, S., Bajpai, A.K., 2007. Dynamics of controlled release of potassium nitrate from a highly swelling binary polymeric blend of alginate and carboxymethyl cellulose. Journal of Applied Polymer Science 106, 961–972. https://doi.org/10.1002/app.26703

Behera, S., Mahanwar, P.A., 2019. Superabsorbent polymers in agriculture and other applications: a review. Polymer-Plastics Technology and Materials 0, 1–16. https://doi.org/10.1080/25740881.2019.1647239

Bokias, G., Durand, A., Hourdet, D., 1998. Molar mass control of poly(N-isopropylacrylamide) and poly(acrylic acid) in aqueous polymerizations initiated by redox initiators based on persulfates. Macromolecular Chemistry and Physics 199, 1387–1392. https://doi.org/10.1002/(SICI)1521-3935(19980701)199:7<1387::AID-MACP1387>3.0.CO;2-K

Caccavo, D., Cascone, S., Lamberti, G., Barba, A.A., 2018. Hydrogels: experimental characterization and mathematical modelling of their mechanical and diffusive behaviour. Chem. Soc. Rev. 47, 2357–2373. https://doi.org/10.1039/C7CS00638A

Cândido, J. de S., Leitão, R.C.F., Ricardo, N.M.P.S., Feitosa, J.P.A., Muniz, E.C., Rodrigues, F.H.A., 2012. Hydrogels composite of poly(acrylamide-co-acrylate) and rice husk ash. I. Synthesis and characterization. Journal of Applied Polymer Science 123, 879–887. https://doi.org/10.1002/app.34528

Chang, C., Han, K., Zhang, L., 2011. Structure and properties of cellulose/poly(N-isopropylacrylamide) hydrogels prepared by IPN strategy. Polymers for Advanced Technologies 22, 1329–1334. https://doi.org/10.1002/pat.1616

Cheng, D., Liu, Y., Yang, G., Zhang, A., 2018. Water- and Fertilizer-Integrated Hydrogel Derived from the Polymerization of Acrylic Acid and Urea as a Slow-Release N Fertilizer and Water Retention in Agriculture. J. Agric. Food Chem. 66, 5762–5769. https://doi.org/10.1021/acs.jafc.8b00872

Demitri, C., Scalera, F., Madaghiele, M., Sannino, A., Maffezzoli, A., 2013. Potential of Cellulose-Based Superabsorbent Hydrogels as Water Reservoir in Agriculture [WWW Document]. International Journal of Polymer Science. https://doi.org/10.1155/2013/435073

Detellier, C., Letaief, S., 2013. Chapter 13.2 - Kaolinite–Polymer Nanocomposites, in: Bergaya, F., Lagaly, G. (Eds.), Developments in Clay Science, Handbook of Clay Science. Elsevier, pp. 707–719. https://doi.org/10.1016/B978-0-08-098258-8.00022-5

Elliott, J.E., Macdonald, M., Nie, J., Bowman, C.N., 2004. Structure and swelling of poly(acrylic acid) hydrogels: effect of pH, ionic strength, and dilution on the crosslinked polymer structure. Polymer 45, 1503–1510. https://doi.org/10.1016/j.polymer.2003.12.040

Eno, C.F., Blue, W.G., Good, J.M., 1955. The Effect of Anhydrous Ammonia on Nematodes, Fungi, Bacteria, and Nitrification in Some Florida Soils. Soil Science Society of America Journal 19, 55–58. https://doi.org/10.2136/sssaj1955.03615995001900010013x

Fu, J., Wang, C., Chen, X., Huang, Z., Chen, D., 2018. Classification research and types of slow controlled release fertilizers (SRFs) used - a review. Communications in Soil Science and Plant Analysis 49, 2219–2230. https://doi.org/10.1080/00103624.2018.1499757

Fumihiko Tanaka, 2011. Applications to Molecular Association and Thermoreversible Gelation, Chemical Engineering. ed, Cambridge Core.

Garay, M.T., Alava, C., Rodriguez, M., 2000. Study of polymer–polymer complexes and blends of poly(N-isopropylacrylamide) with poly(carboxylic acid). 2. Poly(acrylic acid) and poly(methacrylic acid) partially neutralized. Polymer 41, 5799–5807. https://doi.org/10.1016/S0032-3861(99)00765-X

Gardolinski, J.E., Carrera, L.C.M., Cantão, M.P., Wypych, F., 2000. Layered polymer-kaolinite nanocomposites. Journal of Materials Science 35, 3113–3119. https://doi.org/10.1023/A:1004820003253

Głowińska, A., Trochimczuk, A.W., Jakubiak-Marcinkowska, A., 2019. Novel acrylate/organophosphorus-based hydrogels for agricultural applications. New outlook and innovative concept for the use of 2-(methacryloyloxy)ethyl phosphate as a multi-purpose monomer. European Polymer Journal 110, 202–210. https://doi.org/10.1016/j.eurpolymj.2018.11.020

Guilherme, M.R., Aouada, F.A., Fajardo, A.R., Martins, A.F., Paulino, A.T., Davi, M.F.T., Rubira, A.F., Muniz, E.C., 2015. Superabsorbent hydrogels based on polysaccharides for application in agriculture as soil conditioner and nutrient carrier: A review. European Polymer Journal 72, 365–385. https://doi.org/10.1016/j.eurpolymj.2015.04.017

Guo, Y., Liu, Z., Zhang, M., Tian, X., Chen, J., Sun, L., 2018. Synthesis and Application of Urea-Formaldehyde for Manufacturing a Controlled-Release Potassium Fertilizer. Ind. Eng. Chem. Res. 57, 1593–1606. https://doi.org/10.1021/acs.iecr.7b04629

Hirashima, Y., Tamanishi, H., Sato, H., Saito, K., Naito, A., Suzuki, A., 2004. Formation of hydrogen bonding in ionized poly(N-isopropylacrylamide) gels by continuous water exchange. Journal of Polymer Science Part B: Polymer Physics 42, 1090–1098. https://doi.org/10.1002/polb.10783

Katsoulos, C., Karageorgiadis, L., Vasileiou, N., Mousafeiropoulos, T., Asimellis, G., 2009. Customized hydrogel contact lenses for keratoconus incorporating correction for vertical coma aberration. Ophthalmic and Physiological Optics 29, 321–329. https://doi.org/10.1111/j.1475-1313.2009.00645.x

Khan, F., Tare, R.S., Oreffo, R.O.C., Bradley, M., 2009. Versatile Biocompatible Polymer Hydrogels: Scaffolds for Cell Growth. Angewandte Chemie International Edition 48, 978–982. https://doi.org/10.1002/anie.200804096

Kotal, M., Bhowmick, A.K., 2015. Polymer nanocomposites from modified clays: Recent advances and challenges. Progress in Polymer Science, Environmentally Relevant and Hybrid Polymer Materials 51, 127–187. https://doi.org/10.1016/j.progpolymsci.2015.10.001

Kuśtrowski, P., Natkański, P., Rokicińska, A., Witek, E., 2018. Polymer Hydrogel-Clay (Nano)Composites, in: Thakur, V.K., Thakur, M.K. (Eds.), Polymer Gels: Science and Fundamentals, Gels Horizons: From Science to Smart Materials. Springer, Singapore, pp. 1–62. https://doi.org/10.1007/978-981-10-6086-1_1

Lawrencia, D., Wong, S.K., Low, D.Y.S., Goh, B.H., Goh, J.K., Ruktanonchai, U.R., Soottitantawat, A., Lee, L.H., Tang, S.Y., 2021. Controlled Release Fertilizers: A Review on Coating Materials and Mechanism of Release. Plants 10, 238. https://doi.org/10.3390/plants10020238

Lee, K.Y., Mooney, D.J., 2001. Hydrogels for Tissue Engineering. Chem. Rev. 101, 1869–1880. https://doi.org/10.1021/cr000108x

Lee, Y.-J., Braun, P.V., 2003. Tunable Inverse Opal Hydrogel pH Sensors. Advanced Materials 15, 563–566. https://doi.org/10.1002/adma.200304588

Liang, R., Liu, M., 2007. Preparation of poly(acrylic acid-co-acrylamide)/kaolin and release kinetics of urea from it. J. Appl. Polym. Sci. 106, 3007–3015. https://doi.org/10.1002/app.26919

Liang, R., Yuan, H., Xi, G., Zhou, Q., 2009. Synthesis of wheat straw-g-poly(acrylic acid) superabsorbent composites and release of urea from it. Carbohydrate Polymers 77, 181–187. https://doi.org/10.1016/j.carbpol.2008.12.018

Ma, J., Xu, Y., Fan, B., Liang, B., 2007. Preparation and characterization of sodium carboxymethylcellulose/poly(N-isopropylacrylamide)/clay semi-IPN nanocomposite hydrogels. European Polymer Journal 43, 2221–2228. https://doi.org/10.1016/j.eurpolymj.2007.02.026

Nagahama, K., Ouchi, T., Ohya, Y., 2008. Temperature-Induced Hydrogels Through Self-Assembly of Cholesterol-Substituted Star PEG-b-PLLA Copolymers: An Injectable Scaffold for Tissue Engineering. Advanced Functional Materials 18, 1220–1231. https://doi.org/10.1002/adfm.200700587

Omar, S.A., Ismail, M.A., 1999. Microbial populations, ammonification and nitrification in soil treated with urea and inorganic salts. Folia Microbiol 44, 205–212. https://doi.org/10.1007/BF02816244

Paranhos, C.M., Soares, B.G., Oliveira, R.N., Pessan, L.A., 2007. Poly(vinyl alcohol)/Clay-Based Nanocomposite Hydrogels: Swelling Behavior and Characterization. Macromol. Mater. Eng. 292, 620–626. https://doi.org/10.1002/mame.200700004

Parvathy, P.C., Jyothi, A.N., 2014. Rheological and thermal properties of saponified cassava starch-g-poly(acrylamide) superabsorbent polymers varying in grafting parameters and absorbency. Journal of Applied Polymer Science 131. https://doi.org/10.1002/app.40368

Pereira, E.I., Giroto, A.S., Bortolin, A., Yamamoto, C.F., Marconcini, J.M., de Campos Bernardi, A.C., Ribeiro, C., 2015. Perspectives in Nanocomposites for the Slow and Controlled Release of Agrochemicals: Fertilizers and Pesticides, in: Rai, M., Ribeiro, C., Mattoso, L., Duran, N. (Eds.), Nanotechnologies in Food and Agriculture. Springer International Publishing, Cham, pp. 241–265. https://doi.org/10.1007/978-3-319-14024-7_11

Ramli, R.A., 2019. Slow release fertilizer hydrogels: a review. Polym. Chem. 10, 6073–6090. https://doi.org/10.1039/C9PY01036J

Shaviv, A., 2001. Advances in controlled-release fertilizers, in: Advances in Agronomy. Academic Press, pp. 1–49. https://doi.org/10.1016/S0065-2113(01)71011-5

Shaviv, A., Mikkelsen, R.L., 1993. Controlled-release fertilizers to increase efficiency of nutrient use and minimize environmental degradation - A review. Fertilizer Research 35, 1–12. https://doi.org/10.1007/BF00750215

Sorber, J., Steiner, G., Schulz, V., Guenther, M., Gerlach, G., Salzer, R., Arndt, K.-F., 2008. Hydrogel-Based Piezoresistive pH Sensors: Investigations Using FT-IR Attenuated Total Reflection Spectroscopic Imaging. Anal. Chem. 80, 2957–2962. https://doi.org/10.1021/ac702598n

Ullah, F., Othman, M.B.H., Javed, F., Ahmad, Z., Akil, H.Md., 2015. Classification, processing and application of hydrogels: A review. Materials Science and Engineering: C 57, 414–433. https://doi.org/10.1016/j.msec.2015.07.053

Wu, L., Liu, M., Rui Liang, 2008. Preparation and properties of a double-coated slow-release NPK compound fertilizer with superabsorbent and water-retention. Bioresource Technology 99, 547–554. https://doi.org/10.1016/j.biortech.2006.12.027

Zhang, S., Shi, Z., Xu, H., Ma, X., Yin, J., Tian, M., 2016. Revisiting the mechanism of redox-polymerization to build the hydrogel with excellent properties using a novel initiator. Soft Matter 12, 2575–2582. https://doi.org/10.1039/C5SM02910D

# CHAPTER I

## Influencing parameters of mechanochemical intercalation of kaolinite with urea

**CHAPTER I. INFLUENCING PARAMETERS OF MECHANOCHEMICAL INTERCALATION OF KAOLINITE WITH UREA ..... 15**

# Chapter I. Influencing parameters of mechanochemical intercalation of kaolinite with urea

## I.1. Introduction

Kaolinite is a 1:1 type clay mineral built from stacked layers of tetrahedral silica sheet and octahedral Gibbsite-like sheet. The individual layers are firmly held together by hydrogen bonds. Mainly, there are two ways to intercalate urea into kaolinite layers. The first way is by the displacement of pre-intercalate molecules such as hydrazine (Ledoux and White, 1966) or DMSO (Liu et al., 2014). The second way is direct intercalation of urea into the interlayer space of pristine kaolinite, by aqueous suspension (Frost et al., 2000; Gardolinski and Lagaly, 2005a; Seifi et al., 2016), mechanochemical (Yan et al., 2005; Letaief et al., 2006a; Makó et al., 2009, 2013), and homogenization (Makó et al., 2015, 2019) methods. In the aqueous suspension method, kaolinite is mixed with a concentrated aqueous solution of urea at 25-110°C for 2-8 days, followed by centrifugation to recover the kaolinite-urea (Kaol-U) complex (Frost et al., 1997b; Gardolinski and Lagaly, 2005a; Zhang et al., 2017; Cheng et al., 2018). The mechanochemical method is based on the manual or mechanical co-grinding of urea and kaolinite with or without the presence of a small amount of water (Tsunematsu and Tateyama, 1999; Valášková et al., 2007; Makó et al., 2009; Horváth et al., 2010). A considerable number of studies reported on the effect of grinding and milling time on the structure of kaolinite (Aglietti et al., 1986a; Gonzalez Garcia et al., 1991; Sánchez-Soto et al., 2000; Frost et al., 2001a, 2001b; Franco et al., 2004; Frost et al., 2004; Valášková et al., 2007; Pardo et al., 2009; Vdović et al., 2010; Valášková et al., 2011; Hamzaoui et al., 2015; Ondruška et al., 2018). Frost et al. (2004) found that the delamination of kaolinite surfaces taking place for short milling times (< 30 min to 2 h) was followed by reaggregation of the ground crystals. During dry milling, surface hydroxyls of the kaolinite were lost and replaced with water molecules coordinated to the new surface active sites (Frost et al., 2001a, 2004). In another study, Sánchez-Soto et al., (2000) showed that grinding Georgia kaolin produced a strong structural alteration, mainly along the c axis, resulting in disorder and total degradation of the crystal structure of the kaolinite and the formation of an amorphous product. As with the grinding of kaolin, the co-grinding of kaolin and urea resulted in structural disorders and a reduction in particle size (Makó et al., 2013). Structural disorders induced by milling can make it difficult to incorporate other organic molecules by the direct displacement method. In the homogenization method, which has been reported more recently, kaolinite is mixed with urea in an agate mortar with a small amount of distilled water and the mixture is aged in a closed or opened sample holder (Makó et al., 2015, 2016, 2017). The amount of urea used in the mechanochemical and homogenization methods was an order of

magnitude less than in the suspension aqueous method. The homogenization method advantageously makes it possible to obtain a more ordered Kaol-U complex compared to mechanochemical method, but still, we are not aware of any study reporting complete intercalation of urea through this method. The optimal conditions for the preparation of the Kaol-U complex by the homogenization method were as follows: 55 m% kaolinite content, 0.7 mass fraction of urea, and aging in an open sample holder at 80°C for 24 h (Makó et al., 2019). Under these conditions, there was still about 15% kaolinite not intercalated by urea. In view of the current research status of Kaol-U intercalates, the preparation methods still need to be improved to be simple, fast, and cost-effective. In this work, ball milling in dry conditions low-defect kaolinite with urea was further explored by investigating the effect of milling conditions (milling times and urea-to-kaolin mass ratio) on the intercalation process. 10 to 40 m% urea loadings are usually used for the preparation of Kaol-U intercalates by co-grinding kaolin with solid urea (Tsunematsu and Tateyama, 1999; Letaief and Detellier, 2009; Rutkai et al., 2009). Higher urea loadings (> 40 m%) for which only a few studies are reported so far (Letaief et al., 2006a) were also tested for comparison. The weakening of the interlayer hydrogen bonds caused by the intercalation of urea may facilitate the delamination/exfoliation of kaolinite after a subsequent treatment of the Kaol-U complex (Tsunematsu and Tateyama, 1999; Valášková et al., 2011). Therefore, the structural characteristics of kaolinite after washing the Kaol-U intercalates with water were also investigated in this chapter. Another scientific problem addressed in this chapter concerns the removal of excess urea (not intercalated). This purification step is important from different aspects: excess urea may decrease the efficiency of the displacement method when the Kaol-U complex is used as a pre-intercalate. On the other hand, the excess urea can lead to a significant burst release of urea in the environment which can be harmful when the intended application requires a controlled release of urea, for example for the preparation of urea controlled-release fertilizers. A further point to consider is that the washing can be accompanied by a partial deintercalation of urea, hence the need to control this purification step. To our knowledge, this problem of purification by the washing of the Kaol-U complex has not been investigated so far.

## I.2. Experimental details

### I.2.1. Intercalation of kaolinite with urea

The kaolin used in this study was low defect kaolinite (KGa-1b; Georgia) from the *Source* Clays *Repository* of the *Clay Mineral Society* (CMS) with a Hinckley index (HI) of around 1.09 (Hinckley, 1962). The chemical composition of the kaolin in m% of the various oxides is : $SiO_2$, 44.2; $Al_2O_3$, 39.7; $TiO_2$, 1.39; $Fe_2O_3$, 0.13; FeO, 0.08; MnO, 0.002; MgO, 0.03; $Na_2O$, 0.013; $K_2O$, 0.05; F, 0.013; $P_2O_5$, 0.034 (https://www.clays.org/sourceclays_data/). The dehydroxylation mass loss of KGa-1b is 13.47%

(theoretical mass loss 13.95%) indicating that KGa-1b contains 96 m% kaolinite with minor phases such as quartz, anatase, and mica (Pruett and Webb, 1993). All the particles of the original sample were passed through a 635-mesh sieve that means kaolin particles are less than 20 µm. KGa-1b was mixed with 25, 50, 66, and 80 m% of urea (Fisher, >99%), and the mixtures (15 g) were ground for different times (5 min to 2 h) with a planetary ball mill (PM100; Retsch corporation) in a 125 $cm^3$ agate jar with 30 agate balls (10 mm diameter). The applied rotation speed was 400 rpm and the direction of rotation was reversed every 10 min to avoid any agglomeration with a 1 min break to prevent the powder from reaching too high temperatures. For isopropanol washing, the as-ground mixture (2g) was suspended in 15 ml isopropanol with gentle shaking for 30 s before applying vacuum to rapidly filter the dispersion. Afterwards, the product was dried at 40°C for 48 h. The total removal of urea was carried out by vigorously shaking a suspension of the as-ground mixture (1 g) in 100 ml water for 24 h at room temperature. The operation was repeated two times and then, the solid was separated by centrifugation (3000 rpm for 10 min), resuspended in 100 ml water and shaken for 1 h in an ultrasonic bath. The resulting suspension was centrifuged (3000 rpm for 10 min) to isolate the solid that was dried at 60°C for 24 h. For comparison, a KGa-1b sample was also prepared following the same treatments as Kaol-U intercalated samples.

## I.2.2. Experimental methods

Powder X-ray diffraction (XRD) analyses were implemented on a Siemens D5000 type diffractometer equipped with a vertical goniometer and diffracted beam monochromator. The radiation applied was Cu K$\alpha$ ($\lambda$ = 0.1541 nm) generated at 40 kV and 40 mA. The samples were measured in step scan mode with 0.04° step size and 4 s step scan. The degree of intercalation $\alpha$ was calculated using the integral intensity of the (001) reflections of the unexpanded kaolinite, $I_0$ and the intercalation compound, $I$ (Gardolinski and Lagaly, 2005b): $\alpha = 100.I/(I+I_0)$. Simultaneous DSC/TGA was performed using a TA Instruments SDT600 heating rate under continuous nitrogen purge of 100 mL/min. The samples (ca. 10 mg) were typically equilibrated at 30°C and ramped to 800°C at a rate of 10°C/min and data analysis was performed using Universal Analysis 2000 software package. The Fourier transform infrared (FTIR) spectra were recorded on a FTIR spectrometer Nexus, (ThermoNicolet) equipped with an attenuated total reflectance diamond crystal unit (Thermo Scientific Smart iTR). 32 scans were obtained at a resolution of 4 $cm^{-1}$ and over a spectral range of 600-4000 $cm^{-1}$. Scanning electron microscopy (SEM) images were recorded with a Zeiss Supra 40 VP Field Emission Scanning Electron Microscope in the secondary electron mode and at an accelerating voltage of 3 kV. The samples were mounted on aluminum stubs with a double-sided adhesive carbon disk and coated with a thin layer of gold to prevent charging of the surface.

## I.3. Results and discussion

### I.3.1. Effect of milling conditions on the characteristics of Kaol-U intercalate

A urea loading of 25 m% was selected because it corresponds to commonly used loading conditions. Ball milling was more rarely carried out with > 40 m% urea loadings. Consequently, it seemed interesting to study samples with urea loadings of 50 m%, 66 m%, and 80 m%, in addition to the 25 m% urea loading sample. When kaolin was ground with 80 m% urea, the powder stuck to the jar walls and the balls even after short milling times. This sample was therefore not further studied. In agreement with previous studies (Letaief et al., 2006b; Makó et al., 2009, 2013, 2017, 2019), the intercalation of urea into kaolinite resulted in a displacement of the (001) reflection to a lower angle (Figure I.1 and Figure I.2).

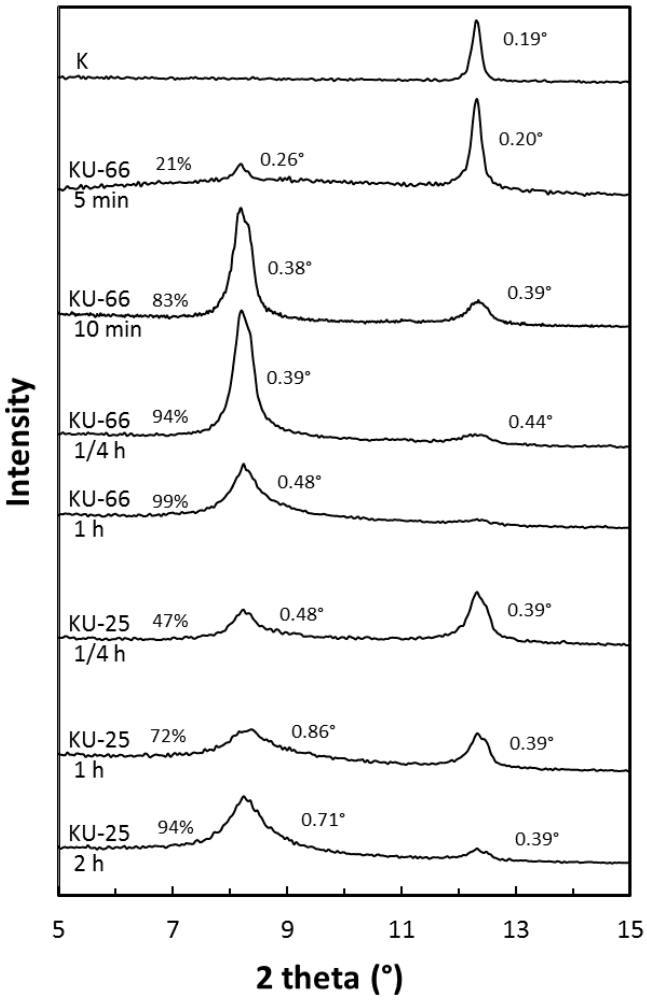


*Figure I.1. X-ray diffraction patterns of the (001) reflection of original kaolin (KGa-1b) and kaolin mechanically ground together with 66 m% and (KU-66) and 25 m% (KU-25) solid urea (5 min-2h). The degree of intercalation, $\alpha$ (%) and the FWHM values (°) of the reflections of the expanded and non-expanded kaolinite are indicated. KU-25 and KU-66 were as ground samples.*

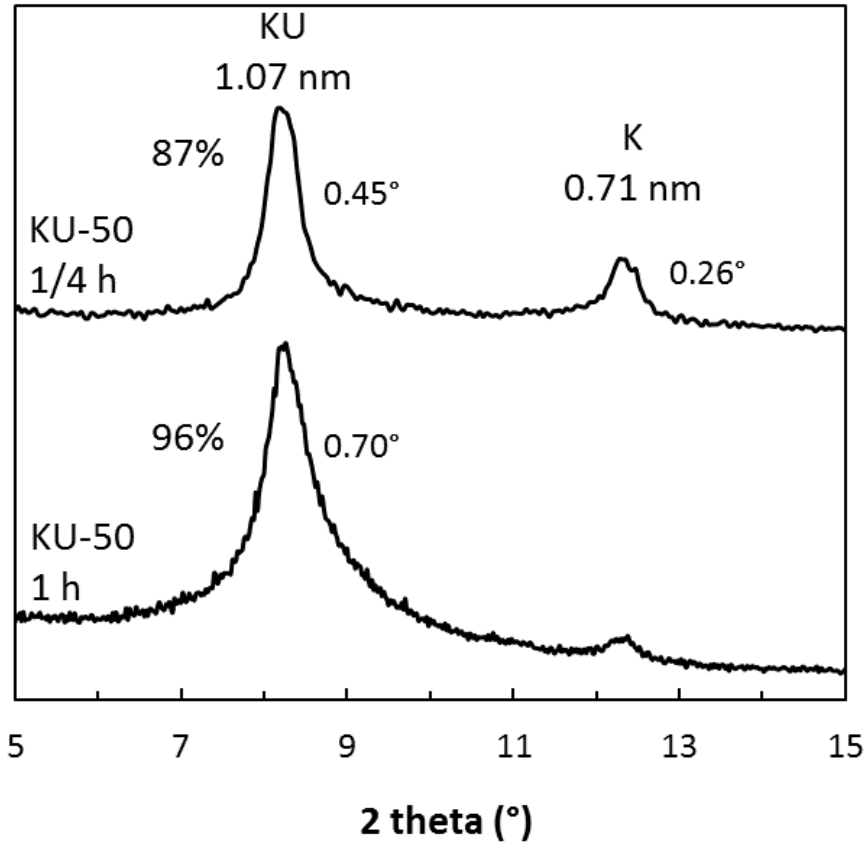


*Figure. I.2. X-ray diffraction patterns of the (001) reflection of kaolin mechanically ground together with 50 m% (KU-50) solid urea for (1/4, 1 h). The degree of intercalation (%), the FWHM values of the reflections (°) and d-values (nm) of the expanded and non-expanded kaolinite are indicated. KU-50 was as ground sample.*

For the raw kaolinite, the d-value was 0.71 nm, but when it was intercalated by urea, the d-value was shifted to 1.07 nm. The degree of intercalation increased significantly with the grinding time. The kaolin co-ground 1/4 h with 66 m% solid urea led to 94% intercalation while the rate of intercalation was only 47% when kaolin was co-ground with 25 m% solid urea. 1 h of co-grinding kaolin with 66 m% urea led to almost 100% intercalation while 2 h of grinding was necessary to obtain a high degree of intercalation (94%) with 25 m% urea. The efficiency of urea intercalation with the 50 m% urea loading sample was intermediate (87 and 96% intercalation were calculated after 1/4 h and 1 h grinding time, respectively) between that of the sample loaded with 25 m% urea and that of the sample loaded with 66 m% urea. The XRD results showed that an excess of urea increases the ability of the kaolinite layers to be expanded by urea. High degrees of urea intercalation by mechanochemical treatment were reported in the literature for grinding times greater than 1 hour (Makó et al., 2013). Here, 1/4 h of co-grinding was sufficient to achieve almost complete intercalation when kaolin is co-ground with a small

excess of urea (66 m% urea). This is the most interesting result of the present study. Moreover, the relatively sharp profile of the (001) reflection at 1.07 nm after 1/4 h co-grinding showed that the Kaol-U complex was well-ordered with a large crystallite size along the *c* axis. It is noted that the influence of the urea content on the degree of intercalation by the mechanochemical method appears opposite to that observed by the homogenization method which led to an increasing degree of intercalation with the level of kaolinite up to 70 m% of kaolinite (Makó et al., 2019). A significant broadening of the 1.07 nm reflection was observed when grinding time increased which can be related to the increase of the mean lattice strain and/or to the reduction of the crystallite size during mechanochemical process (Makó et al., 2009). The full width at half-maximum (FWHM) value of the 1.07 nm reflection was slightly broader for the intercalate prepared with 25 m% urea compared to those prepared with 66 m% urea. This result suggests that co-grinding kaolinite with an excess of urea led to the formation of greater crystallite size of Kaol-U complexes along the *c* axis. For the rest of the study, we studied more specifically two urea loadings, 25 m% (the most common loading) and 66 m% which gave the higher efficiency of intercalation. The morphology of the untreated kaolin and the different treated kaolin samples was observed by SEM (Figure I.3).

Micrograph of the untreated kaolin revealed the typical booklet morphology of kaolinite with many stacked euhedral pseudohexagonal platelets with a lateral size mostly less than 4 µm. After 1 h grinding without urea, kaolinite did not exhibit the booklet morphology and there was less stacking of the kaolinite particles, but the hexagonal shape of the particles was largely preserved (Figure I.3,b). Figure I.3,f showed XRD patterns of starting kaolin before and after one hour of dry grinding. The HI value of raw kaolinite was 1.09 which indicated that KGa-1b belongs to the category of ordered kaolinite. After 1 h grinding, a significant loss in the definition of reflections occurring between 19 and 24° ($2\theta$) was observed, suggesting that grinding results in some structural disorder. At the same time, the width and intensity of the (001) reflection remained almost unchanged while the d-value slightly increased from 0.713 nm to 0.718 nm. Overall, XRD results indicated that the applied milling regime resulted in small structural changes for kaolinite, which agrees with SEM observations. These results can be compared with those obtained recently by Ondruška et al. (2018). These authors have indeed used the same type of planetary mill. Milling balls made of a high-density material lead to high kinetic energy provided in the collision (Štefanić et al., 2007). Despite the use of heavier corundum balls ($\rho$ = 3.8 g/cm$^3$) instead of agate balls ($\rho$ = 2.4 g/cm$^3$), the XRD reflections of kaolinite after 1 h grinding time also showed little amorphization of kaolinite (Ondruška et al., 2018). After 1/4 h grinding kaolin with 66 m% urea still showed many stacks of euhedral pseudohexagonal platelets with no delamination (Figure I.3,c). The SEM observations fit well with the XRD results which suggested the formation of well-ordered Kaol-U intercalates after 1/4 h co-grinding. Co-grinding kaolin with solid urea for longer grinding times (1 or 2 h) led to more significant changes in morphology (Figure I.3,d and e).

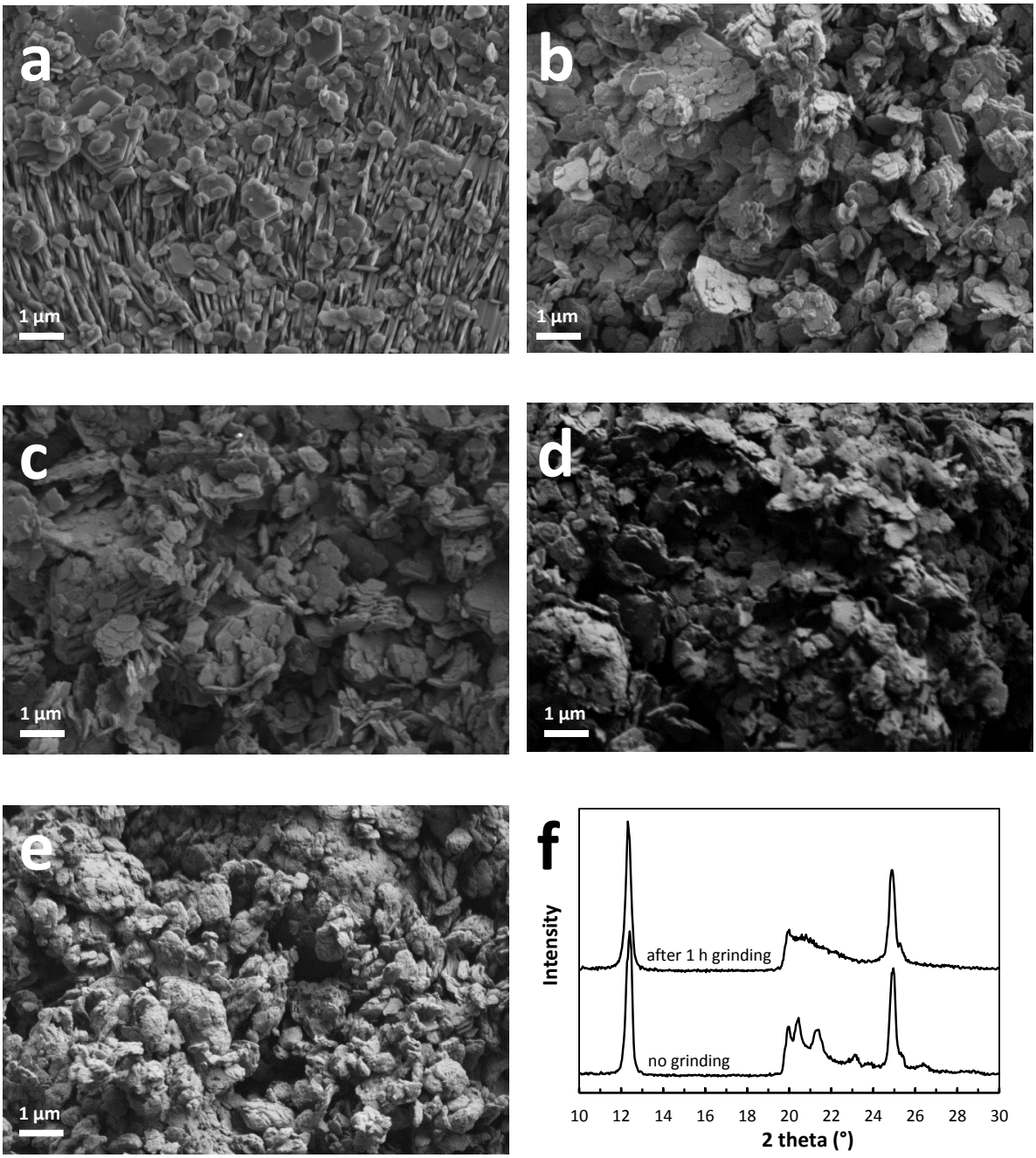


*Figure I.3. SEM images showing the morphology of (a) original kaolin, (b) kaolin ground 1 h, (c) kaolin ground 1/4 h with 66 m% urea, (d) kaolin ground 1 h with 66 m% urea, (e) kaolin ground 2 h with 25 m% urea (samples c, d and e after repeated washing with isopropanol to remove excess urea) and (f) XRD of kaolin before and after 1 h grinding.*

After 1 h grinding kaolin with 66 m% urea, a few plates still showed developed euhedral edges but most of them were somewhat irregular. It was seen that 2 h grinding kaolin with 25 m% urea led to an even greater modification of the morphology of the original kaolinite with the formation of shapeless

agglomerates consisting of partially fused nanometer-sized particles giving them an apparent rugged surface.

The derivative thermogravimetric (DTG) curves in Figure I.4 showed the complex nature of the decomposition of the Kaol-U samples.

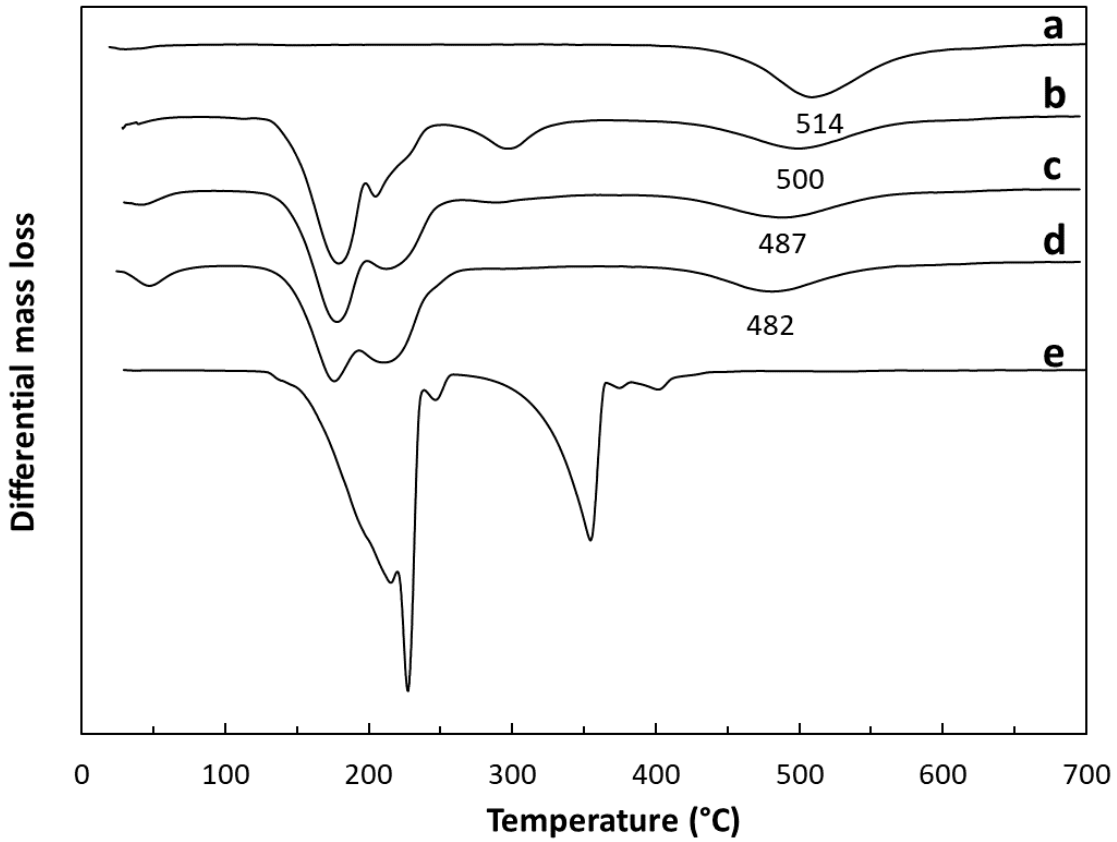


*Figure I.4. Derivative thermogravimetric (DTG) curves of (a) original kaolin, (b) kaolin ground with 25 m% urea for 1/4 h (as ground), (c) kaolin ground with 25 m% urea for 1 h (as ground), (d) kaolin ground with 25 m% urea for 2 h (as ground) and (e) urea (the DTG peak temperatures of the thermal dehydroxylation of the kaolinite are indicated).*

The first mass loss, below 125°C, was assigned to the removal of adsorbed/coordinated water. The amount of water loss increased as the grinding time increased, following other reported works (Gonzalez Garcia et al., 1991; Sánchez-Soto et al., 2000; Frost et al., 2001b; Hamzaoui et al., 2015). The increase in the amount of water loss in TGA is attributed to "gel water" formed by mechanochemical dehydroxylation from the structural hydroxyl groups of kaolinite (Makó et al., 2009). The second mass loss step, between 135 and 400°C indicated the existence of a complex multistep mechanism which is related to the loss of urea (non-intercalated and intercalated) and the residue of coordinated water (Kristóf et al., 1998). The decomposition pattern of urea drastically changed with grinding time (and

thus, an increasing amount of intercalated urea) which suggests that the intercalated urea does not follow the same decomposition pathway as the adsorbed (external) urea. Notably, after 2 h grinding and near-complete intercalation of urea (from XRD results), no mass loss was observed between 250 and 350°C, as discussed below. The third mass loss step, between 400 and 800°C, is due to the dehydroxylation of kaolinite with the formation of meta-kaolinite (Miller and Oulton, 1970; Aglietti et al., 1986a; Frost et al., 1997a, 1997b, 2000, 2003; Horváth et al., 2003; Makó et al., 2009, 2013). The dehydroxylation of kaolinite took place at 514°C for original kaolinite and at 500, 487 and 482°C for the kaolin milled with 25 m% urea for 1/4, 1, and 2 h, respectively. Thus, the dehydroxylation peak temperature of kaolinite shifted to a lower temperature as the grinding time increased. This feature will be further discussed later in this chapter.

## I.3.2. Isopropanol washes for excess urea removal

The objective of the washing step with isopropanol was to eliminate the excess urea crystals. The solubility of urea in isopropanol is lower than in other alcohols (such as methanol or ethanol) which should allow better control of the washing process by decreasing the risk of removal of interlayer urea during washing (House and House, 2017). Figure I.5 showed the thermogravimetric analyses of the kaolin ground with 66 m% solid urea for 1 h before and after three and seven successive washing steps with isopropanol. Figure I.5 also displayed the TGA curve of urea. The thermal decomposition of urea under an $N_2$ atmosphere is a very complex process. Based on the study by Schaber et al. (2004), the mass loss below 190°C was principally associated with urea decomposition, first resulting in the evolution of $NH_3$ (g) and HNCO (g). From 160°C, HNCO (g) reacts with intact urea to produce biuret and from 175°C, small amounts of cyanuric acid(s) and ammelide(s) commence to be produced from common reactants, biuret, and HNCO. Between 190 and 250°C, urea continues and biuret begins to decompose to produce large quantities of cyanuric acid and ammelide. Ammeline begins to be formed in this temperature range. The mass loss above 250°C was related to the sublimation and eventual decomposition of cyanuric acid, ammeline, and ammelide. TGA curves in Figure I.5 showed a progressive decrease in mass losses above 250°C during successive washes, *i.e.* when excess external urea is eliminated. This suggests that decomposition of intercalated urea takes place by a reaction process different in terms of total product distribution and/or intermediates observed than urea. As no mass loss was observed above 250°C when external urea was totally eliminated, intercalated urea most likely degrades without producing appreciable amounts of cyanuric acid, ammeline, and ammelide. Simultaneous DSC/TGA can be used to study the morphological state of urea in the samples obtained after co-grinding kaolin with solid urea. The DSC curves of the ground samples before and after isopropanol washes are shown in Figure I.6. The endothermic peak at 135°C in the DSC curves was attributed to the melting of urea crystallites.

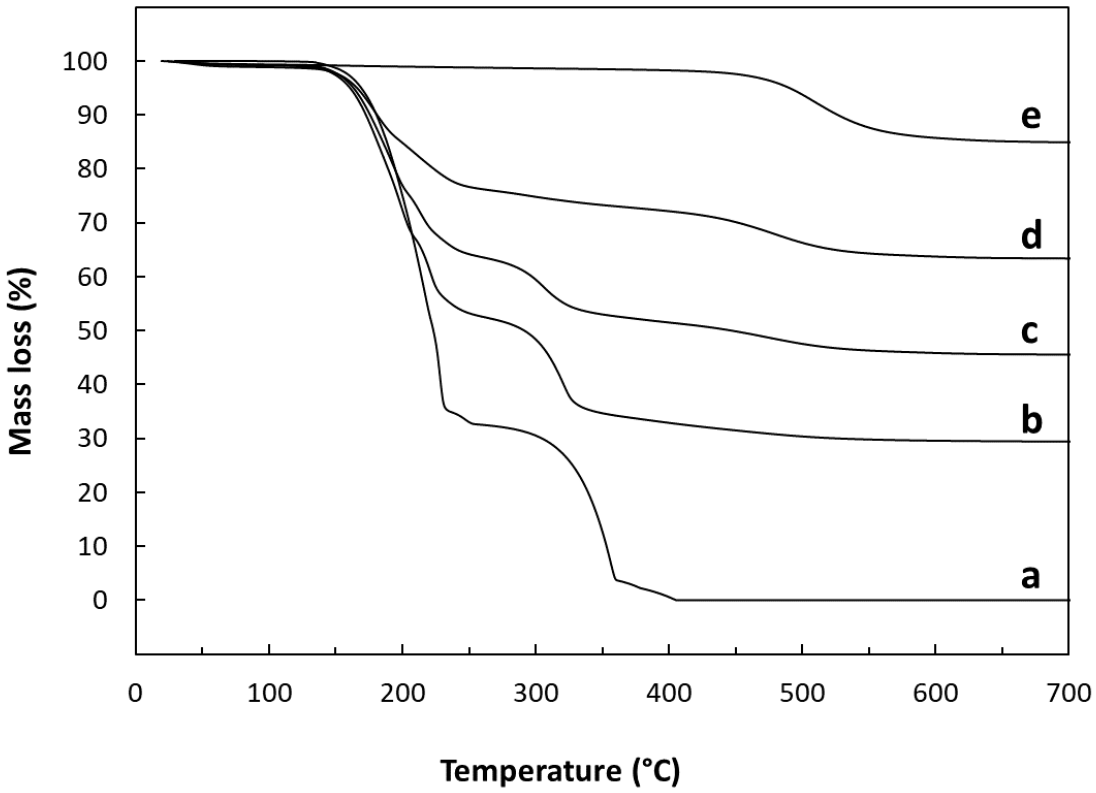


*Figure I.5. Thermogravimetric analysis of (a) urea, (b) kaolin ground for 1 h with 66 m% urea, (c) sample (b) washed three times with isopropanol, (d) sample (b) washed seven times with isopropanol and (e) original kaolin.*

In the DSC curves of the ground samples, it is clearly seen that the amount of crystalline urea decreased with isopropanol washings. It is reasonable to suppose that the intercalated urea is in an amorphous state because the interlayer space is not large enough for urea crystallization. The area of the endothermic peak at 135°C is thus directly proportional to the amount of external surface urea crystallites. The above results showed that external urea was progressively removed after isopropanol washing. From the DSC curves of the kaolin ground for 2 h with 25 m% urea, it is seen that total elimination of external urea required three successive washes with isopropanol. On the other hand, DSC curves of the kaolin ground for 1 h with 66 m% urea still showed an endothermic melting peak of urea even after seven successive washing steps, indicating that much more washings are needed for the total elimination of external urea when large amounts of urea were used in the kaolin-urea mixture. The following method can be implemented to give a more quantitative description of the type and amount of urea in the kaolin-urea samples.

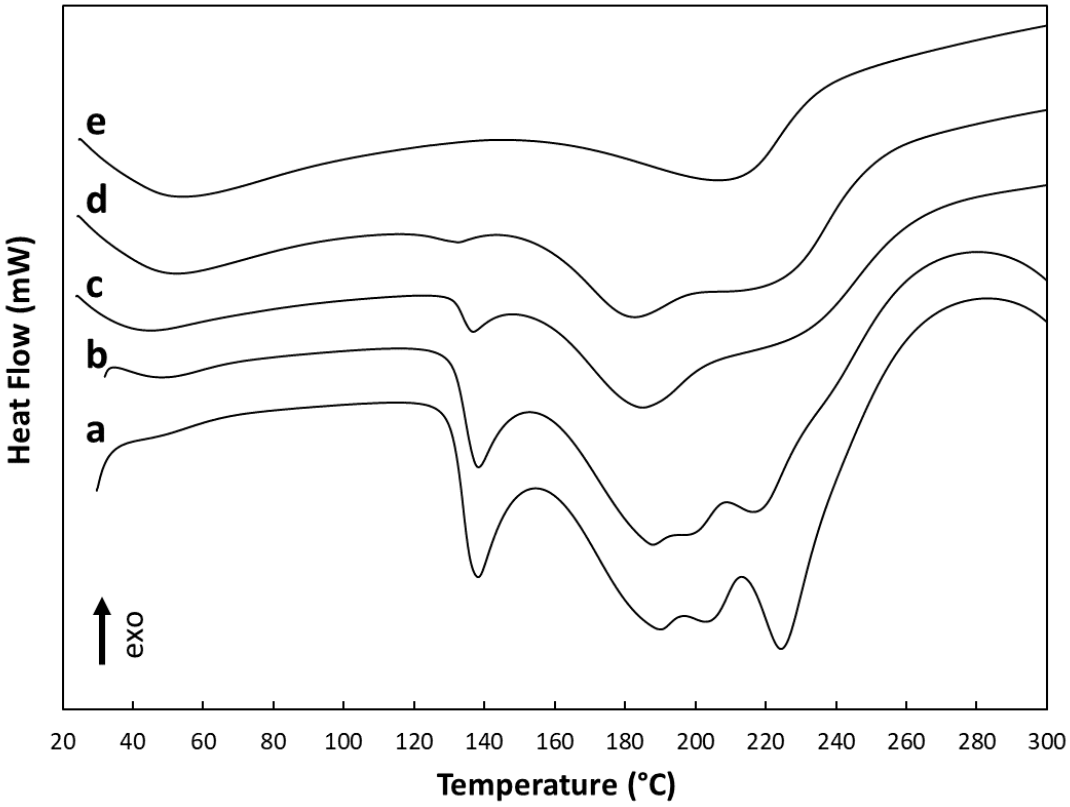


*Figure I.6. DSC curves of (a) kaolin ground for 1h with 66 m% urea (b) sample (a) washed three times with isopropanol, (c) sample (a) washed seven times with isopropanol, (d) kaolin ground for 2h with 25 m% urea and (e) sample (d) washed three times with isopropanol.*

The mass loss in TGA between 135 and 400°C was used to determine the total urea content. Based on this method, the amount of urea in the as ground kaolin-urea samples (corrected from the physisorbed water loss below 135°C) was 27 m% for the kaolin co-ground with 25 m% urea and 67 m% for the kaolin co-ground with 66 m% urea, which is close to the expected values. The slight differences between the expected and calculated values are likely due to a small contribution from the coordinated water produced during the mechanochemical degradation to the loss of mass measured between 135 and 400°C. The percentage of intercalated (*i.e.* amorphous) urea in the samples relative to total urea, $\%X_a$, was calculated as:

Since *W*(%) is the mass percentage of urea in the kaolin-urea sample, the heat of fusion that should have been measured if the urea contained in the kaolin-urea mixture was 100% crystallized, HF (100%), is given by :

$$HF\ (100\%) = \frac{\Delta H_0 . W(\%)}{100}$$

Where $\Delta H_0$ is the heat of fusion of 100% crystalline urea determined from the DSC thermogram of urea. Since the measured heat of fusion of urea in the kaolin-urea sample determined in the DSC thermogram was $\Delta H_m$, the % of crystallized urea, $U_{cryst}$(%), in the kaolin-urea mixture is expressed as :

$$U_{\text{cryst}}(\%) = \frac{100.\Delta H_m}{HF\ (100\%)} = \frac{100.\Delta H_m}{\frac{\Delta H_0.W(\%)}{100}}$$

Then, the % of amorphous (intercalated) urea relative to total urea in the kaolin-urea mixture is given by,

$$\%X_a = 100 - U_{cryst}(\%) = 100 - \frac{100.\Delta H_m}{\frac{\Delta H_0.W(\%)}{100}}$$

which can be rearranged to give equation (1) :

$$\%X_a = 100.(1 - \frac{100.\Delta H_m)}{W.\Delta H_0}) \qquad (1)$$

Where *W(%)* was determined from TGA by the mass loss measured in the 135-400°C range and the heat of fusion relative to the fusion of urea (in J/g) was determined from the area under the melting endotherm of urea between 129 and 152°C in the DSC signal. The percentage of total urea, $\%U_{Tot}$, in the sample calculated by removing the contribution of physisorbed water was determined from equation (2) :

$$\%U_{\text{Tot}} = 100.\frac{W}{(100-W_w)} \qquad (2)$$

Where $W_w$ is the mass % of physisorbed water in the kaolin-urea sample determined from TGA by the mass loss measured in the 20-135°C range. The percentage of intercalated urea ($\%U_{Int}$) in the kaolin-urea sample was determined using the following equation :

$$\%U_{\text{Int}} = \frac{X_a.\%U_{\text{Tot}}}{100} \qquad (3)$$

Figure I.7 showed the amount of intercalated urea relative to total urea, $\%X_a$, and the amount of intercalated urea, $\%U_{Int}$, in the kaolin-urea samples. After grinding for 2 h kaolin with 25 m% urea (KU-25), the intercalated urea content was 24.6 m% corresponding to 92 m% of the total urea. Three successive washing in isopropanol allowed the total elimination of external surface urea but this was accompanied by a partial deintercalation of urea, giving an intercalated urea content of 14.4 m%.

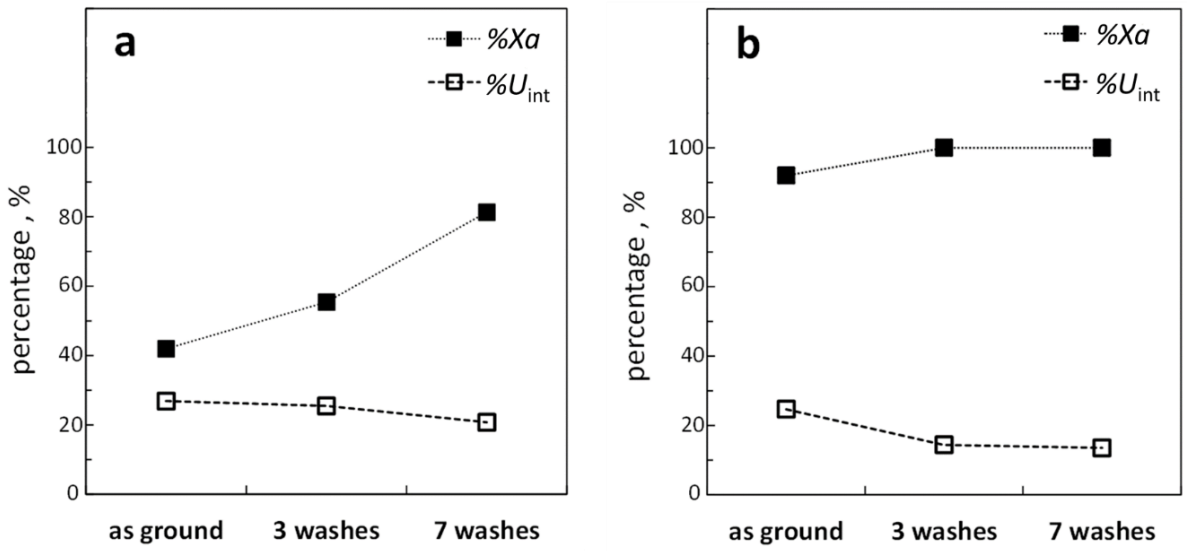


*Figure I.7. Effect of isopropanol washes on the amount of intercalated urea relative to total urea ($\%X_a$) or relative to the kaolin-urea content ($\%U_{Int}$) for (a) kaolin ground with 66 m% urea for 1 h and (b) kaolin ground with 25 m% urea for 2 h. The error bars (the average deviation from the mean of duplicate measurements) are smaller than the size of the symbols.*

The elimination of external urea required more extensive washing when kaolin was co-ground with 66 m% urea (KU-66). After seven successive rinses with isopropanol, the intercalated urea content in KU-66 was 20.8 m% corresponding to 79 m% of the total urea. Note that the content of intercalated urea is certainly slightly overestimated because of loss of water between 135 and 400°C (gel water formed during co-grinding and/or thermal dehydroxylation below 400°C during TGA ramp). XRD analyses of the samples were also carried out to determine the changes in the degree of intercalation after isopropanol washes (Figure I.8).

XRD patterns of KU-25 showed that the (001) reflection collapsed partially to a *d*-value of 0.71 nm after the successive rinses with isopropanol. This agrees with the DSC/TGA results that showed a significant deintercalation of urea after isopropanol washes. On the other hand, KU-66 exhibited no collapse to a *d*-value of 0.71 nm after isopropanol washing. DSC/TGA results of KU-66 indicated that intercalated urea reduces from 26.8 m% to 20.8 m%, before and after seven successive washes. These results suggest that a small deintercalation of urea during isopropanol rinses was not necessarily accompanied by the collapse of the kaolinite layer.

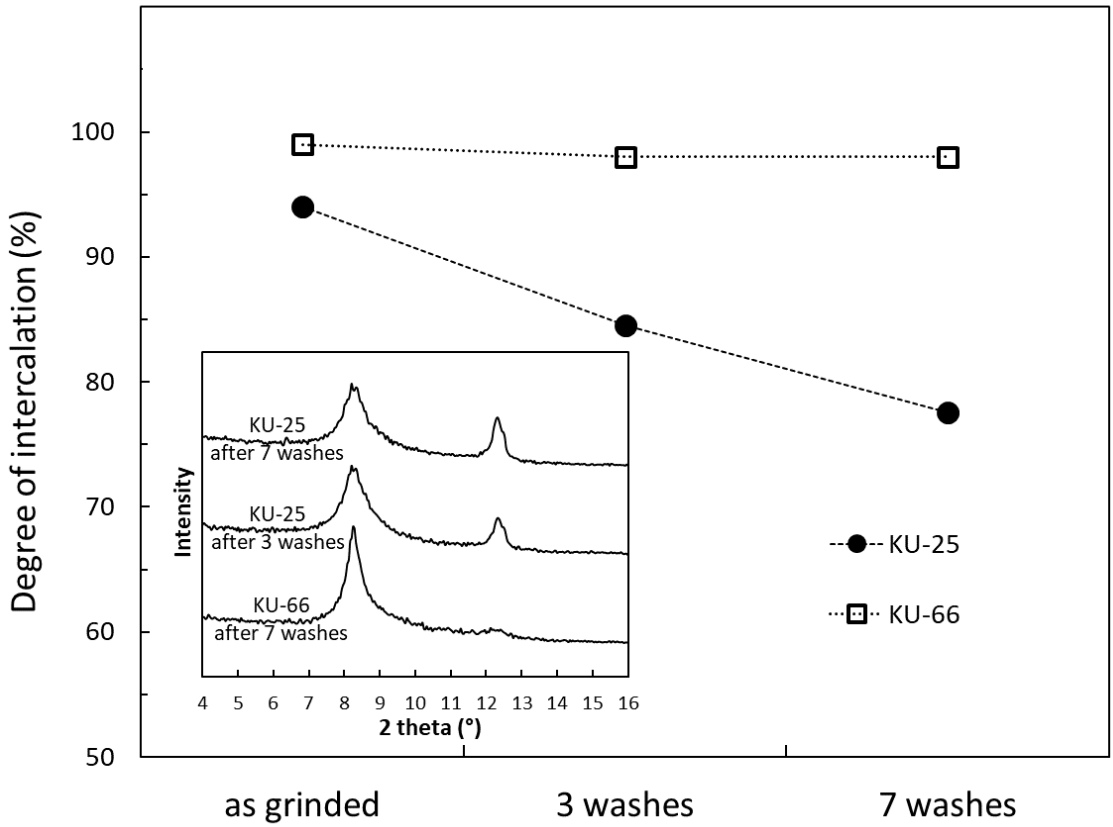


*Figure I.8. Changes in the degree of intercalation calculated for the kaolin ground with 66 m% urea for 1 h (KU-66) and for kaolin ground with 25 m% urea for 2 h (KU-25) after isopropanol washes (XRD of KU-66 and KU-25 after washes with isopropanol are shown as inset). The error bars (the average deviation from the mean of duplicate measurements) are smaller than the size of the symbols.*

## I.3.3. FTIR analysis

FTIR spectra of the original kaolin and the ground kaolin-urea (25 m%) mixtures were shown in Figure I.9. KGa-1b had the characteristic OH stretching pattern with 3687, 3669, and 3651 $cm^{-1}$ bands attributed to the inner surface hydroxyl groups of the alumina surface. The surface –OH groups were accessible for hydrogen bonding with the intercalated molecules. Their intensity and location are thus usually sensitive to the intercalation of organic molecules. Another characteristic band at 3620 $cm^{-1}$ is attributed to the stretching of the inner hydroxyl groups. The inner-OH are located within the kaolinite framework and rarely interact with organic intercalates (Elbokl and Detellier, 2009). Upon grinding kaolin with 25 m% urea for different times, the absorption bands at 3687, 3669, and 3651 $cm^{-1}$ from inner-surface hydroxyl groups decreased with grinding times while the band at 3619 $cm^{-1}$ remained unperturbed.

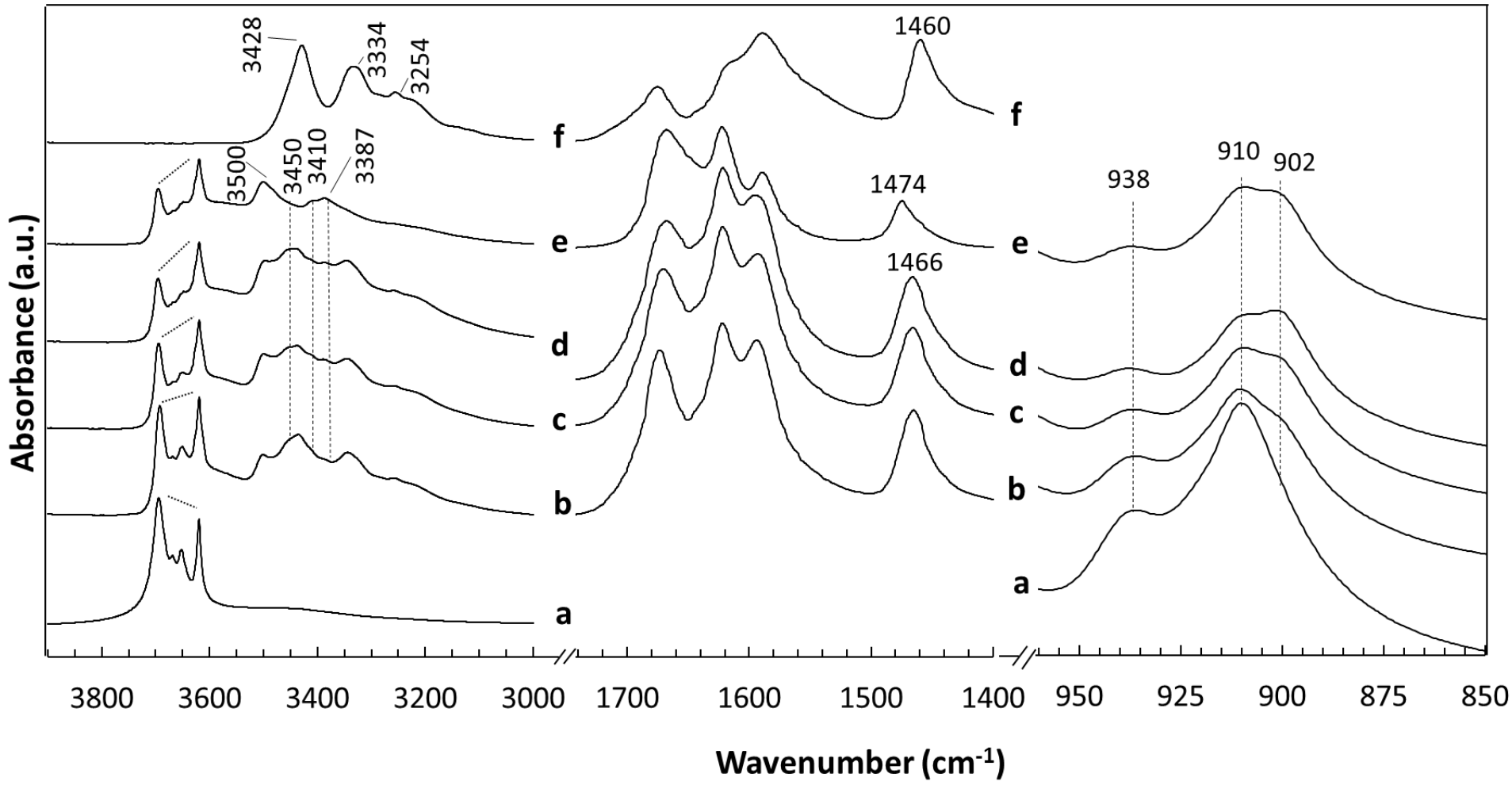


***Figure I.9. Infrared spectra of (a) original kaolin, (b) the kaolin ground with 25 m% urea for (b) 1/4 h, (c) 1 h and (d) 2 h, (e) sample (d) washed three times with isopropanol and (f) urea.***

The infrared spectrum of urea was characterized by two strong bands at 3428 and 3334 $cm^{-1}$ assigned to the $NH_2$ stretching vibrations. The weak band at 3254 $cm^{-1}$ is assigned to a combination band of the symmetrical $NH_2$-deformation and the CO stretching vibration (Keuleers et al., 1999). These bands were observed in the infrared spectra of the as-ground samples showing the presence of external urea for these samples. However, they disappeared completely after washing with isopropanol, indicating that the excess external urea was totally removed during the isopropanol washing. This is identical to the DSC/TGA results. New bands also appeared at 3500, 3410, and 3387 $cm^{-1}$. The position of these new bands was similar to those previously reported (Letaief et al., 2006a; Zhang et al., 2017). They were related to $NH_2$ groups of urea involved in hydrogen bonds with inner-surface hydroxyls. The antisymmetric and symmetric $NH_2$ stretching vibrations of urea in urea-water solutions were reported at 3488 and 3379 $cm^{-1}$, respectively (Keuleers et al., 1999). The corresponding bands shifted to higher wavenumbers in the FTIR spectra of Kaol-U intercalates, supporting the weak hydrogen bonds between occluded urea and kaolinite. The amine group of urea can interact as an H-donor with the oxygens of the tetrahedral sheet ($NH_2$…O-Si) and with the oxygens of the hydroxyl groups on the alumina surface. The broad 3500 $cm^{-1}$ band contains the contribution of the NH antisymmetric stretching of intercalated urea with alumina and siloxane sheets in different environments. The bands at 3410 and 3387 $cm^{-1}$ were due to the corresponding NH symmetric stretching vibrations. In the literature, it was postulated that the 3380 $cm^{-1}$ band corresponded to $NH_2$ groups interacting with the siloxane sheet (Ledoux and White, 1966). It was more recently reported using molecular dynamics simulation that the interaction energy of urea with alumina surfaces was greater than that with siloxane surfaces (Zhang et al., 2017). The assignment of each of the two bands at 3410 and 3387 $cm^{-1}$ to a specific interaction with the siloxane or alumina sheet is thus rather speculative. Another difference in the NH stretching region was the appearance of a poorly resolved band around 3450 $cm^{-1}$. The intensity of this band increased with grinding time but it is strongly reduced after extensive isopropanol washing. Seifi et al., (2016) noted absorption in the same wavelength range for Kaol-U intercalates and assigned this band to NH groups of urea linked to kaolinite by hydrogen bonding. The FTIR spectrum of KGa-1b (KBr pellet) gave two bands at 3457 and 1635 $cm^{-1}$ that are related to OH stretching and OH deformation of water, respectively (Madejová and Komadel, 2001). The infrared spectra of the ground kaolin-urea mixtures did not show a well-resolved band at 1635 $cm^{-1}$ due to overlapping with the strong $NH_2$ deformation bands but the intensity of the absorption around 1635 $cm^{-1}$ increased with grinding time and strongly decreased after isopropanol washing. Thus, the most likely explanation of the 3450 $cm^{-1}$ band is that it corresponded to adsorbed water formed by mechanochemical dehydroxylation and which was largely removed during extensive isopropanol washing. In the infrared spectrum of urea, the bands at 1674, 1618, 1588 and 1460 $cm^{-1}$ were assigned to $\delta_s$ ($NH_2$), $\delta_{as}$($NH_2$), $\nu$(CO) and $\nu_{as}$(CN) vibrations, respectively (Grdadolnik and Maréchal, 2002). As

the symmetrical $NH_2$ deformation and CO stretching vibrations are strongly coupled, any further discussion concerning the shifts of the 1674 and 1588 $cm^{-1}$ bands would be purely speculative. The CN stretching vibration was shifted from 1460 to 1466 $cm^{-1}$ in the spectra of the 2 h-ground kaolin-urea mixtures. After elimination of external urea by isopropanol washing, the CN stretching vibration of the intercalated urea was shifted to 1474 $cm^{-1}$. The increase in wavenumber indicated interactions in intercalated urea that strengthen the C-N bond. It suggests the formation of charge-transfer complex in which the oxygen atom of CO acts as an electron donor and the hydrogen atom of $NH_2$ as an electron acceptor resulting in C-N bond having more double bond character. This positive shift of $\nu_{as}$(CN) band was similar to that found by Zhang et al. (2017) and it supports their conclusion that the C=O groups of urea acted as H-acceptors for the hydroxyl groups on alumina surfaces while the amino group of urea acted as H-donor with basal oxygens on siloxane surfaces and/or with the oxygens of hydroxyl groups on alumina surfaces. The position of the CN stretching vibration of the as-ground samples (no isopropanol washing) reflected the presence of intercalated urea and of some external crystals of urea.

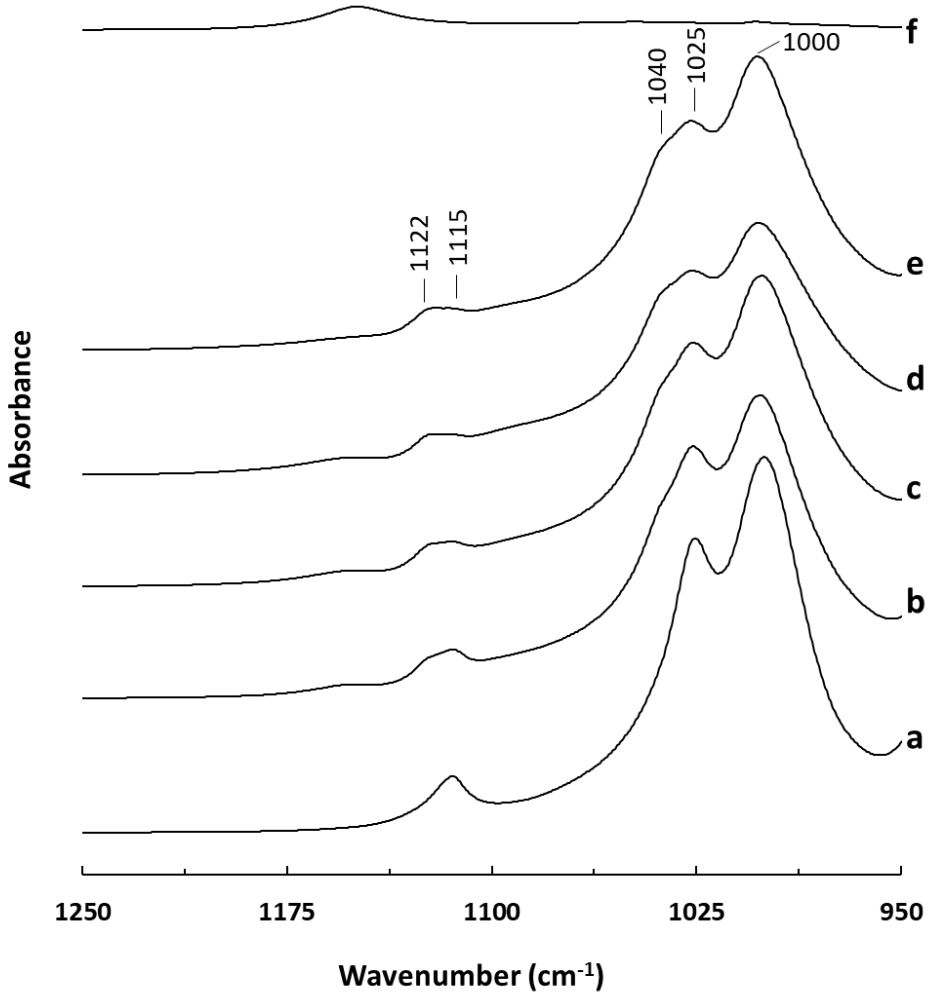


*Figure I.10. Infrared spectra (950-1250 $cm^{-1}$) of (a) original kaolin, (b) the kaolin ground with 25 m% urea for (b) 1/4 h, (c) 1 h and (d) 2 h, (e) sample (d) washed three times with isopropanol and (f) urea.*

The bands at 1000 , 1025 (Si-O-Si in plane vibrations) and 1115 $cm^{-1}$ (apical Si-O) seen in Figure I.10 are the typical SiO bands of kaolinite (Horváth et al., 2010). The bands at 1000 and 1025 $cm^{-1}$remained constant in position in the spectra of Kaol-U intercalates; however two shoulders appear at ~1040 and ~1122 $cm^{-1}$ that were both increasing in intensity with grinding time. Thus, the local environment of Si atoms was changed upon the intercalation of urea. Similar band shifts in the υ(Si-O) region have been reported for hydrazine intercalated kaolinite (Johnston et al., 2000). Another means of evaluating the changes in the structure of kaolinite upon intercalation is the study of the AlOH bending region between 850 and 960 $cm^{-1}$. Kaolinite had two bands at 938 and 910 $cm^{-1}$ that can be assigned to the bending vibrations of the inner-surface hydroxyl and inner hydroxyl, respectively. On grinding kaolin with urea an additional absorption appeared at 902 $cm^{-1}$. The intensity of 902 $cm^{-1}$ bands increased with grinding time. Due to the concomitant decrease of the 938 $cm^{-1}$ band with increasing grinding time, it seems reasonable to assign the 902 $cm^{-1}$ band to the hydroxyl deformation vibration of the inner surface hydroxyls hydrogen bonded to the C=O of urea, as proposed by Makó et al. (2009). The decreasing intensity of the band at 902 $cm^{-1}$ following washing with isopropanol suggested that urea was partially deintercalated from kaolinite by washing. This result is consistent with the XRD observations.

## I.3.4. Structural characteristics of kaolinite after urea washing

The morphological changes which took place in the Kaol-U complexes after water washing treatment were studied by XRD, FTIR, and TGA.

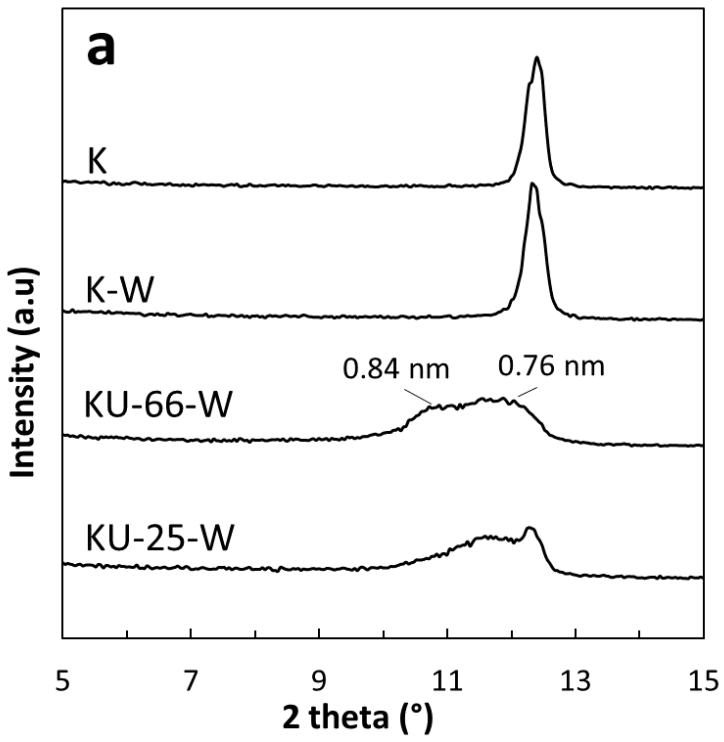

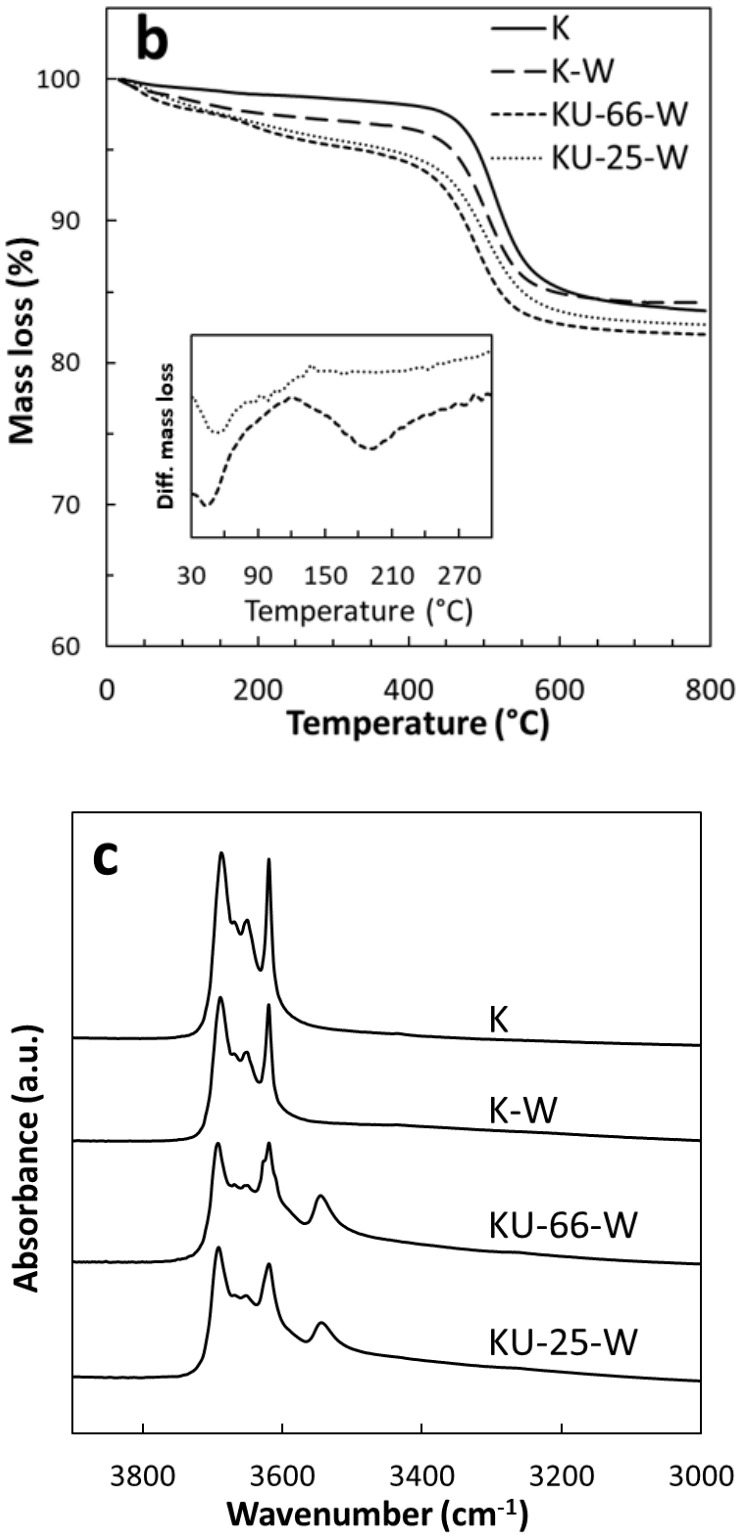


*Figure I.11. (a) X-ray diffraction patterns of the (001) reflection, (b) thermogravimetric analysis and (c) Infrared spectra in the range 3000-3900 $cm^{-1}$ of original kaolin (K), kaolin ground for 1 h after water washing process (K-W), kaolin ground with 66 m% urea for 1 h after water washing process (KU-66-W) and kaolin ground with 25 m% urea for 2 h after water washing process (KU-25-W). The embedded graph in (b) shows the dehydration section of the DTG curves of KU-25-W and KU-66-W.*

Figure I.11,a showed the first basal diffractions of kaolinite and Kaol-U intercalates after water washing treatments. Upon water washing of the original KGa-1b or KGa-1b after 1 h grinding, the non-expanded (001) diffraction at 0.71 nm remained unchanged. The washed Kaol-U intercalates showed a more interesting XRD pattern with a broad (001) reflection indicating the formation of a hydrate phase with a poorly resolved XRD reflection centered around 0.84 nm and an additional phase at a slightly higher interlayer distance than the original kaolinite (mean 0.76 nm). The XRD pattern of the non-expanded kaolinite was thus not restored after the removal of urea by water washing. Various synthetic kaolinite hydrates were reported with d-values near 0.84 nm (Tunney and Detellier, 1994; Gardolinski et al., 2000; Valášková et al., 2007). A 0.76 nm reflection appeared when a potassium acetate complex of a Georgia kaolinite was washed with water (Deeds et al., 1966). Residual unexpanded (d-value = 0.71 nm) kaolinite was observed for the washed Kaol-U intercalate prepared with 25 m% urea, which is not surprising when we take into account that the Kaol-U intercalate with 25 m% urea contains 6% of non-expanded kaolinite. The intensity in the 0.84 nm reflection of the hydrate as relative to the intensity of the 0.76 nm reflection was slightly higher for the intercalate prepared with the higher amount of urea (66 m%). Compared to the Kaol-U intercalates prepared with 25 m% urea, a more pronounced reduction of the 001 diffraction intensity was observed for the kaolinite intercalated with 66 m% urea. This suggests that the exfoliation/delamination of kaolinite is more efficient when a high concentration of urea is used in the preparation of the Kaol-U intercalate, in agreement with previous studies (Tsunematsu and Tateyama, 1999; Valášková et al., 2007). The results of the thermal analyses of the water-washed samples were given in Figure I.11,b. The complete disappearance of the DTG peaks related to urea decomposition indicated that urea was almost totally removed by the water washing procedure. The TGA curves showed a continuous mass loss in the temperature range of 20-300°C due to dehydration (and possibly residual urea for the co-ground samples) while the second mass loss step between 350 and 700°C was due to the elimination of structural water. It was noticeable that the DTG curve of the washed KU-66 intercalated with 66 m% urea showed two distinct peaks at 44 and 190°C related to dehydration which suggested two types of water in kaolinite. The sample prepared with 25 m% urea lost water in an apparently continuous mass loss between 20 and 300°C. The mass loss due to dehydration corresponded to 4.8% for the sample prepared with 66 m% urea and 4.4% for the sample prepared with 25 m% urea, giving a stoichiometry of $Al_2Si_2O_5(OH)_4(H_2O)_{0.72}$ and $Al_2Si_2O_5(OH)_4(H_2O)_{0.66}$, respectively. The stoichiometry of the water molecules thus found was in accordance with the stoichiometry reported for 0.84 nm kaolinite hydrates prepared from other kaolinite intercalates (Costanzo et al., 1984).

Table I.1. Influence of milling conditions and washing steps on the DTG dehydroxylation peak temperature (°C)

| Milling conditions | Post-milling treatment | | | |
|---|---|---|---|---|
| | as ground | after three washes with isopropanol | after seven washes with isopropanol | after removal of urea with water |
| Kaolin no grinding | 514 | - | - | - |
| Kaolin ground for 1 h | 508 | - | - | 502 |
| Kaolin ground for 1/4 h with 66 m% urea | 486 | 491 | 498 | 502 |
| Kaolin ground for 1 h with 66 m% urea | n.d.[a] | 478 | 480 | 489 |
| Kaolin ground for 1/4 h with 25 m% urea | 500 | 504 | 506 | 513 |
| Kaolin ground for 1 h with 25 m% urea | 487 | 495 | 497 | 513 |
| Kaolin ground for 2 h with 25 m% urea | 482 | 488 | 489 | 507 |

[a] n.d. : not determined due to weak and broad signal

Table I.1 showed the variations in the DTG dehydroxylation peak temperature with the milling and post-treatment conditions. With increased grinding time, the dehydroxylation temperatures shifted to lower values and it may be noted that the shift was more pronounced when kaolin was co-ground with

a large fraction of urea. Further, it appeared that when the crushed samples were subjected to washing with isopropanol or urea removal upon immersion in water, the thermal dehydroxylation temperature increased significantly again, while remaining lower than the dehydroxylation temperature of the original kaolinite. The effect of isopropanol washes on the dehydroxylation temperature was more pronounced with kaolin co-ground with low fraction of urea (25 m%). This, combined with the fact that the washes of Kaol-U intercalates with isopropanol induced a higher degree of deintercalation with urea loading of 25 m%, implies that the drop in the dehydroxylation temperature was partly linked to the interactions established by intercalated urea. Urea is almost completely decomposed when thermal dehydroxylation of kaolinite occurs. Therefore, it is in fact the residues of the decomposition of urea which, by interacting with the kaolinite, would be at the origin of the drop in the dehydroxylation temperature. On the other hand, dry grinding or co-grinding produced an increased amount of disordered and amorphous kaolinite phase (Aglietti et al., 1986a, 1986b; Gonzalez Garcia et al., 1991; Suraj et al., 1997; Sánchez-Soto et al., 2000; Frost et al., 2001b; Pardo et al., 2009; Vdović et al., 2010). The effect of the irreversible structural changes induced by grinding can be illustrated by observing the thermal behavior of the ground samples after the removal of urea by repeated washing with water. Compared to the original kaolinite, after co-grinding kaolin with 66 m% urea for 1 h and subsequent removal of urea by immersion in water, the dehydroxylation temperature showed a decrease of around 25°C. On the contrary, when kaolin was co-ground with 25 m% urea, there was a marginal decrease in the dehydroxylation temperature (~7°C after 2 h co-grinding). The decrease in dehydroxylation temperatures observed in this study appeared to be lower than that reported in a previous study about the Kaol-U complex obtained by mechanochemical intercalation (Makó et al., 2013). This confirmed that ball milling was performed under relatively mild conditions that did not result in a strong disorder of kaolinite. The remaining structural water after grinding kaolin or co-grinding kaolin with solid urea and subsequent washing of urea with water can be related to the relative mass losses in the range 400-800°C (Makó et al., 2009, 2013; Hamzaoui et al., 2015) (the amount of dehydroxylation water of the unground kaolin was considered to be 100% (Makó et al., 2009)). After 1 h of grinding, the relative mass loss of KGa-1b was 93%. After the kaolin was co-ground with 66 m% urea for 1/4 h and 1 h, the relative mass losses of dehydroxylation were 97% and 93%, respectively. After 1/4, 1 and 2 h co-grinding kaolin with 25 m% urea, the relative mass losses of dehydroxylation were 100%, 95%, and 92%, respectively. These results indicated that amorphization increased with the grinding time, with only a minor effect of the urea content on the amorphization rate. On the other hand, the above values showed that the ball milling conditions used in the present study led to minor amorphization of kaolinite (after grinding or co-grinding with urea), notably comparing with other milling conditions reported in previous studies (Makó et al., 2009, 2013). These findings are consistent with the former XRD and SEM observations. The infrared spectra of the not-

ground kaolin and kaolin ground for 1 h after water washing were nearly identical to the infrared spectrum of the original kaolin (Figure I.11,c). The infrared spectra of the Kaol-U intercalates after water washing showed a OH stretching band at 3545 $cm^{-1}$ and a water deformation band at 1652 $cm^{-1}$ which support the formation of a kaolinite hydrate. These spectral features were in good accord with those observed in the infrared spectra of the 0.84 nm hydrate prepared by washing with water an ethylene glycol intercalated kaolinite (Tunney and Detellier, 1994). Additional changes were observed in the inner -OH band at 3619 $cm^{-1}$ which was broader with the appearance of two shoulders at 3627 and 3609 $cm^{-1}$. The shoulder at 3609 $cm^{-1}$ can be interpreted as a red-shift of the 3619 $cm^{-1}$ inner OH band. The perturbance of the inner hydroxyls, as a red-shift, had been observed previously in other 0.84 nm hydrates and it supported the partial keying of water into the siloxane ditrigonal cavity (Costanzo and Giese, 1990; Tunney and Detellier, 1994).

## I.4. Conclusion

A summary of the advantages and limitations of the described mechanochemical intercalation method can be given as follows. On the one hand, when kaolin is co-ground with excess urea, a well-ordered complex is formed after a short grinding time but repeated isopropanol washing is needed to remove excess urea. On the other hand, co-grinding carried out with a lower amount of urea (close to the maximum urea content in the Kaol-U complex) promotes amorphization of kaolinite and requires long grinding times but no need for additional treatment. Complete intercalation of urea was achieved with very little amorphization of the kaolinite by grinding kaolin KGa1b with a small excess of urea (66 m%) in a ball mill for a short time (1/4 h). It was proposed that these results could be related to the specific grinding conditions used in this study: milling device, the jar and ball materials, and the use of a slight excess of urea relative to kaolinite. The Kaol-U intercalates prepared in this work will be used for the preparation of controlled-release fertilizer formulations through encapsulation with hydrogels to provide a humid- and nutrient-stable environment for plant growth.

## I.5. References

Aglietti, E.F., Porto Lopez, J.M., Pereira, E., 1986a. Mechanochemical effects in kaolinite grinding. II. Structural aspects. International Journal of Mineral Processing 16, 135–146. https://doi.org/10.1016/0301-7516(86)90080-3

Aglietti, E.F., Porto Lopez, J.M., Pereira, E., 1986b. Mechanochemical effects in kaolinite grinding. I. Textural and physicochemical aspects. International Journal of Mineral Processing 16, 125–133. https://doi.org/10.1016/0301-7516(86)90079-7

Cheng, H., Liu, Q., Xu, P., Hao, R., 2018. A comparison of molecular structure and de-intercalation kinetics of kaolinite/quaternary ammonium salt and alkylamine intercalation compounds. Journal of Solid State Chemistry 268, 36–44. https://doi.org/10.1016/j.jssc.2018.08.009

Costanzo, P.M., Giese, R.F., 1990. Ordered and Disordered Organic Intercalates of 8.4-Å, Synthetically Hydrated Kaolinite. Clays Clay Miner. 38, 160–170. https://doi.org/10.1346/CCMN.1990.0380207

Costanzo, P.M., Giese, R.F., Lipsicas, M., 1984. Static and Dynamic Structure of Water in Hydrated Kaolinites. I. The Static Structure. Clays Clay Miner. 32, 419–428. https://doi.org/10.1346/CCMN.1984.0320511

Deeds, C., Van Olphen, H., Bradley, W., 1966. Intercalation and interlayer hydration of minerals of the kaolinite group, in: Proceedings of the International Clay Conference. Jerusalem, Israel, pp. 183–199.

Elbokl, T.A., Detellier, C., 2009. Kaolinite–poly(methacrylamide) intercalated nanocomposite via in situ polymerization. Can. J. Chem. 87, 272–279. https://doi.org/10.1139/v08-142

Franco, F., Pérez-Maqueda, L.A., Pérez-Rodríguez, J.L., 2004. The effect of ultrasound on the particle size and structural disorder of a well-ordered kaolinite. Journal of Colloid and Interface Science 274, 107–117. https://doi.org/10.1016/j.jcis.2003.12.003

Frost, R.L., Horváth, E., Makó, É., Kristóf, J., 2004. Modification of low- and high-defect kaolinite surfaces: implications for kaolinite mineral processing. Journal of Colloid and Interface Science 270, 337–346. https://doi.org/10.1016/j.jcis.2003.10.034

Frost, R.L., Horváth, E., Makó, É., Kristóf, J., Rédey, Á., 2003. Slow transformation of mechanically dehydroxylated kaolinite to kaolinite—an aged mechanochemically activated formamide-intercalated kaolinite study. Thermochimica Acta 408, 103–113. https://doi.org/10.1016/S0040-6031(03)00316-2

Frost, R.L., Kristof, J., Rintoul, L., Kloprogge, J.T., 2000. Raman spectroscopy of urea and urea-intercalated kaolinites at 77 K. Spectrochimica Acta Part A: Molecular and Biomolecular Spectroscopy 56, 1681–1691. https://doi.org/10.1016/S1386-1425(00)00223-7

Frost, R.L., Makó, É., Kristóf, J., Horváth, E., Kloprogge, J.T., 2001a. Modification of Kaolinite Surfaces by Mechanochemical Treatment. Langmuir 17, 4731–4738. https://doi.org/10.1021/la001453k

Frost, R.L., Makó, É., Kristóf, J., Horváth, E., Kloprogge, J.T., 2001b. Mechanochemical Treatment of Kaolinite. Journal of Colloid and Interface Science 239, 458–466. https://doi.org/10.1006/jcis.2001.7591

Frost, R.L., Thu Ha, T., Kristof, J., 1997a. FT-Raman spectroscopy of the lattice region of kaolinite and its intercalates. Vibrational Spectroscopy 13, 175–186. https://doi.org/10.1016/S0924-2031(96)00049-5

Frost, R.L., Tran, T.H., Kristof, J., 1997b. The structure of an intercalated ordered kaolinite; a Raman microscopy study. Clay Minerals 32, 587–596.

Gardolinski, J.E., Carrera, L.C.M., Cantão, M.P., Wypych, F., 2000. Layered polymer-kaolinite nanocomposites. Journal of Materials Science 35, 3113–3119. https://doi.org/10.1023/A:1004820003253

Gardolinski, J.E.F.C., Lagaly, G., 2005a. Grafted organic derivatives of kaolinite: II. Intercalation of primary n-alkylamines and delamination. Clay Minerals 40, 547–556. https://doi.org/10.1180/0009855054040191

Gardolinski, J.E.F.C., Lagaly, G., 2005b. Grafted organic derivatives of kaolinite: I. Synthesis, chemical and rheological characterization. Clay Minerals 40, 537–546. https://doi.org/10.1180/0009855054040190

Gonzalez Garcia, F., Ruiz Abrio, M.T., Gonzalez Rodriguez, M., 1991. Effects of dry grinding on two kaolins of different degrees of crystallinity. Clay miner 26, 549–565.

Grdadolnik, J., Maréchal, Y., 2002. Urea and urea–water solutions—an infrared study. Journal of Molecular Structure 615, 177–189. https://doi.org/10.1016/S0022-2860(02)00214-4

Hamzaoui, R., Muslim, F., Guessasma, S., Bennabi, A., Guillin, J., 2015. Structural and thermal behavior of proclay kaolinite using high energy ball milling process. Powder Technology 271, 228–237. https://doi.org/10.1016/j.powtec.2014.11.018

Hinckley, D.N., 1962. Variability in "crystallinity" Values among the Kaolin Deposits of the Coastal Plain of Georgia and South Carolina. Clays Clay Miner. 11, 229–235. https://doi.org/10.1346/CCMN.1962.0110122

Horváth, E., Frost, R.L., Makó, É., Kristóf, J., Cseh, T., 2003. Thermal treatment of mechanochemically activated kaolinite. Thermochimica Acta 404, 227–234. https://doi.org/10.1016/S0040-6031(03)00184-9

Horváth, E., Kristóf, J., Frost, R.L., 2010. Vibrational Spectroscopy of Intercalated Kaolinites. Part I. Applied Spectroscopy Reviews 45, 130–147. https://doi.org/10.1080/05704920903435862

House, K.A., House, J.E., 2017. Thermodynamics of dissolution of urea in water, alcohols, and their mixtures. Journal of Molecular Liquids 242, 428–432. https://doi.org/10.1016/j.molliq.2017.07.020

Johnston, C.T., Bish, D.L., Eckert, J., Brown, L.A., 2000. Infrared and Inelastic Neutron Scattering Study of the 1.03- and 0.95-nm Kaolinite−Hydrazine Intercalation Complexes. J. Phys. Chem. B 104, 8080–8088. https://doi.org/10.1021/jp001075s

Keuleers, R., Desseyn, H.O., Rousseau, B., Van Alsenoy, C., 1999. Vibrational Analysis of Urea. J. Phys. Chem. A 103, 4621–4630. https://doi.org/10.1021/jp984180z

Kristóf, J., Frost, R., Horváth, E., Kocsis, L., Inczédy, J., 1998. Thermoanalytical Investigations on Intercalated Kaolinites. Journal of Thermal Analysis and Calorimetry 53, 467–475. https://doi.org/10.1023/a:1010189324654

Ledoux, R.L., White, J.L., 1966. Infrared studies of hydrogen bonding interaction between kaolinite surfaces and intercalated potassium acetate, hydrazine, formamide, and urea. Journal of Colloid and Interface Science 21, 127–152. https://doi.org/10.1016/0095-8522(66)90029-8

Letaief, S., Detellier, C., 2009. Clay−Polymer Nanocomposite Material from the Delamination of Kaolinite in the Presence of Sodium Polyacrylate. Langmuir 25, 10975–10979. https://doi.org/10.1021/la901196f

Letaief, S., Elbokl, T.A., Detellier, C., 2006a. Reactivity of ionic liquids with kaolinite: Melt intersalation of ethyl pyridinium chloride in an urea-kaolinite pre-intercalate. Journal of Colloid and Interface Science 302, 254–258. https://doi.org/10.1016/j.jcis.2006.06.008

Letaief, S., Martín-Luengo, M.A., Aranda, P., Ruiz-Hitzky, E., 2006b. A Colloidal Route for Delamination of Layered Solids: Novel Porous-Clay Nanocomposites. Advanced Functional Materials 16, 401–409. https://doi.org//10.1002/adfm.200500190

Liu, Q., Zhang, S., Cheng, H., Wang, D., Li, X., Hou, X., Frost, R.L., 2014. Thermal behavior of kaolinite–urea intercalation complex and molecular dynamics simulation for urea molecule orientation. J Therm Anal Calorim 117, 189–196. https://doi.org/10.1007/s10973-014-3646-1

Madejová, J., Komadel, P., 2001. Baseline studies of the clay minerals society source clays: infrared methods. Clays and Clay Minerals 49, 410–432.

Makó, É., Kovács, A., Antal, V., Kristóf, T., 2017. One-pot exfoliation of kaolinite by solvothermal cointercalation. Applied Clay Science 146, 131–139. https://doi.org/10.1016/j.clay.2017.05.042

Makó, É., Kovács, A., Ható, Z., Kristóf, T., 2015. Simulation assisted characterization of kaolinite–methanol intercalation complexes synthesized using cost-efficient homogenization method. Applied Surface Science 357, 626–634. https://doi.org/10.1016/j.apsusc.2015.09.081

Makó, É., Kovács, A., Katona, R., Kristóf, T., 2016. Characterization of kaolinite-cetyltrimethylammonium chloride intercalation complex synthesized through eco-friend kaolinite-urea pre-intercalation complex. Colloids and Surfaces A: Physicochemical and Engineering Aspects 508, 265–273. https://doi.org/10.1016/j.colsurfa.2016.08.035

Makó, É., Kovács, A., Kristóf, T., 2019. Influencing parameters of direct homogenization intercalation of kaolinite with urea, dimethyl sulfoxide, formamide, and N-methylformamide. Applied Clay Science 182, 105287. https://doi.org/10.1016/j.clay.2019.105287

Makó, É., Kristóf, J., Horváth, E., Vágvölgyi, V., 2013. Mechanochemical intercalation of low reactivity kaolinite. Applied Clay Science 83–84, 24–31. https://doi.org/10.1016/j.clay.2013.08.002

Makó, É., Kristóf, J., Horváth, E., Vágvölgyi, V., 2009. Kaolinite–urea complexes obtained by mechanochemical and aqueous suspension techniques—A comparative study. Journal of Colloid and Interface Science 330, 367–373. https://doi.org/10.1016/j.jcis.2008.10.054

Miller, J.G., Oulton, T.D., 1970. Prototropy in Kaolinite during Percussive Grinding. Clays Clay Miner. 18, 313–323. https://doi.org/10.1346/CCMN.1970.0180603

Ondruška, J., Csáki, Š., Trnovcová, V., Štubňa, I., Lukáč, F., Pokorný, J., Vozár, L., Dobroň, P., 2018. Influence of mechanical activation on DC conductivity of kaolin. Applied Clay Science 154, 36–42. https://doi.org/10.1016/j.clay.2017.12.038

Pardo, P., Bastida, J., Serrano, F.J., Ibáñez, R., Kojdecki, M.A., 2009. X-Ray Diffraction Line-Broadening Study on Two Vibrating, Dry-Milling Procedures in Kaolinites. Clays and Clay Minerals 57, 25–34. https://doi.org/10.1346/CCMN.2009.0570102

Pruett, R.J., Webb, H.L., 1993. Sampling and Analysis of KGa-1B Well-Crystallized Kaolin Source Clay. Clays Clay Miner. 41, 514–519.

Rutkai, G., Makó, É., Kristóf, T., 2009. Simulation and experimental study of intercalation of urea in kaolinite. Journal of Colloid and Interface Science 334, 65–69. https://doi.org/10.1016/j.jcis.2009.03.022

Sánchez-Soto, P.J., Haro, M. del C.J. de, Pérez-Maqueda, L.A., Varona, I., Pérez-Rodríguez, J.L., 2000. Effects of Dry Grinding on the Structural Changes of Kaolinite Powders. Journal of the American Ceramic Society 83, 1649–1657. https://doi.org/10.1111/j.1151-2916.2000.tb01444.x

Schaber, P.M., Colson, J., Higgins, S., Thielen, D., Anspach, B., Brauer, J., 2004. Thermal decomposition (pyrolysis) of urea in an open reaction vessel. Thermochimica Acta 424, 131–142. https://doi.org/10.1016/j.tca.2004.05.018

Seifi, S., Diatta-Dieme, M.T., Blanchart, P., Lecomte-Nana, G.L., Kobor, D., Petit, S., 2016. Kaolin intercalated by urea. Ceramic applications. Construction and Building Materials 113, 579–585. https://doi.org/10.1016/j.conbuildmat.2016.03.095

Štefanić, G., Musić, S., Gajović, A., 2007. A comparative study of the influence of milling media on the structural and microstructural changes in monoclinic ZrO2. Journal of the European Ceramic Society, Refereed Reports IX Conference & Exhibition of the European Ceramic Society 27, 1001–1016. https://doi.org/10.1016/j.jeurceramsoc.2006.04.136

Suraj, G., Iyer, C.S.P., Rugmini, S., Lalithambika, M., 1997. The effect of micronization on kaolinites and their sorption behaviour. Applied Clay Science 12, 111–130. https://doi.org/10.1016/S0169-1317(96)00044-0

Tsunematsu, K., Tateyama, H., 1999. Delamination of Urea-Kaolinite Complex by Using Intercalation Procedures. Journal of the American Ceramic Society 82, 1589–1591. https://doi.org/10.1111/j.1151-2916.1999.tb01963.x

Tunney, J., Detellier, C., 1994. Preparation and Characterization of an 8.4 Å Hydrate of Kaolinite. Clays Clay Miner. 42, 473–476. https://doi.org/10.1346/CCMN.1994.0420414

Valášková, M., Barabaszová, K., Hundáková, M., Ritz, M., Plevová, E., 2011. Effects of brief milling and acid treatment on two ordered and disordered kaolinite structures. Applied Clay Science 54, 70–76. https://doi.org/10.1016/j.clay.2011.07.014

Valášková, M., Rieder, M., Matějka, V., Čapková, P., Slíva, A., 2007. Exfoliation/delamination of kaolinite by low-temperature washing of kaolinite–urea intercalates. Applied Clay Science 35, 108–118. https://doi.org/10.1016/j.clay.2006.07.001

Vdović, N., Jurina, I., Škapin, S.D., Sondi, I., 2010. The surface properties of clay minerals modified by intensive dry milling — revisited. Applied Clay Science 48, 575–580. https://doi.org/10.1016/j.clay.2010.03.006

Yan, C., Chen, J., Zhang, C., Han, K., 2005. Kaolinite-urea intercalation composites. American Ceramic Society Bulletin.

Zhang, S., Liu, Q., Gao, F., Li, X., Liu, C., Li, H., Boyd, S.A., Johnston, C.T., Teppen, B.J., 2017. Mechanism Associated with Kaolinite Intercalation with Urea: Combination of Infrared Spectroscopy and Molecular Dynamics Simulation Studies. J. Phys. Chem. C 121, 402–409. https://doi.org/10.1021/acs.jpcc.6b10533

# CHAPTER II

## Effect of nitrogen fertilizer loading on the properties of polyacrylic acid hydrogels

# Chapter II. Effect of nitrogen fertilizer loading on the properties of polyacrylic acid hydrogels

## II.1. Introduction

The crucial elements in plant growth are water and fertilizers. Rapid global population growth, reduction of arable land and intensive use of fertilizers implies an optimization of these elements.

To meet the inevitable increase in demand for global food, the agricultural sector increases the quantities of fertilizers which results in undesirable environmental impacts (Azeem et al., 2014; Zhou et al., 2018). On the other hand, good management of water resources appears inevitable.

Superabsorbent hydrogels are three dimensional cross-linked polymeric structures able to incorporate and retain large amounts of water (Teodorescu et al., 2009; Zhang et al., 2014). Superabsorbent polymers are increasingly used in the agricultural sector in particular to better regulate water supplies to the plant (Kazanskii and Dubrovskii, 1992). Increasingly intensive use of fertilizers to improve agricultural yields has a negative impact on the quality of surface water, soil, causing disturbance to aquatic ecosystems. The incorporation of fertilizer into superabsorbent hydrogel to control the quantity delivered to crops is a way to dwindle the environmental pollution (Zhang et al., 2006) and to reduce fertilizer losses (Singh et al., 2011; Bortolin et al., 2016; Xiang et al., 2017).

Among the N fertilizers, urea is extensively used due to its high nitrogen content (46%) and low cost. Many researchers have studied the way to control the urea supply to reduce these losses in environment by the use of slow release fertilizers. As noted in the general introduction, matrix-based formulations formed the largest category of SRFs. The fertilizer is dispersed in a polymer matrix and diffuses through pores in the carrier phase. Superabsorbent polymers have been frequently used as polymer matrix in matrix based SRF formulations (M. Guo et al., 2005; Helaly et al., 2005; Liu et al., 2006; Zhang et al., 2006; Liu et al., 2007; Akelah, 2013; Ianchis et al., 2019; Ramli, 2019). The release of a low molecular weight solute from hydrogel matrix is classically assumed to take place by diffusion (Muhr and Blanshard, 1982). The effect of the structure of the polymer gel on this diffusion is complex and is still the subject of many studies (Anseth et al., 1996; Favre and Girard, 2001). Two main routes to load hydrogels with fertilizer are possible: the first method consists in synthesizing the 3D hydrogel network in the presence of the fertilizer while in the second method, the hydrogel is first synthesized before being loaded with the fertilizer in a second step. In this chapter, polyacrylic acid hydrogels with urea fertilizer have been prepared using the two previously described loading methods. The objective of this study was to compare the advantages and disadvantages of each of these two methods in terms of swelling capacity, recycling swelling capability, water retention and slow release properties of urea

fertilizer Biopolymers have been a very popular area of research in recent years but hydrogels based on polyacrylic acid have several advantages: they are non-toxic, the structure of the gels obtained during synthesis is easier to control and they have high swelling capacity, swelling being tunable by the partial neutralization of the acid groups of the polymer. Among all the synthesis parameters of polyacrylate hydrogels, the concentration of crosslinking agent and neutralization degree are the most effective parameters for modulating the swelling properties of hydrogels (El-Rehim and A, 2006; Pourjavadi et al., 2007; Teodorescu et al., 2009; Cândido et al., 2012). The effect of these two parameters on the properties of swelling and urea release kinetics will be studied within the framework of this work.

## II.2. Materials and methods

### II.2.1. Materials

Acrylic acid (AA, Aldrich, 99%) was distilled under vacuum to remove the polymerization initiator and stored in the freezer. Other reagents including N,N'–methylene-bis-acrylamide, MBA, urea and ammonium persulfate, APS, were purchased commercially as analytical grade products and were used as received.

### II.2.2. Methods

Preparation of urea-loaded hydrogels. Urea-loaded hydrogels were prepared by an in-situ loading method and by a post-loading method as follows.

#### *II.2.2.1. In situ loading method*

The proper amounts of urea (8 M stock solution), AA and MBA (60 mM stock solution) were stirred together to give a 1 :1 wt ratio of urea :(AA+MBA). The monomer concentration AA was held at a constant value of 2 M for all syntheses. The neutralization of AA was carried out with a 10 M sodium hydroxide solution This reaction mixture was placed into a glass tube of 6 mm inner diameter which was sealed by a rubber septum. After nitrogen bubbling for 10 min to remove dissolved oxygen, the tube was placed in a water bath at 60°C. Then, a certain amount of a 0.1M APS aqueous solution was added to give an APS concentration of 15 mM. Polymerization was carried at 60°C for 3 h. After the reaction was completed, the product was dried at 50°C to a constant weight, ground with a cryogenic freezer mill and screened. All dried hydrogel samples investigated in this study had a particle size in the range 35-50 meshes (300-500 µm). The samples were coded PAA/urea.

#### *II.2.2.2. Post-loading method*

A similar protocol to that described in the in situ loading method was followed for the synthesis of hydrogels but without the addition of urea (PAA). Dried PAA (0.1 g), previously sieved to 35-50 mesh

was placed into a tea-bag with a 170 mesh nylon screen and the bag was immersed entirely in an aqueous solution of urea for 24 hours at room temperature. Preliminary experiments showed that 24 h immersion allowed to reach equilibrium. The typical concentration of urea solution was 10 g/L but samples were also loaded in a 500 g/L urea solution. Thereafter, the swollen gel was dried in vacuum oven at 50°C to constant weight. The loading percentage was calculated by the following equation (1).

$$\text{Loading Capacity} = \frac{M_1 - M_0}{M_0} \qquad (1)$$

where $M_0$ and $M_1$ are the weights of unloaded and loaded dry gel, respectively. The samples prepared by the post loaded method were designated urea-loaded PAA.

Materials were designated CL x% where x represents the mol% of MBA relative to AA.

Figures II.1 and 2 show respectively the nitrogen line for removing $O_2$ before reaction and the hydrogels obtained after synthesis in glass tubes.

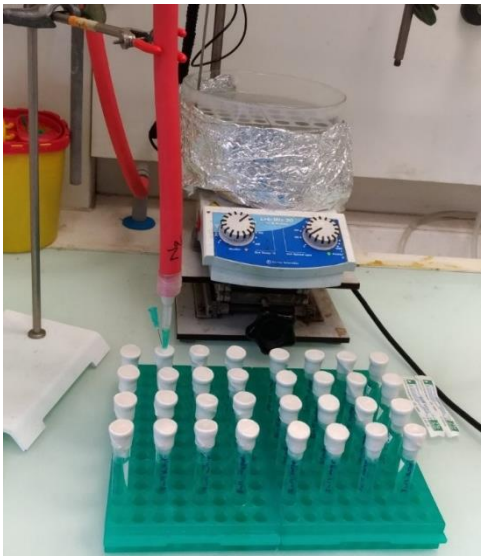

*Figure II.1. $O_2$ removal before reaction.*

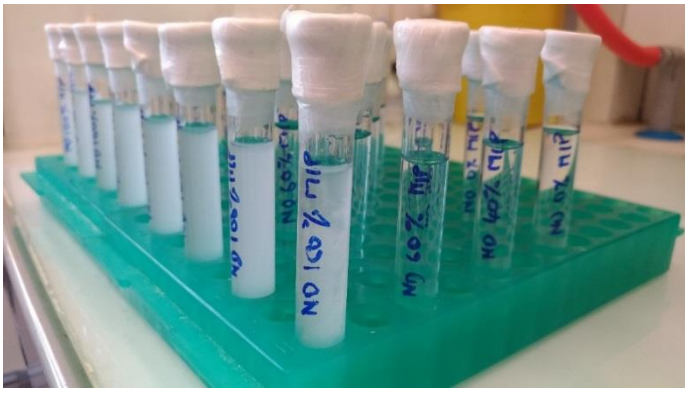

*Figure II.2. Hydrogels after synthesis in glass tube.*

### *II.2.2.3. Swelling measurements*

The gel samples were placed in a 170 mesh nylon screen tea-bag and this set was immersed entirely in 500 mL distilled water at ambient temperature (25°C). The bag was removed from the solution at

different time intervals with the excess of water removed superficially with tissue paper and the weight, Ws of the swollen gel was measured. The sample swelled for 5 h was dried in a vacuum oven at 50°C for 24h and the weight of the dried sample, WD was measured. The weight swelling ratio, Q, was determined according to

$$Q = \frac{W_S - W_D}{W_D} \qquad (2)$$

Figures II.3 and II.4 show the tea bags used for swelling tests and photos of the xerogel before and after swelling.

*Figure II.3. Tea bags during swelling tests.*

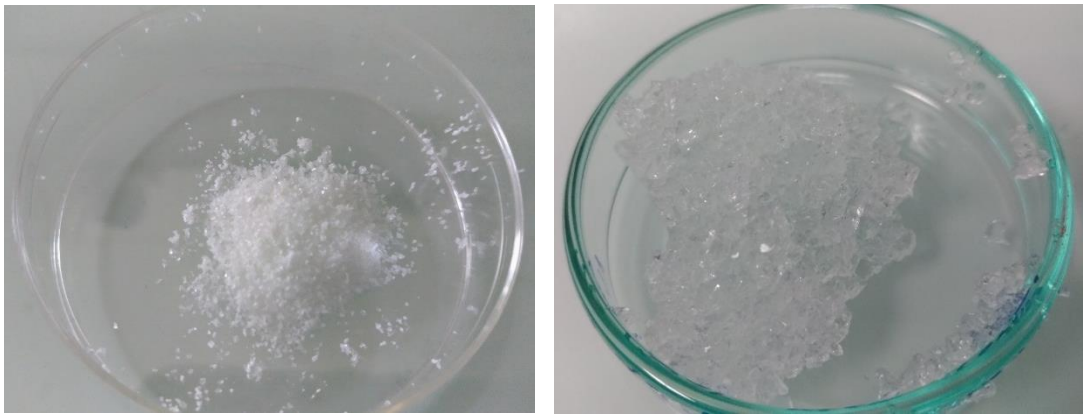

*Figure II.4. 300-500 µm diameter xerogel powder and the swollen gel.*

### *II.2.2.4. Water retention capacity*

25-30 mg of dried gel was placed in 500 mL distilled water for 24 hours. The swollen gel was centrifuged at 2000 rpm or heated at 60°C in an air oven at different times, weighed and WRC (%) was calculated according to Eq 3.

$$WR(\%) = \frac{M_t}{M_S} x100 \qquad (3)$$

where $M_S$ and $M_t$ are the weights of the gel before and after centrifugation or thermal drying, respectively.

### *II.2.2.5. Effect of drying-swelling cycles on hydrogel swelling capacity*

The dried material was immersed in water at ambient temperature for 5 h and the swelling degree was determined as previously described. The swollen material dried at 50°C for 24h was again submitted to swelling process. This drying-swelling cycle was repeated five times. The following equation (4) was used to calculate the percent extractables (E%) after each swelling-deswelling cycle:

$$E\% = 100x\frac{M_{D_1} - M_{D_2}}{M_{D_1}} \qquad (4)$$

where $M_{D_1}$ and $M_{D_2}$ are the weight of the dry gel before and after a swelling-deswelling cycle.

### *II.2.2.6. Release of urea in water*

The urea concentration in solution was determined by UV-vis spectrophotometry (Shimadzu 2501 PC), according to Watt method (Watt and Chrisp, 1954) (Watt, Chrisp, Anal Chem, 1954,26, 452). This method is based on the yellow-green color produced when p-dimethylaminobenzaldehyde is added to urea in dilute hydrochloric acid solution. The calibration curve for urea as a function of urea concentration (ppm) was prepared as follows. The standard urea solution was prepared by dissolving 0.4 g of urea in 100 mL of deionized water. The color reagent consists of 6 g of p-dimethylaminobenzaldehyde, 300 ml of ethanol absolute and 30ml of concentrated hydrochloric acid (37%). Ten ml of color reagent was added to appropriate urea aliquots and this mixture was diluted to a volume of 25 mL with deionized water.

The reaction between p-dimethylaminobenzaldehyde and urea gives the yellow-green colored complex which exhibits a maximum absorbance at 420-430 nm.

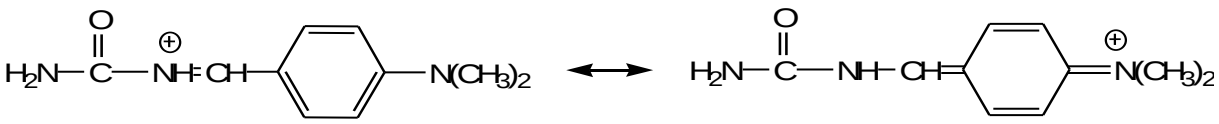

Figure II.5 shows that the plot of absorbance at 420 nm as a function urea concentration follows Beer-Lambert's law within the concentration range 16 to 480 ppm.

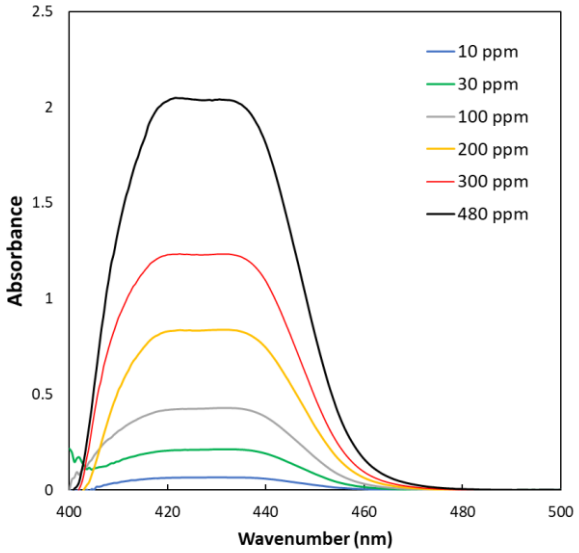


*Figure.II.5. Spectral curve for the reaction product of urea (ppm) with p-dimethylaminobenzaldehyde.*

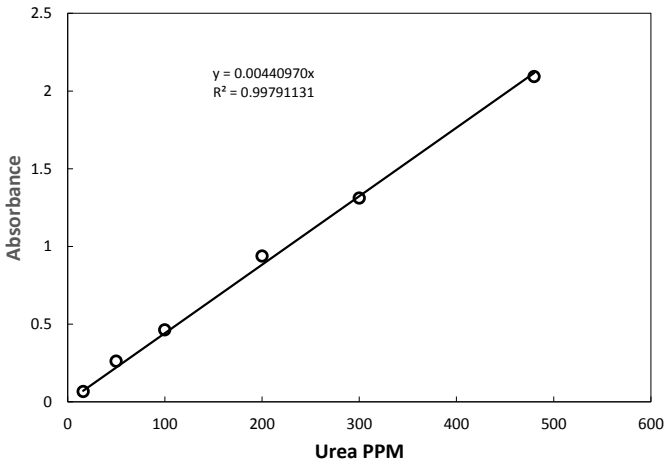


*Figure II.6. Calibration curve for urea at 420 nm.*

0.1 g of urea loaded xerogel was embedded into a tea bag and then immersed in 75mL of distilled water. At various intervals, 2 mL solution was taken out to which was added 5 ml of color reagent and deionized water to give a total volume of 10 mL.

The fertilizer release percentage (FR %) was calculated using Eq. (5)

$$\%FR = \frac{0.01x\sum_{i=1}^{n} C_i + 5xC_n x0.073}{W_0} x100 \qquad (5)$$

Where and $W_0$ is the initial fertilizer weight (mg) in the loaded hydrogel and $C_i$ is the fertilizer concentration (in ppm) of the $i^{th}$ sample collection

Each measurement was replicated three times and the average result was taken as the result. Some measurements of nitrogen content remained in the gels were also made. To do this, the tea bag with

the swollen granules was retrieved at the given time, placed on a filter paper and dried. Then the dry granules were removed from the tea bag and assessed for nitrogen content.

The weight fraction of urea in the loaded xerogel was also determined from the elemental analysis results.

Let's consider that 1g xerogel contains x g of urea and y g of water. Then the N % and C % in the loaded xerogel can be calculated using Eqs. (6) and (7)

$$\%N : (28x/60.05+\%N_{th}/100)/(1+x+y) \quad (6)$$

$$\%C : (12x/60.05+\%C_{th}/100)/(1+x+y) \quad (7)$$

Where $\%C_{th}$ and $\%N_{th}$ are the carbon percentage and nitrogen percentage of the xerogel calculated from the monomer feed composition (acrylic acid and MBA content) as follows:

For PAA-urea hydrogels prepared by the in-situ loading method

$$\%C_{th}\ (mol\%_{(MBA)}) = 100*((420+7*\%mol_{(MBA)})*M_C)/((420+7*\%mol_{(MBA)})*M_C)+((240+2*\%mol_{(MBA)})*M_N)+((320+2*\%mol_{(MBA)})*M_O)+((880+10*\%mol_{(MBA)})*M_H)$$

$$\%N_{th}\ (mol\%_{(MBA)}) = 100*((240+2*\%mol_{(MBA)})*M_N)/((420+7*\%mol_{(MBA)})*M_C)+((240+2*\%mol_{(MBA)})*M_N)+((320+2*\%mol_{(MBA)})*M_O)+((880+10*\%mol_{(MBA)})*M_H)$$

For PAA-urea hydrogels prepared by the post-loading method

$$\%C_{th}\ (mol\%_{(MBA)}) = 100*((300+7*\%mol_{(MBA)}+\%mol_{urea\_loaded})*M_C)/((300+7*\%mol_{(MBA)}+\%mol_{urea\_loaded})*M_C)+((2*\%mol_{(MBA)}+2*\%mol_{urea\_loaded})*M_N)+((200+2*\%mol_{(MBA)}+\%mol_{urea\_loaded})*M_O)+((400+10*\%mol_{(MBA)}+4*\%mol_{urea\_loaded})*M_H)$$

$$\%N_{th}\ (mol\%_{(MBA)}) = 100*((2*\%mol_{(MBA)}+2*\%mol_{urea\_loaded}))/((300+7*\%mol_{(MBA)}+\%mol_{urea\_loaded})*M_C)+((2*\%mol_{(MBA)}+2*\%mol_{urea\_loaded})*M_N)+((200+2*\%mol_{(MBA)}+\%mol_{urea\_loaded})*M_O)+((400+10*\%mol_{(MBA)}+4*\%mol_{urea\_loaded})*M_H)$$

With $M_C$, $M_N$, $M_O$ and $M_H$ the molecular weight of carbon, nitrogen, oxygen and hydrogen, respectively (g/mol)

The relative amount of urea x can then be determined from Eqs (6) and (7) using Eq.(8) :

$$x = (0.6005*(\%C_{th}-\%N_{th}(\%C/\%N))/(28*(\%C/\%N)-12) \quad (8)$$

with the carbon and nitrogen percentages in the loaded xerogel %C and %N given by elemental analysis measurements.

## II.2.3. Characterization

The infrared spectra of the dried samples were recorded on a Thermo Nicolet Nexus instrument at a resolution of 4 $cm^{-1}$. Contents of nitrogen and carbon element in the dried gels were determined by an elemental analysis instrument (Thermo Scientific, Flash 2000). The network structure in molecular level was studied by $^{13}C$ and $^{1}H$ HR-MAS and $^{13}C$ cross-polarization/magic-angle spinning CP-MAS. The samples for $^{13}C$ and $^{1}H$ HR-MAS analysis were prepared by mixing 20 mg of dried gel with 100 µL of $D_2O$. The samples analyzed by SEM were prepared by soaking the swollen gels into liquid nitrogen and then placing these samples into the chamber of the freeze-dryer. Lyophilization was then carried out at a temperature of -110°C and under vacuum for 96 hours. SEM investigations were performed on freeze-dried hydrogels coated with a thin layer of gold. A Supra 40VP electron microscope, operating at an accelerating voltage of 5 kV was used for the observations. Tensile mechanical measurements were performed at room temperature on as prepared hydrogels of the same size (6.0 mm $\phi$ x 160 mm length) and the same water/polymer ratio (SD=6) using an Instron 5982 tensile testing machine fitted with a 1 kN load cell using a crosshead speed of 100 $mm.min^{-1}$. The elastic modulus was determined by the slope of the stress–strain curve over the strain range 0–10%. The samples to be tested have been coated with a thin layer of polymethyl siloxane fluid (50 cst, Dow Corning Corp) to keep the water content unchanged.

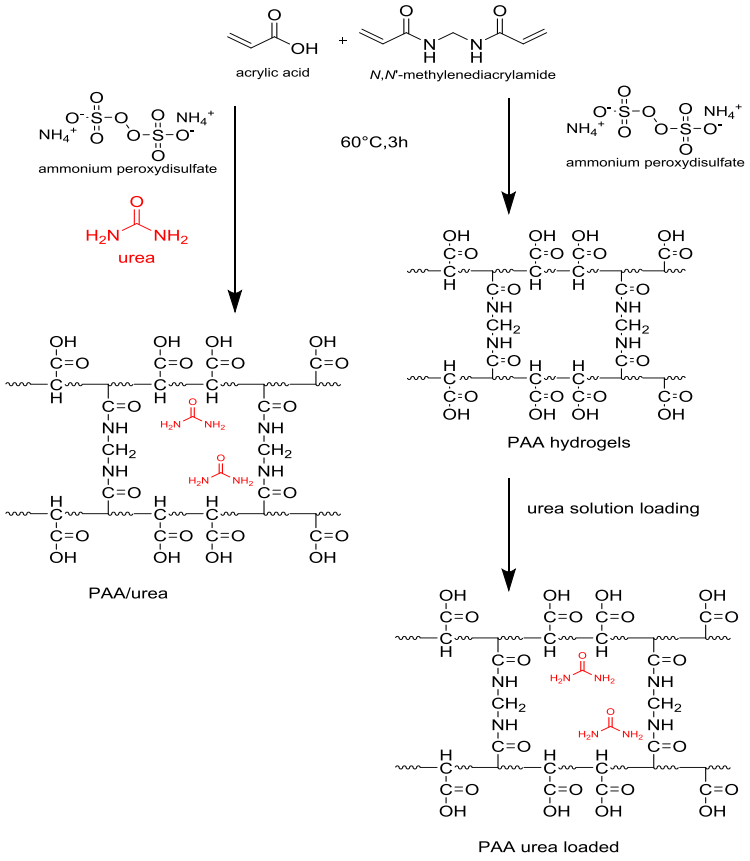


*Scheme II.1. The two routes for the preparation of PAA urea hydrogels.*

## II.3. Results and discussion

The polymer materials prepared in this work are polyacrylic acid hydrogels obtained by radical polymerization of acrylic acid using ammonium persulfate as initiator and methylene-bis-acrylamide, MBA as crosslinker. Scheme II.1 shows the two routes used to load urea into hydrogels, (i) prepare the gel in presence of urea or (ii) synthesize the gel and then load urea into the gel via equilibrium partitioning. Gelation of the polymerization medium rapidly occurred (< 4 min) in all cases.

To the best of our knowledge, a systematic comparison of the effect of the mode of urea loading in hydrogels on the macroscopic material properties such as water absorption and urea release properties of hydrogels has never been carried out.

We will successively study the swelling kinetics and swelling capacity, the reswelling cycling capacity, the water retention properties and the release kinetics of urea fertilizer.

### II.3.1. Swelling kinetics

We first investigated the effect of crosslinker content (CL) on the kinetics of swelling. Time-dependent swelling behaviors of the PAA hydrogels in deionized water are plotted in Figure II.7. For each swelling curve, swelling of the hydrogels increased with time until a stable value was reached after less than 5 hours. This constant weight is related to the equilibrium swelling value (Isık and Kıs, 2004).

Several kinetic models could be used to investigate the controlling mechanism of the hydrogel swelling process. The portion of the water absorption curve with a fractional uptake less than 0.60 was analysed using the following empirical equation (Ritger and Peppas, 1987).

$$F = K\,t^{n} \qquad (9)$$

Where F is the fractional water uptake at time t (=$Q/Q_{eq}$), k is a characteristic constant of the polymer and n is the diffusional exponent, which is indicative of the transport mechanism. LnF vs lnt graphs were made for PAA and urea loaded PAA gels and the diffusional coefficient n was obtained from the slope of the lines (Figure II.8). The model was not used for PAA/urea because water absorption was too fast resulting in a lack of kinetic data.

Ritger and Peppas (1987) showed that the transition from Fickian to non-Fickian diffusion occurs at a value of n that depends on the geometry of the absorbing material. The limiting value of n for Fickian and non-Fickian transport is 0.50 for thin film, 0.45 for cylindrical sample and 0.43 for spherical samples. The polydispersity of the absorbing material also affects the diffusion time, giving lower limiting values of n in comparison with a monodisperse system (Ritger and Peppas, 1987). The gel particles used for absorption are polydisperse granular samples with a more or less spherical shape (Figure II.9) and a polydisperse size distribution (dried particles between 300 and 500 µm). It is thus reasonable to assume that Fickian diffusion will be characterized by n values lower than 0.43. The

values of n determined for PAA swollen in water or in water-urea solution correspond to a Fickian diffusion except for the samples prepared with the lower CL content which gives values of n>0.43 corresponding to anomalous diffusion. For low CL content, the diffusion process thus occurs simultaneously by diffusion and relaxation of the hydrogel chains.

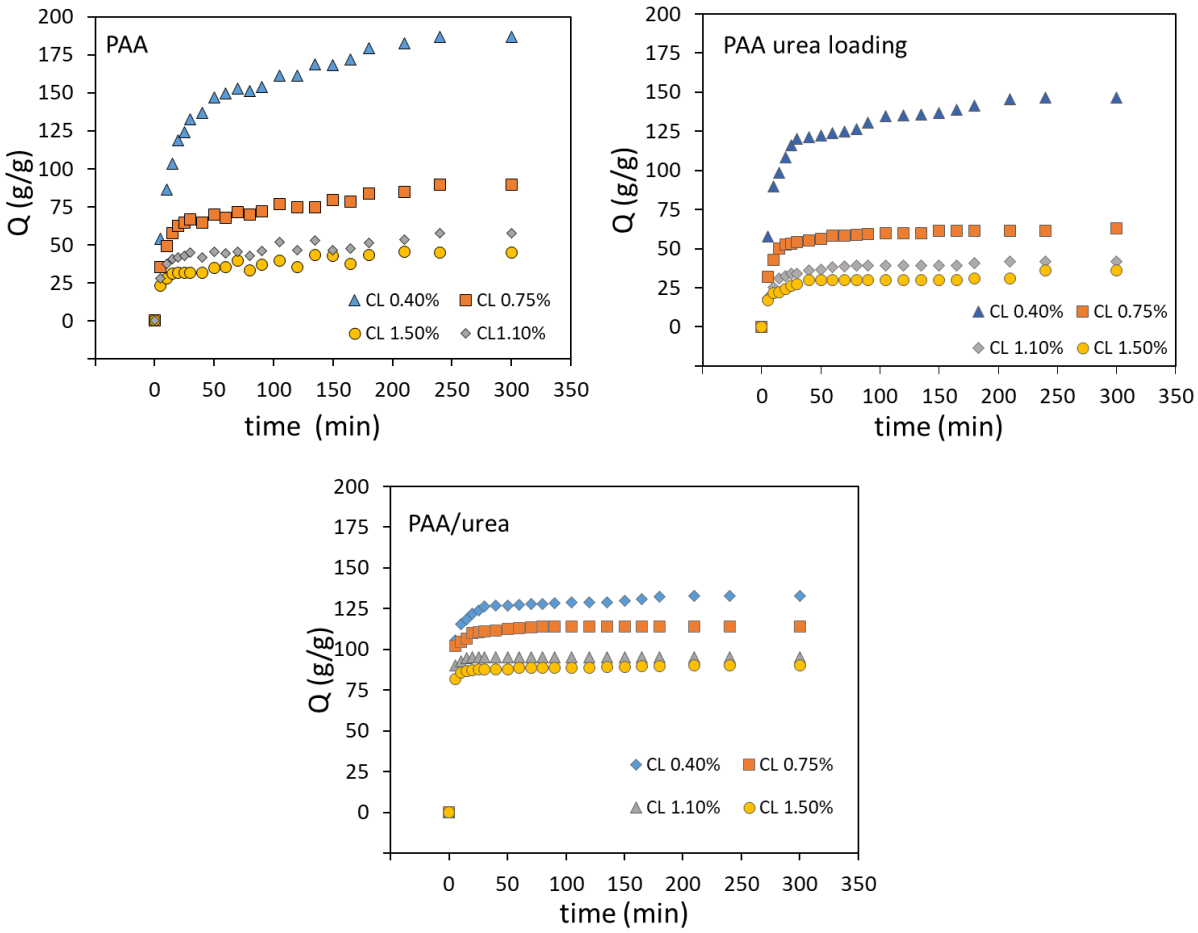


*Figure.II.7. Time-depending swelling behaviors of the PAA hydrogels.*

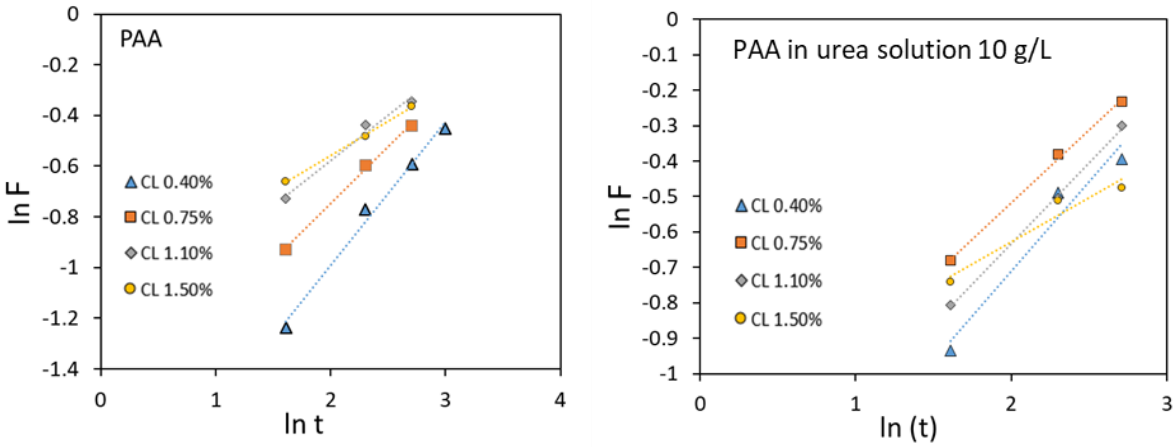


*Figure II.8. LnF vs lnt graphs for PAA gels immersed in water or in urea 10 g/L urea solution ($r^2$ > 0.98 in all cases).*

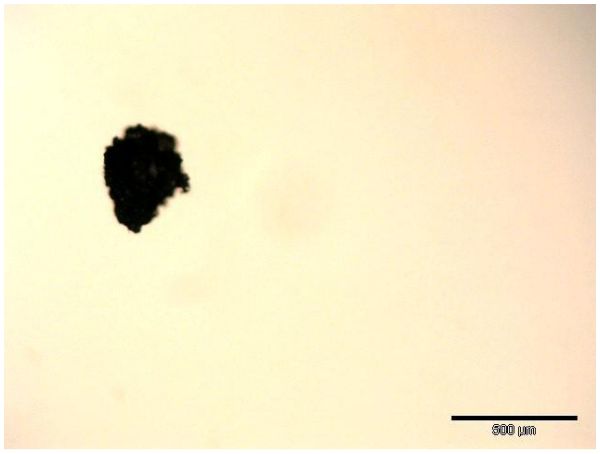


*Figure.II.9. A typical dried particle used for absorption.*

For extensive swelling of polymers, (Schott, 1992) proposed the following expression

$$\frac{t}{Q} = A + Bt \qquad (10)$$

where Q is the swelling ratio at time t, $A = 1/K_s\, Q_{eq}^2$, the reciprocal of the initial swelling rate $(dQ/dt)_0$ and $B=1/Q_{eq}$, the inverse of the equilibrium swelling ratio. Schott demonstrated that Eq.(2) implies a second-order swelling kinetics in the form of

$$\frac{dQ}{dt} = K_S(Q_{eq} - Q)^2 \qquad (11)$$

Where Ks is the rate constant.

The second-order kinetics model has been used for particles shapes with a range of diameters (Cândido et al., 2012) as those used in our work. Figure II.9 shows the linear regression by means of Eq.(10) for the swelling data. A good correlation with the Schott model is observed for all the hydrogels.

The results in Figure II.10 and Tables II. 1, 2, 3 show that the time taken to reach the steady state and the swelling rate constant increase when the CL content decreases. These observations are in agreement with those reported by (Omidian et al., 1998). These results can be interpreted by considering that crosslinking lowers the resistance to permeation presumably by preventing the chains from packing as closely in the drying step. Over the range of crosslinking investigated, permeability increased with crosslinking probably by restricting the collapse of the polymer network during the drying process. The swelling rate constant Ks rose when the crosslinker content increases. In the second-order kinetic model, Ks depends on the initial rate of swelling and the equilibrium swelling ratio. The initial swelling rate is related to the relaxation rate of the chain segments in the network of the dry gel. The relaxation rate is affected by the following factors: the rigidity/flexibility, the hydrophobicity/hydrophilicity and the degree of crosslinking and the size of dry gel powder (Ofner and

Schott, 1986) . The initial swelling rate of PAA hydrogels loaded in water and in urea solution decreased when crosslinker content increases. Thus, the rose in Ks is related to the higher ability to absorb large amounts of water of the gels prepared with low MBA content. The decrease in the initial rate of swelling with the increase in the amount of MBA because of the increase in the rigidity of the network with the increase in the degree of crosslinking. The rate of swelling of PAA gels is faster in an urea solution than in water. The presence of urea in water resulted in an increase in swelling over that in pure water in interpenetrated hydrogels based on poly(vinyl alcohol) and poly(2-hydroxyethylmemthacrylate) (Ramaraj and Radhakrishnan, 1994). This was explained by the ability of urea to break hydrogen bonding of the bound water and counteract the polymer-polymer interaction. Here, PAA gels showed larger swelling ratios in water than in urea solution. Hydrogels prepared by Ramaraj absorbed much less water (Qeq < 5) than PAA gels prepared in this work. The sorbed water is mainly free water and the bound water contributes little to the sorbed water at equilibrium. Therefore, it is assumed that the decrease water swelling in urea solution is caused by an increase in osmotic pressure of the external medium. Our observations agree with the decrease in swelling in urea solution for polyacrylamide/polyacrylate and polyacrylamide/polymethacrylate hydrogels with high sorption capacities reported by others (Abd El-Rehim et al., 2006; Karadağ et al., 2010). On the other hand, it is seen that that the gels containing urea, PAA/urea, swells faster in water compared to their counterpart prepared without urea. This behavior can be attributed to an initially large chemical potential or osmotic driving force for swelling due to the presence of solute (urea) within the gel. The initial swelling rate is maximum for an MBA level of 0.75 mol% and, consequently, is not controlled by the amount of crosslinking agent. The fact that PAA/urea hydrogels rapidly absorbs water is a positive point for the targeted applications in the agricultural sector.

Table II.1 Swelling kinetics parameters for the second-order kinetics model as well as the value of n exponent of the empirical model Eq (9) of PAA gels in deionized water.

| MBA (%mol) | $Q_{eq}$(exp) | $Q_{eq}$(calc) | $K_s$($min^{-1}$) | $(dQ/dt)_0$ ($min^{-1}$) | $R^2$ | n |
|---|---|---|---|---|---|---|
| 0.40 | 187 | 196 | $2.98 \times 10^{-4}$ | 11.4 | 0.9971 | 0.5665 |
| 0.75 | 89 | 91 | $7.08 \times 10^{-4}$ | 5.9 | 0.9919 | 0.4472 |
| 1.10 | 58 | 57 | $1.27 \times 10^{-3}$ | 4.1 | 0.9840 | 0.4199 |
| 1.50 | 45 | 46 | $1.44 \times 10^{-3}$ | 3.0 | 0.9856 | 0.2598 |

Table II.2 Swelling kinetics parameters for the second-order kinetics model as well as the value of n exponent of PAA gels in 10 g/L urea solution.

| MBA (%mol) | $Q_{eq}$(exp) | $Q_{eq}$(calc) | $K_s$($min^{-1}$) | $(dQ/dt)_0$ ($min^{-1}$) | $R^2$ | n |
|---|---|---|---|---|---|---|
| 0.40 | 146 | 149 | $6.54 \times 10^{-4}$ | 14.5 | 0.9986 | 0.6401 |
| 0.75 | 63 | 63 | $2.96 \times 10^{-3}$ | 11.7 | 0.9998 | 0.4310 |
| 1.10 | 42 | 43 | $3.09 \times 10^{-3}$ | 5.7 | 0.9999 | 0.4353 |
| 1.50 | 36 | 35 | $2.41 \times 10^{-3}$ | 3.0 | 0.9857 | 0.3309 |

Table II.3 Swelling kinetics parameters for the second-order kinetics model of PAA/urea gels in deionized water.

| samples | $Q_{eq}$(exp) | $Q_{eq}$(calc) | $K_s$($min^{-1}$) | $(dQ/dt)_0$ ($min^{-1}$) | $R^2$ |
|---|---|---|---|---|---|
| CL0.40% | 133 | 133 | $2.94 \times 10^{-3}$ | 52 | 0.9998 |
| CL0.75% | 114 | 115 | $1.05 \times 10^{-2}$ | 138 | 1 |
| CL1.50% | 90 | 90 | $1.02 \times 10^{-2}$ | 82 | 1 |

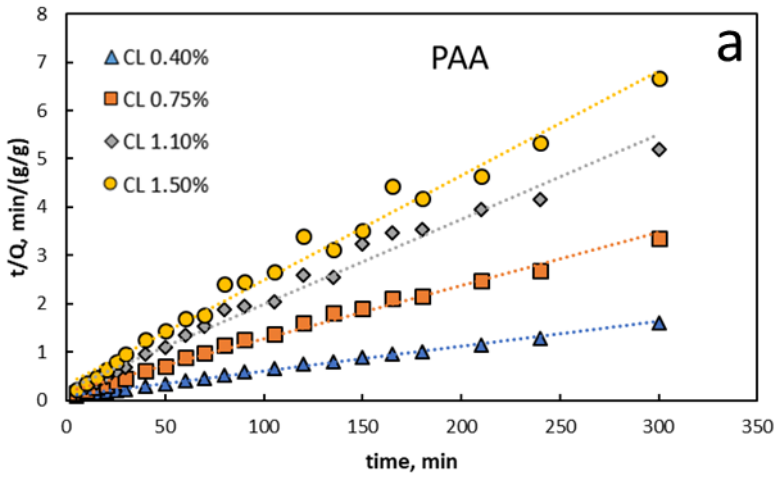


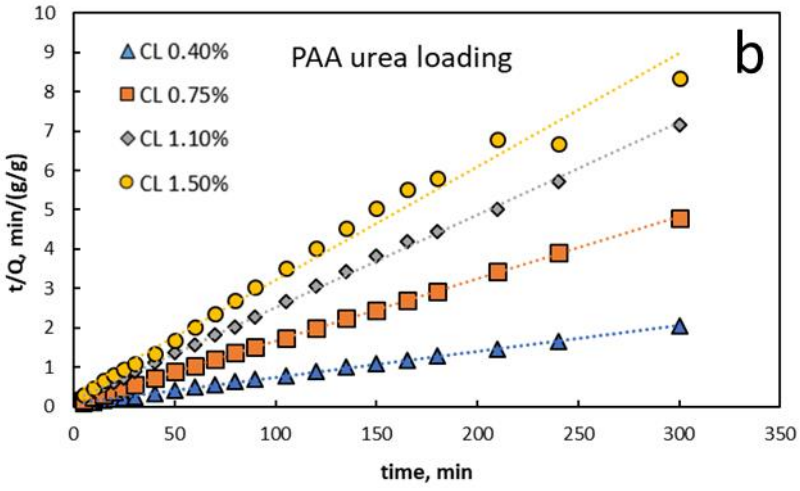

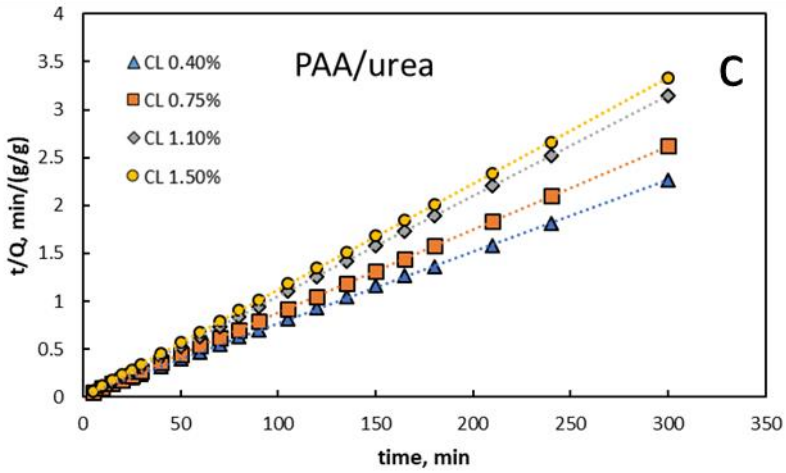


*Figure II.10. The plot of t/Q versus time for (a) PAA in water, (b) PAA in urea solution (10 g/L) and (c) PAA/urea.*

## II.3.2. Swelling and reswelling cycling capacity

Figure II.11 and II.12 shows the water absorbency ($Q_{eq}$) obtained after successive swelling – deswelling cycles. Five cycles were performed. The effects of MBA content and neutralization degree of AA have been studied.

When the crosslinker amount increased from 0.40 mol% to 1.50 mol%, the swelling ratio decreases. Indeed, higher crosslinker content implies more crosslink nodes, which, in turn densifies the network and decreases the free volume in the hydrogel (Li et al., 2004; Jin et al., 2011a). It must be noted that the water absorbency of PAA/urea hydrogels is much less dependent on the amount of crosslinker. Overall, the water absorbency of PAA and PAA/ urea hydrogels is close with low or moderate amount of MBA, while the PAA/urea hydrogels obtained with a high amount of MBA swell more than their counterpart prepared without urea. It thus seems that the presence of urea in the polymerization medium can result in a more swellable structure. The neutralization degree of acrylic acid is specified as the molar percentage of acidic groups in acrylic acid neutralized by sodium hydroxide. The effect of the neutralization of acidic groups on the water absorption capacities was studied while keeping the other synthesis parameters fixed. Figure shows that the water absorbency of PAA hydrogels increases with the neutralization degree of AA. This is due to the electrostatic repulsion of negative charges which makes possible to widen the network and therefore to incorporate more water. As we have already observed with the effect of MBA content, the water absorbency of PAA/urea hydrogels is much less dependent on the degree of neutralization of AA.

The swelling of PAA hydrogels was found to increase during the five successive cycles but much more during the three first cycles. Urea is known to break hydrogen bonds so it is believed that urea can break the H bonds between COOH groups of PAA chains. The degree of swelling is thus much more

stable during successive swelling-deswelling cycles with PAA/urea as COOH bonds were disrupted by urea. On the other hand, it is seen that the greatest increase in swelling is observed for the sample prepared at the lowest MBA content. At a low level of crosslinking, when the synthesized gel is thermally dried, the network is loose enough to allow chain reorganization accompanied by the formation of interchain bonds between COOH groups. This is not the case with higher MBA contents because in this case, some of these COOH groups would remain "free" during drying due to a lack of molecular mobility and water can therefore have easier access to these groups when the xerogel is put back into the water.

With PAA hydrogels, it takes several successive swelling-deswelling cycles to break the intermolecular bonds between COOH groups. This hypothesis is in agreement with the results of the neutralized PAA hydrogels for which the maximum degree of swelling is reached from the 1st cycle even in the absence of urea during the polymerization. Intermolecular COOH bonds are less operative in these hydrogels due to the partial neutralization of COOH groups. The observed decrease in the degree of swelling during cycling of the PAA neutralized gels is undoubtedly linked to a partial reprotonation of the carboxylates by exchanges between $Na^+$ and $H^+$ (Wu et al, 2001). Even when the urea is completely eliminated, which is nearly the case soon after the first cycle (see next section), there is a large difference in the degree of swelling depending on whether the hydrogel was prepared without or with urea when the PAA is partially neutralized. PAA-Na/urea hydrogels swelled less than PAA-Na hydrogels.

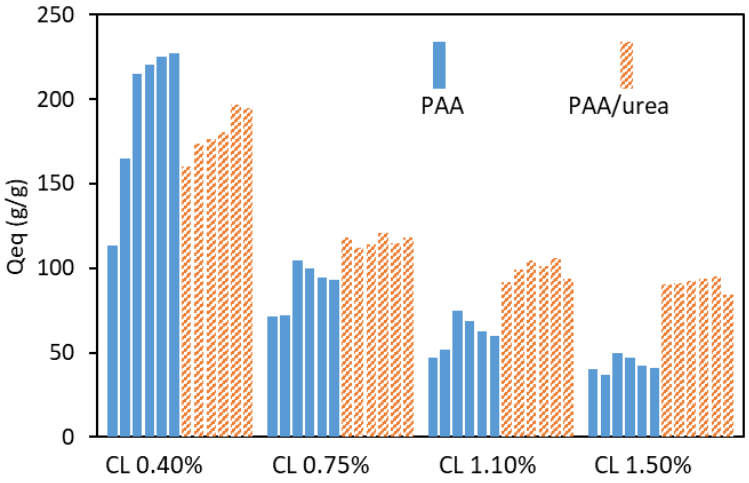


*Figure II.11. Variation of water absorbency ($Q_{eq}$) of PAA and PAA/urea hydrogels prepared with different MBA content CL (mol% vs AA) after 5 successive swelling-deswelling cycles (swelling for 5h at 22°C).*

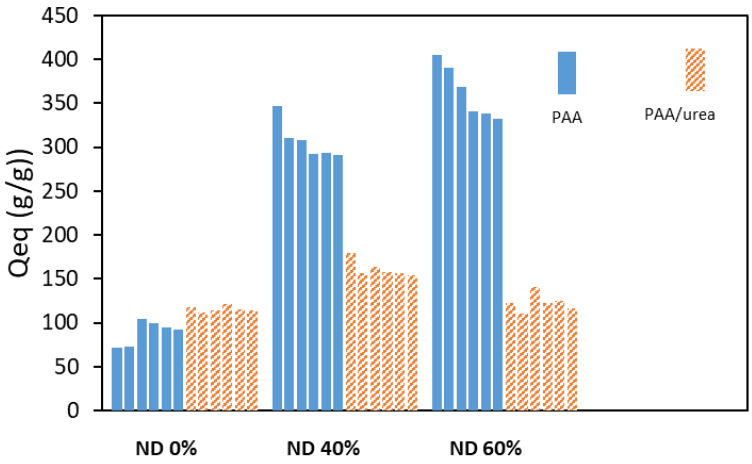


*Figure II.12. Variation of water absorbency ($Q_{eq}$) of PAA and PAA/urea hydrogels prepared with different neutralization degree ND of AA after 5 successive swelling-deswelling cycles (swelling for 5h at 22°C; CL content=0.75 mol%).*

## II.3.3. Loading and partition of urea in PAA gels

The loading of urea in PAA gels has been realized by swelling the gels in 10 g $L^{-1}$ urea solution. Figure II.13 shows that urea loading percentage is strongly affected by the crosslinker content, decreasing with increasing content of MBA. The change in urea loading with MBA content follows the same trend than that of the swelling ratio which suggests that urea is mainly distributed in water channels.

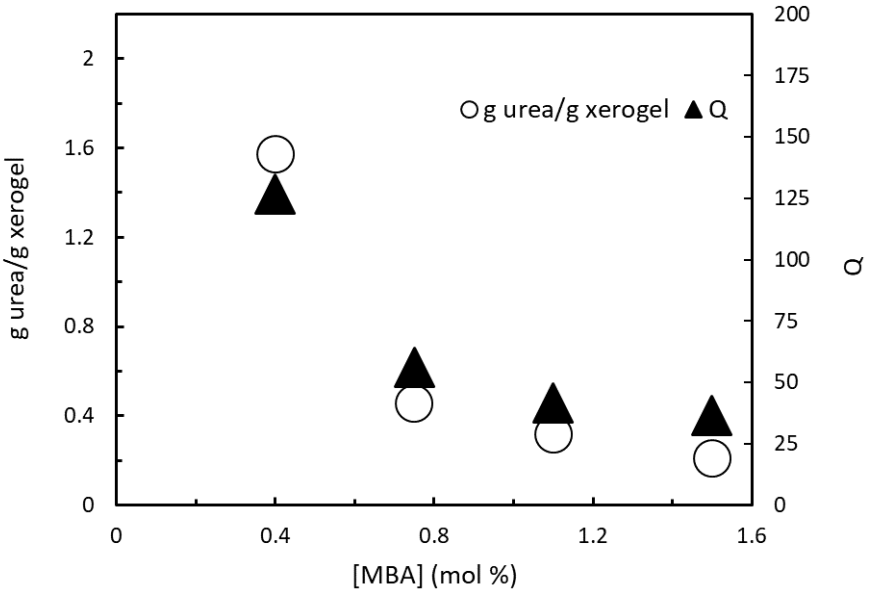


*Figure II.13. The relative urea vs polymer amount and equilibrium water content of the PAA hydrogels loaded for 24 h in 10 g/l urea solution as a function of MBA content. The data corresponds to the mean value of duplicates and error bars are smaller than the symbol size.*

The partition coefficient of urea in PAA gels is defined as,

$$K_D = \frac{\frac{C_{gw}.V_w}{(V_{dry}+V_w)}}{C_{sol}} \qquad (12)$$

Where $C_{sol}$ = concentration of external solution after sorption, $C_{gw}$ = concentration of the solute in water channels of the swollen gel, $V_{dry}$= volume of the polymer, $V_w$= volume of water channels in the swollen gel

The water volume fraction of the swollen gel is defined as,

$$\varphi_{w,s} = \frac{V_w}{V_{dry}+V_w} = \frac{Q}{Q+\frac{\rho_w}{\rho_p}} \qquad (13)$$

with $\rho_p$ and $\rho_w$ , the densities of polymer and water (1.2 g/cm$^3$ for PAA at 298K (Van Krevelen, 1990)).

it follows that the partition coefficient is related to the swelling degree, Q, according to the following relation:

$$K_D = \frac{C_{gw}}{C_{sol}} \frac{Q}{(Q+\frac{\rho_w}{\rho_p})} \qquad (14)$$

Thus, $K_D$ is expected to increase with Q.

The partition coefficient ($K_D$) of urea was determined from the elemental composition using the C/N ratio of the loaded gels. Water absorption is difficult to avoid in particular for gels obtained at low levels of MBA, particularly hygroscopic. TGA analysis of urea loaded gels showed that urea loaded gels rapidly absorbed 4 to 6% water before being transferred to the thermogravimetric analyzer. The method using the C/N ratio has the advantage of being free from the possible absorption of water by the gel preceding the elemental analysis. This is not the case of the method using only the N content. Figure II.14 and 15 show that the elemental analysis method give a satisfactory agreement with the expected values from the feed composition.

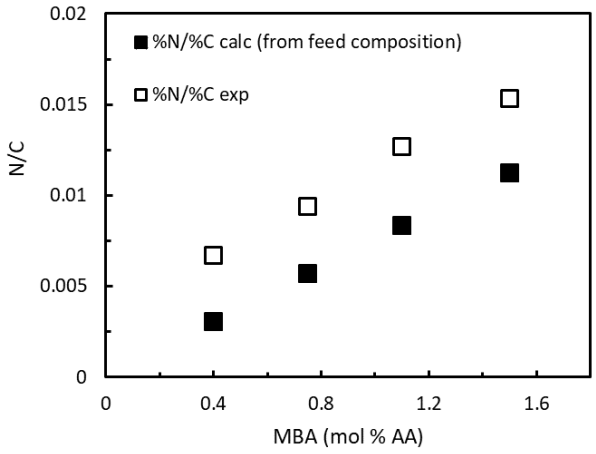


*Figure II.14. Experimental N/C ratio as a function of MBA content and comparison with the values calculated form the feed composition.*

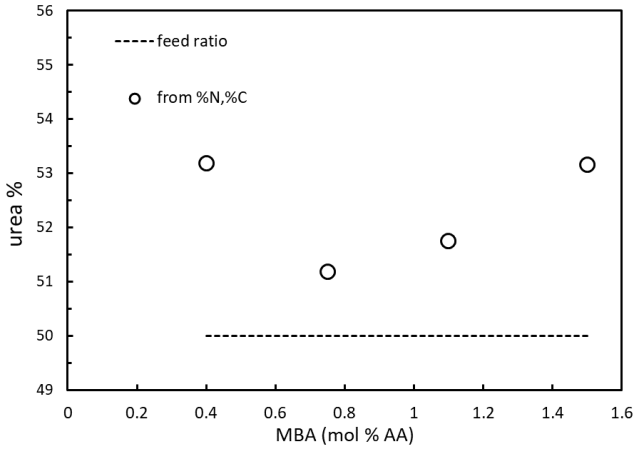


*Figure II.15. Urea (wt%) of the PAA/urea gels as a function of MBA content.*

The change in partition coefficient with the equilibrium swelling ratio is shown in Figure II.16.

The partition coefficient $K_D$ did not significantly change with the equilibrium swelling ratio. The mean value of $K_D$ was 0.69±0.06. It was reported that the partition coefficient of urea for 2-hydroxyethyl methacrylate (HEMA) hydrogel membranes crosslinked with various amounts of hexamethylene diisocyanate, increased linearly with $\varphi_{w,s}$ (Yoon and Jhon, 1982). Therefore, urea partitioned only into the water-containing region. It is important to note that the poly(HEMA) membranes studied by Yoon et al. contained significantly lower water contents (Q between 0.3 and 0.7) than the polyacrylic acid hydrogels studied in this work (Q values greater than 20). Eq.14 shows that the partition coefficient becomes almost constant when the value of Q becomes significantly greater than 1, which corresponds to the hydrogels studied in this work.

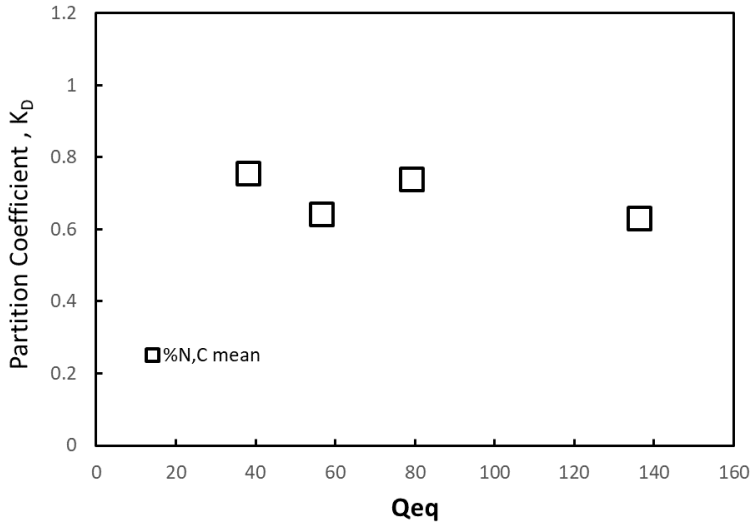


*Figure II.16. The partition coefficient of urea as a function of equilibrium water content, $Q_{eq}$, of the PAA hydrogel samples. The data corresponds to the mean value of duplicates and error bars are smaller than the symbol size.*

## II.3.4. Water retention ability

The water retention ability of hydrogels is an important parameter because it helps to mitigate the adverse effects of drought periods on the growth of the plant, prolongs irrigation cycles and reduces irrigation frequencies. The water retention properties were studied by subjecting the saturated hydrogels to a centrifugal force or placing them in a normally ventilated oven at a temperature of 60 °C. The results of water retention test are shown in Figure II.17 and 18. WR%, as a function of the centrifugation time at 2000 rpm is shown in Figure II.17. It is noteworthy that the PAA/urea gels do not contain urea because urea was released completely during the swelling phase preceding the water retention test. In all cases, the initial water loss is rapid followed by a slower water loss phase. The highest loss rate at the first stage is related to the water weakly bound to the gel, principally localized at the gel surface. After this first phase, the water must gradually come out of a gel having an increasing concentration of polymer and increasing diffusion path with an increasingly contribution of water bound in interaction with the carboxylic groups of the polymer. The initial phase of water loss occurs at the same rate for PAA and PAA/urea hydrogels but the loss of water following this first phase occurs at a slower rate with PAA/urea gels compared to PAA gels. The loose network of the gels prepared with a low MBA content (0.40 mol%) cannot retain efficiently water under the effect of a pressure or centrifugal force. Increasing the crosslinking density by increasing MBA content allows to obtain a more rigid polymer which increases its ability to retain water under the effect of pressure. Tensile tests (Figure II.19) realized on the as prepared gels gave Young's modulus increasing from 22 kPa to 84 kPa for PAA gels and from 24 kPa to 104 kPa for PAA/urea gels when MBA content increases from 0.4 mol% to 1.5 mol %. Urea loaded PAA gels resulted in the same WR behavior under centrifugal force than their unloaded counterpart which confirms that the WR capacity under centrifugal force is controlled by the strength of the polymer network. This also seems to agree the higher modulus of PAA/urea gel prepared with 1.5 mol % MBA relative to PAA gel. However, it is important to remain cautious when comparing the values of Young's modulus of the two types of hydrogel because of the presence of urea in PAA/urea gels which can impact the mechanical properties of the PAA/urea gels. The effect of the degree of crosslinking on the water content under thermal stress is opposite to that observed under centrifugal force. The desorption rate increases when the crosslinker content increases. It is believed that looser networks can immediately reorganize during thermal drying resulting in more collapsed chains which hinders the release of water molecules. Urea loaded PAA gels retain more water than PAA gels because under thermal stress, desorption is not controlled by the crosslinking density as it was the case under mechanical stress. This result can be attributed to the osmotic driven force for desorption due to the presence of urea within the gel. The PAA/urea gels obtained at low MBA

contents (0.4 and 0.75 mol%) retained less water when thermally dried compared to PAA gels. This effect could be related to a lower ability of polymer chains to rearrange during thermal drying of PAA/urea gels or to interact with water molecules.

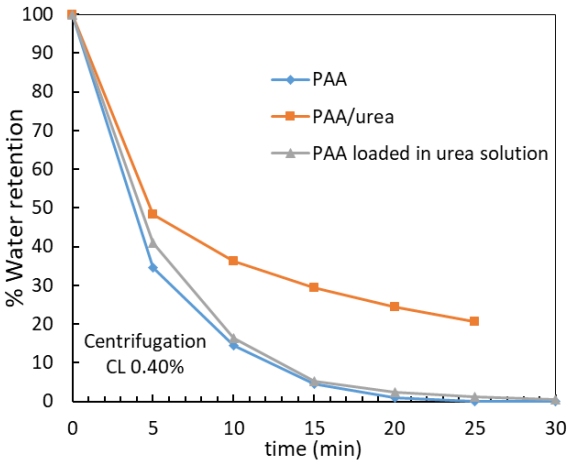


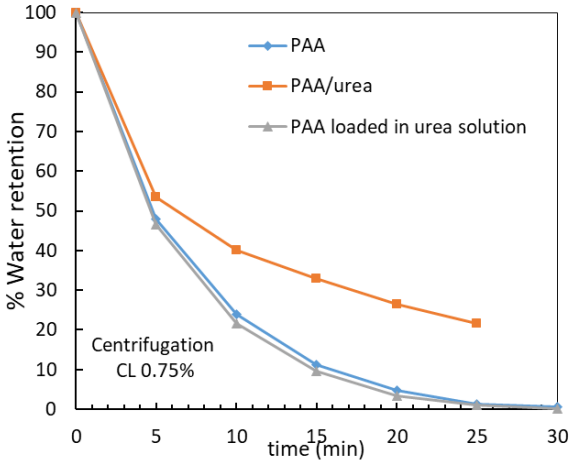


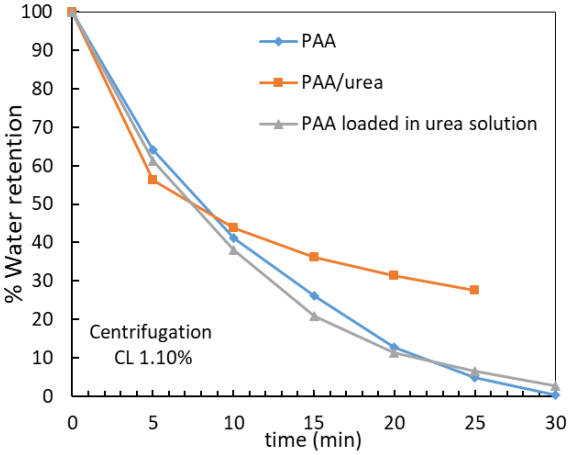


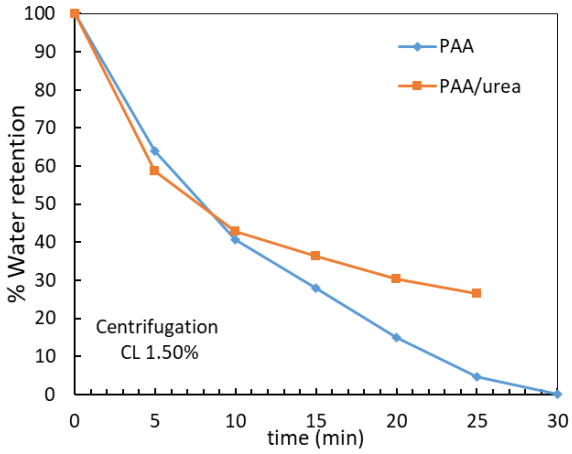


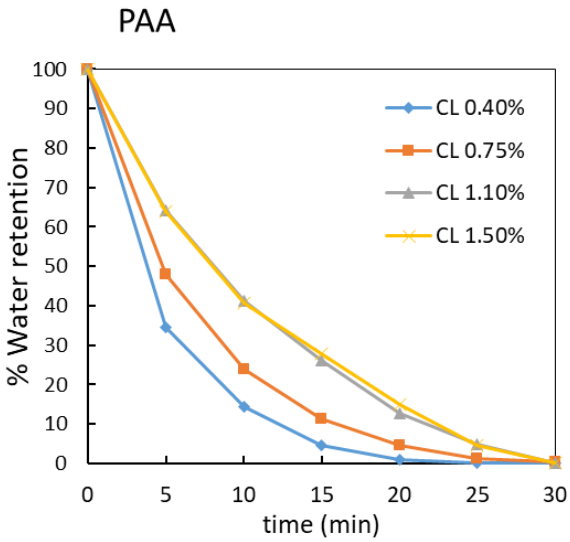


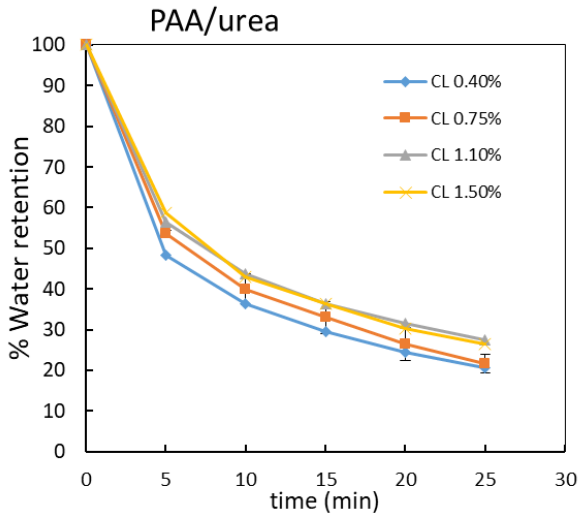

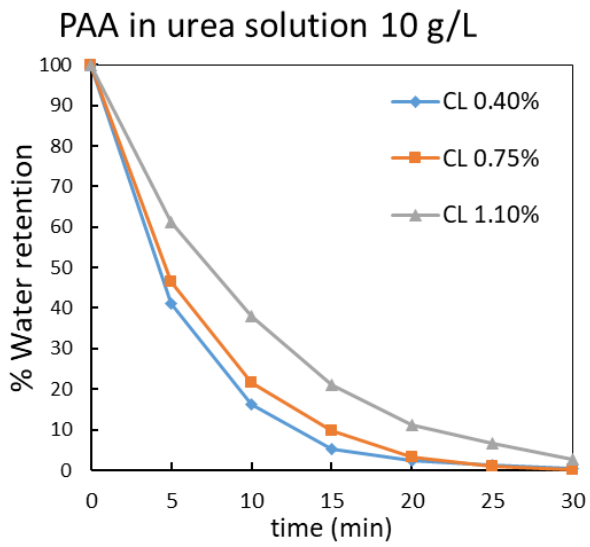


*Figure II.17. Water retention % as a function of time of centrifugation at 2000 rpm for PAA gels, PAA/urea gels and urea loaded PAA gels prepared at different MBA contents.*

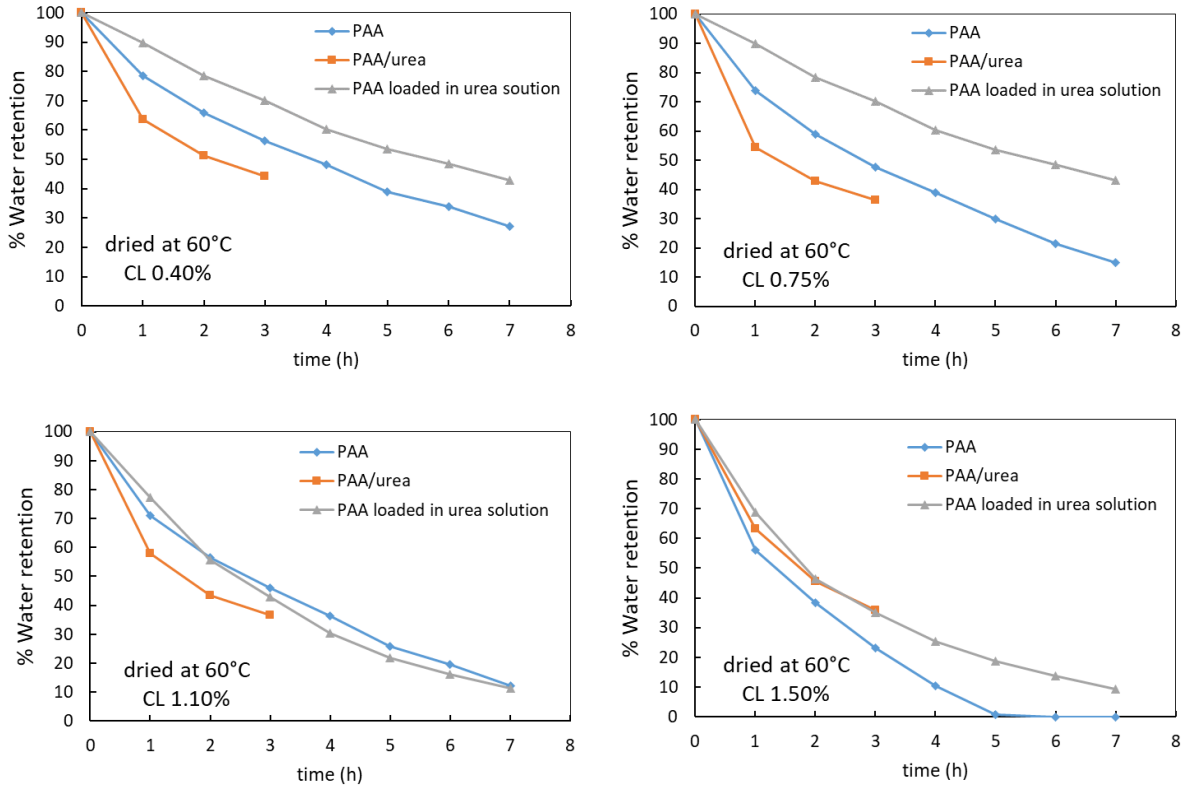

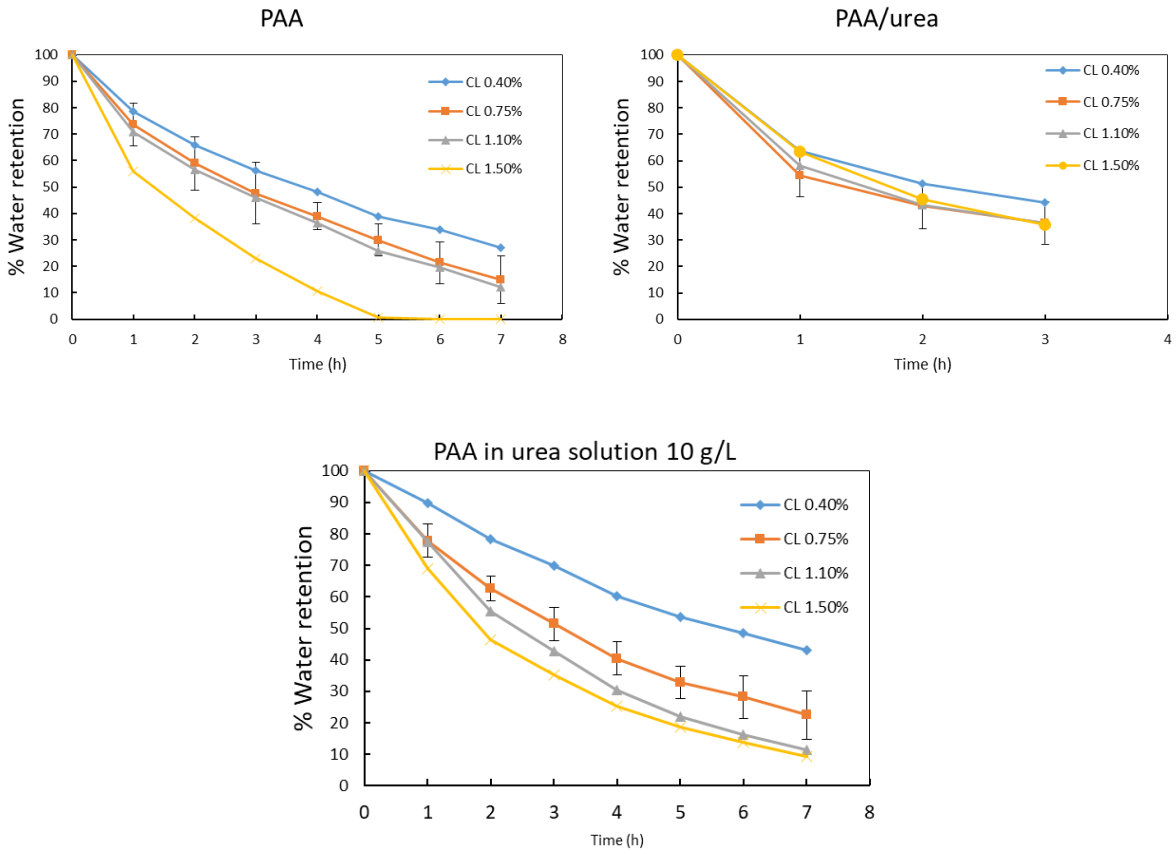


*Figure II.18. Water retention % as a function of time of drying at 60°C for PAA gels, PAA/urea gels and urea loaded PAA gels prepared at different MBA contents.*

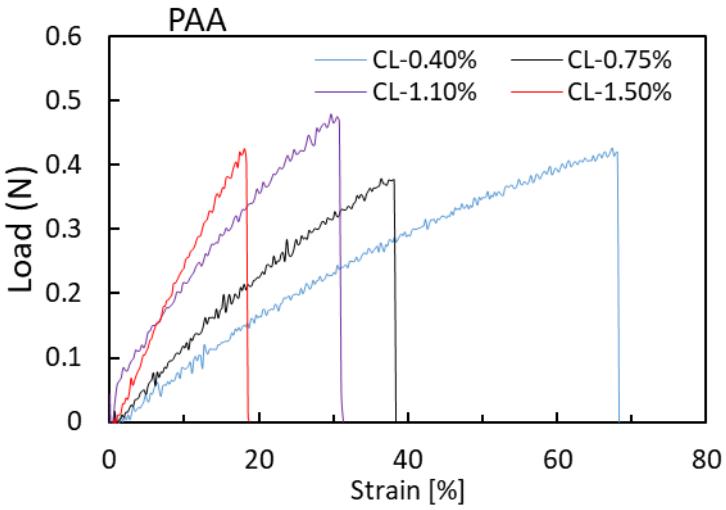

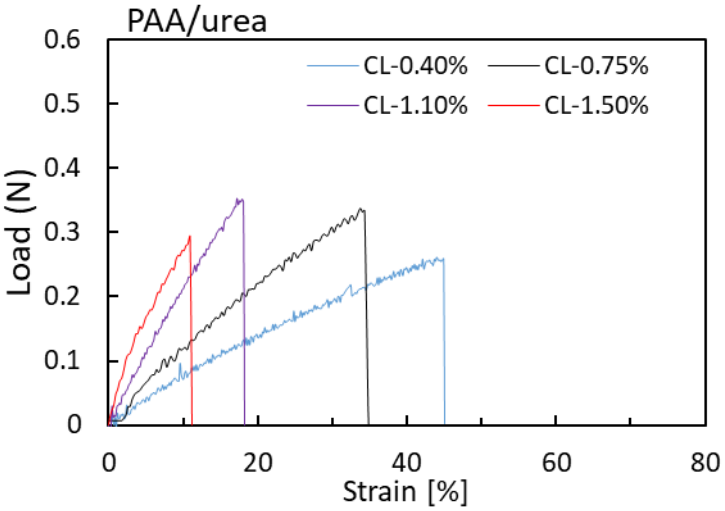


*Figure II.19. Representative tensile load-strain curves of PAA and PAA/urea hydrogels.*

## II.3.5. Study of network parameters

The polymer volume fraction of the swollen gel, was determined using Eq. 15.,

$$\varphi_{p,s} = \frac{1}{1+Q(\frac{\rho_p}{\rho_w})} \qquad (15)$$

With $\rho_p$ and $\rho_w$ , the densities of polymer and water (1.2 g/cm$^3$ for PAA at 298K ).

Experimental values of $\bar{M}_c$ were evaluated from the tensile properties of hydrogels measured at a constant Q value (=6). Due to its high Tg (ca. 106°C (Brandrup et al., 1999), the polyacrylic acid chains are frozen in a glassy state at room temperature. However, with hydrogels containing a sufficient quantity of water, the PAA chains are solvated and behave like a network of flexible chains in the rubbery state. The PAA hydrogels thus behave according to the rules of rubber elasticity at room temperature. According to the theory of rubber elasticity, the molecular weight between crosslinks, $\bar{M}_c$, can be determined from the following equation (Peppas and Merrill, 1977; Huglin et al., 1986; Horkay and Zrinyi, 1988; Powers and Stein, 2006; C. Walowski, 2010):

$$E(\varphi_p) = \frac{3RT\rho_p\varphi_p^{1/3}}{\bar{M}_C} \qquad (16)$$

Where E is the Young's modulus, $\varphi_p$ is the fraction of polymer in hydrogel, R is the gas constant (8.314 J K$^{-1}$ mol$^{-1}$) and T is the temperature.

The $\bar{M}_c$ values determined from tensile properties using Eq.(16) are summarized in Table II.4. These calculations were not performed for PAA/urea gels because of the presence of urea in these gels which

has certainly an impact on the mechanical properties. The theoretical values of $\bar{M}_c$, $\bar{M}_{c,th}$, were calculated using Eq(16 and 17) and are also included in Table II.4:

$$\bar{M}_{c,th} = \frac{M_r}{2X} \qquad (17)$$

with X, the crosslinking ratio (mol MBA/mol PAA repeating unit) and $M_r$, the molecular weight of the repeating unit (72 g/mol).

Table II.4 Parameters characterizing network structure of PAA hydrogels

| Sample | X (mol MBA/mol AA) | Swelling ratio Q | $\bar{M}_{c,exp}$ (g/mol) | $\bar{M}_{c,th}$ (g/mol) | Mesh size $\xi$ (Å) |
|---|---|---|---|---|---|
| PAA-0.4 | 0.004 | 187 | 15084 | 9006 | 2142 |
| PAA-0.75 | 0.0075 | 89 | 9094 | 4803 | 1405 |
| PAA-1.1 | 0.011 | 58 | 7819 | 3275 | 1238 |
| PAA-1.5 | 0.015 | 45 | 4198 | 2401 | 738 |

An increased concentration of MBA crosslinker resulted in a reduction in the value of Mc.

The molecular weights obtained from tensile tests were higher than the theoretical values, irrespective of the crosslinker content. The tensile tests were carried out on the as prepared hydrogels with therefore an identical water content for all the samples (Q=6). Free PAA chains are therefore certainly present and contribute to increasing the mobility of the chains which resulted in lower Young's modulus. This thus leads to higher effective $\bar{M}_c$ than the theoretical $\bar{M}_c$ values calculated by considering an ideal lattice. On the other hand, the presence of dangling chains could also contribute to the difference observed between the experimental and theoretical $\bar{M}_c$ values.

The gel mesh size, $\xi$, defined as the statistical length between two crosslinks, is another important parameter used to describe the gel structure (Figure II.20).

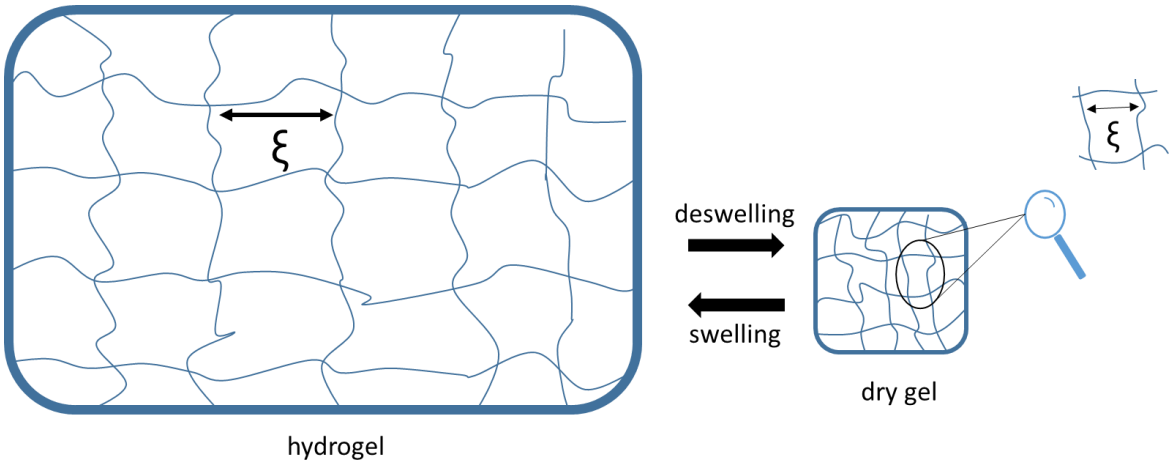


*Figure II.20. Schematic of mesh size in hydrogels (adapted from* (Peppas et al., 1999) *).*

The mesh size, ξ, was determined according to Eq. (18) (Canal and Peppas, 1989):

$$\zeta = \varphi_p{}^{-1/3}.l_{C-C}\sqrt{2C_n\frac{\overline{M_c}}{M_r}} \qquad (18)$$

where $l_{C\text{-}C}$ is the length of the covalent carbon-carbon bond (1.54 Å) and $C_n$ is the the Flory characteristic ratio of PAA (6.7 (Brandrup et al., 1999) VII-34). The mesh size of the PAA networks decreased with increase in CL content from 214 nm to 74 nm.

The morphology of cryofixed -swollen PAA hydrogels is shown in Figure II.21 and 22. The pore size distribution determined form SEM images is given in Figure II.23. All SEM pictures show irregular macropores with sizes ranging from 2 to 20 µm. Identical structures were found for pictures taken at different locations indicating that pictures shown in Figure. can be considered as representative of the overall morphology. SEM images have been analyzed to extract a statistical relevant pore size distribution by Image J software analysis. PAA hydrogels prepared with urea showed some differences in morphology compared to hydrogels prepared without urea. Honeycomb -like networks are formed without urea with a severe distortion from spherical shape of hole while the pores of hydrogels prepared in the presence of urea have a more spherical shape and appear separated by large portions of polymer films.

SEM images show that PAA gels with a low crosslinking degree have bigger pores than PAA/urea gels, which is in agreement with the greater water uptake capability of PAA gels. The size of the pores depends much more on the amount of crosslinking agent used in the synthesis for the PAA gels than for the PAA/urea gels. Consequently, the pore sizes of the PAA and PAA/urea gels becomes closer together when CL content increases. However, PAA/urea gels still appear les porous than PAA gels even for high CL contents. It thus seems that the little higher water uptake capability of PAA/urea gels prepared at high CL contents is not related to the formation of a larger number of macropores during swelling. This might indicate that a more homogeneous network is formed when urea is present in the polymerization medium which results in the formation of a large amount of small pores upon swelling in water. Similar trends were found for the effect of crosslinker content on the pore size than that found from the estimate of mesh size by swelling or tensile measurements. However, the pore sizes by SEM are one decade higher than the estimate values of mesh size. Paterson et al. (2013) have shown that the method of dehydration by quenching with liquid nitrogen made it possible to preserve the morphology of the hydrated sample better than the method consisting in freezing the hydrated sample in a freezer before freeze-drying. The plunge freeze/freeze-drying method was therefore used in our case. The differences in pore size observed with SEM and from the swelling measurements or tensile properties suggest that the liquid nitrogen quenching method may not completely prevent the formation of ice crystals excluding the polymer from the growing crystal domains. Moreover, the swollen gels were all transparent in appearance which suggest a pore size in the submicrometer range

(Chirila et al., 1993) It is thus not certain that the morphology of pores observed with SEM represent the native morphology of the hydrated gels.

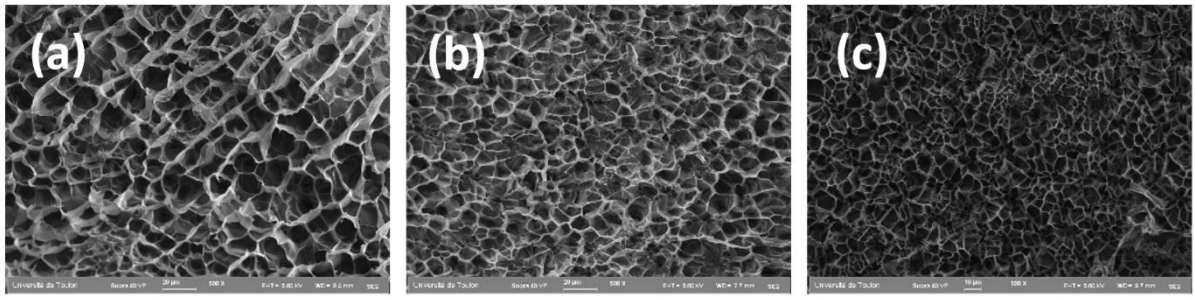


*Figure II.21. SEM images of lyophilized PAA gels prepared with different MBA content (a) 0.4, (b) 0.75 and (c) 1.5 mol%.*

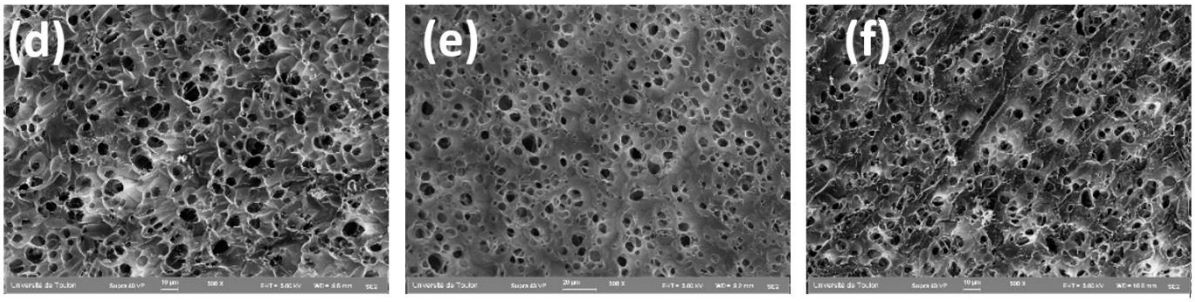


*Figure II.22. SEM images of lyophilized PAA/urea gels prepared with different MBA content (a) 0.4 , (b) 0.75 and (c) 1.5 mol%.*

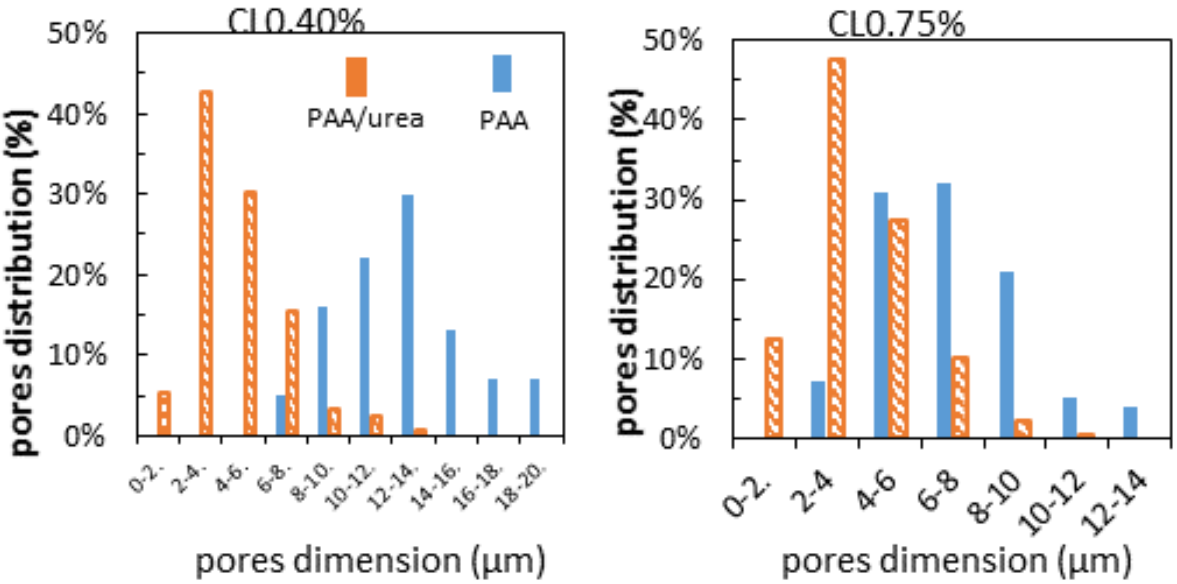

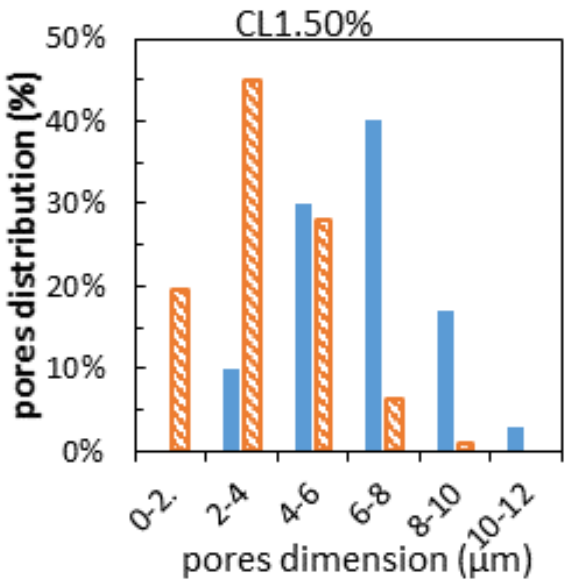


*Figure II.23. Pore size distribution of the lyophilized PAA and PAA/urea hydrogels prepared at different MBA content.*

## II.3.6. Urea release properties

The release curves of urea fertilizer in deionized water are shown in Figure II.24. There is good agreement between the data from the photometric analyzes and those from the elementary analysis. The release curves indicate a slower release of urea in the case of PAA/urea gels, in particular when the gels are prepared at intermediate levels in MBA. A more quantitative analysis of these results can be carried out by modelling the diffusional release of urea from the PAA gels.

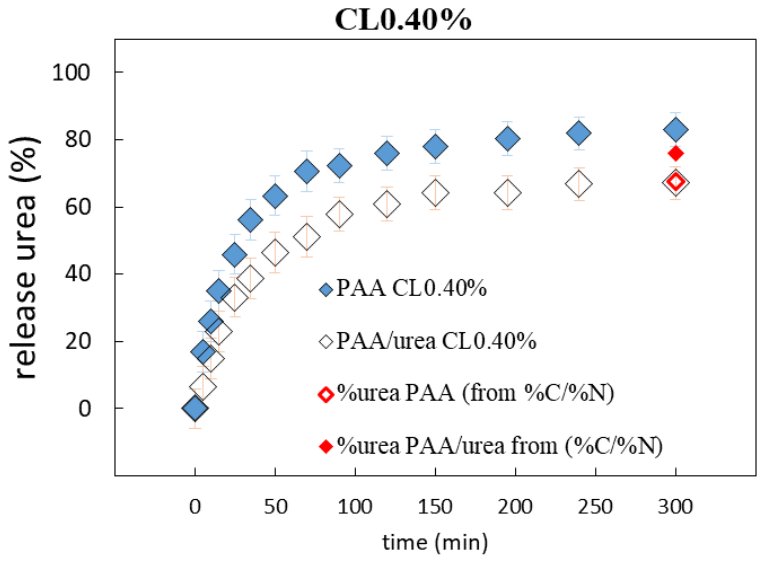

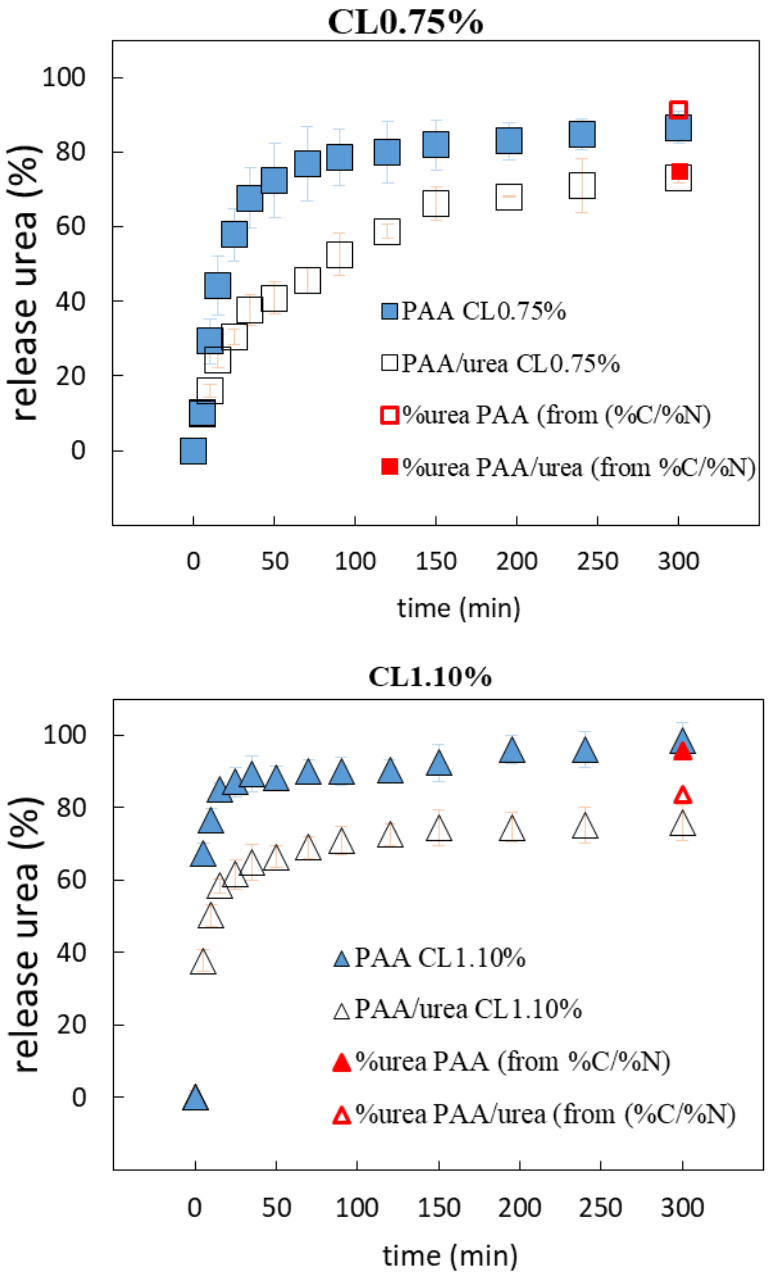
CL0.75%
release urea (%)
time (min)
PAA CL0.75%
PAA/urea CL0.75%
%urea PAA (from (%C/%N)
%urea PAA/urea (from %C/%N)
CL1.10%
release urea (%)
time (min)
PAA CL1.10%
PAA/urea CL1.10%
%urea PAA (from %C/%N)
%urea PAA/urea (from (%C/%N)

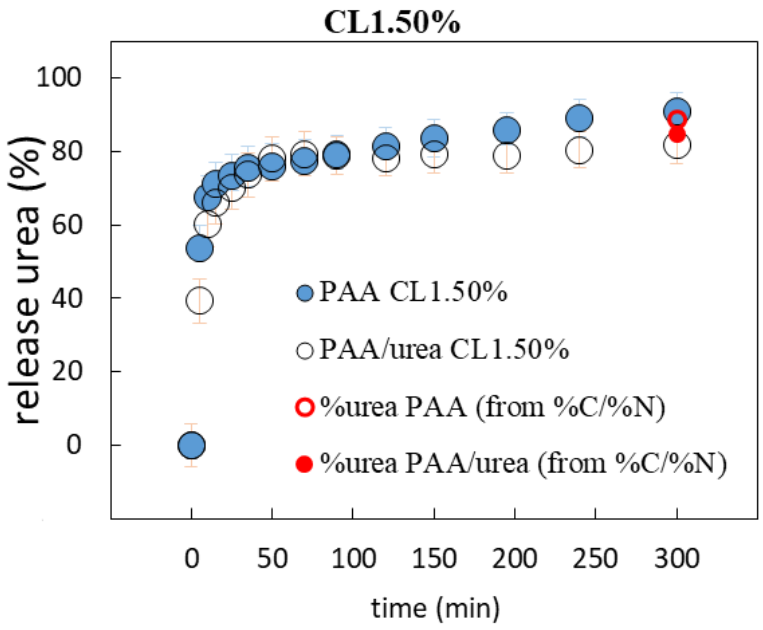


*Figure II.24. Urea release in deionized water for urea loaded PAA and PAA/urea gels prepared at different crosslinker content, the points correspond to the results of the photometric analysis, the data from elemental analysis carried out at 5 hours immersion time are also represented.*

The release of an active agent from hydrogel is classically assumed to take place by diffusion (Muhr & Blanshard, 1982). A kinetic equation (Cobby et al., 1974) with a cubic form had been derived to describe the diffusion control release behaviors of solute for a porous matrix ($M_t/M_0 < 60\%$):

$$\alpha = \frac{M_t}{M_0} = 3Kt^{1/2} - 3(Kt^{1/2})^2 + (Kt^{1/2})^3 \qquad (19)$$

where α is the fraction of weight released at time t, and K is the release rate constant.

This expression can be written in a linear form as:

$$(1-\alpha)^{\frac{1}{3}} = 1 - Kt^{\frac{1}{2}} \qquad (20)$$

By plotting the left-hand side of the above expression as a function of the square root of time, a linear plot with slope K is obtained.

The release rate constant K is defined as:

$$K = \left(\frac{1}{C_0} r_0\right)[D(2C_0 - C_s)C_s]^{\frac{1}{2}} \qquad (21)$$

where $C_0$ is the weight of urea per unit volume of granular, Cs is the equilibrium solubility of the urea in the dissolution liquid, D is the diffusion coefficient of the urea in the swollen granular (including the effect of porosity and tortuosity) and $r_0$ is the granular radius (0.2 mm).

The diffusion coefficient D was calculated from the release rate K according to:

$$D = \frac{(KC_0 r_0)^2}{(2C_0 - C_s)C_s} \qquad (22)$$

The values calculated for the diffusion coefficient D of urea in PAA and PAA/urea hydrogels are given in Table II.5. The obtained values are in general agreement with the values reported in literature , ie in the range $10^{-5}$-$10^{-6}$ cm² $s^{-1}$ (Shavit et al., 1995; Helaly et al., 2005b) . The diffusion coefficient of the loose network of the urea loaded PAA obtained at a 0.4 mol% MBA is smaller than the D values obtained at higher CL content. This result may seem surprising at first glance since this gel contains the largest mesh sizes and absorbs a large amount of water.

It can be explained from the results of water absorption kinetics which showed that rate constant parameter and the initial swelling rate are lower with PAA/urea prepared at the lowest content of crosslinker, noting that the same trend should be obtained for the swelling kinetics of urea loaded PAA gels. It may be due to the fact that the network prepared at low CL contents have more ability to rearrange itself during the drying of the gel to form multi-site hydrogen bond interactions between COOH groups of polymer chains and urea. These interactions would slow down the access of water and therefore the departure of urea from the dried gels when they are immersed in water.

The diffusion coefficient D is up to one decade smaller for PAA/urea gels compared to the values found for urea loaded PAA gels with a crosslinker content in the medium range (0.75 mol % and 1.10 mol%). The slower rate of urea release may be related to the more homogeneous nature of the network leading to smaller pore sizes than PAA gels, as suggested by SEM results. It could also be due to urea molecules establishing on average more interactions with the polymer when the polymerization is carried out in the presence of urea. The urea release kinetics of the two types of gels prepared at the highest content of MBA (1.5 mol%) are almost similar. It may be related to the higher water absorption capacity of the PAA/urea gels compared to PAA at this content of MBA.

Long-term release tests were carried out in the case of gels prepared with 0.75 mol% of MBA. The results in Figure II.25 indicate a continuous and slow release of urea up to a 100% release obtained after approximately 32 hours for urea loaded PAA gels and ca. 45 hours for PAA/urea gels.

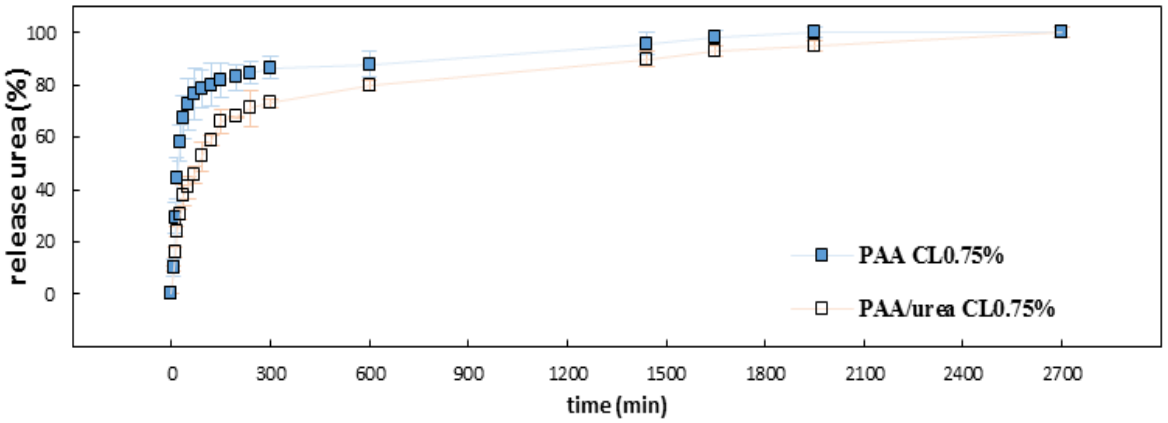


*Figure II.25. Urea release in deionized water for urea loaded PAA and PAA/urea gels prepared with 0.75 mol% MBA, up to a 100% release.*

Table II.5. Diffusion coefficient of urea for urea loaded PAA and PAA/urea gels.

| samples | D ($cm^2/s$) | | $R^2$ | |
|---|---|---|---|---|
| | Urea loaded PAA | PAA/urea | Urea loaded PAA | PAA/urea |
| CL0.40% | $4.4 \times 10^{-6}$ | $2.1 \times 10^{-6}$ | 0.997 | 0.983 |
| CL0.75% | $1.0 \times 10^{-5}$ | $1.5 \times 10^{-6}$ | 0.821 | 0.989 |
| CL1.10% | $1.2 \times 10^{-5}$ | $1.4 \times 10^{-6}$ | 0.998 | 0.865 |
| CL1.50% | $1.1 \times 10^{-5}$ | $6.5 \times 10^{-6}$ | 0.952 | 0.869 |

## II.3.7. $^{13}C$ NMR Spectroscopic investigation of PAA hydrogels

To investigate the structural change in molecular level and the influence of urea fertilizer in different networks formation, $^{13}C$ HR-MAS for swollen gel was carried out in order to clarify the nature of the gel/urea interactions.

The $^{13}C$ NMR spectra of PAA, urea loaded PAA and PAA/urea before and after immersion in water for 24 h are shown in Figure II.26 and 27 for samples prepared with 0.75 mol% and 1.5 mol% of urea, respectively. The $^{13}C$ HR-MAS spectra show four main groups of signals, (i) in the range δ=34.6-36.3 ppm for the $CH_2$ groups, (ii) in the range δ=42.2-43.6 ppm for the CH groups, (iii) at δ=163.5 ppm corresponding to carbonyl of urea (Kuchel et al., 2014) and finally (iv) in the range δ=179.4-181.1 ppm assigned to carbonyl groups of the polymer.

Although the formation of diacyl ureas by condensation of urea with carboxylic acids in the presence of a metal catalyst (iron or zinc oxide) has been speculated in the patent literature (Dean, 2002), no characterization data confirming the structure of the products formed was presented. On the other hand, it is clearly established that urea has the ability to form hydrogen-bonded crystalline structures with a wide variety of dicarboxylic acids (Alhalaweh et al., 2010). Based on $^{13}C$ spectral data of fatty

acid-derived diacyl ureas (Stec and Pecic, 2020) and on the chemical shift predictions by ChemDraw Software, the urea and diacyl carbonyl peaks of diacyl urea structures are respectively expected at around 150 ppm and 174 ppm. No signals assigned to diacyl urea crosslinks were identified. In PAA gels, the $^{13}C$ NMR spectrum only contains the signals related to the polymer network. The immersion of the PAA gel in an urea solution results in the appearance of the urea peak at $\delta$=163.5 ppm, confirming that urea has been loaded in the PAA and that it has not been degraded during the thermal drying of the gel. The characteristic peak of urea at $\delta$=163.5 ppm almost completely disappeared after immersion of PAA/urea gels in water for 24 hours. These results are in agreement with the photometric titration and elemental analysis results and confirm that almost all of the urea incorporated in the gel can be released after a sufficiently long time of immersion in water.

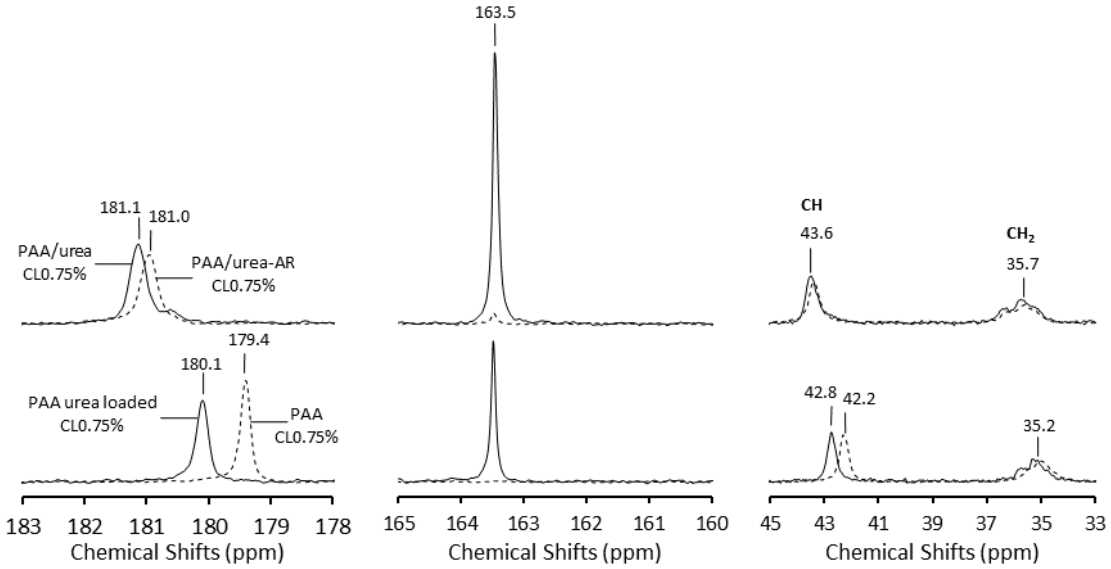


*Figure II.26. Swollen-state $^{13}C$ HR-MAS NMR spectra ($d_1$=40s, 20mg + 100µL $D_2O$) of PAA/urea before and after immersion in water for 24 h (top) and of PAA synthetized without fertilizer before and after urea loading (bottom). All samples prepared with a crosslinker content of 0.75 mol%.*

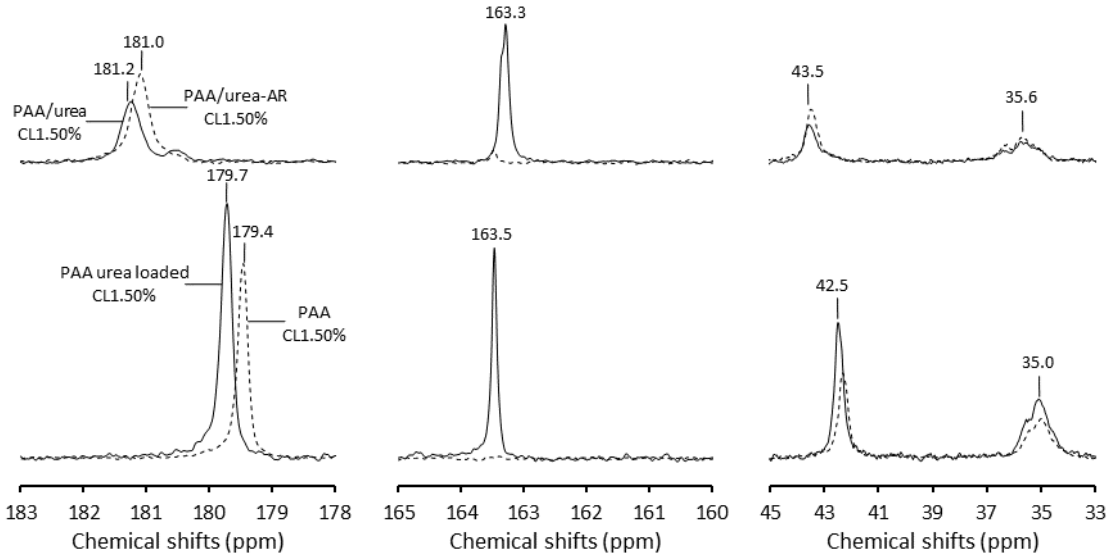


*Figure II.27. Swollen-state $^{13}C$ HR-MAS NMR spectra ($d_1$=40s, 20mg + 100µL $D_2O$) of PAA/urea before and after immersion in water for 24 h (top) and of PAA synthetized without fertilizer before and after urea loading (bottom). All samples prepared with a crosslinker content of 1.5 mol%.*

## II.4. Conclusion

In this part, we have developed polyacrylic acid hydrogels loaded with urea as nitrogen fertilizer. The objective was to evaluate the influence of the urea loading method on the properties important for the intended agricultural application, namely the swelling properties and the ability of these gels to release the fertilizer over a long period. Loading of the urea was thus carried out either during the polymerization or once the polymer had been formed to give PAA/urea and PAA gels, respectively. Contrary to what several studies in the literature advance, we have shown that the urea incorporated in these two types of hydrogels is not chemically linked to the polymer network but only establishes hydrogen bond interactions with the COOH groups of the network. The previous studies were based only on unconvincing FTIR spectrometry results. In our case, $^{13}C$ solid state NMR analyzes of the urea loaded gels clearly rejected any chemical link between urea and the polymer network. The gels prepared at low crosslinker content imbibed more than 100 times their dry weight of water and can consequently be categorized as superabsorbent polymers. The variations in the degree of swelling at equilibrium with the amount of crosslinking agent or neutralisation degree of acrylic acid are less when the urea is incorporated into the polymerization medium. PAA/urea gels swell less than PAA gels at low crosslinker content and more at high crosslinker content. Moreover, compared to PAA gels, PAA/urea gels are more stable during successive swelling-deswelling cycles. Besides, we found that

urea in these hydrogels mainly partition in the water-containing region in the swollen gel. PAA/urea retain more water than PAA gels under mechanical stress but less under thermal stress. SEM observations indicated that these hydrogels are macroporous gels with pore size in the micrometer range. The size of pores decreases with increasing crosslinker content for both types of hydrogels but the variations are less for the PAA/urea gels compared to those observed with PAA gels. The results obtained suggested that PAA/urea network is more homogeneous than PAA network which leads to the formation of smaller pores when the gel swells. The diffusion coefficient D is up to one decade smaller for PAA/urea gels compared to the values found for urea loaded PAA gels with a crosslinker content in the medium range (0.75 mol % and 1.10 mol%). The slow release properties of PAA/urea gels was related to the more homogeneous nature of the network leading to smaller pore sizes than PAA gels and/or to urea molecules establishing on average more interactions with the polymer when the polymerization is carried out in the presence of urea.

## II.5. References

Abd El-Rehim, H.A., Hegazy, E.-S.A., Abd El-Mohdy, H.L., 2006. Effect of various environmental conditions on the swelling property of PAAm/PAAcK superabsorbent hydrogel prepared by ionizing radiation. Journal of Applied Polymer Science 101, 3955–3962. https://doi.org/10.1002/app.22904

Akelah, A., 2013. Polymers in the Controlled Release of Agrochemicals, in: Functionalized Polymeric Materials in Agriculture and the Food Industry. Springer, Boston, MA, pp. 133–192. https://doi.org/10.1007/978-1-4614-7061-8_3

Alhalaweh, A., George, S., Boström, D., Velaga, S.P., 2010. 1:1 and 2:1 Urea−Succinic Acid Cocrystals: Structural Diversity, Solution Chemistry, and Thermodynamic Stability. Crystal Growth & Design 10, 4847–4855. https://doi.org/10.1021/cg100823p

Anseth, K.S., Bowman, C.N., Brannon-Peppas, L., 1996. Mechanical properties of hydrogels and their experimental determination. Biomaterials 17, 1647–1657. https://doi.org/10.1016/0142-9612(96)87644-7

Azeem, B., KuShaari, K., Man, Z.B., Basit, A., Thanh, T.H., 2014. Review on materials & methods to produce controlled release coated urea fertilizer. Journal of Controlled Release 181, 11–21. https://doi.org/10.1016/j.jconrel.2014.02.020

Bortolin, A., Serafim, A.R., Aouada, F.A., Mattoso, L.H.C., Ribeiro, C., 2016. Macro- and Micronutrient Simultaneous Slow Release from Highly Swellable Nanocomposite Hydrogels. J. Agric. Food Chem. 64, 3133–3140. https://doi.org/10.1021/acs.jafc.6b00190

Brandrup, J., Immergut, E.H., Grulke, E.A., Abe, A., Bloch, D.R., 1999. Polymer handbook. Wiley New York.

Canal, T., Peppas, N.A., 1989. Correlation between mesh size and equilibrium degree of swelling of polymeric networks. Journal of Biomedical Materials Research 23, 1183–1193. https://doi.org/10.1002/jbm.820231007

Cândido, J. de S., Leitão, R.C.F., Ricardo, N.M.P.S., Feitosa, J.P.A., Muniz, E.C., Rodrigues, F.H.A., 2012. Hydrogels composite of poly(acrylamide-co-acrylate) and rice husk ash. I. Synthesis and characterization. Journal of Applied Polymer Science 123, 879–887. https://doi.org/10.1002/app.34528

Chirila, T.V., Chen, Y.-C., Griffin, B.J., Constable, I.J., 1993. Hydrophilic sponges based on 2-hydroxyethyl methacrylate. I. effect of monomer mixture composition on the pore size. Polymer International 32, 221–232. https://doi.org/10.1002/pi.4990320303

Cobby, J., Mayersohn, M., Walker, G.C., 1974. Influence of shape factors on kinetics of drug release from matrix tablets I: Theoretical. Journal of Pharmaceutical Sciences 63, 725–732. https://doi.org/10.1002/jps.2600630516

Dean, F.W., 2002. Methods for preparing and using diacyl ureas. US6448440B1.

El-Rehim, A., A, H., 2006. Characterization and possible agricultural application of polyacrylamide/sodium alginate crosslinked hydrogels prepared by ionizing radiation. Journal of Applied Polymer Science 101, 3572–3580. https://doi.org/10.1002/app.22487

Favre, E., Girard, S., 2001. Release kinetics of low molecular weight solutes from mixed cellulose ethers hydrogels: a critical experimental study. European Polymer Journal 37, 1527–1532. https://doi.org/10.1016/S0014-3057(01)00024-6

Guo, M., Liu, M., Hu, Z., Zhan, F., Wu, L., 2005. Preparation and properties of a slow release NP compound fertilizer with superabsorbent and moisture preservation. J. Appl. Polym. Sci. 96, 2132–2138. https://doi.org/10.1002/app.21140

Helaly, F.M., Essawy*, H.A., El-Nashar, D.E., Maziad, N.A., 2005a. Slow Release of Urea as a Source of Nitrogen from Some Acrylamide and Acrylic Acid Hydrogels. Polymer-Plastics Technology and Engineering 44, 253–263. https://doi.org/10.1081/PTE-200048712

Helaly, F.M., Essawy*, H.A., El-Nashar, D.E., Maziad, N.A., 2005b. Slow Release of Urea as a Source of Nitrogen from Some Acrylamide and Acrylic Acid Hydrogels. Polymer-Plastics Technology and Engineering 44, 253–263. https://doi.org/10.1081/PTE-200048712

Horkay, F., Zrinyi, M., 1988. Studies on mechanical and swelling behavior of polymer networks on the basis of the scaling concept. 7. Effect of deformation on the swelling equilibrium concentration of gels. Macromolecules 21, 3260–3266. https://doi.org/10.1021/ma00189a022

Huglin, M.B., Rehab, M.M.A.M., Zakaria, M.B., 1986. Thermodynamic interactions in copolymeric hydrogels. Macromolecules 19, 2986–2991. https://doi.org/10.1021/ma00166a019

Ianchis, R., Ninciuleanu, C.M., Gifu, I.C., Alexandrescu, E., Nistor, C.L., Nitu, S., Petcu, C., 2019. Hydrogel-clay Nanocomposites as Carriers for Controlled Release [WWW Document]. https://doi.org/info:doi/10.2174/092986732566180831151055

Isık, B., Kıs, M., 2004. Preparation and determination of swelling behavior of poly(acrylamide-co-acrylic acid) hydrogels in water. Journal of Applied Polymer Science 94, 1526–1531. https://doi.org/10.1002/app.21074

Jin, S., Yue, G., Feng, L., Han, Y., Yu, X., Zhang, Z., 2011. Preparation and Properties of a Coated Slow-Release and Water-Retention Biuret Phosphoramide Fertilizer with Superabsorbent. J. Agric. Food Chem. 59, 322–327. https://doi.org/10.1021/jf1032137

Karadağ, E., Kırıştı, T., Kundakcı, S., Üzüm, Ö.B., 2010. Investigation of sorption/swelling characteristics of chemically crosslinked AAm/SMA hydrogels as biopotential sorbent. Journal of Applied Polymer Science 117, 1787–1797. https://doi.org/10.1002/app.32125

Kazanskii, K.S., Dubrovskii, S.A., 1992. Chemistry and physics of “agricultural” hydrogels, in: Polyelectrolytes Hydrogels Chromatographic Materials, Advances in Polymer Science. Springer, Berlin, Heidelberg, pp. 97–133. https://doi.org/10.1007/3-540-55109-3_3

Kuchel, P.W., Naumann, C., Chapman, B.E., Shishmarev, D., Håkansson, P., Bacskay, G., Hush, N.S., 2014. NMR resonance splitting of urea in stretched hydrogels: Proton exchange and 1H/2H isotopologues. Journal of Magnetic Resonance 247, 72–80. https://doi.org/10.1016/j.jmr.2014.08.004

Li, A., Wang, A., Chen, J., 2004. Studies on poly(acrylic acid)/attapulgite superabsorbent composite. I. Synthesis and characterization. J. Appl. Polym. Sci. 92, 1596–1603. https://doi.org/10.1002/app.20104

Liu, M., Liang, R., Zhan, F., Liu, Z., Niu, A., 2007. Preparation of superabsorbent slow release nitrogen fertilizer by inverse suspension polymerization. Polymer International 56, 729–737. https://doi.org/10.1002/pi.2196

Liu, M., Liang, R., Zhan, F., Liu, Z., Niu, A., 2006. Synthesis of a slow-release and superabsorbent nitrogen fertilizer and its properties. Polym. Adv. Technol. 17, 430–438. https://doi.org/10.1002/pat.720

Muhr, A.H., Blanshard, J.M.V., 1982. Diffusion in gels. Polymer 23, 1012–1026. https://doi.org/10.1016/0032-3861(82)90402-5

Ofner, C.M., Schott, H., 1986. Swelling Studies of Gelatin I: Gelatin Without Additives. Journal of Pharmaceutical Sciences 75, 790–796. https://doi.org/10.1002/jps.2600750814

Omidian, H., Hashemi, S.A., Sammes, P.G., Meldrum, I., 1998. A model for the swelling of superabsorbent polymers. Polymer 39, 6697–6704. https://doi.org/10.1016/S0032-3861(98)00095-0

Paterson, S.M., Casadio, Y.S., Brown, D.H., Shaw, J.A., Chirila, T.V., Baker, M.V., 2013. Laser scanning confocal microscopy versus scanning electron microscopy for characterization of polymer morphology: Sample preparation drastically distorts morphologies of poly(2-hydroxyethyl methacrylate)-based hydrogels. Journal of Applied Polymer Science 127, 4296–4304. https://doi.org/10.1002/app.38034

Peppas, N.A., Keys, K.B., Torres-Lugo, M., Lowman, A.M., 1999. Poly(ethylene glycol)-containing hydrogels in drug delivery. Journal of Controlled Release 62, 81–87. https://doi.org/10.1016/S0168-3659(99)00027-9

Peppas, N.A., Merrill, E.W., 1977. Crosslinked poly(vinyl alcohol) hydrogels as swollen elastic networks. Journal of Applied Polymer Science 21, 1763–1770. https://doi.org/10.1002/app.1977.070210704

Pourjavadi, A., Ghasemzadeh, H., Soleyman, R., 2007. Synthesis, characterization, and swelling behavior of alginate-g-poly(sodium acrylate)/kaolin superabsorbent hydrogel composites. Journal of Applied Polymer Science 105, 2631–2639. https://doi.org/10.1002/app.26345

Powers, J., Stein, R.S., 2006. Topics in polymer physics. World Scientific Publishing Company.

Ramaraj, B., Radhakrishnan, G., 1994. Modification of the dynamic swelling behaviour of poly(2-hydroxyethyl methacrylate) hydrogels in water through interpenetrating polymer networks (IPNs). Polymer 35, 2167–2173. https://doi.org/10.1016/0032-3861(94)90245-3

Ramli, R.A., 2019. Slow release fertilizer hydrogels: a review. Polym. Chem. 10, 6073–6090. https://doi.org/10.1039/C9PY01036J

Ritger, P.L., Peppas, N.A., 1987. A simple equation for description of solute release II. Fickian and anomalous release from swellable devices. Journal of Controlled Release 5, 37–42. https://doi.org/10.1016/0168-3659(87)90035-6

Schott, H., 1992. Swelling kinetics of polymers. Journal of Macromolecular Science, Part B 31, 1–9. https://doi.org/10.1080/00222349208215453

Shavit, U., Shaviv, A., Zaslavsky, D., 1995. Solute diffusion coefficient in the internal medium of a new gel based controlled release fertilizer. Journal of Controlled Release 37, 21–32. https://doi.org/10.1016/0168-3659(95)00043-8

Singh, B., Chauhan, N., Sharma, V., 2011. Design of Molecular Imprinted Hydrogels for Controlled Release of Cisplatin: Evaluation of Network Density of Hydrogels. Ind. Eng. Chem. Res. 50, 13742–13751. https://doi.org/10.1021/ie200758b

Stec, J., Pecic, S., 2020. Facile synthesis of the fungus-derived natural products: N,N'-dipalmitoleyl urea (C16:1) and N,N'-dioleyl urea (C18:1). Natural Product Research 0, 1–8. https://doi.org/10.1080/14786419.2020.1844694

Teodorescu, M., Lungu, A., Stanescu, P.O., Constantin Neamţu, 2009. Preparation and Properties of Novel Slow-Release NPK Agrochemical Formulations Based on Poly(acrylic acid) Hydrogels and Liquid Fertilizers. Ind. Eng. Chem. Res. 48, 6527–6534. https://doi.org/10.1021/ie900254b

Van Krevelen, D.W., 1990. Properties of Polymers, 3rd completely revised ed.

Watt, G.W., Chrisp, J.D., 1954. Spectrophotometric Method for Determination of Urea. Anal. Chem. 26, 452–453. https://doi.org/10.1021/ac60087a006

Xiang, Y., Ru, X., Shi, J., Song, J., Zhao, H., Liu, Y., Guo, D., Lu, X., 2017. Preparation and Properties of a Novel Semi-IPN Slow-Release Fertilizer with the Function of Water Retention. J. Agric. Food Chem. 65, 10851–10858. https://doi.org/10.1021/acs.jafc.7b03827

Yoon, S.C., Jhon, M.S., 1982. The transport phenomena of some model solutes through postcrosslinked poly(2-hydroxyethyl methacrylate) membranes with different tactic precursors. Journal of Applied Polymer Science 27, 3133–3149. https://doi.org/10.1002/app.1982.070270834

Zhang, J., Liu, R., Li, A., Wang, A., 2006. Preparation, Swelling Behaviors, and Slow-Release Properties of a Poly(acrylic acid-co-acrylamide)/Sodium Humate Superabsorbent Composite. Ind. Eng. Chem. Res. 45, 48–53. https://doi.org/10.1021/ie050745j

Zhang, M., Cheng, Z., Zhao, T., Liu, M., Hu, M., Li, J., 2014. Synthesis, Characterization, and Swelling Behaviors of Salt-Sensitive Maize Bran–Poly(acrylic acid) Superabsorbent Hydrogel. J. Agric. Food Chem. 62, 8867–8874. https://doi.org/10.1021/jf5021279

Zhou, T., Wang, Y., Huang, S., Zhao, Y., 2018. Synthesis composite hydrogels from inorganic-organic hybrids based on leftover rice for environment-friendly controlled-release urea fertilizers. Science of The Total Environment 615, 422–430. https://doi.org/10.1016/j.scitotenv.2017.09.084

# CHAPTER III

## Hydrogel composites based on kaolinite-urea intercalates for slow release fertilizers

# Chapter III. Hydrogel composites based on kaolinite-urea intercalates for slow release fertilizers

## III.1. Introduction

In agriculture, an adequate supply of fertilizer and water are two essential factors for the growth of a plant. It is therefore important to improve the efficiency of use of water resources and nutrient fertilizer (Azeem et al., 2014; Wanyika, 2014; Campos et al., 2015). Increasing the efficiency of fertilizer use by preventing the loss of fertilizer in the environment is a key objective agronomic management. One of the solutions considered to limit the losses of fertilizer and thus increase their efficiency is to use slow or controlled release fertilizer (SRFs) systems (Wu and Liu, 2007). Among fertilizers, urea is extensively used as an effective nitrogen source in agriculture due to its high nitrogen content (46%), formula $CO(NH_2)_2$, and low cost (Liang and Liu, 2007; Zheng et al., 2009; Kim et al., 2011; Azeem et al., 2014). However, excessive supplies of urea leads to losses in soils and causes pollution of soils and underground water by transformation into ammonia as explained in the general introduction. Different strategies have been used to control the release of urea in the environment (Liang and Liu, 2007; Pereira et al., 2012; Azeem et al., 2014). Hydrogel-based slow release fertilizer SRFs (gel-based SRFs) are matrix-type formulations, based on mixtures of natural and/or synthetic hydrophilic polymers and conventional fertilizers.

Superabsorbent hydrogels are cross-linked polymeric networks with the ability to absorb large quantities of water, ie more than 100 times their dry weight of water (Cipriano et al., 2014). Superabsorbent hydrogels can be obtained by radical polymerization of acrylic acid (AA) or its salt and acrylamide (Am) as monomer, using methylene-bis-acrylamide (MBA) as crosslinker agent. This polymer network included very hydrophilic groups ($COO^-$, COOH, $CONH_2$) which allow it to absorb a very large quantity of water (Zhang et al., 2006; Liang and Liu, 2007; Ahmed, 2015). Relative to their application in agriculture, another interesting property of hydrogels is their capacity to retain water that can help to reduce the excess loss of water by evaporation in soils and limit the effects of drought periods.

The incorporation of fertilizers can be operated during (Zheng et al., 2009; D. Cheng et al., 2017) or after (Liang and Liu, 2007) the polymerization step. Recently, clays were incorporated with hydrogel matrix to achieve a slower release of fertilizer (Bortolin et al., 2016; Cheng et al., 2017).

Kaolin group include dickite, nacrite, halloysite and kaolinite the most abundant mineral clay in the group. The chemical composition of kaolinite $Al_2Si_2O_5(OH)_4$ composed of silicon tetrahedral

sheets and aluminum octahedral sheets (Letaief et al., 2006). Kaolinite allows by spacing its interlayer space the intercalation of organic molecules such as urea, hydrazine, dimethyl sulfoxide. Intercalation of urea in kaolinite was studied by Ledoux and White, (1966) by using aqueous suspension, one of different techniques to intercalate kaolinite. Mechanochemical intercalation of urea using ball mills is also a technique to intercalate kaolinite as means of powder activation during reactions (Frost et al., 2001; Makó et al., 2009). The mechanochemical intercalation of fertilizer in kaolinite interlayer and other clays to reduce the rate of fertilizer release has interested several authors (Zhang and Saito, 2009; Solihin et al., 2011; AlShamaileh et al., 2018). (Solihin et al., 2011) prepared by mechanochemical reaction, the incorporation of $KH_2PO_4$ and $NH_4H_2PO_4$ into the kaolin structure for slow release of fertilizer. At 25 m% kaolin addition, release of dispersed nutrients in water reached over 85% and closer to 100%, but decreased to between 30 and 50% for kaolin content at 50 m% and was further reduced to below 10% for sample mixture with kaolin content at 75 m%. (Pereira et al., 2012) described the preparation and characterization of a novel urea slow-release nanocomposite, based on urea intercalation into montmorillonite clay by an extrusion process at room temperature, the release rate of active components in water showed that the nanocomposite showed a slow release behavior for urea dissolution, even in low montmorillonite amounts (20% in mass). (Roshanravan et al., 2015) used intercalated kaolinite-urea as the fertilizer base with a chitosan was used as the binder to prepare controlled release of fertilizer (CRFs). (Borges et al., 2015) also prepared by mechanochemical intercalation of phosphate fertilizer in kaolinite layer. Recently, (Rudmin et al. 2020) also prepared the formulation of slow release fertilizers by the mechanical activation of a mixture of powdered clays and urea using planetary or ring milling techniques. (Xiaoyu et al., 2013) implemented a new method for slow release urea using bentonite and organic polymer to form three-dimensional lattice structure by melting urea.

In this study, we focus on the preparation of kaolinite-urea/hydrogel composites, by varying the amount of kaolinite in the hydrogel matrix (0 to 25 m%) and by varying the amount of urea (0 to 30 m%). The gel matrix used in this study is poly(acrylic acid-co-acrylamide), p(AA-co-Am) hydrogels. The gel time, the swelling ratio, the release of urea in deionized water and the water retention capacity was investigated. The mechanochemical intercalation of kaolinite-urea complex was first prepared by a planetary ball milling by varying the amount of urea and the complex obtained was used to prepare hydrogel composite. Kaolinite/urea/hydrogel composites with the same composition were prepared for comparison using non-intercalated kaolinite-urea mixtures.

Scheme III.1 describes the preparation of two types of kaolinite-hydrogel composites by using kaolinite-urea intercalate complexes and kaolinite not intercalated with urea.

## III.2. Materials and methods

### III.2.1. Materials

Acrylic Acid (AA, Aldrich, 99%) was distilled under vacuum to remove the polymerization inhibitor and stored in the freezer. N,N'–methylenebisacrylamide (MBA, Sigma Aldrich, 99%), ammonium persulfate (APS, Acros Organic, 98+%), sodium hydroxide (NaOH, Acros Organic, 98.5%), acrylamide (Am, Fluka, 98%), absolute ethanol 99%, 4-(dimethylamino)benzaldehyde (Aldrich 98%), hydrochloric acid (HCl, Fisher 37%), urea (Fisher, >99%) and Kaolin (KGa-1b; Georgia) were used without further purification.

### III.2.2. Kaolinite-urea intercalation

The mechanochemical intercalation of urea in the interlayer space of kaolinite was carried out in the same conditions than those described in Chapter 1. The samples prepared by mechanochemical intercalation in this chapter were kaolinite-urea complexes (KU) KU-25m%, KU-50m% KU-66m% and KU-80m% with m% the mass percentage of urea. For sample KU-25m%, the ball milling time was 2 hours and for the samples KU-50, 66, 80m%, the ball milling time was 1 hour. Table III.1 listed the m% of kaolin and urea in samples prepared.

Table III.1. List of kaolinite-urea complexes prepared by mechanochemical intercalation.

| KU samples | m% kaolin | m% urea |
|---|---|---|
| KU-25m% | 75 | 25 |
| KU-50m% | 50 | 50 |
| KU-66m% | 34 | 66 |
| KU-80m% | 20 | 80 |

### III.2.3. Preparation of the kaolinite-hydrogel composites with urea fertilizer p(AA-co-Am)/kaolinite/urea

A series of samples were prepared with different amounts of kaolinite-urea complex treated by mechanochemically intercalation, and with fixed amounts of acrylamide co-monomer (30 mol%), N,N'-methylenebisacrylamide (MBA) (0.75 mol%), 60% of neutralization degree of AA (with sodium hydroxide) and ammonium persulfate (APS) 0.75mol% (all mol% relative to AA). The total concentration of monomers was 2 mol/l. Stock solutions of Am 2.5 mol/l, MBA 0.12 mol/l, APS 0.1 mol/l and NaOH 10 mol/l were prepared. Acrylic acid solution 1.54 mol/l was first added to glass tube and appropriate quantities of Am, MBA, deionized water, NaOH and APS were successively added to obtain 0.46 mol/l Am, 15 mmol/l MBA and 15 mmol/l APS. The solution was purged for 5 minutes with nitrogen just before the introduction of the APS. The final solution was added to kaolinite-urea powder and mixed manually by shaking for few seconds and then placed in a water bath at 60°C. Before

gelation (ca. less than 5 minutes), the glass tube was shaken at regular intervals maintain a good dispersion of kaolinite. After the 3 hours of reaction, the glass tube was broken to recover the gel in the form of discs 1 cm thick. The discs were dried at 40°C in oven to constant weight. Lastly, the dried xerogel, was cryo-grinded and screened to a particle size of 30-50 mesh. In order to evaluate the effect of the intercalation of urea in kaolinite, kaolinite/urea hydrogel composites were prepared using non-intercalated kaolinite-urea mixtures. The composition of the hydrogel composite samples are summarized in Table III.2.

Table III.2. Composition of hydrogel composites prepared with kaolinite-urea intercalates, HG-KU-X-Y and with kaolinite/urea non-intercalated mixtures, HG-K-U-X-Y (not listed). X corresponds to the amount of urea (m%) in KU complex and Y is the mass % of KU relative to the mass of polymer.

| Sample Code | Polymer (m%) | Kaolin (m%) | Urea (m%) |
|---|---|---|---|
| HG-KU-25-2 | 98.0 | 1.5 | 0.5 |
| HG-KU-25-5 | 95.2 | 3.6 | 1.2 |
| HG-KU-25-20 | 83.3 | 12.5 | 4.7 |
| HG-KU-25-50 | 66.7 | 25 | 8.3 |
| HG-KU-50-2 | 98.0 | 1.0 | 1.0 |
| HG-KU-50-5 | 95.2 | 2.4 | 2.4 |
| HG-KU-50-20 | 83.3 | 8.3 | 8.3 |
| HG-KU-50-50 | 66.7 | 16.7 | 16.7 |
| HG-KU-66-2 | 98.0 | 0.7 | 1.3 |
| HG-KU-66-5 | 95.2 | 1.6 | 3.2 |
| HG-KU-66-20 | 83.3 | 5.6 | 11.1 |
| HG-KU-66-50 | 66.7 | 11.1 | 22.2 |
| HG-KU-80-2 | 98.0 | 0.4 | 1.6 |
| HG-KU-80-5 | 95.2 | 1.0 | 3.8 |
| HG-KU-80-20 | 83.3 | 3.3 | 13.3 |
| HG-KU-80-50 | 66.7 | 6.7 | 26.7 |

Hydrogel composites were also prepared without urea by varying the amount of kaolin (1 to 50m% relative to the mass of polymer) HG-K-m% and without kaolin by varying the amount of urea (1 to 50m% relative to the mass of polymer), HG-U-m%.

## III.2.4. Methods

### *III.2.4.1. Gel time.*

The gel time was measured by inverting test tube. When a test tube containing a solution is tilted, it is defined as a sol phase if the solution deforms by flow, or a gel phase if there is no flow.

### *III.2.4.2. Swelling measurements.*

The bag containing an accurately weighed specimen (0.1 g 300-500 µm particles) was immersed entirely in 500 mL deionized water at room temperature. After 5 hours immersion, the bag was removed from the solution, the excess of water was removed superficially with tissue paper and the bag was weighed. A balance with $10^{-4}$ g precision was used for weighing. The swelling ratio Q at equilibrium was calculated using equation (1).

$$Q = \frac{m_t - m_0}{m_0} \qquad (1)$$

Where $m_0$ is the weight of dry gel, $m_t$ is the weight of the swollen gel at equilibrium.

### *III.2.4.3. Water retention properties.*

A 0.1 g of xerogel was immersed in deionized water (500 mL) for 24h. The swollen hydrogel $M_0$ was placed at 40°C in an oven. For different intervals, the mass of remaining hydrogel was weighed and denoted by $M_t$. the water retention of the sample is calculated by using the equation (2).

$$WR(\%) = \frac{M_t}{M_0}.100 \qquad (2)$$

Were $M_t$ = weight hydrogel – (weight polymer + kaolinite) at t time and $M_0$ = weight hydrogel – (weight polymer + kaolinite) after swelling 24 hours in deionized water).

### *III.2.4.4. Release of urea from hydrogel-clay composite.*

The release of urea was studied by following the same method as that described in chapter 2. Each measurement was replicated three times and the average result was taken as the result.

Powder X-ray diffraction (XRD) analyses were carried out on a Siemens D5000 type diffractometer equipped with a vertical goniometer and diffracted beam monochromator. The radiation applied was Cu K$\alpha$ ($\lambda$=0.1541 nm) generated at 40 kV and 40 mA. The samples were measured in step scan mode with 0.04° step size and 4s step scan.

An elemental analysis instrument (Thermo Scientific, Flash 2000) was used to determine the contents of nitrogen and carbon element in dried gels before and after swelling different times in deionized water.

The Fourier-transform infrared (FTIR) spectra were recorded on a FTIR spectrometer Nexus, (ThermoNicolet) equipped with an attenuated total reflectance diamond crystal unit (Thermo Scientific Smart iTR). Spectra were acquired at a resolution of 4 $cm^{-1}$ over a spectral range of 600-4000 $cm^{-1}$.

## III.3. Results and discussion

Scheme III.1 resume the procedure adopted to prepare kaolinite hydrogel composites. In the one step process (1), urea loaded hydrogel composites are prepared by in situ polymerization after adding all ingredients individually. In the two steps process (2), urea was first mechanochemically intercalated in interlayers of kaolinite and then, the kaolinite-urea complex is added to the reaction mixture before polymerization and crosslinking. Urea was intercalated between interlayer of kaolinite in order to delay the release of urea in water. We used the denomination KU-m% for kaolinite urea samples mechanochemically ground and K-U-m% for samples obtained by simply mixing kaolin and urea together in the reaction mixture.

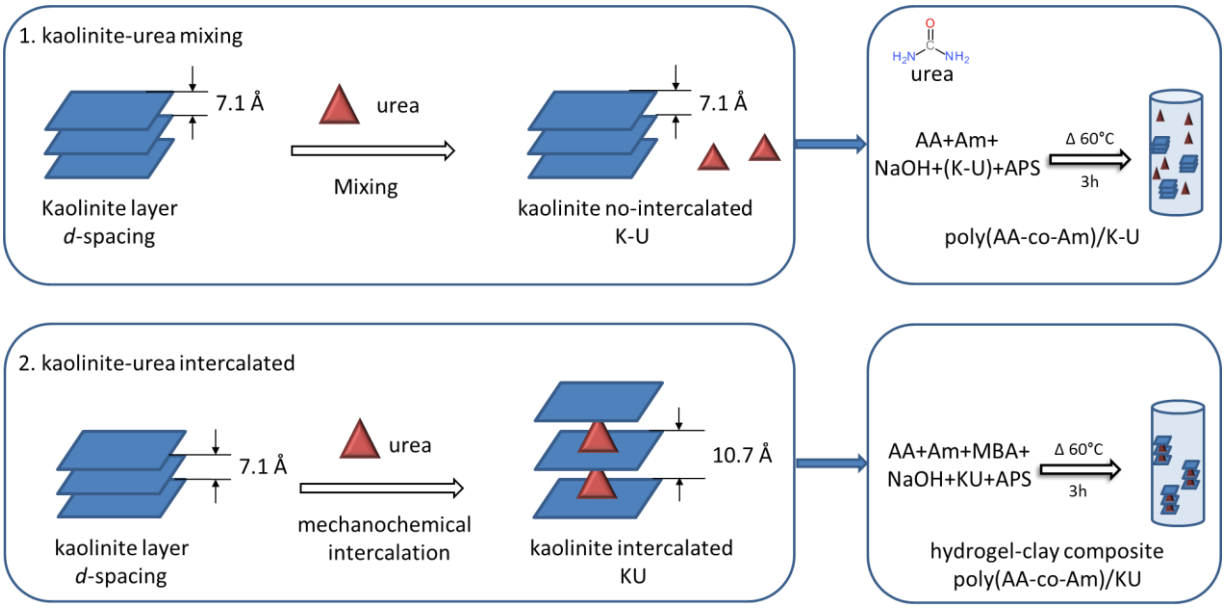


*Scheme III.1. A schematic presentation of the two routes for the preparation of poly(acrylic acid-co-acrylamide)/kaolinite-urea composite hydrogels.*

### III.3.1. Kaolinite-urea complexes

Firstly, we will study the kaolinite-urea complexes obtained by mechanochemical intercalation of urea in the interlayer of kaolinite using different amounts of urea. The amount of urea was varied in a wide range, from 25m% to 80m% as indicated in table III.1. The mechanochemical intercalation was operated by planetary ball mill in the same conditions than those described in Chapter 1. It is important to emphasize that the kaolin urea intercalates were incorporated without washing into the reaction mixture. The KU samples thus obtained contain an excess of non-intercalated urea increasing with the amount of urea used during grinding. This excess urea present at the outer surface of the kaolinite

sheets is likely to limit de-intercalation during polymerization and potentially combine two types of urea within the hydrogel: easily releasable urea and urea released over longer durations.

XRD patterns of kaolin and kaolin mechanochemically ground with urea at different mass% of urea, are shown in (Figure III.1). As noted in Chapter 1, we observed an agglomeration of the powder at a urea content of 80 m%: the powder stuck to the jar walls and the balls even after short milling times. In this case, the agglomerated powder was crushed by a pestle mortar by hand to obtain a fine powder. As reported by many studies (Makó et al., 2009, 2013), for pure kaolinite the d-value was 0.71 nm and after mechanochemical grinding, the d-value was shifted to 1.07 nm after intercalation of urea. The degree of intercalation α (%) was 94% for sample KU-25m%, 96% for KU-50m%, 99% for KU-66m% and 99% for KU-80m%. X-ray diffraction results thus confirm the nearly quantitative intercalation of urea in kaolinite. These complexes will be used for the synthesis of composite hydrogels. Considering that the amount of urea in the kaolinite urea intercalates is of the order of 25 m% (from the results in chapter 1), the percentage of non-intercalated (ie in excess) urea amounts to around 0 %, 33 m%, 54 m% and 73 m% for KU-25m%, KU-50m%, KU-66m% and KU-80m%, respectively.

Kaolinite-urea complexes were also studied by infrared spectroscopy. Pure kaolinite KGa-1b (Figure III.2,a) shows the typical infrared absorption bands of well-crystallized kaolinite. In the high wavenumber region (4000 to 3000 $cm^{-1}$), OH stretching bands observed at 3687, 3669 and 3651 correspond to inner surface hydroxyl groups while the band at 3619 $cm^{-1}$ corresponds to inner OH groups, usually not affected by intercalation. (Ledoux and White, 1966; Letaief and Detellier, 2005; Letaief et al., 2006). Intercalation of urea into kaolinite layers result in the striking reduction in intensity of the 3687, 3669 and 3651 $cm^{-1}$ absorption bands of kaolinite (Figure III.2,b c d e). As expected, the band at 3619 $cm^{-1}$ is not influenced by the interlamellar modification. The bands at 3440 $cm^{-1}$ and 3345 $cm^{-1}$ correspond to the NH stretching vibrations of urea. The intensity of these bands increase with the amount of urea in the KU complex.

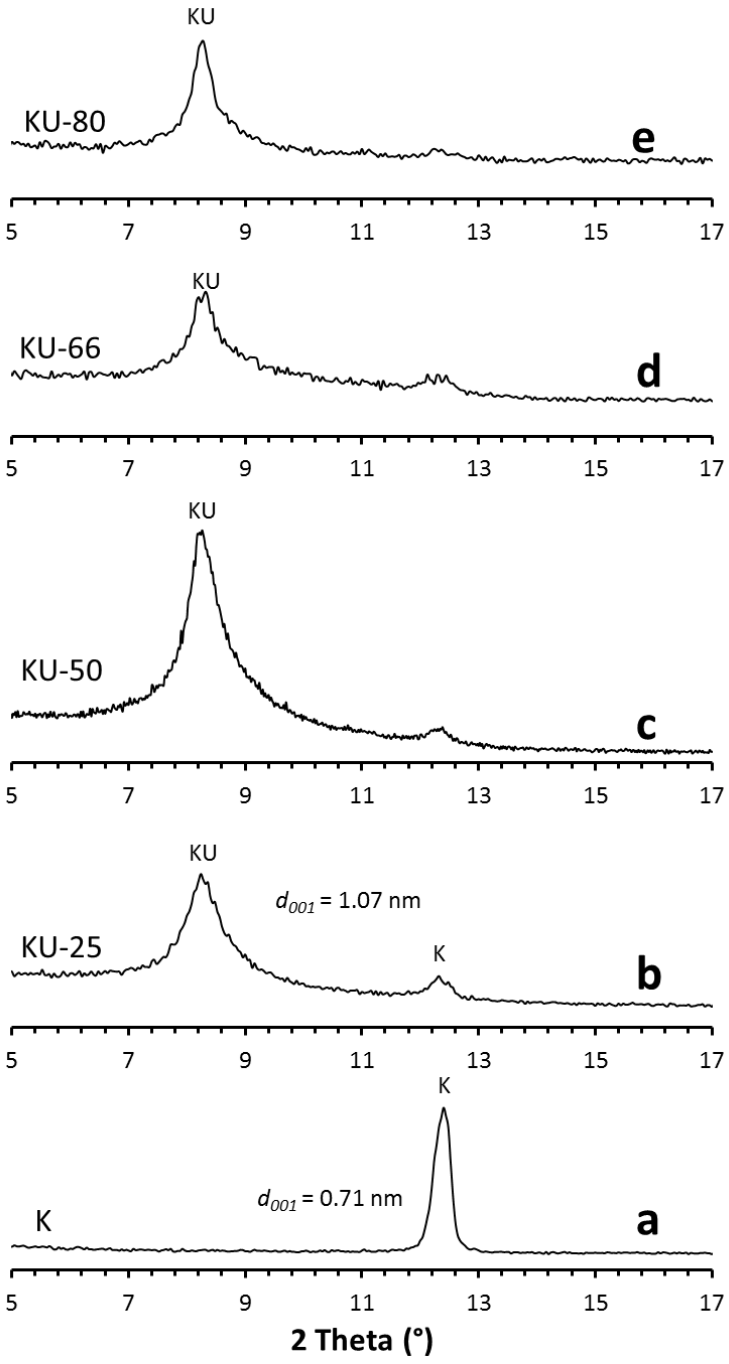


*Figure III.1. X-ray diffraction of (a) kaolin, kaolin mechanochemically ground with (b) 25m% urea (KU-25m%), (c) 50m% urea (KU-50m%) (d) 66 m% urea (KU-66m%) and (e) 80 m% urea (KU-80m%).*

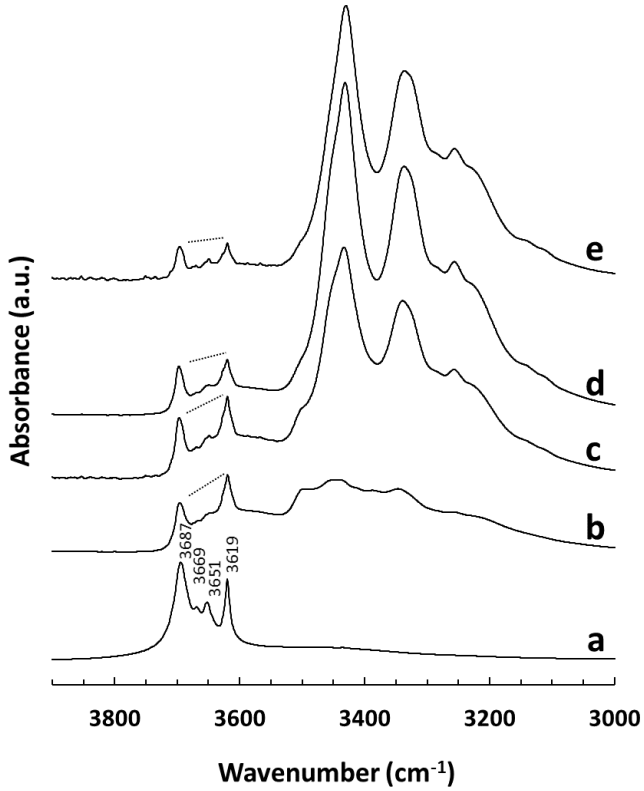


*Figure III.2. FTIR spectra of (a) kaolin, kaolin mechanochemically ground with (b) 25m% urea (KU-25m%), (c) 50m% urea (KU-50m%) (d) 66 m% urea (KU-66m%) and (e) 80 m% urea (KU-80m%).*

## III.3.2. Kaolinite-urea hydrogel composites

### *III.3.2.1. Preparation and physico-chemical characterization of hydrogel composites*

The incorporation of kaolin and urea is liable to modify the conditions of formation of the crosslinked polymer network. These effects were studied by measuring the gel time in the different reaction mixtures studied. First, the effect of adding kaolin alone or urea was studied (Figure III.3). Kaolin has a significant effect on gel time. The gel time decreases for low kaolin contents (less than 2%) and then increases until a gel time comparable to the unfilled polymer is reached. The kaolin incorporated in the reaction medium in a small proportion appears to be well dispersed with a translucent appearance of the gel obtained. On the other hand, the kaolin incorporated in high proportion leads to an opaque gel. Faster gelation in the presence of a small proportion of kaolin could be related to the hydrophilic nature of the kaolin surface which involves hydrogen bonds interactions with the polymer chains being formed and thus, play a role of physical crosslinking node contributing to the gelation of the medium reaction. Increasing amounts of kaolin lead to an agglomeration of the kaolinite which decreases the exchange surface with the polymer chains. On the other hand, a high level of kaolin can also partially block the diffusion of reactive species within the reaction medium, thus leading to an increase in the gel time. Unlike kaolin, the incorporation of urea did not induce a significant variation in the gel time.

The gel times measured on the composites prepared from the kaolin-urea complexes are shown in Figure III.4. There is no clear trend in the evolution of gel times with the content of KU complex in the various hydrogels. In all cases, gelation is rapid (less than 5 minutes) showing that the kaolin urea complex does not significantly modify the kinetics of the polymerization reactions and building of the 3D organic network. A fundamental point in this study is to ensure that the urea trapped between the kaolinite sheets is not partially or totally released in the reaction medium knowing that the reaction occurs in water and that urea has a high solubility in water. This risk is undoubtedly maximum before gelation and therefore the short gel times obtained constitute a positive aspect of the polymerization process retained in this study.

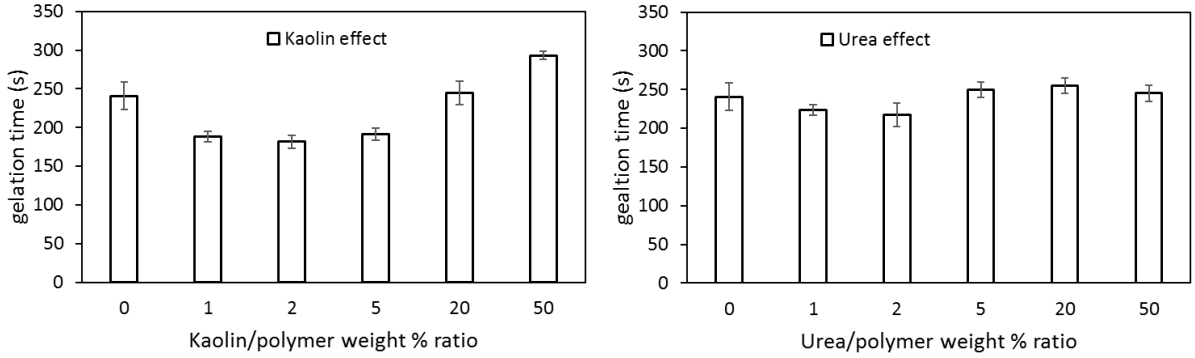


*Figure III.3. Gel times for kaolin hydrogel composites and urea loaded hydrogels.*

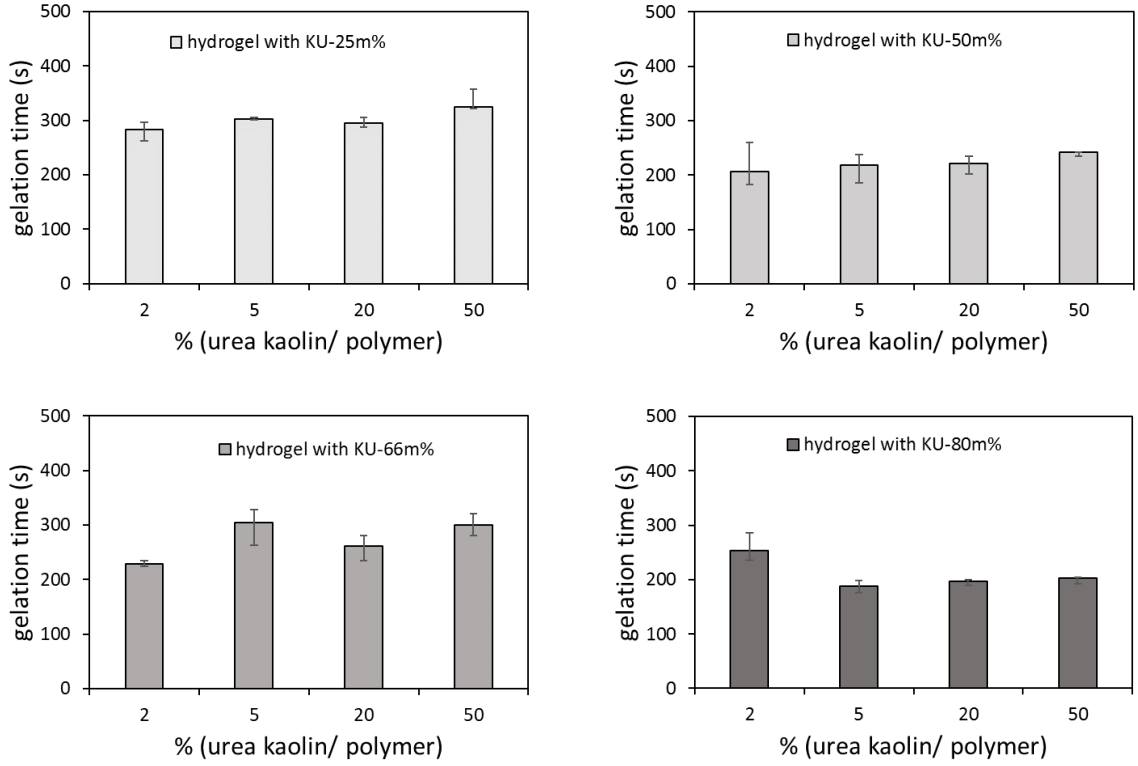


*Figure III.4. Gel times for kaolin-urea hydrogel composites based on kaolinite urea intercalates.*

The FTIR spectra of the hydrogel composites prepared by the one step and by the two step methods are shown in Figure III.5. As noted previously, the OH stretching region of kaolinite is very sensitive to the effects of interlayer modification. For hydrogel built by mixing kaolinite and urea without mechanochemical intercalation (Figure III.5,e), the relative intensity of the inner and surface hydroxyl groups at 3619 and 3687 $cm^{-1}$ remains identical to that of pure kaolinite. Therefore, urea was not intercalated during the mixing of ingredients or during the *in-situ* polymerization. On the contrary, the infrared spectrum of the hydrogel composite prepared by the two steps method shows the band at 3687 $cm^{-1}$ still having a lower intensity than the band at 3619 $cm^{-1}$. This indicates that the inner surface OH groups of kaolinite are still in interaction with urea and, consequently, that urea is still intercalated in the interlayer space of kaolinite.

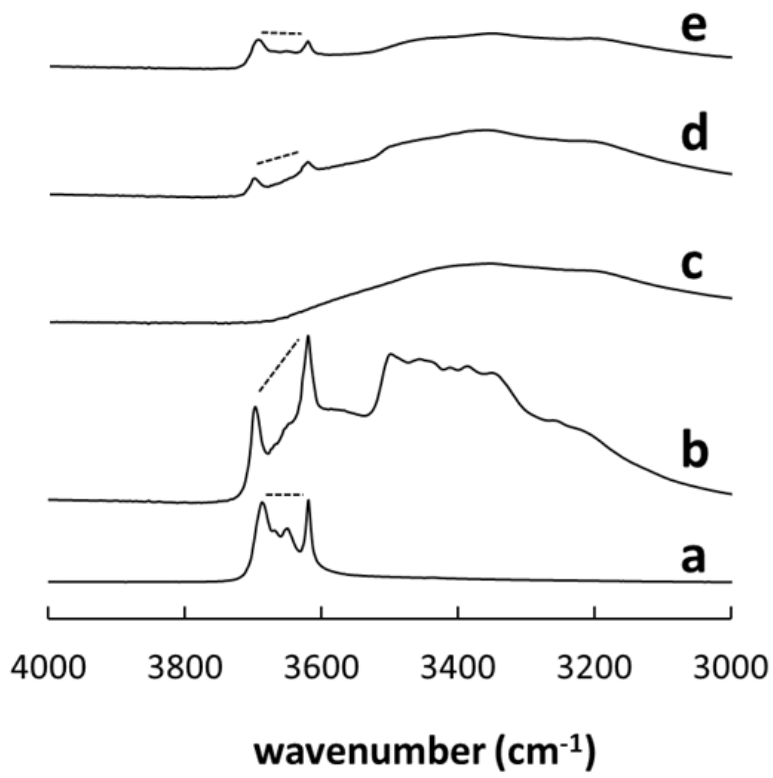


*Figure III.5. The FTIR spectra (4000-3000 $cm^{-1}$) of kaolinite (a), kaolinite-urea intercalated KU-25m% (b), poly(AA-co-Am) hydrogel (c), hydrogel composite HG-KU-25-50 prepared by the two steps method and (d) hydrogel composite HG-K-U-25-50 prepared by the one step method).*

The X-ray diffraction patterns of the hydrogel composites prepared by the on step and by the two steps method are shown in Figure III.6. The hydrogel composite prepared by the one step method shows the characteristic non-expanded (001) reflection of kaolinite at 0.71 nm. Urea was thus not intercalated during the *in-situ* polymerization process. On the contrary, the hydrogel composite prepared by the

two steps method still shows the (001) reflection at 1.07 nm characteristic of urea kaolinite intercalates. XRD results are in agreement with FTIR analysis.

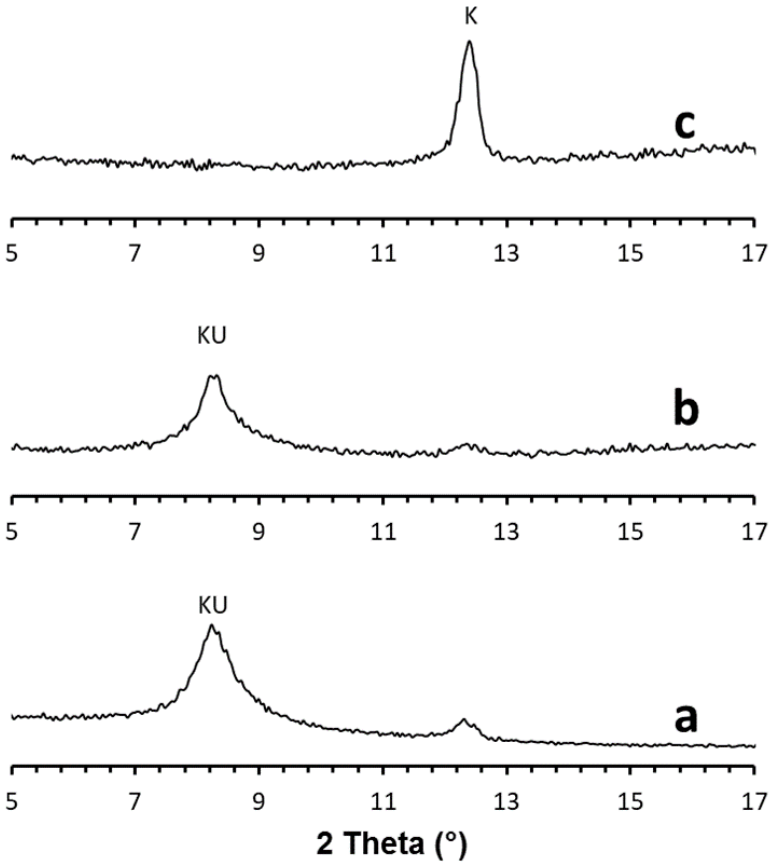


*Figure III.6. X-ray diffraction pattern of (a) kaolinite-urea intercalate, KU-25m%, (b) hydrogel composite prepared with KU-25m% and (c) hydrogel composite prepared by the one step method (mixing kaolinite and urea directly in the reaction mixture).*

### *III.3.2.2. Swelling properties*

The swelling ratio of hydrogel composites was studied by the tea bag method. The effect on swelling ratio of kaolin content, urea content intercalated KU complex and not intercalated K-U content in the hydrogel composites was successively investigated (Figure III.7, Figure III.8 and Figure III.9). The swelling ratio did not change significantly at low kaolin loadings (below 5 m%) but it significantly decreased at higher loadings. In general, increasing the amount of kaolin in hydrogels decrease the swelling ratio (W.-M. Cheng et al., 2017, Liang, 2007 ). At low loadings, kaolinite is well dispersed and water certainly interacts with the external surface of kaolinite particles. The physical nodes between kaolinite and polymer chains are certainly broken when the water molecules accumulate in the swollen hydrogel and, thus, do not lead to a decrease in swelling ratio. At high kaolin loadings, kaolin particles are more agglomerated and water can not have access to the whole surface of agglomerated particles.

This leads to a decrease in the swelling ratio. Urea alone also resulted in a decrease in swelling ratio when added at a high content as already noted in Chapter 2. In the case of hydrogel composites prepared from the kaolin-urea intercalates, the swelling ratio does not decrease even at high loadings of kaolinite. There is even a significant increase in the swelling ratio at intermediate loadings of kaolin, (see for example the sample HG-KU-25-20). Such evolution has been noted in the literature with more expandable clays than kaolinite such as bentonite (Cheng et al, 2017). This suggests that kaolinite in these samples is more well-dispersed than in the hydrogel composites obtained without urea. It is noteworthy that the swelling ratio of hydrogel composites obtained by the one step method significantly decreased at high kaolinite loadings. These results suggest that the high swelling degree of high loaded kaolinite urea hydrogel composites prepared from KU intercalates is related to the presence of urea in the interlayer space. The expansion of the kaolinite by urea allows an easier access to the interlayer space to water molecules. This can be combined with a partial exfoliation after long times swelling in water. XRD patterns of the two types of hydrogel composites after 24 hours swelling are shown in Figure III.10. After swelling for 24 hours, the intensity of the (001) reflection strongly decreased in the case of the hydrogel composite prepared by the two step method. This is not accompanied by an increasing intensity of the 0.71 nm reflection, related to the collapsed kaolinite. On the contrary, the composite prepared by the one step method still shows the same XRD pattern after swelling than before swelling, related to unexpanded kaolinite. The XRD analysis of the hydrogels after swelling for 24 hours in water thus confirmed the partial exfoliation of kaolinite in the case of hydrogel composites prepared by the two step method. As seen in Chapter 1, when KU-25m% was immersed alone in deionized water, hydrates of kaolinite are formed. On the contrary, when the KU-25m% was introduced into the matrix hydrogels before immersion in water, the hydrates of the kaolinite are not formed because kaolinite interlayer was partially exfoliated. This suggests that the partial exfoliation of the kaolin sheets is associated with the hydrophilicity of the polymer network and its superabsorbent properties. It thus seems that the stresses generated during the swelling of the polymer would promote the exfoliation of the kaolinite.

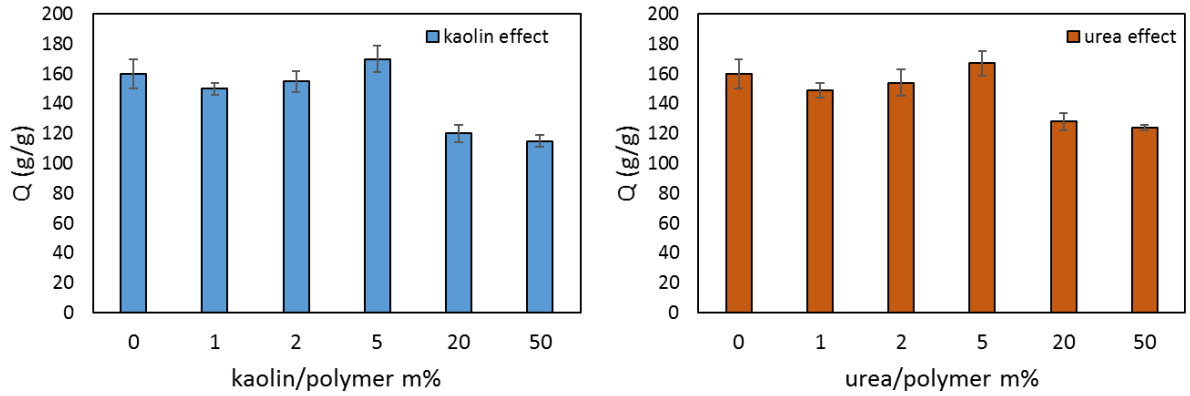


*Figure III.7. The effect of kaolin and urea content on the swelling ratio of poly(acrylic acid-co-acrylamide) hydrogels.*

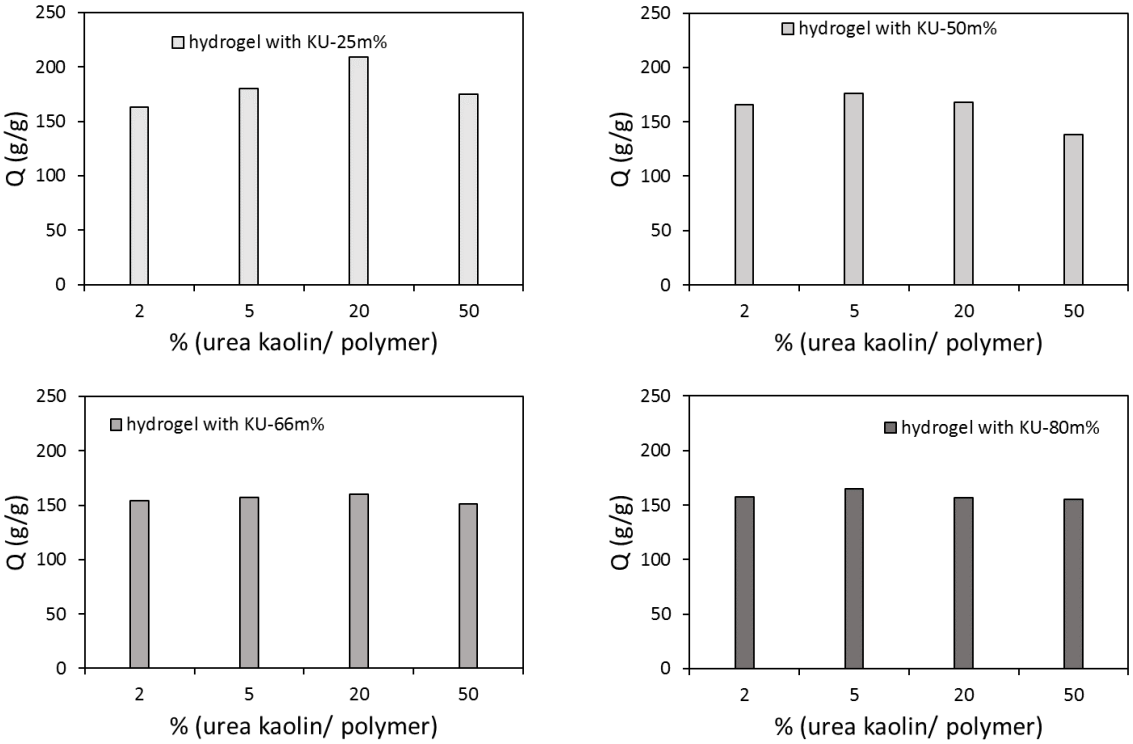


*Figure III.8. Swelling ratio of hydrogel composites prepared by the two step method with KU-25m%, KU-50m%, KU-66m%, KU-80m%, as a function of KU-m% in the composite.*

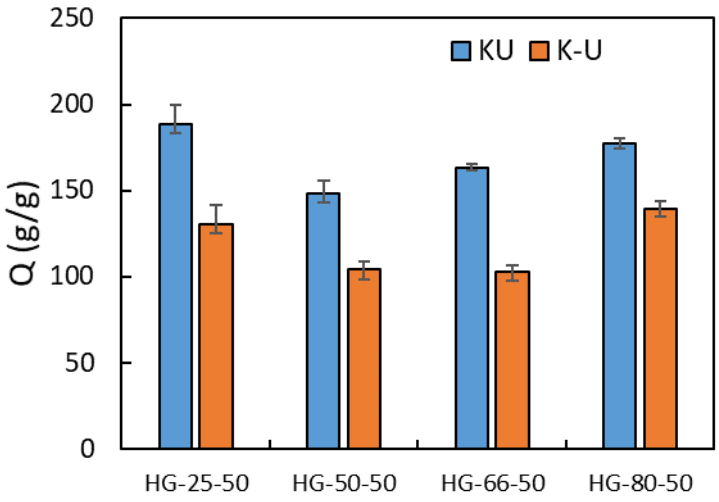


*Figure III.9. Comparison of the swelling ratio of hydrogel composites prepared by the two step method (based on KU intercalates) with those prepared by the one step method.*

The graph in Figure III.10,c,d presented the hydrogel prepared with mixed without intercalation kaolinite urea. In this case the (001) reflection was not perturbed after polymerization and after 24 hours in deionized water (0.71 nm).

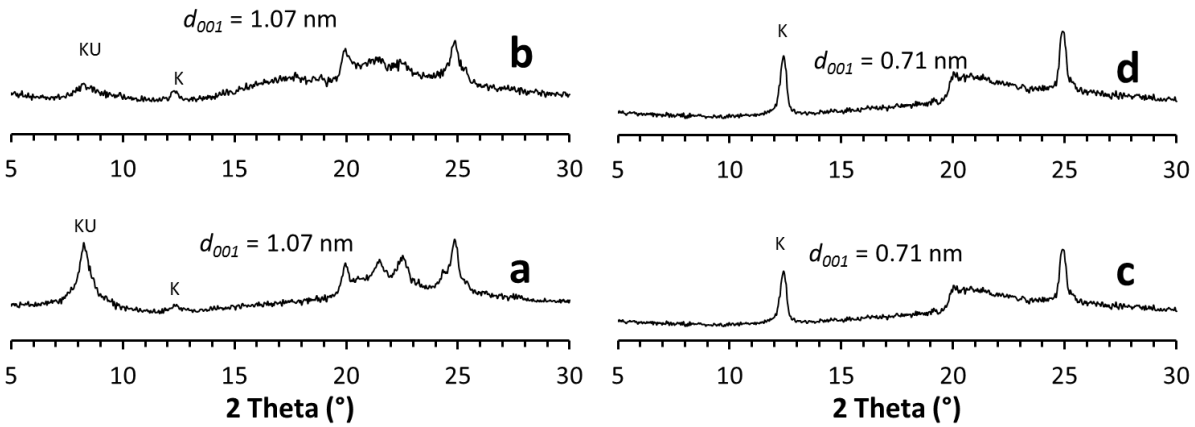


*Figure III.10. X-ray diffraction (2θ = 5°-30°) of (a) xerogel HG-KU-25-50, (b) xerogel HG-KU-25-50 after 24h swelling in deionized water, (c) xerogel HG-K-U-25-50 and (d) HG-K-U-25-50 after 24h swelling in deionized water.*

### *III.3.2.3. Water retention properties*

In drought periods the water retention capacity of hydrogels is essential in order to keep the water as long as possible for plants. For this purpose many studies are looking into this aspect (Liang and Liu,

2006; Abedi-Koupai et al., 2008; Jamnongkan and Kaewpirom, 2010; Jin et al., 2011; Yang et al., 2013; Xiang et al., 2017). A large quantity of studies investigated water retention capacity of hydrogels in soil at room temperature. This implies that the monitoring of water loss until dryness is done for days. In our work, the water retention capacity was measured by placing the swelled hydrogels in oven at 40°C, desorption takes place for hours.

Figure III.11 shows the % water retention as a function of time for hydrogel composites prepared by the one step method and those prepared by the two step method. Hydrogels composites prepared with KU-25m%, K-U-25m%, KU-66m% and K-U-66m%, were investigated. After 22 hours drying time, hydrogel composite HG-KU-25-50 and HG-K-U-25-50 retained respectively 40% and 26% of water. And HG-KU-66-50 retains 13% more water compared to HG-K-U-66-50.

Hydrogels prepared with kaolin urea intercalates have a better ability to retain water than samples prepared by simply mixing individual ingredients. This can be explained on the one hand by the partial exfoliation during the swelling of the hydrogels prepared with the kaolin urea intercalates. This exfoliation is likely to increase the diffusion path of the water molecules and therefore to delay the departure of the water. Besides, the results associated with the study of the release of urea (see following part) indicated a higher residual urea content after 24 hours of swelling in the case of the samples prepared from the KU intercalates. The osmotic pressure associated with the presence of urea in the hydrogels is therefore higher in this case, which can also help to retain more water within the swollen gel. It is also noted that the amount of kaolin urea strongly impacts the capacity of hydrogels to retain water. For all the systems studied, this capacity to retain water increases with the amount of kaolinite urea and reaches an optimum at a KU loading of 20 m%. Beyond 20 m%, the capacity to retain water decreases. It is thus noted that the capacity to retain water of the hydrogels HG-KU-25-20 and HG-KU-50-20 is the highest of all the samples tested and that it is in particular higher than the uncharged hydrogel (Figure III.12, Figure III.13 and Figure III.14).

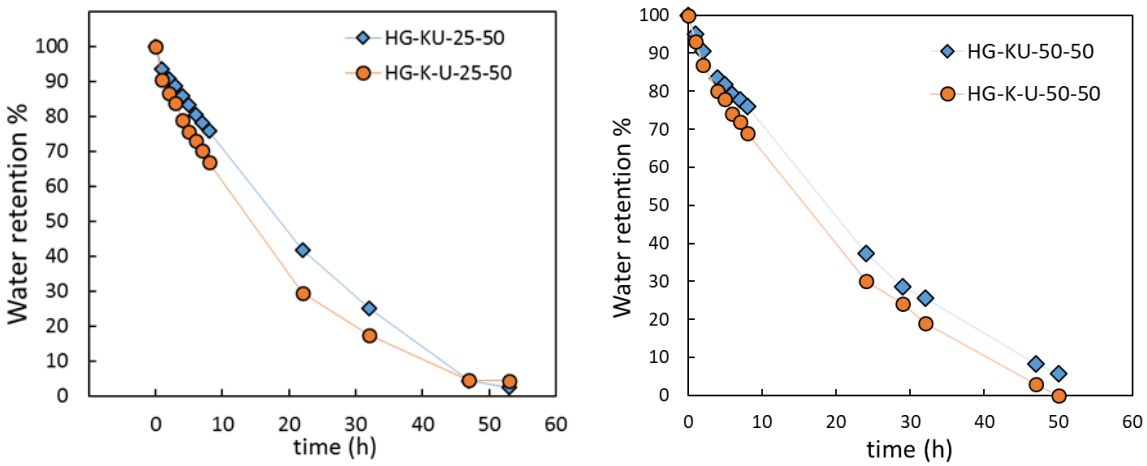

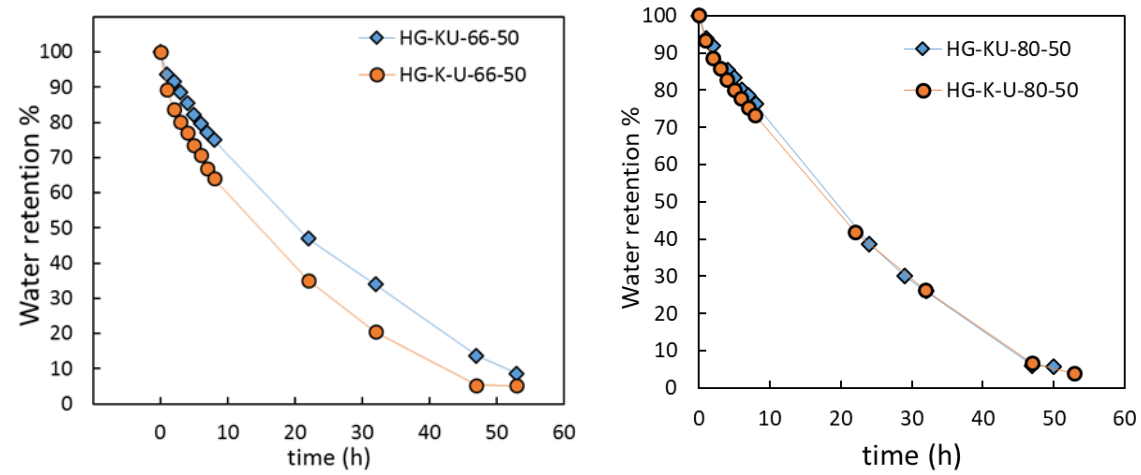


*Figure III.11. Water retention capacity at 40°C of hydrogel composites prepared by the one step method (HG-K-U-25-20, HG-K-U-50-20, HG-K-U-25-50 and HG-K-U-66-50) and by the two step method (HG-KU-25-20, HG-KU-50-20, HG-KU-25-50 and HG-KU-66-50).*

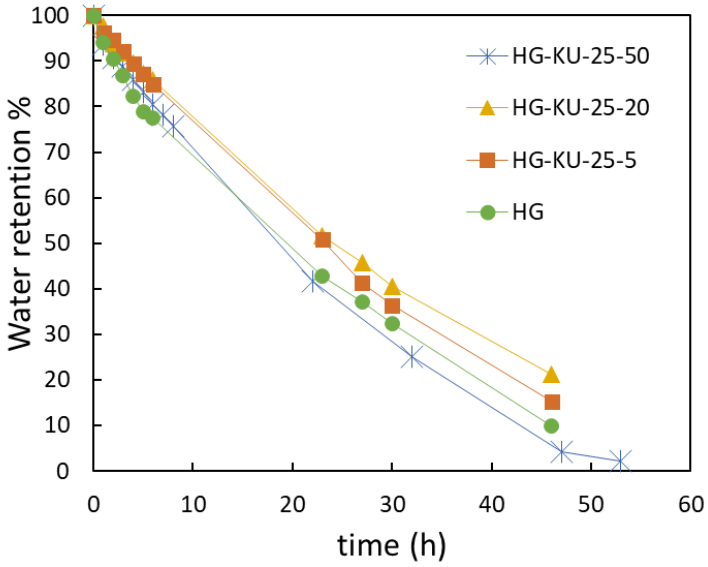


*Figure III.12. Water retention capacity at 40°C of hydrogel composites prepared by the two step method with different KU-25 m% loadings (0, 5, 20 and 50 m%).*

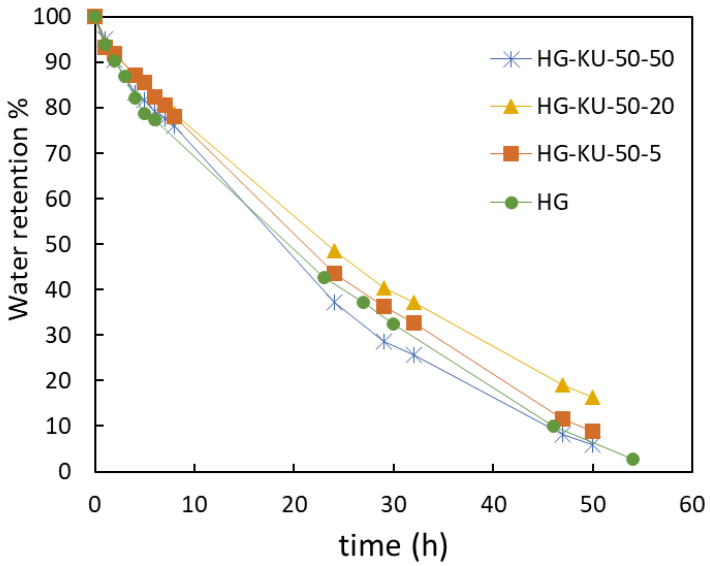


*Figure III.13. Water retention capacity at 40°C of hydrogel composites prepared by the two step method with different KU-50 m% loadings (0, 5, 20 and 50 m%).*

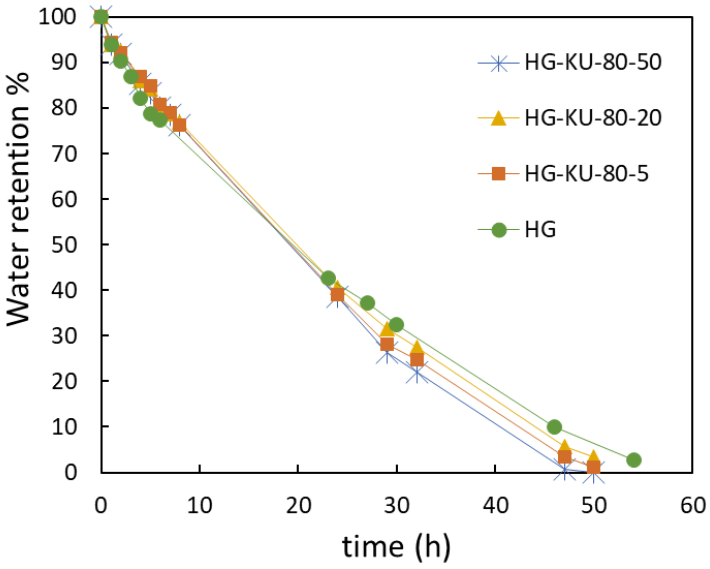


*Figure III.14. Water retention capacity at 40°C of hydrogel composites prepared by the two step method with different KU-80 m% loadings (0, 5, 20 and 50 m%).*

### *III.3.2.4. Release properties*

The release of urea from p(AA-co-Am) hydrogel composites was done by spectrophotometric determination of the amount of urea released in water using a method adapted from the Watt's method (Watt and Chrisp, 1954).

Firstly, we studied the release of urea for the kaolin urea complex at 25% by weight of urea and we compared it to the manual mixing of kaolin and urea in the same proportions as the complex. The results are shown in Figure III.15. It is observed that the release kinetics are slower in the KU complex than in the mixture ground manually. The urea is completely released in just 10 minutes in the case of the manually ground mixture while 90 minutes are required in the case of the KU complex. The intercalation of urea between the kaolinite sheets therefore makes it possible to slow down the release kinetics of urea.

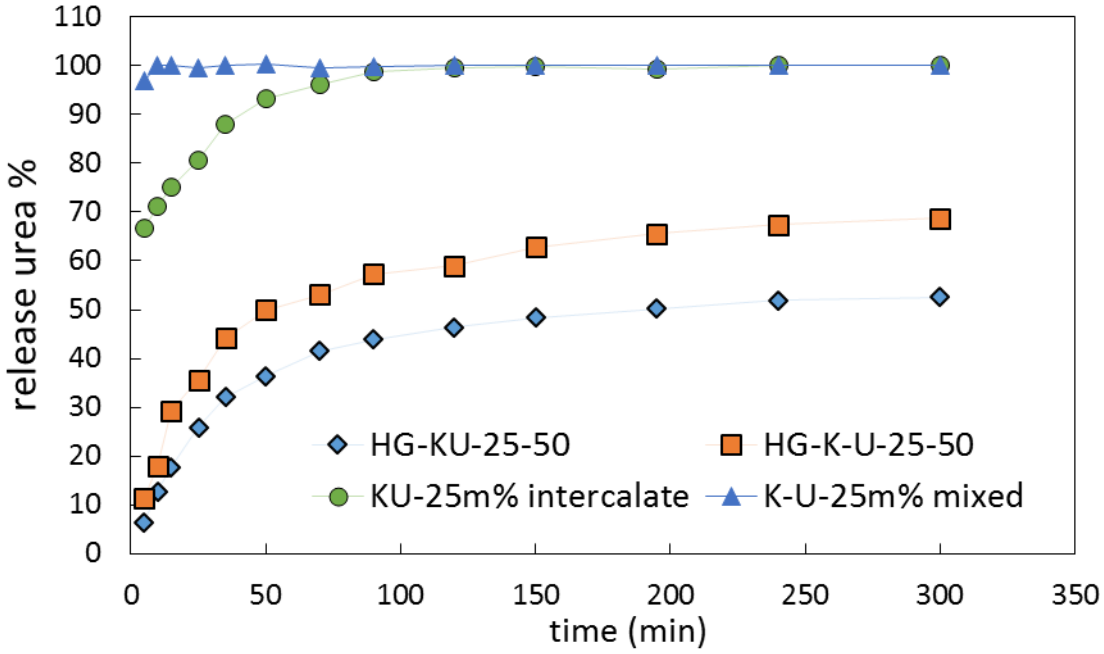


*Figure III.15. Urea release curves in deionized water for the KU complex, KU-25m%, for kaolin urea mixture (25 m%) obtained by manual grinding and for hydrogel composites prepared by the one step method (HG-K-U-25-50) and by the two step method (HG-KU-25-50).*

The kinetics of urea release in the composite hydrogels were then studied. Release curves for composites prepared from kaolin urea complexes (25m%), i.e. according to the two-step method and for composites of the same composition but prepared by simple mixing of the individual ingredients (one-step method) are shown in Figure III.16. It is clear that the incorporation of urea into a hydrogel matrix makes it possible to reduce the release kinetics. It is also observed that the kinetics are slower when the urea is incorporated into a kaolin urea intercalate than when it is directly in contact with the polymer hydrogel matrix. The release kinetics were prolonged over long periods in order to assess

whether all of the incorporated urea is releasable or if part of the incorporated urea is not releasable, for example, due to its partial decomposition during the formation and/or drying of the composite (thermally activated hydrolysis) or due to chemical bonds established with the constituents of the hydrogel.

A slow but continuous release is observed over long periods of time. This result is particularly interesting for the targeted application because it indicates that the plants will have a progressive nutrient supply over long periods of time. In addition to the results obtained from the spectrophotometric analysis, Figure III.16 indicates two measurement points resulting from the elementary analysis of C, H and N elements. There is a very good agreement between the two methods. Urea is completely released in 83 hours in the case of the hydrogel prepared by the one-step method and in 120 hours for the hydrogel prepared in two steps, i.e. from the kaolin urea intercalates. Consequently, there is no loss of urea or all of the urea incorporated is therefore released, which is advantageous in terms of cost efficiency of the process. The diffusion coefficient D of urea was calculated from equation (3) detailed in chapter 2.

$$D = \frac{(KC_0r_0)^2}{(2C_0 - C_s)C_s} \qquad (3)$$

The D values shown in Table III.3 indicate a diffusion coefficient twice as low for the composite prepared from the kaolin urea intercalate. On the other hand, the diffusion coefficient of the composite obtained by mixing the individual ingredients is close to the diffusion coefficient of the hydrogel polymer not comprising kaolin. This result could suggest that the slower release with the composite loaded with the kaolin-urea intercalate would be due mainly to a slower release of the intercalated urea. However, it should be remembered that the state of dispersion of kaolin in the two types of composites is different and that this can also have an impact on the release kinetics of urea.

Table III.3. Diffusion coefficient of hydrogels

| samples | HG-KU-25-50 | HG-K-U-25-50 | HG-U-50 |
|---|---|---|---|
| D ($cm^2/s$) x $10^{-9}$ | 3.9 | 7.6 | 7.5 |

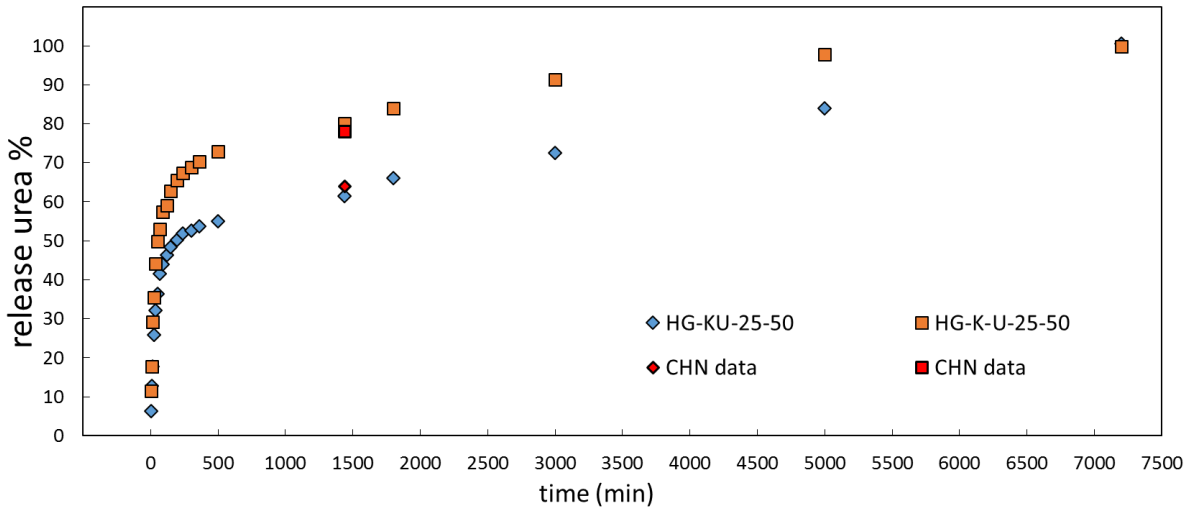


*Figure III.16. Release of urea from hydrogel composites HG-KU-25-50 and HG-K-U-25-50 in deionized water over long release times.*

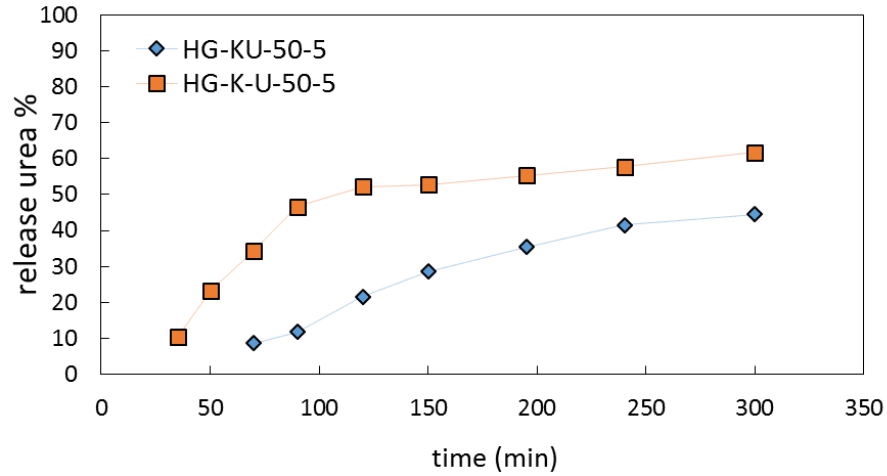


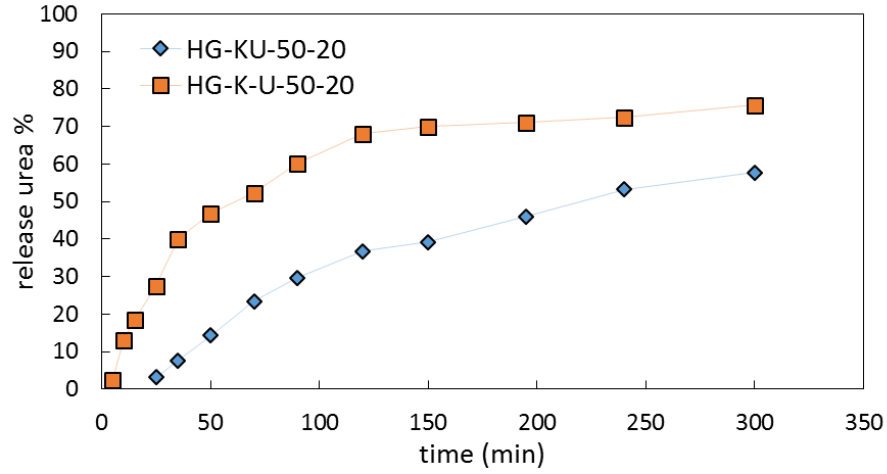

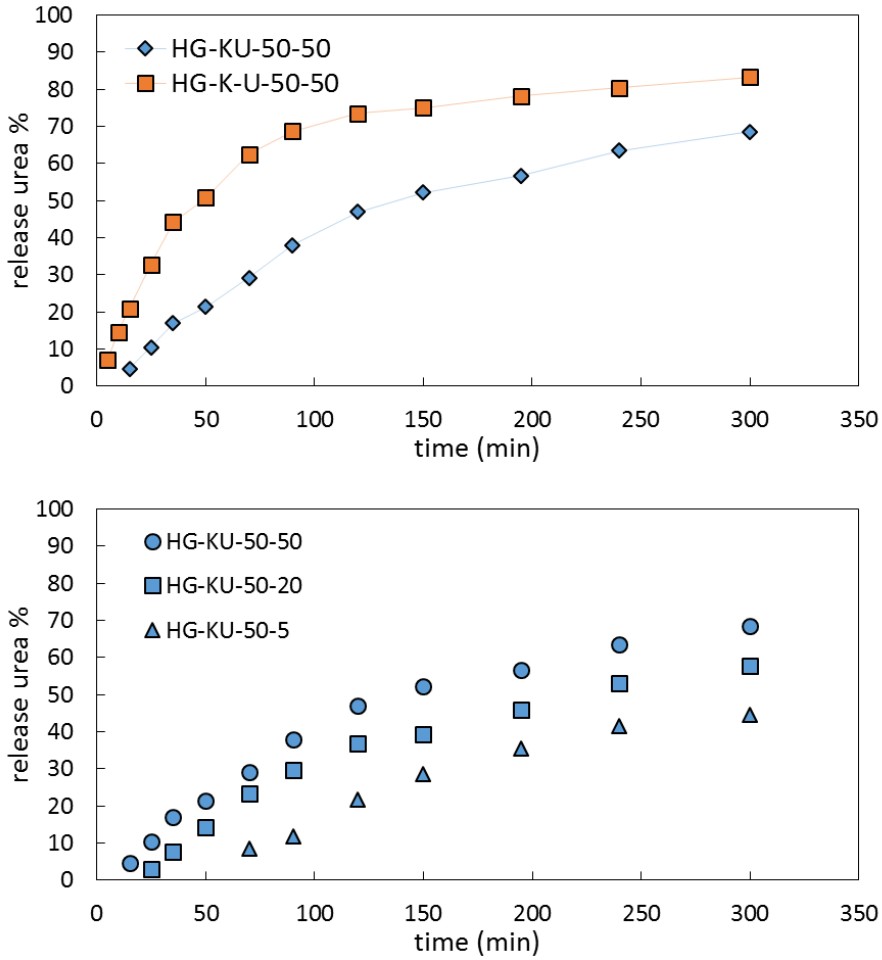


*Figure III.17. The comparison of urea release curves for hydrogel composites prepared from KU-50m% intercalates and from K-U-50m% with different KU (and K-U) loadings*

Figure III.17 illustrates the effect of the kaolin-urea loading rate on the urea release kinetics is illustrated in the case of the composites prepared from the kaolin urea complexes at 50% by mass of urea, KU-50. The results of Figure III.17 confirm that urea is released more slowly in the case of composites prepared by the two-step method compared to composites prepared by the one-step method. On the other hand, the release rate seems to increase with the loading rate and therefore with the quantity of urea and kaolin present in the hydrogel. The low urea rate of the HG-KU-50-5 composite (2.4 m% urea) explains the absence of measurement points on the release curve because the released urea rate cannot be measured because we are in this case at the limit of sensitivity of the method. It is noteworthy that the swelling ratio for all the HG-KU-50 composites reached values greater than 100 after only 5 to 10 minutes of immersion in water. The above results are therefore not correlated with different swelling kinetics between these composites. The swelling kinetics of the hydrogels in this study therefore does not appear to be a determining factor explaining the differences observed in the release curves as a function of the kaolin level in the composites. The urea

concentration gradient between the hydrogel and the surrounding solution increases with the kaolin-urea content of the composites. This could explain the lower urea flux obtained in the case of the HG-KU-5 composite. Figure III.18 shows the release curves for the composites prepared from kaolin-urea at 66% by mass of urea and at 80 m% of urea. Again, the release is slower with the composites prepared with the kaolin-urea intercalates.

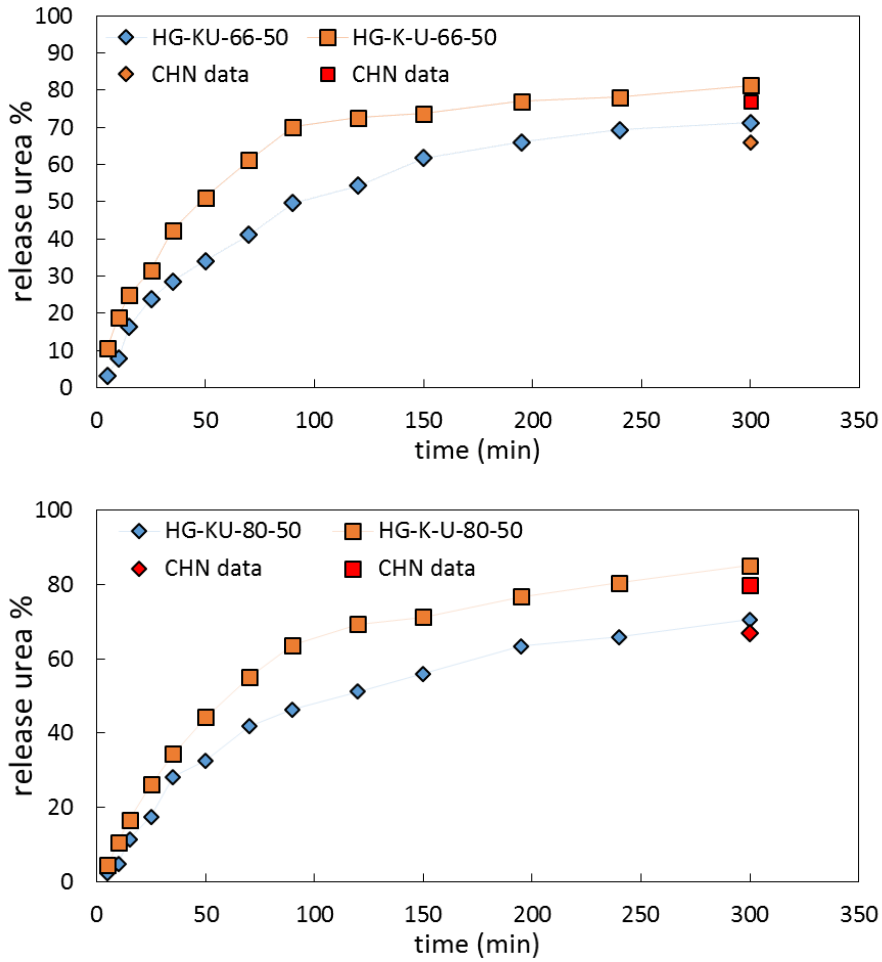


*Figure III.18. The comparison of urea release curves for hydrogel composites prepared from KU-66m%, K-U-66m%, KU-80m% and K-U-80m%*

## III.4. Conclusion

Poly(acrylic acid-co-acrylamide) hydrogel composites have been prepared by in situ polymerization by incorporating in the reaction medium either a kaolin-urea intercalate or kaolin and urea independently. Kaolin urea intercalates with different urea content were prepared in short time by mechanochemical grinding using a planetary ball mill. Gelation occurs in a few minutes in all cases showing that the kaolin and urea do not hinder the formation of the 3D polymer network. The two preparation methods lead to different properties in terms of swelling, water retention and urea release kinetics. Swelling results show a significant decrease in the swelling ratio in composites prepared by simple mixing of individual components. This is due to an agglomeration of the kaolin which decreases the water absorption capacity of the composites compared to the uncharged hydrogel. On the contrary, the composites prepared from the KU intercalates leads to swelling ratio es most often close to the polymer matrix. A significant increase in swelling is even observed at an intermediate loading ratio of 20% with the kaolin - urea (25 m%) intercalate. This was explained by the expansion of the kaolinite by urea which allows an easier access to the interlayer space to water molecules. It is also explained by a partial exfoliation after long times swelling in water as suggested by XRD analysis. Moreover, hydrogel composites prepared with kaolin urea intercalates have a better ability to retain water than samples prepared by simply mixing individual ingredients. This was mainly related to the better dispersion of kaolinite in the former case which results in a more tortuous path for water molecules. Finally, we found that the release of urea from the hydrogel composites prepared with the KU intercalates is slower than with the composite prepared by the one-step method. This slow release is related to embedding of KU with the hydrogel matrix together with the urea location in the interlayer space of kaolinite.

## III.5. References

Abedi-Koupai, J., Sohrab, F., Swarbrick, G., 2008. Evaluation of Hydrogel Application on Soil Water Retention Characteristics. Journal of Plant Nutrition 31, 317–331. https://doi.org/10.1080/01904160701853928

Ahmed, E.M., 2015. Hydrogel: Preparation, characterization, and applications: A review. Journal of Advanced Research 6, 105–121. https://doi.org/10.1016/j.jare.2013.07.006

AlShamaileh, E., Al-Rawajfeh, A.E., Alrbaihat, M., 2018. Mechanochemical Synthesis of Slow-Release Fertilizers: A Review. The Open Agriculture Journal 12. https://doi.org/10.2174/1874331501812010011

Azeem, B., KuShaari, K., Man, Z.B., Basit, A., Thanh, T.H., 2014. Review on materials & methods to produce controlled release coated urea fertilizer. Journal of Controlled Release 181, 11–21. https://doi.org/10.1016/j.jconrel.2014.02.020

Borges, R., Brunatto, S.F., Leitão, A.A., Carvalho, G.S.G.D., Wypych, F., 2015. Solid-state mechanochemical activation of clay minerals and soluble phosphate mixtures to obtain slow-release fertilizers. Clay Minerals 50, 153–162. https://doi.org/10.1180/claymin.2015.050.2.01

Bortolin, A., Serafim, A.R., Aouada, F.A., Mattoso, L.H.C., Ribeiro, C., 2016. Macro- and Micronutrient Simultaneous Slow Release from Highly Swellable Nanocomposite Hydrogels. J. Agric. Food Chem. 64, 3133–3140. https://doi.org/10.1021/acs.jafc.6b00190

Campos, E.V.R., Oliveira, J.L. de, Fraceto, L.F., Singh, B., 2015. Polysaccharides as safer release systems for agrochemicals. Agron. Sustain. Dev. 35, 47–66. https://doi.org/10.1007/s13593-014-0263-0

Cheng, D., Liu, Y., Yang, G., Hao, G., Wang, Y., Zhang, A., 2017. Preparation of low cost superabsorbent hydrogel by urea and acrylic acid. Materials Letters 204, 16–18. https://doi.org/10.1016/j.matlet.2017.05.136

Cheng, D., Liu, Y., Yang, G., Zhang, A., 2018. Water- and Fertilizer-Integrated Hydrogel Derived from the Polymerization of Acrylic Acid and Urea as a Slow-Release N Fertilizer and Water Retention in Agriculture. J. Agric. Food Chem. 66, 5762–5769. https://doi.org/10.1021/acs.jafc.8b00872

Cheng, W.-M., Hu, X.-M., Zhao, Y.-Y., Wu, M.-Y., Hu, Z.-X., Yu, X.-T., 2017. Preparation and swelling properties of poly(acrylic acid-co-acrylamide) composite hydrogels. e-Polymers 17, 95–106. https://doi.org/10.1515/epoly-2016-0250

Cipriano, B.H., Banik, S.J., Sharma, R., Rumore, D., Hwang, W., Briber, R.M., Raghavan, S.R., 2014. Superabsorbent Hydrogels That Are Robust and Highly Stretchable. Macromolecules 47, 4445–4452. https://doi.org/10.1021/ma500882n

Frost, R.L., Makó, É., Kristóf, J., Horváth, E., Kloprogge, J.T., 2001. Mechanochemical Treatment of Kaolinite. Journal of Colloid and Interface Science 239, 458–466. https://doi.org/10.1006/jcis.2001.7591

Guo, M., Liu, M., Hu, Z., Zhan, F., Wu, L., 2005. Preparation and properties of a slow release NP compound fertilizer with superabsorbent and moisture preservation. J. Appl. Polym. Sci. 96, 2132–2138. https://doi.org/10.1002/app.21140

Jamnongkan, T., Kaewpirom, S., 2010. Potassium Release Kinetics and Water Retention of Controlled-Release Fertilizers Based on Chitosan Hydrogels. J Polym Environ 18, 413–421. https://doi.org/10.1007/s10924-010-0228-6

Jin, S., Yue, G., Feng, L., Han, Y., Yu, X., Zhang, Z., 2011. Preparation and Properties of a Coated Slow-Release and Water-Retention Biuret Phosphoramide Fertilizer with Superabsorbent. J. Agric. Food Chem. 59, 322–327. https://doi.org/10.1021/jf1032137

Kim, K.S., Park, M., Choi, C.L., Lee, D.H., Seo, Y.J., Kim, C.Y., Kim, J.S., Yun, S.-I., Ro, H.-M., Komarneni, S., 2011. Suppression of NH<Subscript>3</Subscript> and N<Subscript>2</Subscript>O emissions by massive urea intercalation in montmorillonite. J Soils Sediments 11, 416–422. https://doi.org/10.1007/s11368-010-0326-z

Ledoux, R.L., White, J.L., 1966. Infrared studies of hydrogen bonding interaction between kaolinite surfaces and intercalated potassium acetate, hydrazine, formamide, and urea. Journal of Colloid and Interface Science 21, 127–152. https://doi.org/10.1016/0095-8522(66)90029-8

Letaief, S., Detellier, C., 2005. Reactivity of kaolinite in ionic liquids : preparation and characterization of a 1-ethyl pyridinium chloride–kaolinite intercalate. Journal of Materials Chemistry 15, 4734–4740. https://doi.org/10.1039/B511282F

Letaief, S., Elbokl, T.A., Detellier, C., 2006. Reactivity of ionic liquids with kaolinite: Melt intersalation of ethyl pyridinium chloride in an urea-kaolinite pre-intercalate. Journal of Colloid and Interface Science 302, 254–258. https://doi.org/10.1016/j.jcis.2006.06.008

Liang, R., Liu, M., 2007. Preparation of poly(acrylic acid-co-acrylamide)/kaolin and release kinetics of urea from it. J. Appl. Polym. Sci. 106, 3007–3015. https://doi.org/10.1002/app.26919

Liang, R., Liu, M., 2006. Preparation and Properties of a Double-Coated Slow-Release and Water-Retention Urea Fertilizer. J. Agric. Food Chem. 54, 1392–1398. https://doi.org/10.1021/jf052582f

Makó, É., Kristóf, J., Horváth, E., Vágvölgyi, V., 2013. Mechanochemical intercalation of low reactivity kaolinite. Applied Clay Science 83–84, 24–31. https://doi.org/10.1016/j.clay.2013.08.002

Makó, É., Kristóf, J., Horváth, E., Vágvölgyi, V., 2009. Kaolinite–urea complexes obtained by mechanochemical and aqueous suspension techniques—A comparative study. Journal of Colloid and Interface Science 330, 367–373. https://doi.org/10.1016/j.jcis.2008.10.054

Pereira, E.I., Minussi, F.B., da Cruz, C.C.T., Bernardi, A.C.C., Ribeiro, C., 2012. Urea–Montmorillonite-Extruded Nanocomposites: A Novel Slow-Release Material. J. Agric. Food Chem. 60, 5267–5272. https://doi.org/10.1021/jf3001229

Roshanravan, B., Soltani, S.M., Rashid, S.A., Mahdavi, F., Yusop, M.K., 2015. Enhancement of nitrogen release properties of urea–kaolinite fertilizer with chitosan binder. Chemical Speciation & Bioavailability 27, 44–51. https://doi.org/10.1080/09542299.2015.1023090

Rudmin, M., Banerjee, S., Yakich, T., Tabakaev, R., Ibraeva, K., Buyakov, A., Soktoev, B., Ruban, A., 2020. Formulation of a slow-release fertilizer by mechanical activation of smectite/glauconite and urea mixtures. Applied Clay Science 196, 105775. https://doi.org/10.1016/j.clay.2020.105775

Solihin, Zhang, Q., Tongamp, W., Saito, F., 2011. Mechanochemical synthesis of kaolin–KH2PO4 and kaolin–NH4H2PO4 complexes for application as slow release fertilizer. Powder Technology 212, 354–358. https://doi.org/10.1016/j.powtec.2011.06.012

Wanyika, H., 2014. Controlled Release of Agrochemicals Intercalated into Montmorillonite Interlayer Space [WWW Document]. The Scientific World Journal. https://doi.org/10.1155/2014/656287

Watt, G.W., Chrisp, J.D., 1954. Spectrophotometric Method for Determination of Urea. Anal. Chem. 26, 452–453. https://doi.org/10.1021/ac60087a006

Wu, L., Liu, M., 2007. Slow-Release Potassium Silicate Fertilizer with the Function of Superabsorbent and Water Retention. Ind. Eng. Chem. Res. 46, 6494–6500. https://doi.org/10.1021/ie070573l

Xiang, Y., Ru, X., Shi, J., Song, J., Zhao, H., Liu, Y., Guo, D., Lu, X., 2017. Preparation and Properties of a Novel Semi-IPN Slow-Release Fertilizer with the Function of Water Retention. J. Agric. Food Chem. 65, 10851–10858. https://doi.org/10.1021/acs.jafc.7b03827

Xiaoyu, N., Yuejin, W., Zhengyan, W., Lin, W., Guannan, Q., Lixiang, Y., 2013. A novel slow-release urea fertiliser: Physical and chemical analysis of its structure and study of its release mechanism. Biosystems Engineering 115, 274–282. https://doi.org/10.1016/j.biosystemseng.2013.04.001

Yang, Y., Tong, Z., Geng, Y., Li, Y., Zhang, M., 2013. Biobased Polymer Composites Derived from Corn Stover and Feather Meals as Double-Coating Materials for Controlled-Release and Water-Retention Urea Fertilizers. J. Agric. Food Chem. 61, 8166–8174. https://doi.org/10.1021/jf402519t

Zhang, J., Liu, R., Li, A., Wang, A., 2006. Preparation, Swelling Behaviors, and Slow-Release Properties of a Poly(acrylic acid-co-acrylamide)/Sodium Humate Superabsorbent Composite. Ind. Eng. Chem. Res. 45, 48–53. https://doi.org/10.1021/ie050745j

Zhang, Q., Saito, F., 2009. Mechanochemical Synthesis of Slow-Release Fertilizers through Incorporation of Alumina Composition into Potassium/Ammonium Phosphates. Journal of the American Ceramic Society 92, 3070–3073. https://doi.org/10.1111/j.1551-2916.2009.03291.x

Zheng, T., Liang, Y., Ye, S., He, Z., 2009. Superabsorbent hydrogels as carriers for the controlled-release of urea: Experiments and a mathematical model describing the release rate. Biosystems Engineering 102, 44–50. https://doi.org/10.1016/j.biosystemseng.2008.09.027

# CHAPTER IV

## Catalytically activated kaolinite for the preparation of polyacrylamide hydrogel composites at ambient temperature

# Chapter IV. Catalytically activated kaolinite for the preparation of polyacrylamide hydrogel composites at ambient temperature

## IV.1. Introduction

Polyacrylamide (PAAm) based hydrogels have been widely applied in agriculture applications due to their great hydrophilicity and simplicity in synthesis (Gao et al., 1999, 2015; Zhang and Wang, 2007; Guilherme et al., 2010; Mahdavinia et al., 2013; Ferfera-Harrar et al., 2014). PAAm hydrogels are usually produced using free radical polymerization method, in which crosslinking agent (e.g. N,N'-methylene-bis-acrylamide (MBA)) is introduced in the polymerization process. Generally, ammonium persulfate (APS) is used to initiate the polymerization reaction. N,N,N',N'-tetramethylethylenediamine (TEMED) is the most common accelerator which, when combined with APS, allows polymerization to be carried out at room temperature (Guo et al., 1990; Si et al., 1995). The chemically crosslinked PAAm hydrogels are generally weak and brittle due to their structural inhomogeneity (Haraguchi et al., 2002). The formation of polymer clay nanocomposites has been considered over the past 20 years as a means of improving the mechanical properties of polyacrylamide gels.

Most of these studies were done with expandable clays such as montmorillonite, vermiculite and bentonite. In this work, we aimed to develop polyacrylamide-kaolinite composite hydrogels without additional chemical crosslinker i,e; with kaolinite acting as a multifunctional crosslinker in place of an organic crosslinker. To our knowledge, no research has reported the formation of kaolinite-based hydrogels without the addition of a chemical crosslinker (MBA type) in the polymerization medium. Zhang recently showed that polyetheramine having the tertiary amine structures could be used as both the initiation and cross-linking point for the formation of polyacrylamide hydrogels. Based on Zhang results, we decided to explore the possibility of grafting of a dimethylamino fragment with a structure similar to TEMED on kaolinite in order to initiate the growth of polyacrylamide chains from the surface of the clay mineral layers.

In this work, the grafting of 2-(2-dimethylaminoethoxy) ethanol on kaolinite will be first carried out. The functionalized kaolinite will be characterized by thermogravimetric analysis, elemental analysis, X-ray diffraction, $^{13}C$ solid state NMR spectroscopy and FT-IR analysis. The functionalized kaolinite will then be used as an accelerator and co-initiator of the polymerization of acrylamide in order to produce polyacrylamide-kaolinite hydrogel composites. Then, the swelling characteristics and mechanical properties of the hydrogel composites will be reported.

## IV.2. Experimental details

### IV.2.1. Materials

The kaolin (KGa-1b) used was from the Source Clays Repository of the Clay Mineral Society. 2-[2-(dimethylamino)ethoxy]ethanol (DAEE, Fisher), acrylamide (Am, Aldrich), ammonium persulfate (APS, Acros Organic,98+%), dioxane (Aldrich), isopropanol (Fisher), acetone, dimethyl sulfoxide (DMSO) and methanol (MeOH) were of analytical grade and used as received.

### IV.2.2. Kaolinite-dimethyl sulfoxide intercalate

The preparation of kaolinite-dimethyl sulfoxide (K-DMSO) intercalate precursor was carried out as follows. 10 g of kaolinite powder was added to a mixture of 60 ml of DMSO and 5 ml of deionized water. The suspension was maintained under constant stirring for 10 days at 80°C and then allowed to stir for 5 days at room temperature. The resulting material was recovered after two series of washing-centrifugation using successively dioxane (2 x 50 ml) and isopropanol (2 x 50 ml). The product was finally dried at 50°C overnight.

### IV.2.3. Preparation of 2-[2-(dimethylamino)ethoxy]ethanol-grafted kaolinite

1 g of K-DMSO was mixed with 6 g of 2-(2-(dimethylamino)ethoxy)ethanol (DAEE) in a flask equipped with a stirrer, a reflux pipe and a nitrogen line under constant stirring. The temperature of the mixture was increased slowly from room temperature to 180°C and maintained stable during 2 h, giving the sample K-DAEE-2, or during 17 h, giving the sample K-DAEE-17. The samples were recovered after three washing by centrifugation with 50 ml isopropanol. The solids were dried at 60°C overnight.

1 g of sample K-DAEE-2 was remixed with 6 g of DAEE with the same conditions as above (2 hours at 180°C), to give the sample K-DAEE-2C.

The hydrolytic stability of the K-DAEE intercalates was studied. Typically, 100 mg of K-DAEE was added to 100 ml of deionized water under vigorous stirring for 24 hours. The powder was recovered by centrifugation and then dried at 60°C for 48 hours.

### IV.2.4. Preparation of kaolinite-g-DAEE/acrylamide intercalate

Kaolinite-acrylamide intercalate (K-DAEE-Am) was prepared by stirring 0.2 g of K-DAEE-2C in 20 ml of a 2.5 mol/l acrylamide aqueous solution for 3 hours under nitrogen and centrifuged. The solid part was suspended again in the same conditions for 72 hours. The excess acrylamide was displaced from kaolinite by washing with acetone (100 mg of sample in 10 ml acetone). The resulting solid was dried under vacuum at 40°C overnight.

## IV.2.5. Preparation polyacrylamide hydrogels

The list of samples prepared are detailed in Table IV.1. The samples were prepared using a stock solution of acrylamide (2.5 mol/l) and a stock solution of ammonium persulfate (0.1 mol/l). First, acrylamide and an appropriate amount of deionized water are mixed in a flask to give a concentration of 2 mol/l acrylamide in the final solution. $O_2$ is removed by bubbling with nitrogen for 5 min. The other components are added successively to another flask, systematically ending with the stock solution of APS and under vigorous stirring for 2 min. The resulting mixture is transferred to a glass tube and the acrylamide solution was added. The glass tube is closed with a septum and bubbled with nitrogen for 5 min. Before gelation, the glass tube was shaken at regular intervals to maintain a good dispersion of kaolinite. For gelled samples, the glass tube was broken, and the hydrogel was cut into 0.5 cm cylindric discs.

Hydrogels and hydrogel composites were also prepared using conventional cross-linker N,N'-methylene-bis-acrylamide (MBA) to compare their mechanical properties to hydrogels prepared with only clay mineral as a crosslinker. In these formulations, polymerization was carried out at 60°C because there is no TEMED accelerator into the polymerization medium. The composition of the samples including MBA crosslinker is given in Table IV.2.

Table IV.1. Composition of reactants (in g) for the synthesis of polyacrylamide samples without organic cross-linker.

| samples | Am | K | K-DAEE-2C | K-DAEE-Am | DAEE | APS |
|---|---|---|---|---|---|---|
| Am | 0.454 | - | - | - | - | 0.014 |
| Am + DAEE | 0.454 | - | - | - | 0.002 | 0.014 |
| Am + K | 0.454 | 0.028 | - | - | - | 0.014 |
| Am + K + DAEE | 0.454 | 0.028 | - | - | 0.002 | 0.014 |
| Am + K-DAEE | 0.454 | - | 0.028 | - | - | 0.014 |
| Am + K-DAEE-Am | 0.454 | - | - | 0.028 | - | 0.014 |

Table IV.2. Composition of reactants (in g) for the synthesis of polyacrylamide hydrogels prepared with MBA crosslinker.

| samples | Am | MBA | K | K-DAEE-Am | APS |
|---|---|---|---|---|---|
| HG-MBA-0.40 | 0.454 | 0.005 | - | - | 0.014 |
| HG-MBA-0.75 | 0.454 | 0.009 | - | - | 0.014 |
| HG-K-MBA-0.40 | 0.454 | 0.005 | 0.028 | - | 0.014 |
| HG-K-MBA-0.75 | 0.454 | 0.009 | 0.028 | - | 0.014 |

## IV.2.6. Material characterization

Powder X-ray diffraction (XRD) analyses were implemented on a Siemens D5000 type diffractometer equipped with a vertical goniometer and diffracted beam monochromator. The radiation applied was Cu K$\alpha$ ($\lambda$ = 0.1541 nm) generated at 40 kV and 40 mA. The samples were measured in step scan mode with 0.04° step size and 4 s step scan. The CHNS elemental analysis was determined using an elemental analyzer Flash EA 1112 series Thermo Finnigan at dried state. Thermogravimetric analysis (TGA) was performed using a TA Instruments SDT600 under continuous nitrogen purge of 100 mL/min. The samples (ca. 10 mg) were typically equilibrated at 30°C and ramped to 800°C at a rate of 10°C/min and data analysis was performed using Universal Analysis 2000 software package. The Fourier Transform Infrared (FTIR) spectra were recorded on a FTIR spectrometer Nexus, (ThermoNicolet) equipped with an attenuated total reflectance diamond crystal unit (Thermo Scientific Smart iTR). 32 scans were obtained at a resolution of 4 $cm^{-1}$ and over a spectral range of 600-4000 $cm^{-1}$. Solid-state $^{13}C$ NMR Cross-Polarization Magic-Angle-Spinning CP/MAS spectra were collected on a Bruker AVANCE 400 NMR spectrometer operating at 100.68 MHz for $^{13}C$. Approximately 100 mg of sample was packed in 4 mm O.D. Zirconia rotors which was spun at the magic angle at 12 kHz.

For swelling measurements, the as-prepared hydrogel was cut into disc 1 cm in diameter and 0.5 cm in height. Disc was immerged in deionized water (0.5 L) for one week and wiped off before weighing ($M_s$). The swollen disc was dried at 40°C to constant weight ($M_D$). The swelling ratio was calculated from the following equation:

$$Q = \frac{M_S - M_D}{M_D} \qquad (1)$$

TA-DMA Q800 dynamic mechanical analyzer was used to investigate the mechanical properties of hydrogels at swollen state. All test measurements were performed on as prepared hydrogel samples in the form of disc. Samples were tested at 25°C with a compression strain rate of 1000 µm/min and a preload force of 0.001 N and in multi-frequency-strain mode with a preload force of 0.1 N, 5% oscillation strain and a frequency sweep from 0.2 to 10 Hz.

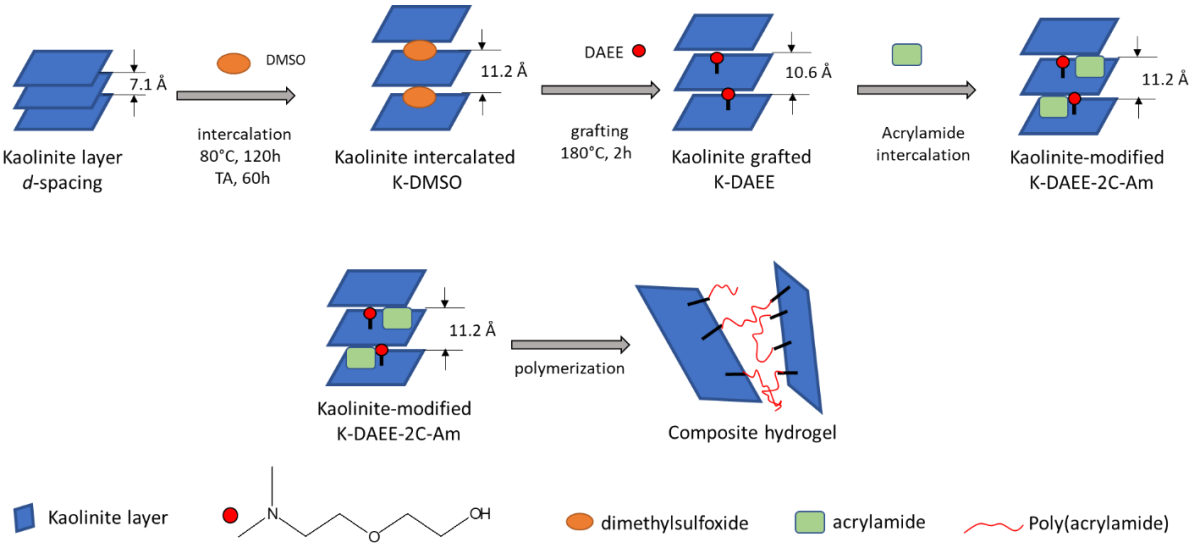


*Scheme IV.1. Schematic illustration of the preparation of the polyacrylamide-kaolinite composite hydrogels.*

## IV.3. Results and discussion

Scheme IV.1 illustrates the different steps adopted to prepare the polyacrylamide-kaolinite hydrogel composites without organic crosslinker. Kaolinite was expanded with DMSO before grafting DAEE on the surface of kaolinite. The polymerization at ambient conditions of acrylamide initiated by the DAEE functionalized clay resulted in the polyacrylamide-kaolinite hydrogel composite.

### IV.3.1 Preparation and characterization of kaolinite grafted with 2-(2-(dimethylamino)ethoxy)ethanol

The grafting of the dimethylamine functionality on the kaolinite surface was carried out by reaction between the OH groups of 2-[2-(dimethylamino)ethoxy]ethanol and aluminol groups present at the surface of kaolinite. This reaction leads to the formation of an Al-O-C bond between the grafted molecule and the kaolinite and generates water as a by-product (scheme IV.2). The grafting reaction was investigated by XRD, TGA, $^{13}C$ CP-MAS NMR, elemental analysis and FTIR spectrometry.

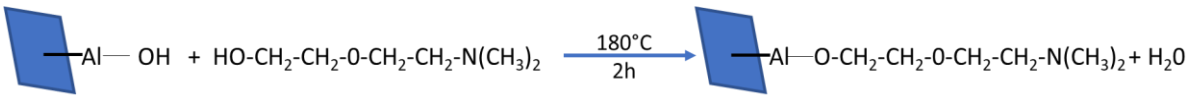


*Scheme IV.2. Grafting of 2-(2-(dimethylamino)ethoxy)ethanol onto the aluminols of the interlayer surface of kaolinite.*

### *IV.3.1.1. X-ray diffraction*

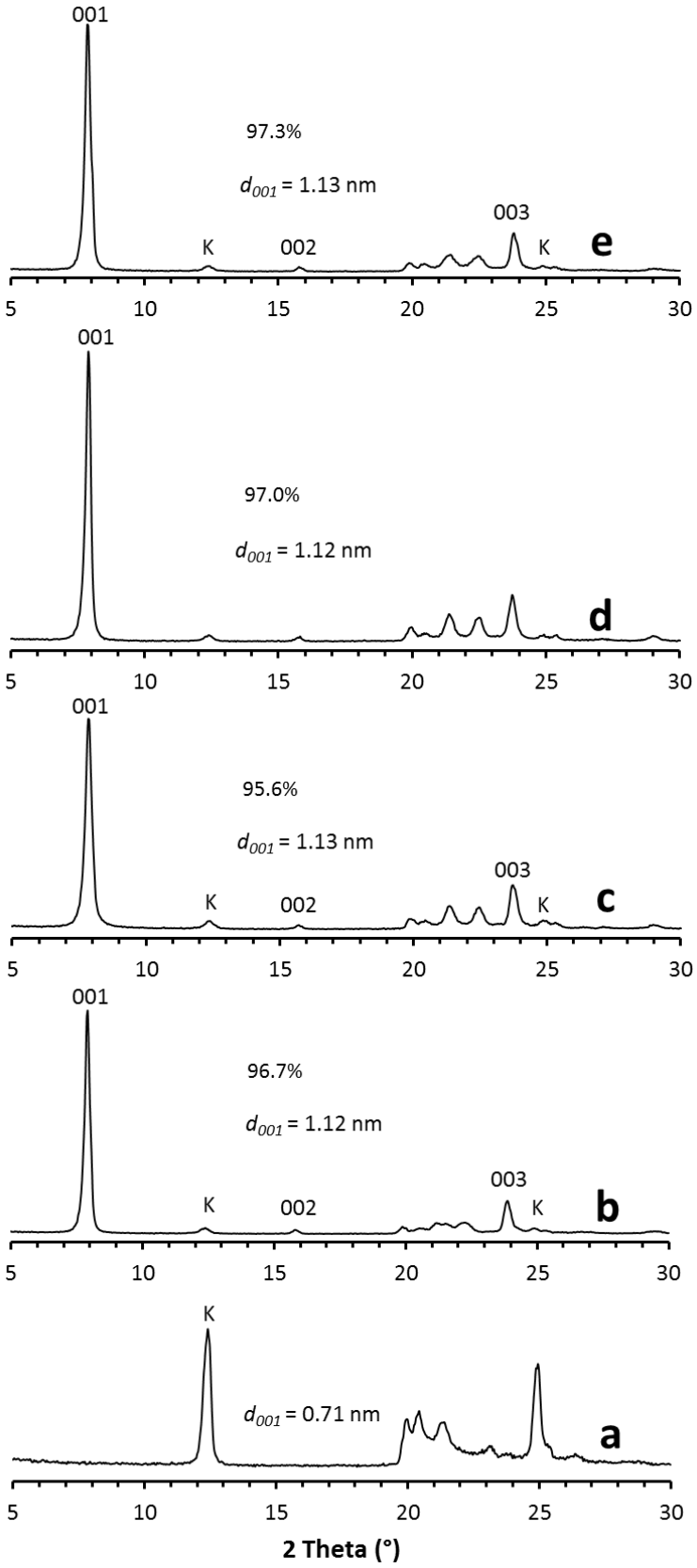


*Figure IV.1. XRD patterns (2θ = 5-30°) of (a) kaolinite, (b) K-DMSO, (c) K-DAEE-2 (reaction time :2h), (d) K-DAEE-2C (2h of reaction repeated twice) and (e) K-DAEE-17 (17h reaction time).*

Figure IV.1,a shows the (001) reflection of raw kaolinite corresponding to an interlayer distance d-value = 0.71 nm. After intercalation with DMSO, the (001) reflection is shifted to 1.12 nm in agreement with previous studies (Olejnik et al., 1968; Gardolinski and Lagaly, 2005a) (Figure IV.1,b). The interlayer distance correspond to the keying of one of the methyl groups of DMSO in the siloxane rings of the tetrahedral sheets (Letaief and Detellier, 2011). After reaction of K-DMSO with DAEE, (Figure IV.1,c ,d ,e), the (001) reflection remained unchanged at 1.12 nm. (Gardolinski et al., 2000; Gardolinski and Lagaly, 2005b) reported basal spacing of kaolinite grafted with a variety of amino alcohols between 1.10 nm and 1.14 nm.

Thorough washing with water was carried out in order to remove the non-grafted organic molecules (Letaief and Detellier, 2007). 0.1 g of K-DMSO, K-DAEE-2, K-DAEE-2C and K-DAEE-17 was suspended in 100 ml of deionized water under magnetic agitation at 300 rpm for 24 hours. The elemental composition of the kaolinite samples before and after washing with water is shown in Table IV.3.

Table IV.3. Elemental composition (CHNS) of the kaolinite samples before and after washing with water.

| Samples | %C | %H | %S | %N |
|---|---|---|---|---|
| K-DMSO | 5.60 | 2.65 | 7.55 | - |
| K-DMSO-w | 0.97 | 1.98 | 0.29 | - |
| K-DAEE-2 | 6.08 | 2.76 | 5.21 | 0.40 |
| K-DAEE-2-w | 2.87 | 2.59 | - | 0.31 |
| K-DAEE-2C | 7.48 | 2.82 | 4.65 | 0.82 |
| K-DAEE-2C-w | 3.87 | 2.83 | - | 0.64 |
| K-DAEE-17 | 6.69 | 2.81 | 6.77 | 0.30 |
| K-DAEE-17-w | 1.30 | 2.03 | - | 0.18 |

XRD patterns of the washed samples are shown in Figure IV.2,b',c',d',e'. It is seen that (001) reflection returned to 0.72 nm as raw kaolinite for K-DMSO. Elemental analysis confirmed that DMSO was strongly displaced by water during water washing. For K-DAEE-2, the (001) reflection shifted from 1.12 nm to 1.03 nm after washing. For K-DAEE-17-w, the (001) reflection shifted from 1.13 m to 0.85 nm. The interlayer space of the washed sample close to the values of kaolinite hydrates. Elemental analysis of K-DAEE-17 indicates that a significant amount of nitrogen is still present in the washed sample. Elemental analysis also shows that a treatment of kaolinite for 17 hours at 180°C with DAEE results in a much lower amount of N than that found for kaolinite treated during shorter times (2 h). The elimination low amount of DAEE and the reduction of the interlayer space suggest that long reaction times at 180°C is detrimental to the efficiency of the grafting reaction, maybe through hydrolysis of the Al-O-C bonds. The non-grafted intercalated DAEE molecule can adopt an orientation parallel to the plane of the layers in order to optimize the interactions between its nitrogen, ethoxy and OH groups

with the oxygen of Si-O-Si and Al-OH of kaolinite. This orientation could explain the low value (0.85 nm) of the interlayer space.

This X-ray result confirmed that a reaction time of two hours results in an efficient grafting of DAEE. Elemental analysis showed that before washing with water, K-DAEE-2 and K-DAEE-2C contain a large amount of S and thus DMSO still intercalated. This would explain that the interlayer distance was the same between K-DAEE and K-DMSO before washing. DMSO was totally removed after washing and this resulted in a smaller interlayer distance for K-DAEE-2 and K-DAEE-2C. The molecule DAEE was grafted and only a low amount of non grafted DAEE was removed from kaolinite interlayer by water washing. The degree of intercalation $\alpha$ (%) was calculated using the integral intensity of the (001) reflections of the expanded and unexpanded kaolinite by the following equation:

$$\alpha(\%) = \frac{I_{i(001)}}{I_{k(001)} + I_{i(001)}} x100 \quad (2)$$

Where $I_{i(001)}$ is the peak intensity observed for the kaolinite intercalate and $I_{k(001)}$ is the peak intensity observed for the non-expanded kaolinite. For sample K-DAEE-2C, repeating the process for grafting led to increase the degree of intercalation $\alpha$ from 95.6 to 97% and from 94% to 97.2 % for the washed samples.

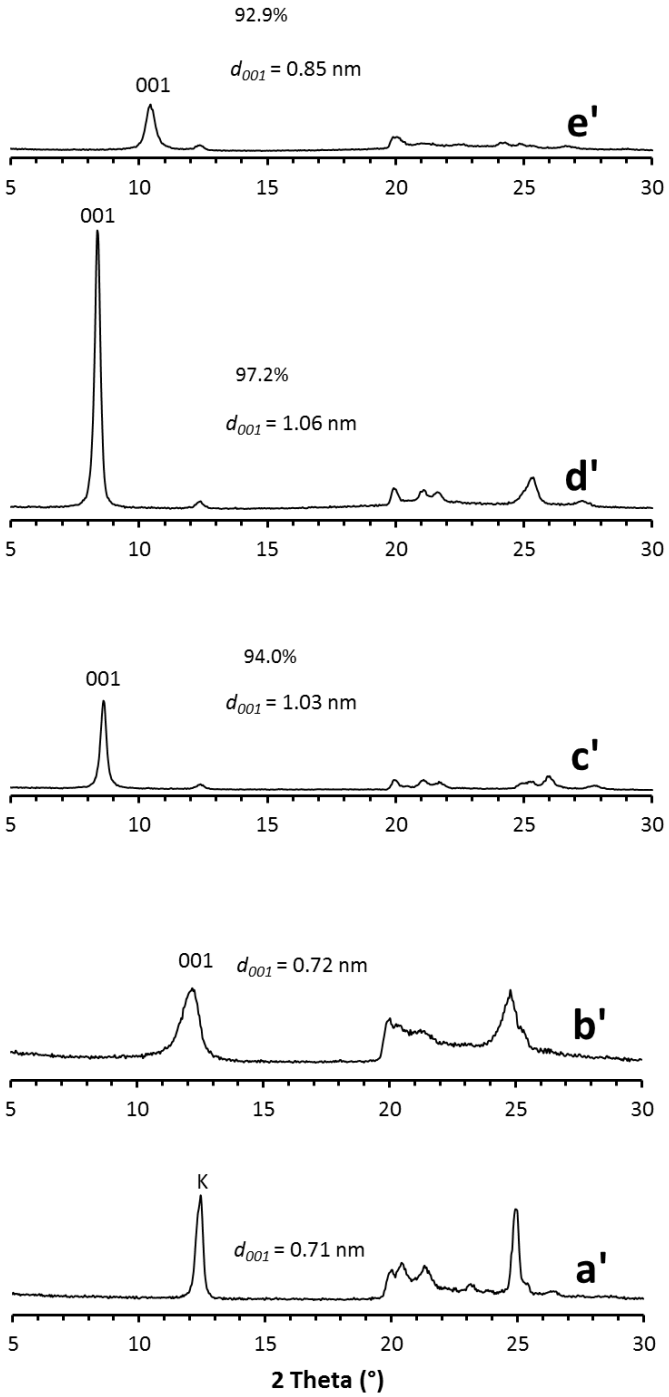


*Figure IV.2. XRD patterns (2θ = 5-30°) after washing with water (a') kaolinite, (b') K-DMSO, (c') K-DAEE-2 (reaction time :2h), (d') K-DAEE-2C (2h of reaction repeated twice) and (e') K-DAEE-17 (17h reaction time).*

### *IV.3.1.2. Thermal analysis*

Thermogravimetric analysis (TGA) was used to determine the amount of organic material loaded in the kaolinite derivatives before and after water washing. Derivative thermogravimetry (DTG) and TGA

traces are shown in Figure IV.3. The first mass loss observed in all samples between 60°C and 150°C correspond to the removal of physically adsorbed water. In the case of intercalated kaolinites, an increase in temperature above 170°C produces release of the organic material. In figure (IV.2,b), TGA of K-DMSO shows a second loss at 179°C which is attributed to the endothermic removal of DMSO. The organic material loaded in the intercalated sample was calculated from the weight loss between 150°C and 350°C. It corresponds to 18.2% mass loss for K-DMSO in agreement with literature reports (Letaief and Detellier, 2005, 2007; Tonlé et al., 2007). The second mass loss was attributed to the dehydroxylation of kaolinite observed at 514°C for pure kaolinite, with a 3.5% mass loss corresponding to the loss of the structural water of kaolinite during the transformation of kaolinite to metakaolinite (Letaief and Detellier, 2011). In Figure IV.3,c ,d ,e, a maximal rate for the decomposition of organic material appeared at 309°C, 319°C and 297°C for K-DAEE-2, K-DAEE-2C and K-DAEE-17, respectively. Elemental analysis revealed a still high amount of DMSO in the unwashed K-DAEE samples. The mass loss between 150 and 350°C therefore corresponds to DMSO and DAEE evaporation and/or decomposition. The mass loss % between 150 and 350°C was 13.8, 14.7 and 17.1% for K-DAEE-2, K-DAEE-2C and K-DAEE-17, respectively. It thus seems to increase with reaction time but it is difficult to separate the amount of DAEE and DMSO in these unwashed samples. These samples must also contain a significant amount of non-grafted DAEE, intercalated or physically adsorbed on the external surface of kaolinite. The third mass loss above 350°C could be first ascribed to the dehydroxylation of kaolinite. For samples K-DMSO, K-DAEE-2, K-DAEE-2C and K-DAEE-17 the dehydroxylation of kaolinite appeared at 508, 467, 461 and 478°C respectively. The dehydroxylation of the grafted amino alcohols hybrid materials was observed at lower temperature (400-460°C) in literature, this effect was attributed to the lower crystallinity of grafted materials (Gardolinski and Lagaly, 2005a; Letaief and Detellier, 2007, 2011; Dedzo and Detellier, 2016).

In Figure IV.4,a the TG curve of K-DMSO-w was close to the TGA curve of raw kaolinite, proving the nearly total elimination of DMSO during water washing, in agreement with elemental analysis. For K-DAEE samples, a sharp decrease in loss between 150 and 350°C is observed for washed samples compared to the loss observed for unwashed samples. The mass loss in the 150-350°C range amounts to 2.50 %, 2.53% and 2.10 % for the washed K-DAEE-2, K-DAEE-2C and K-DAEE-17, respectively. This loss corresponds to the decomposition of the grafted DAEE. The higher efficiency of the grafted reaction appears for the sample treated twice for 2 hours at 180°C, K-DAEE-2C, in agreement with elemental analysis results. After water washing kaolinite hybrid samples, the dehydroxylation appeared at512, 479, 454, 505°C for K-DMSO K-DAEE-2, K-DAEE-2C and K-DAEE-17, respectively (Figure IV.4). The sharp decrease in the dehydroxylation temperature relative to kaolinite for the KDAEE-2C sample suggests that the decomposition of the grafted DAEE is not completed at 350°C and

that it partially overlaps with the dehydroxylation of kaolinite. The loss between 150 and 350°C therefore undoubtedly underestimates the rate of grafted DAEE.

For the washed K-DAEE, 8.2% mass loss correspond to the water adsorbed and/or hydrates kaolinite and ca. 2.50% mass loss of DAEE molecule grafted in kaolinite layers. For K-DAEE-17-w, the TG shows the reduction of the organic with the washing with an accordance with other analysis.

Based on the percentage of mass loss of water and organics to form the metakaolinite $Al_2O_3.2SiO_2$, the TGA data allowed to calculate the formula unit of K-DAEE-2C. The formula calculated for K-DAEE-2C determined from TGA results was $Al_2Si_2O_5(OH)_4[-(OCH_2CH_2\text{-}O\text{-}CH_2CH_2\text{-}N(CH_3)_2]_{0.05}$. The formula determined from elemental analysis (N content) of K-DAE-2C was $Al_2Si_2O_5(OH)_4[H\text{-}(OCH_2CH_2\text{-}O\text{-}CH_2CH_2\text{-}N(CH_3)_2]_{0.12}$. This confirms that TGA largely underestimates the amount of grafted DAEE.

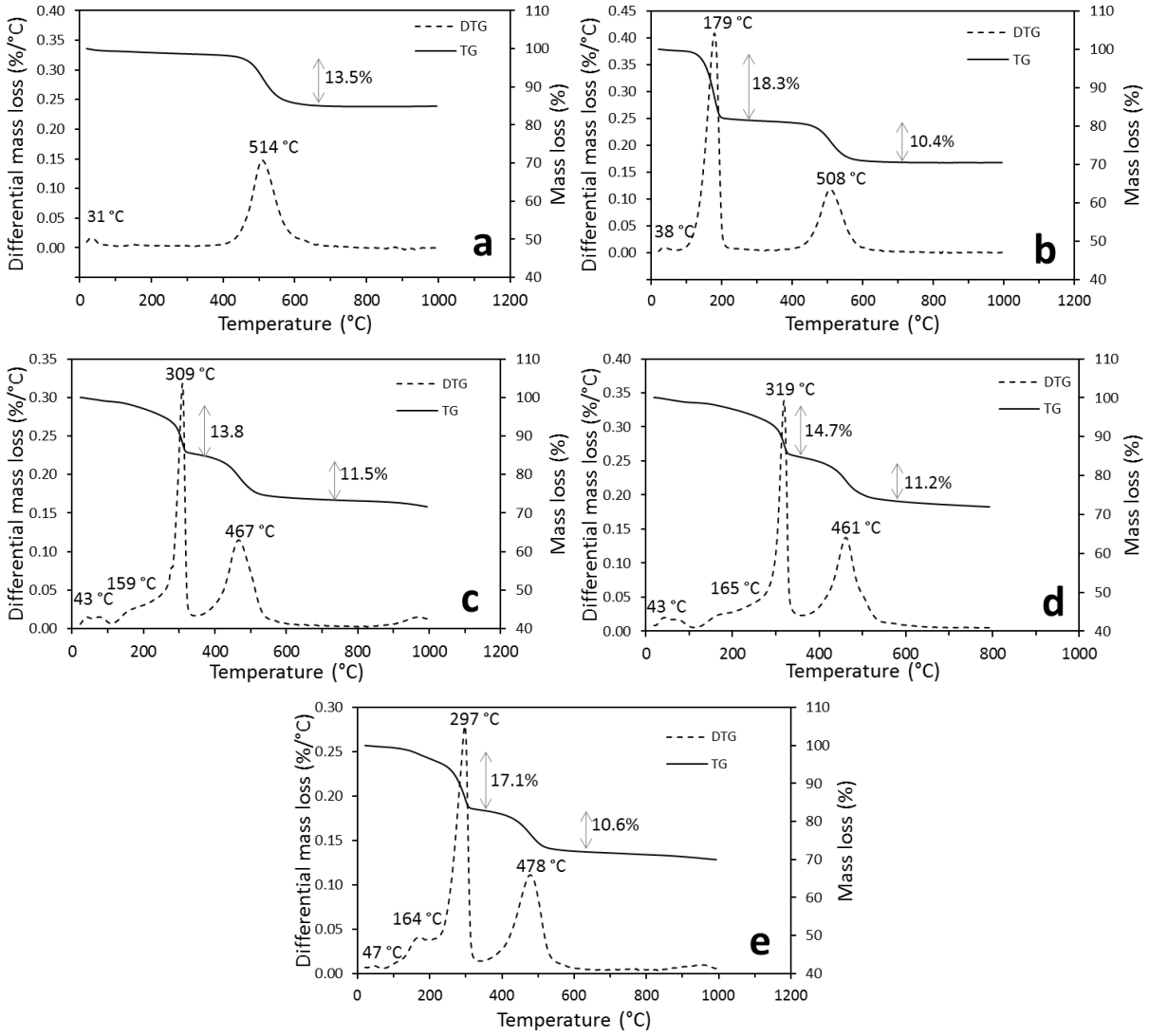


*Figure IV.3. DTG-TG curves of kaolinite (a), K-DMSO (b), K-DAEE-2 (c), K-DAEE-2C (d) and K-DAEE-17 (e).*

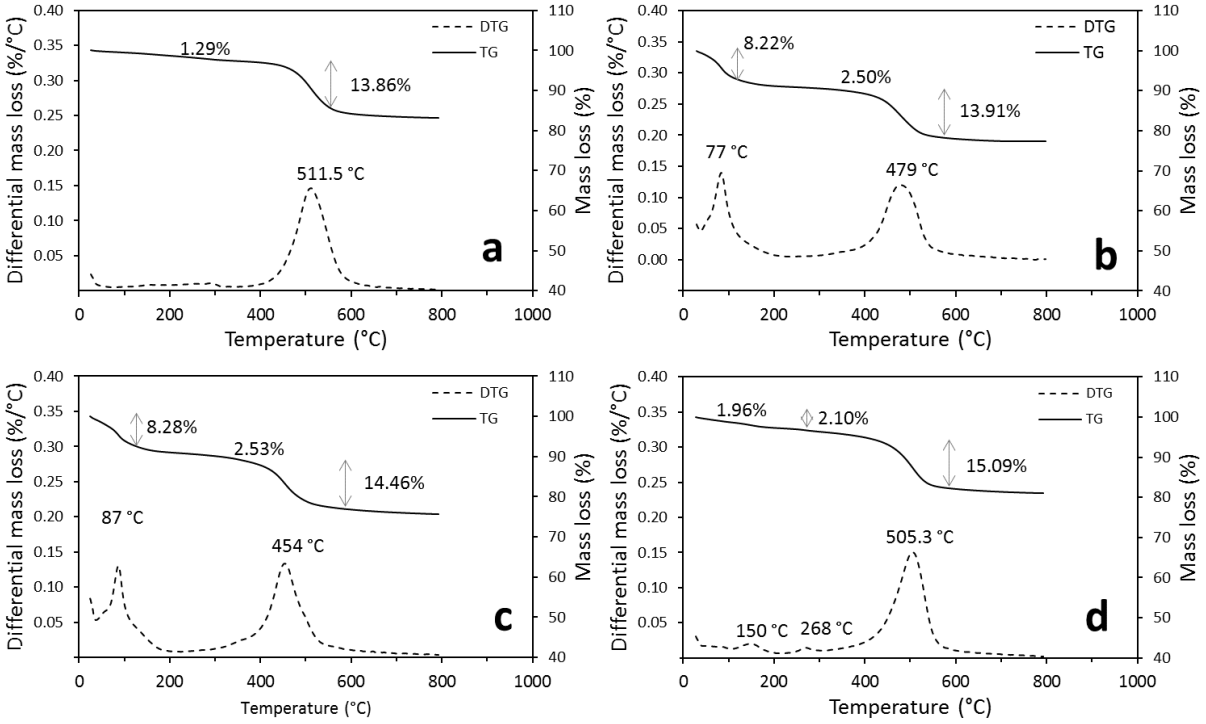


*Figure IV.4. DTG-TG curves of K-DMSO-w (a), K-DAEE-2-w (b), K-DAEE-2C-w (c) and K-DAEE-17-w (d).*

### *IV.3.1.3. FTIR spectrometry*

FTIR spectra (4100-2500 $cm^{-1}$) showed of kaolinite and kaolinite-DAEE hybrids before extensive washing with water are shown in Figure IV.5. Kaolinite has the three typical bands at 3687, 3669 and 3651 $cm^{-1}$ corresponding to inner surface hydroxyl groups. These bands should be significantly modified after intercalation or grafting compound into kaolinite layers, contrary to the band at 3619 $cm^{-1}$ which corresponds to the stretching vibrations of the inner hydroxyl groups (Ledoux and White, 1966; Cheng et al., 2014). After intercalation with DMSO molecules, a significant modification in position and intensity of the bands of the surface hydroxyls is observed while the band of the internal groups remains intense and at the same position. The new vibration bands appearing at 3535 and 3503 $cm^{-1}$ are related to the inner surface OH perturbed by DMSO (Letaief and Detellier, 2008). The new bands appearing at 2937 and 3022 $cm^{-1}$ are assigned to the $CH_3$ vibrations of DMSO. After the reaction with DAEE the surface hydroxyl bands appeared modified in intensity and position. The FTIR spectra of K-DAEE and K-DAEE-2C corresponding to short reaction times show significant changes compared to the FTIR spectrum of K-DMSO. The OH vibration bands appear less well resolved than for K-DMSO. These results suggest that DAEE was intercalated and interact with surface hydroxyl groups of kaolinite. The FTIR spectrum of K-DAEE-17 shows nearly the same features than the K-DMSO. It thus seems that long reaction times are detrimental to the efficient intercalation and grafting of DAEE.

Figure IV.6 shows FTIR spectra of the samples after their extensive washing with water. The FTIR spectrum of the washed K-DMSO shows the same features than raw kaolinite. This confirms the

efficient removal of DMSO during the washing step. The small band at 3544 $cm^{-1}$ corresponds to kaolinite hydrate which suggests the displacement of DMSO by water molecules. This is in accordance with XRD results discussed above. Unlike K-DMSO, the OH bands of the K-DAEE samples after washing still corresponds to perturbated OH inner surface groups. This confirms that DAEE is well-grafted and that the Al-O-C bond resists to water washing. The FTIR spectrum of K-DAEE prepared by long reaction time (K-DAEE-17) shows significant differences relative to the K-DAEE prepared by short immersion times (K-DAEE-2 and K-DAEE-2C). Notably, a strong band appears at 3544 $cm^{-1}$. This band can be ascribed to kaolinite hydrate. As discussed before, the removal of the non-grafted DAEE and/or the hydrolysis of the Al-O-C bond during washing with water resulted in a partial collapse of kaolinite layers, a re-orientation of DAEE intercalated molecules and trapping of water molecules to form kaolinite hydrates. FTIR results are in good agreement with XRD results.

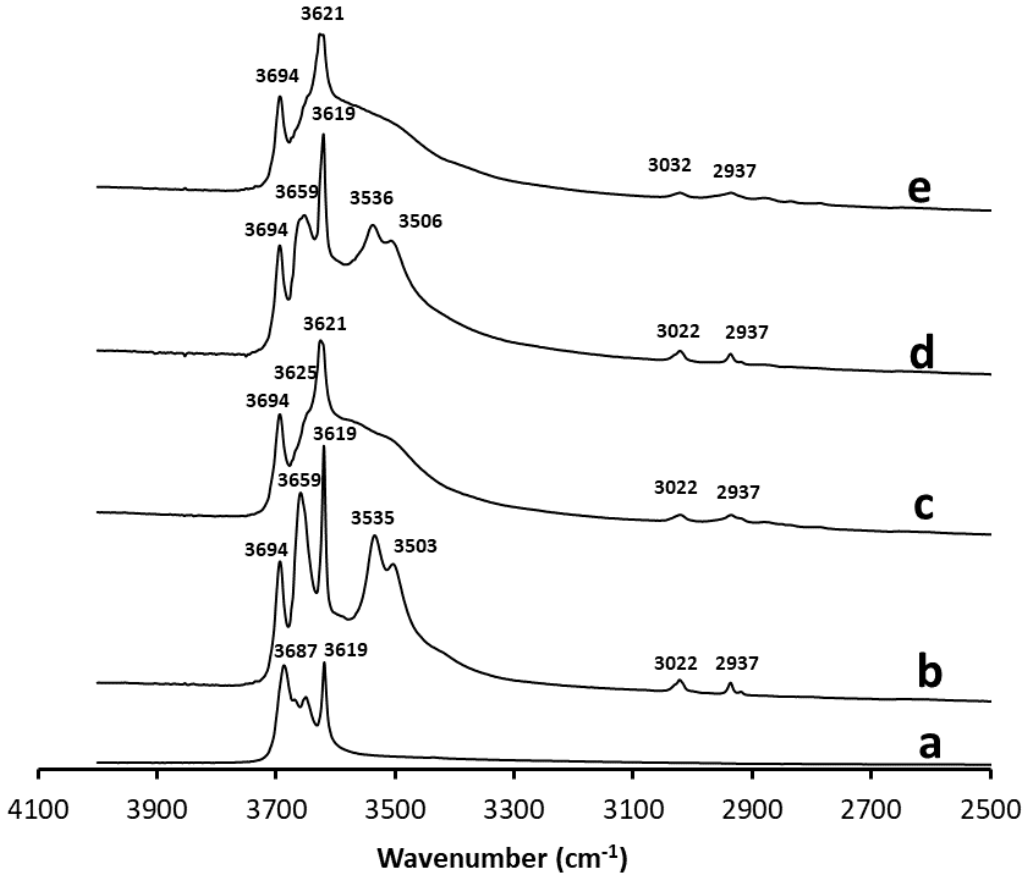


*Figure IV.5. FTIR spectra (4000-2500 $cm^{-1}$) of (a) kaolinite, (b) K-DMSO, (c) K-DAEE-2, (d) K-DAEE-17 and (e) K-DAEE-2C.*

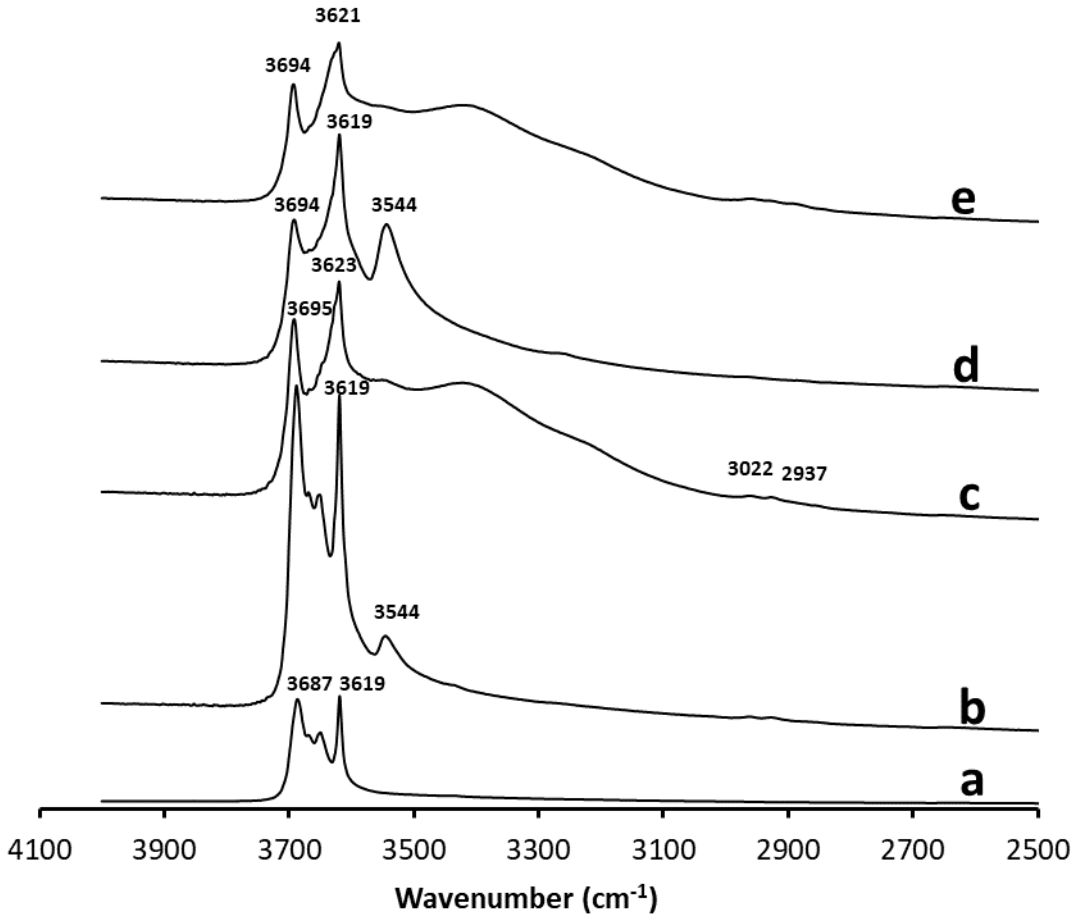


*Figure IV.6. FTIR spectra after water washing of samples (a) kaolinite (K-w), (b) K-DMSO-w, (c) K-DAEE-2-w, (d) K-DAEE-17-w, (e) K-DAEE-2C-w.*

### *IV.3.1.4. NMR spectroscopy*

$^{13}$C CP/MAS-NMR was used to obtain further information on the structure of the intercalated or grafted species into kaolinite. The assignment of carbon signals of DAEE molecule is shown in Figure IV.7. K-DMSO spectrum is characterized by a doublet at 43.2 and 42.1 ppm due to the asymmetric location of DMSO within the interlayer spaces of kaolinite (Letaief and Detellier, 2008). The $^{13}$C NMR spectra of unwashed K-DAEE samples still contains an intense signal at ca. 43 ppm which confirms that DMSO has not been totally displaced by DAEE during the grafting reaction. Extensive washing with water allows to remove DMSO as indicated by the large decrease of the 43 ppm signal in the NMR spectra of the washed samples. The 43 ppm signal is indeed shifted to ca. 44.2 ppm for K-DAEE-2C-w and K-DAEE-2-w which corresponds to the resonance of the dimethylamino units of grafted DAEE. The peak at 55.2 ppm corresponds to the carbon of Al-0-C bond, this peak is shifted compared to the HO-$^{13}$C signal of DAEE molecule (61.3 ppm) (Figure IV.8). In the case of K-DAEE-17-w, the intensity of peak at 55.2 ppm is very low which would confirm that DAEE residues are not chemically grafted. The N-$CH_2$ and $CH_2$-O

give resonance signals at 60.6 and 69.3 ppm. $^{13}C$ NMR thus confirm that DAEE was grafted for short immersion times and that the higher efficiency of grafting was repeated two times during short reaction times (2h).

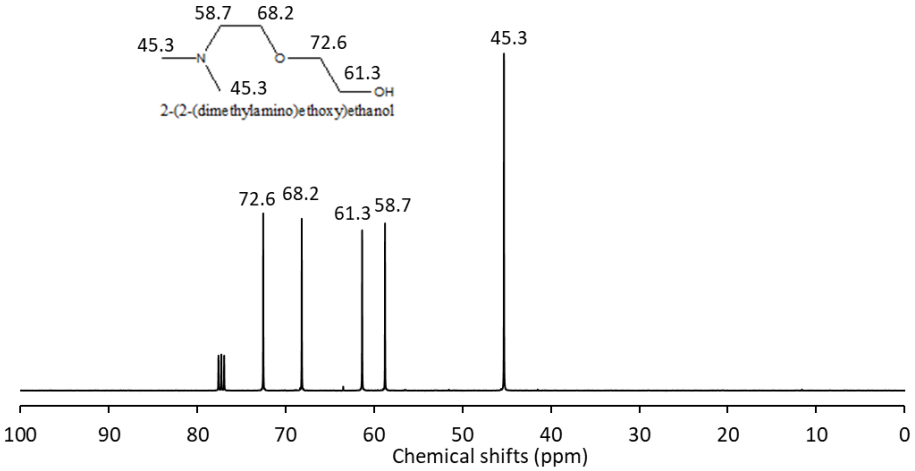


*Figure IV.7. $^{13}C$ NMR spectra for DAEE molecule.*

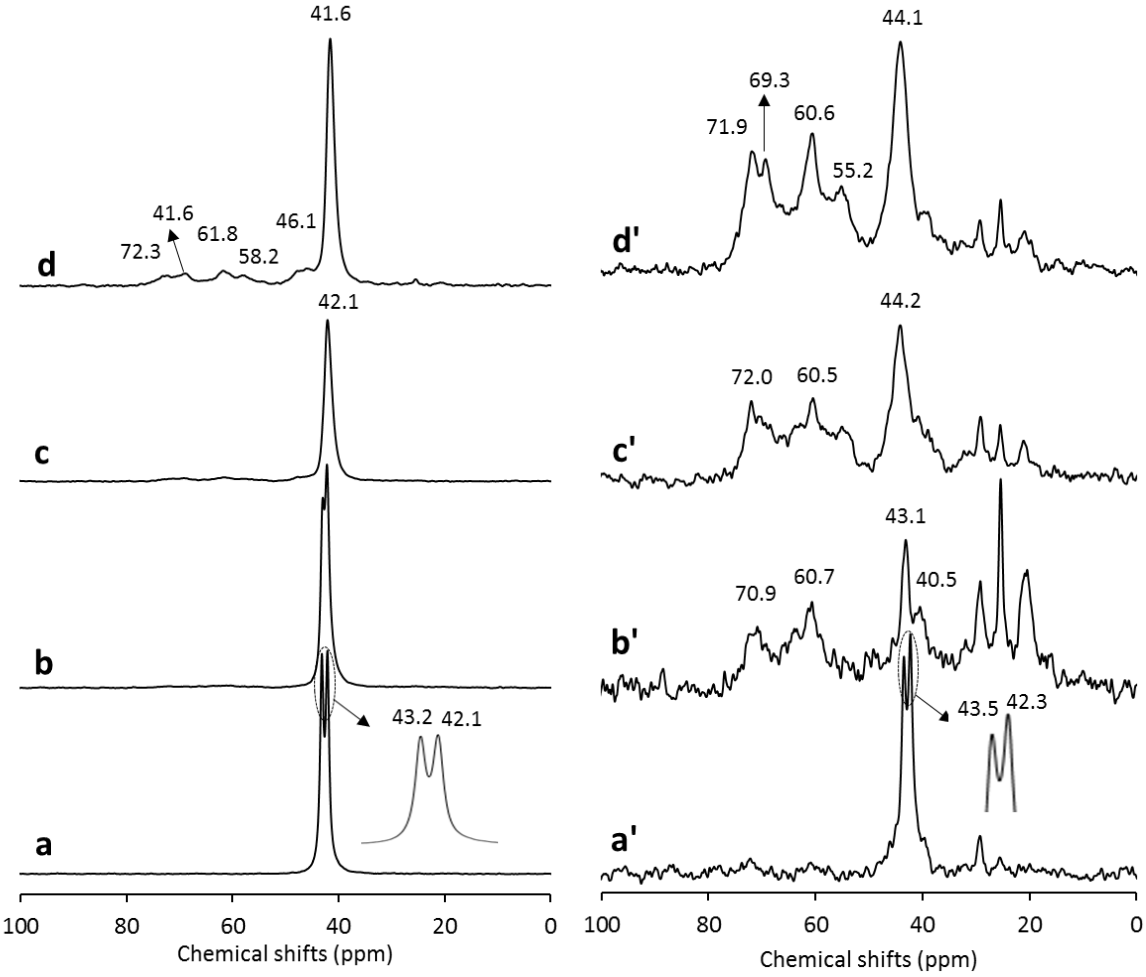


*Figure IV.8. Solid state $^{13}C$ CP/MAS NMR spectra for (a) the starting materials K-DMSO, (b) K-DAEE-17, (c) K-DAEE-2, (d) K-DAEE-2C and (a', b', c', d') for their corresponding water washed samples.*

## IV.3.2. Polymerization of K-modified DAEE with acrylamide

### *IV.3.2.1. Polymerization method*

K-DAEE-2C was used both as initiator and activator of persulfates with respect to the polymerization of acrylamide. Dimethylamino units grafted on kaolin are believed to react with persulfate ions in the same way as TEMED reacts with APS. As represented in Scheme 3, lone pair electrons of nitrogen atoms firstly attack the persulfate and the unstable intermediate (1), (2) and sulfate ion are created. Then, the oxygen anion of sulfate in intermediate (2) abstracts a hydrogen from the dimethyl group to give the free radicals (3) and (4). Therefore, two kinds of free radicals are formed that can both initiate the polymerization of acrylamide. The initiation via radical (4) will result to polyacrylamide chain bonded to the kaolinite surface. In order to understand the role of each component of the system, several preliminary tests were carried out. First, acrylamide was mixed with APS at room temperature for several hours. No change in viscosity was noted. It is well known that the activation of APS requires heating the reaction medium and thus polyacrylamide was not formed in these conditions. The same observations were made when kaolin was added to the reaction medium. With the addition of DAEE (without or with kaolinite) in the reaction medium, a rapid increase in viscosity (less than 5 minutes) is observed at room temperature. DAEE can thus activate the polymerization of acrylamide, certainly in the same way as TEMED. On the other hand, simple mixing of K-DAEE-2C with APS and acrylamide did not lead to an increase in viscosity. At this stage, two hypotheses can be made: either the DAEE loses its capacity to catalyze the initiation reaction when it is immobilized on the surface of the kaolin or the DAEE grafts can still activate the polymerization but the APS and / or more probably the monomer do not have access to the interlamellar space. A final experiment was therefore carried out using a DAEE-kaolinite pre-intercalated with acrylamide together with acrylamide monomer and APS. In this case, an increase in viscosity is observed followed by gelation after approximately 80 minutes of reaction at room temperature. This last result validates the mechanism presented in Schemes 1 and 3 where the polymerization of acrylamide is initiated on the surface of the kaolinite surface and where the kaolinite plays the role of a multifunctional crosslinker to obtain polyacrylamide-kaolinite hydrogel.

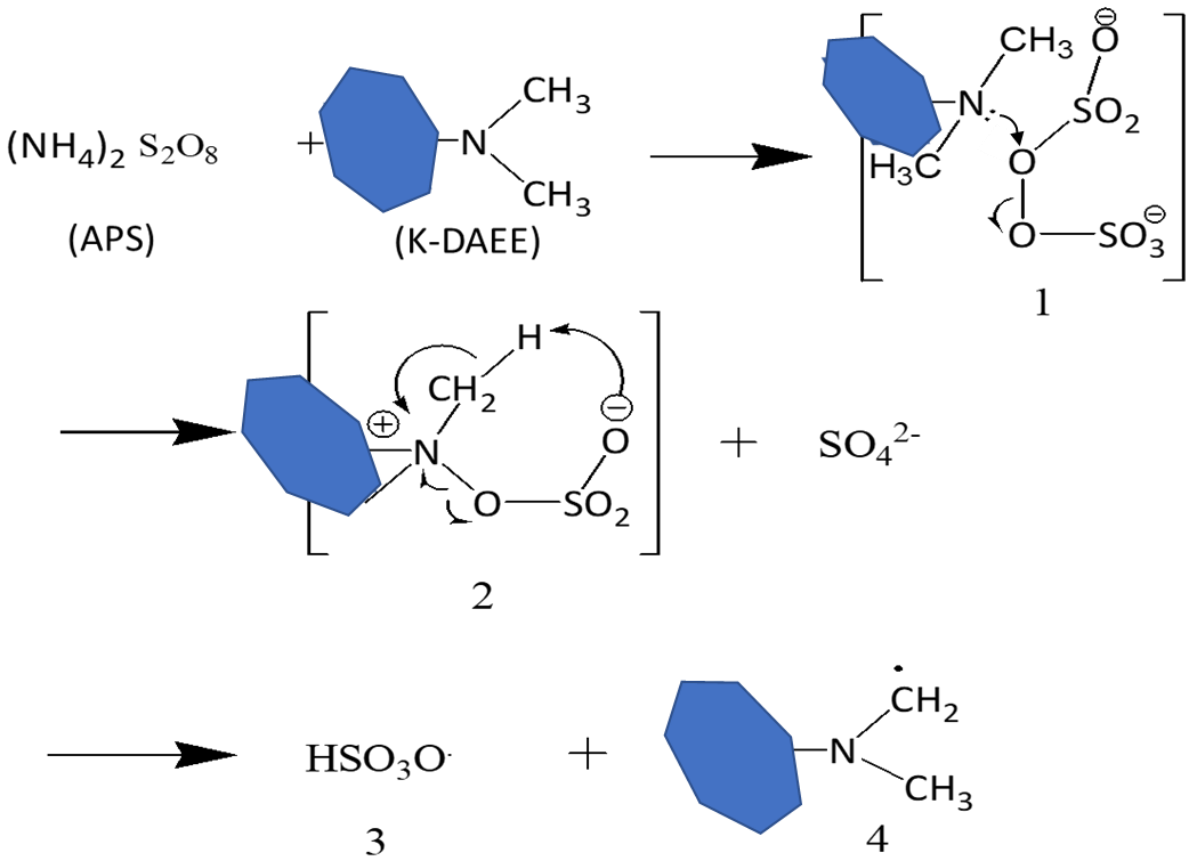


*Scheme IV.3. The initiation mechanism of the system of persulfate tertiary amine grafted on kaolinite interlayer.*

### *IV.3.2.2. Characterization of K-DAEE-Am intercalates*

The XRD pattern of the product obtained by treatment of K-DAEE-2C with an aqueous 18% acrylamide solution is shown in Figure IV.10. The (001) peak shifted from 1.06 nm to 1.12 nm. Elemental analysis of the product gave 9.23% of C, 2.92 % of N and 0.26% of S. The amount of S is a littler lower to the amount of S found after extensive washing of K-DMSO with water and it is much lower than the S amount in K-DAEE-2C. This suggests that DMSO has been largely displaced by acrylamide and that the interlayer distance of 1.12 nm, which is the same value than that found for K-DMSO intercalate is related to the intercalation of acrylamide in kaolinite. The N content related to grafted DAEE for K-DAEE-2C was 0.64 %. By considering that the fraction of grafted DAEE remains unchanged during the intercalation of acrylamide, it is possible to calculate the fraction of C associated with DAEE grafts from their N content knowing that DAEE contains 6 C for 1 N. On the other hand, the difference between the amount of total N and the amount of N level associated with DAEE grafts makes it possible to determine the amount of N coming from acrylamide and therefore the amount of C coming from acrylamide (knowing that acrylamide contains 3 C for 1 N). By summing the amount of C coming respectively from the acrylamide and DAEE grafts, the obtained value was very close to the measured value of total C in the product. It can be concluded that DAEE grafts are preserved during the

intercalation process of acrylamide. Overall, K-DAEE-Am contains ca. 11.4 m% of acrylamide and 6.1 m% of DAEE grafts i.e. a total of 17.5 m% of organic component.

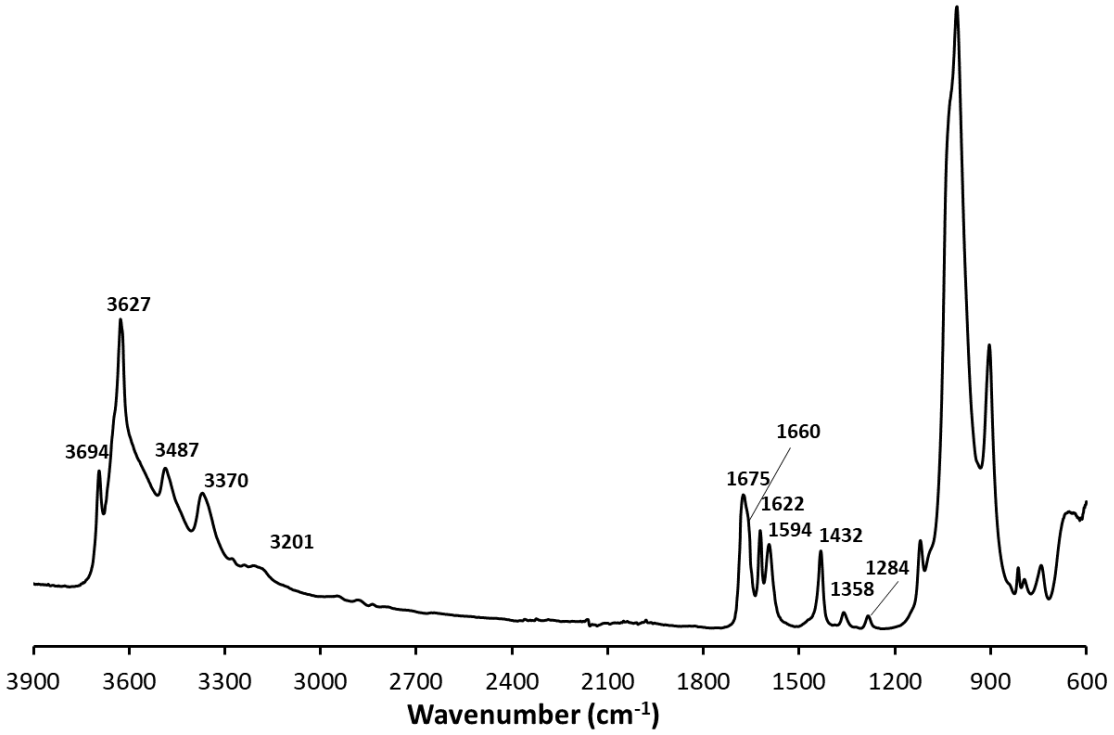


*Figure IV.9. K-DAEE-Am FTIR spectra.*

The FTIR spectrum of KDAEE-Am is shown in Figure IV.9. The inner surface OH bands appear perturbed relative to the bands of the raw kaolinite. The new band that appears at 3627 $cm^{-1}$ (partly overlapped with the 3619 $cm^{-1}$ band of inner OH can be related to hydroxyl groups interacting with carbonyl and amino groups of acrylamide. The bands at 3487 and 3370 $cm^{-1}$ correspond the stretching of $NH_2$ groups of acrylamide. The OH region give a broad band with several shoulders, notably at ca. 3650 $cm^{-1}$ due to the presence of several environments since OH groups strongly interact by hydrogen bonding with grafted-DAEE and intercalated acrylamide. The low wavenumber part of the IR spectrum contain several features confirming the intercalation of acrylamide with bands at 1675 $cm^{-1}$ and 1660 $cm^{-1}$ (as shoulder), assigned to ν(C=0) and ν(C=C), respectively and bands at 1622 and 1594 $cm^{-1}$, attributed to δ($NH_2$) of acrylamide. The FTIR spectral features of K-DAEE-Am supports the formation of a kaolinite-acrylamide intercalation compound.

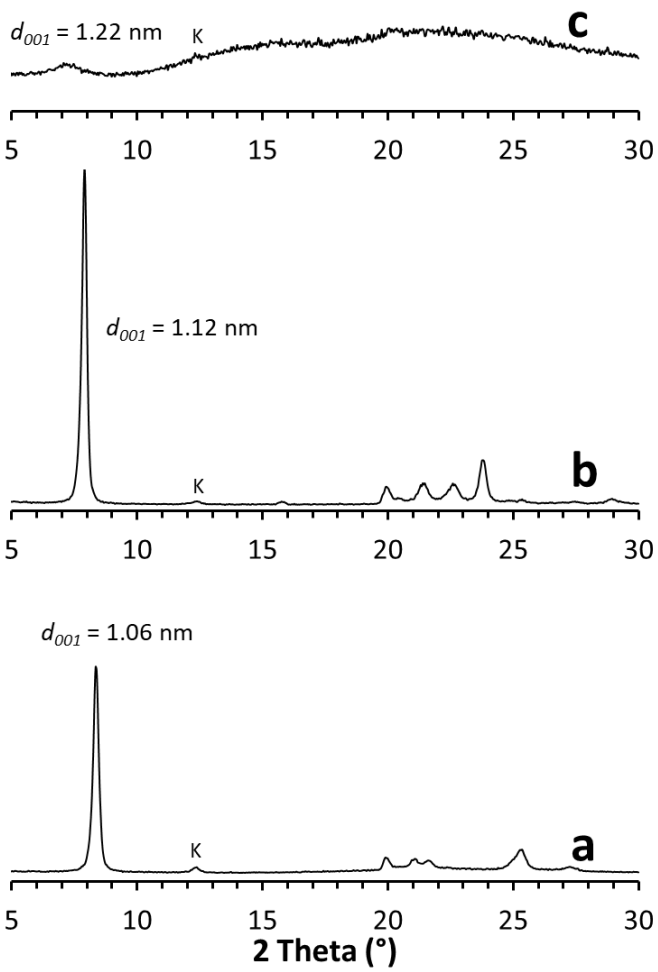


*Figure IV.10. XRD patterns of (a) K-DAEE-2C, (b) K-DAEE-Am intercalate and (c) HG-K-DAEE-Am hydrogel composite.*

The XRD pattern of the PAAm-kaolinite shows a broad (001) peak shifted to 1.22 nm and with a small intensity. The shift of (001) peak suggests the intercalation of polymer chains while the broadness and low intensity of the peak suggests a decrease in the stacking order and/or partial exfoliation of kaolinite.

### *IV.3.2.3. Mechanical properties and swelling capacity*

The viscoelastic properties of polyacrylamide hydrogels has been studied by DMA analysis in compression mode at room temperature and at different frequencies (Figure IV.10). The water content of each sample was 87 wt%. The storage modulus of the hydrogels are more than one decade higher than their viscous modulus, showing that the elastic properties of these gels is more pronounced than their viscous properties. The hydrogels containing kaolinite have relatively higher mechanical properties than their unreinforced polymer matrix. Moreover, the polyacrylamide-kaolinite hydrogel prepared by surface initiated polymerization resulted in a higher storage modulus than the hydrogel composites prepared with MBA conventional crosslinker.

Figure IV.11 showed a typical stress-stain curve recorded during uniaxial compression test of HG-K-MBA-0.40, HG-K-MBA-0.75 and HG-K-DAEE-2C-Am. When the compression strain is above 35%, the compression stress of all the hydrogels begins to increase exponentially because the chain segments are getting closer with compression.

The compressive strength of the hydrogel prepared without adding MBA is between the compressive strength of the gel prepared with an MBA level of 0.4 mol% (relative to acrylamide) and an MBA level of 0.75 mol%.

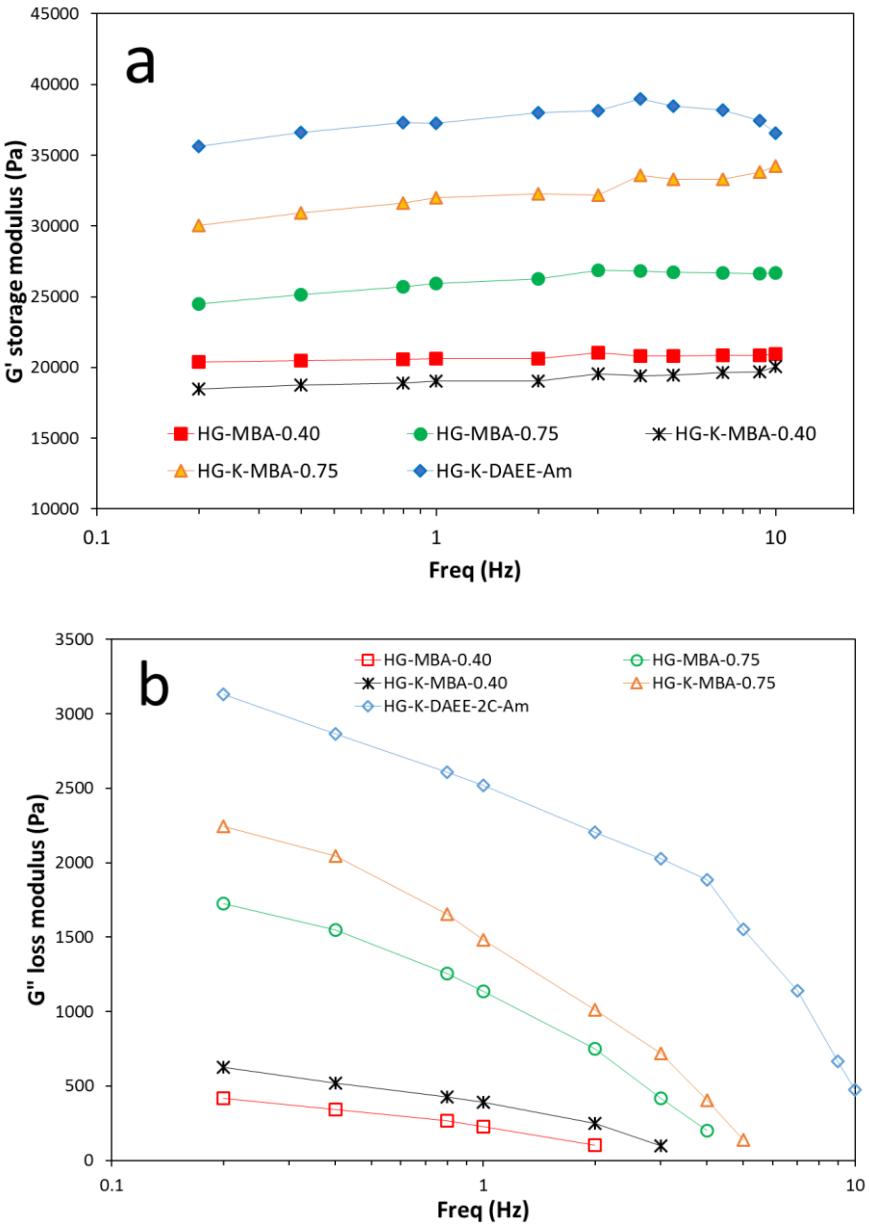


*Figure IV.11. Dynamic rheology of PAAm and K-PAAm gels (a) Storage modulus, G' and (b) loss modulus, G'' as a function of frequency. Reaction conditions: kaolinite content in K-PAAm gels 5.8 wt%, water content of each sample ca 87 wt%.*

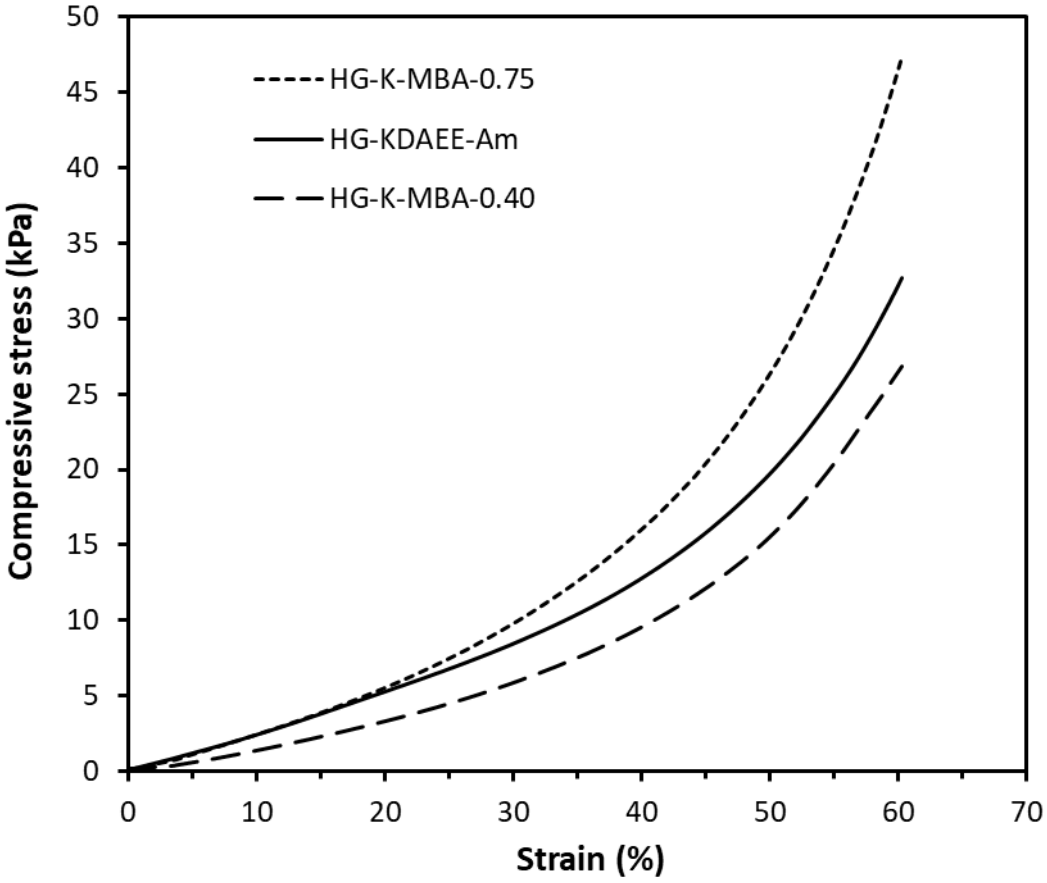


*Figure IV.12. Strain with a compression strain rate of 1000 µm/min and a preload force of 0.001 N of different hydrogels.*

Figure IV.13 shows a comparison of the behavior of the polyacrylamide gels under uniaxial compression. Digital photos of hydrogel before and after compression test illustrated the rigidity and physical aspect of hydrogels (Figure IV.13). As can be seen, hydrogels with conventional MBA cross-linker, HG-MBA-0.40 and HG-MBA-0.75 were brittle and degraded under compressive stress (Figure IV.13,a,b,c,d). The addition of 5.8 wt% of kaolinite to the conventional hydrogel allowed to strengthen the gel when low MBA content is used, HG-K-MBA-0.40. This sample has a good elastic recovery ~90%. The hydrogel prepared with a higher MBA content, HG-K-MBA-0.75, is brittle and broke during compression test (Figure IV.13,e,f,g,h). The HG-K-DAEE-Am hydrogel was soft and did not degraded upon compressive stress and showed a good elastic recovery although lower than HG-MBA-0.4 (Figure IV.13,i,j,k). As vividly shown in Figure IV.13, the as-prepared HG-K-DAEE-Am hydrogels appeared soft, resilient, tough and completely opaque. They can be compressed or stretched, have a good elastic recovery returning instantaneously to their initial length after unloading by hand manipulation. The hand elongation can attain more than 120% (Figure IV.14,a,b,c,d). Cylindrical HG-K-DAEE-Am showed also a good elastic recovery after compressive stress (Figure IV.14,e,f).

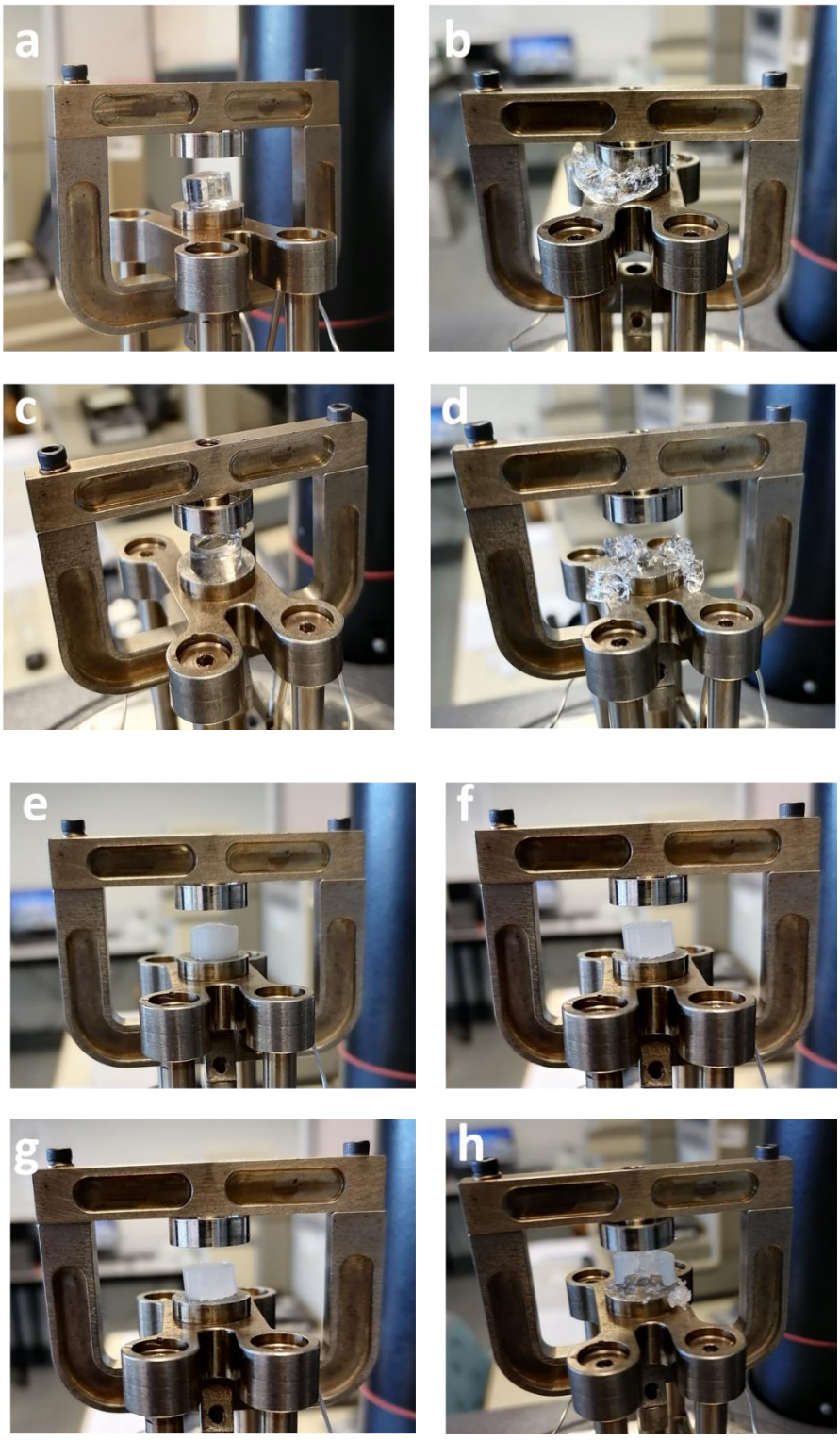
a
b
c
d
e
f
g
h


*Figure IV.13. Comparison of the behavior of polyacrylamide gels under uniaxial compression (*before compressing, under 80% compressing, and after unloading*) HG-MBA-0.40 (a, b), HG-MBA-0.75 (c, d), HG-K-MBA-0.40 (e, f), HG-K-MBA-0.75 (g,h) and HG-K-DAEE-Am (i, j, k).*

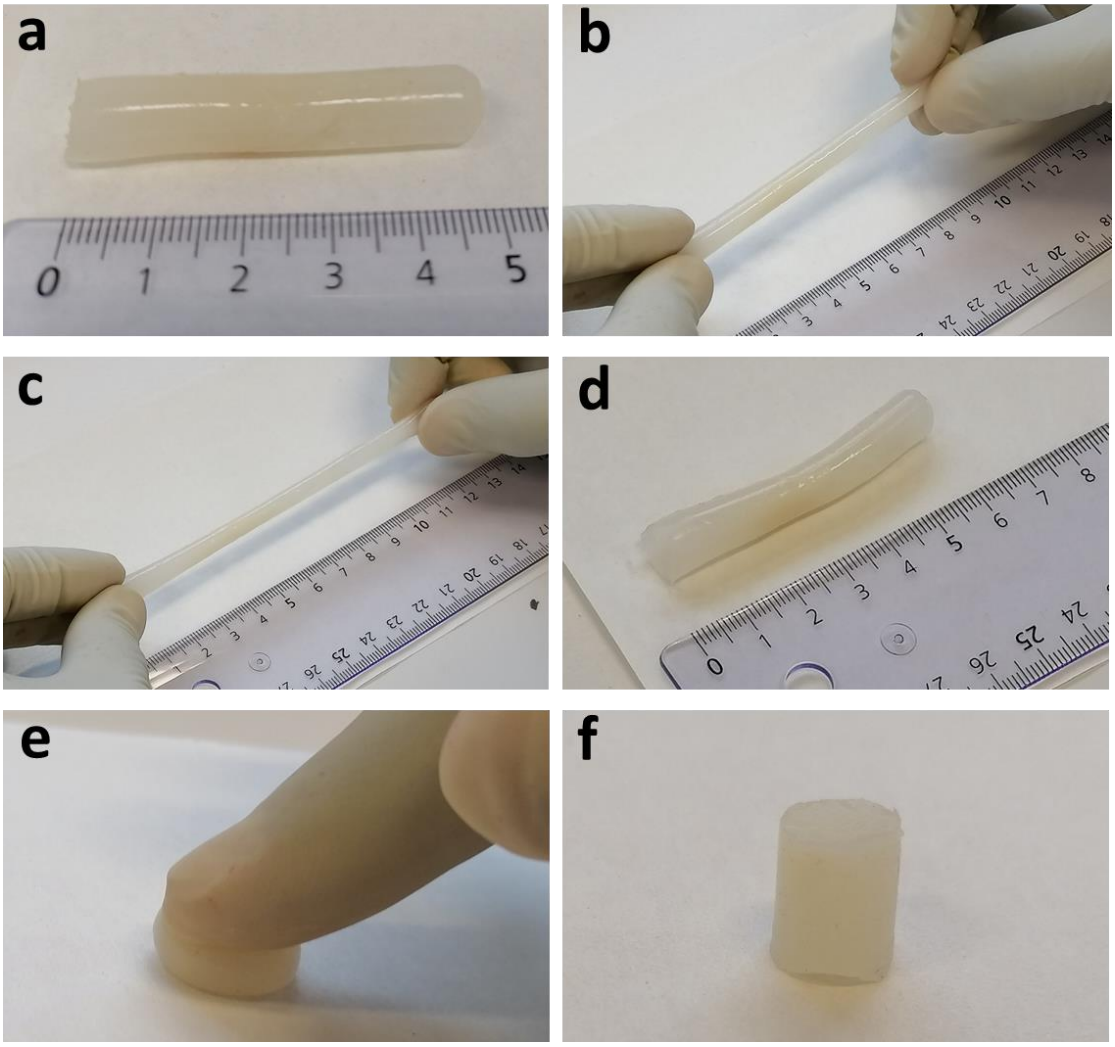


*Figure IV.14. Digital photos of HG-K-DAEE-Am hydrogels (a) as prepared, (b, c) stretched, (d) returned after stretch, compressed with a finger and release (e, f).*

HG-K-DAEE-Am hydrogels did not dissolve but swelled, maintaining its original shape very well. The swelling ratio of HG-KDAEE-Am hydrogel was 30 g/g. Ibraeva et al. (2015) reported a maximum degree of swelling for polyacrylamide-kaolin composites with 10 wt% kaolin prepared using MBA as a crosslinker in the range 4-10 g/g, depending on the MBA content.

## IV.4. Conclusion

In conclusion, in this chapter we have prepared a new functionalized kaolinite by the interlayer attachment of 2-(2-dimethylaminoethoxy)ethanol to the aluminum groups of the octahedral sheets. This grafting reaction was confirmed by XRD, TGA, $^{13}C$ NMR and elemental analysis. Immersion in water under vigorous stirring for 24 hours showed that Al-O-C bond resists to hydrolysis degradation. The DAEE-functionalized kaolinite was used with ammonium persulfate to initiate the polymerization of acrylamide. Several different combinations of reactants lead to conclude that the DAEE-kaolinite hybrid played the role of a multifunctional crosslinker. DAEE graft is a key element in the system by reacting with APS to generate free radicals on the surface which allows the initiated surface polymerization of acrylamide to occur. The pre-intercalation of acrylamide into the interlayer was necessary to obtain the hydrogel composite. The XRD results revealed an expansion of the interlayer during polymerization with a low stacking order and certainly partial exfoliation of kaolinite. The polyacrylamide-kaolinite composites showed good elastic recovery properties and a high swelling capacity.

## IV.5. References

Cheng, H., Liu, Q., Liu, J., Sun, B., Kang, Y., Frost, R.L., 2014. TG–MS–FTIR (evolved gas analysis) of kaolinite–urea intercalation complex. J Therm Anal Calorim 116, 195–203. https://doi.org/10.1007/s10973-013-3383-x

Dedzo, G.K., Detellier, C., 2016. Functional nanohybrid materials derived from kaolinite. Applied Clay Science, SI Euroclay 2015 Part-1 130, 33–39. https://doi.org/10.1016/j.clay.2016.01.010

Ferfera-Harrar, H., Aiouaz, N., Dairi, N., Hadj-Hamou, A.S., 2014. Preparation of chitosan-g-poly(acrylamide)/montmorillonite superabsorbent polymer composites: Studies on swelling, thermal, and antibacterial properties. Journal of Applied Polymer Science 131. https://doi.org/10.1002/app.39747

Gao, D., Heimann, R.B., Williams, M.C., Wardhaugh, L.T., Muhammad, M., 1999. Rheological properties of poly(acrylamide)-bentonite composite hydrogels. Journal of Materials Science 34, 1543–1552. https://doi.org/10.1023/A:1004516330255

Gao, G., Du, G., Sun, Y., Fu, J., 2015. Self-Healable, Tough, and Ultrastretchable Nanocomposite Hydrogels Based on Reversible Polyacrylamide/Montmorillonite Adsorption. ACS Appl. Mater. Interfaces 7, 5029–5037. https://doi.org/10.1021/acsami.5b00704

Gardolinski, J.E., Carrera, L.C.M., Cantão, M.P., Wypych, F., 2000. Layered polymer-kaolinite nanocomposites. Journal of Materials Science 35, 3113–3119. https://doi.org/10.1023/A:1004820003253

Gardolinski, J.E.F.C., Lagaly, G., 2005a. Grafted organic derivatives of kaolinite: II. Intercalation of primary n-alkylamines and delamination. Clay Minerals 40, 547–556. https://doi.org/10.1180/0009855054040191

Gardolinski, J.E.F.C., Lagaly, G., 2005b. Grafted organic derivatives of kaolinite: I. Synthesis, chemical and rheological characterization. Clay Minerals 40, 537–546. https://doi.org/10.1180/0009855054040190

Grattoni, C.A., Al-Sharji, H.H., Yang, C., Muggeridge, A.H., Zimmerman, R.W., 2001. Rheology and Permeability of Crosslinked Polyacrylamide Gel. Journal of Colloid and Interface Science 240, 601–607. https://doi.org/10.1006/jcis.2001.7633

Guilherme, M.R., Fajardo, A.R., Moia, T.A., Kunita, M.H., Gonçalves, M. do C., Rubira, A.F., Tambourgi, E.B., 2010. Porous nanocomposite hydrogel of vinyled montmorillonite-crosslinked maltodextrin-co-dimethylacrylamide as a highly stable polymer carrier for controlled release systems. European Polymer Journal 46, 1465–1474. https://doi.org/10.1016/j.eurpolymj.2010.04.008

Guo, X.Q., Qiu, K.Y., Feng, X.D., 1990. Studies on the kinetics and initiation mechanism of acrylamide polymerization using persulfate/aliphatic diamine systems as initiator. Die Makromolekulare Chemie 191, 577–587. https://doi.org/10.1002/macp.1990.021910313

Haraguchi, K., Takehisa, T., Fan, S., 2002. Effects of Clay Content on the Properties of Nanocomposite Hydrogels Composed of Poly(N-isopropylacrylamide) and Clay. Macromolecules 35, 10162–10171. https://doi.org/10.1021/ma021301r

Ibraeva, Z.E., Zhumaly, A.A., Blagih, E., Kudaibergenov, S.E., 2015. Preparation and Characterization of Organic-Inorganic Composite Materials Based on Poly(acrylamide) Hydrogels and Clay Minerals. Macromolecular Symposia 351, 97–111. https://doi.org/10.1002/masy.201300131

Jeong, D., Kim, C., Kim, Y., Jung, S., 2020. Dual crosslinked carboxymethyl cellulose/polyacrylamide interpenetrating hydrogels with highly enhanced mechanical strength and superabsorbent properties. European Polymer Journal 127, 109586. https://doi.org/10.1016/j.eurpolymj.2020.109586

Ledoux, R.L., White, J.L., 1966. Infrared studies of hydrogen bonding interaction between kaolinite surfaces and intercalated potassium acetate, hydrazine, formamide, and urea. Journal of Colloid and Interface Science 21, 127–152. https://doi.org/10.1016/0095-8522(66)90029-8

Letaief, S., Detellier, C., 2011. Application of thermal analysis for the characterisation of intercalated and grafted organo-kaolinite nanohybrid materials. Journal of Thermal Analysis and Calorimetry 104, 831–839. https://doi.org/10.1007/s10973-010-1269-8

Letaief, S., Detellier, C., 2008. Interlayer grafting of glycidol (2,3-epoxy-1-propanol) on kaolinite. Can. J. Chem. 86, 1–6. https://doi.org/10.1139/v07-130

Letaief, S., Detellier, C., 2007. Functionalized nanohybrid materials obtained from the interlayer grafting of aminoalcohols on kaolinite. Chemical Communications 0, 2613–2615. https://doi.org/10.1039/B701235G

Letaief, S., Detellier, C., 2005. Reactivity of kaolinite in ionic liquids : preparation and characterization of a 1-ethyl pyridinium chloride–kaolinite intercalate. Journal of Materials Chemistry 15, 4734–4740. https://doi.org/10.1039/B511282F

Mahdavinia, G.R., Hasanpour, J., Rahmani, Z., Karami, S., Etemadi, H., 2013. Nanocomposite hydrogel from grafting of acrylamide onto HPMC using sodium montmorillonite nanoclay and removal of crystal violet dye. Cellulose 20, 2591–2604. https://doi.org/10.1007/s10570-013-0004-6

Olejnik, S., Aylmore, L.A.G., Posner, A.M., Quirk, J.P., 1968. Infrared spectra of kaolin mineral-dimethyl sulfoxide complexes. J. Phys. Chem. 72, 241–249. https://doi.org/10.1021/j100847a045

Si, K., Guo, X.Q., Qiu, K.Y., 1995. Initiation Mechanism of Radical Polymerization Using Ammonium Persulfate and Polymerizable Amine Redox Initiators. Journal of Macromolecular Science, Part A 32, 1149–1159. https://doi.org/10.1080/10601329508020336

Tonlé, I.K., Diaco, T., Ngameni, E., Detellier, C., 2007. Nanohybrid Kaolinite-Based Materials Obtained from the Interlayer Grafting of 3-Aminopropyltriethoxysilane and Their Potential Use as Electrochemical Sensors. Chem. Mater. 19, 6629–6636. https://doi.org/10.1021/cm702206z

Zaharia, A., Sarbu, A., Radu, A.-L., Jankova, K., Daugaard, A., Hvilsted, S., Perrin, F.-X., Teodorescu, M., Munteanu, C., Fruth-Oprisan, V., 2015. Preparation and characterization of polyacrylamide-modified kaolinite containing poly [acrylic acid-co-methylene bisacrylamide] nanocomposite hydrogels. Applied Clay Science 103, 46–54. https://doi.org/10.1016/j.clay.2014.11.009

Zhang, J., Wang, A., 2007. Study on superabsorbent composites. IX: Synthesis, characterization and swelling behaviors of polyacrylamide/clay composites based on various clays. Reactive and Functional Polymers 67, 737–745. https://doi.org/10.1016/j.reactfunctpolym.2007.05.001

# Conclusion and perspectives

# Conclusion and perspectives

The need for innovative strategies for water and soil protection that substitute the time-, energy- and resource-consuming remediation processes with other more efficient and environmentally-friendly is becoming urgent. In this respect, the interest of this project was to promote such solutions for public and private practitioners and to up-rise industrial competitiveness through economically sustainable technologies/products, in the Agriculture Field and indirectly in the Water Management area. Therefore, this project practically developed acrylic-kaolinite composite hydrogel with a controlled release of nitrogen fertilizers. To achieve this objective, first, the mechanochemical intercalation of kaolinite with urea fertilizers was thoroughly investigated. Secondly, acrylic-hydrogels with urea fertilizers were prepared following two different strategies, a one step method with the presence of urea during the network formation and two step method by post loading urea into the preformed polymer. Thirdly, acrylic-kaolinite composite with urea were developed at various amounts of kaolinite and urea. Finally, kaolinite was functionalized to allow the surface initiated polymerization of acrylamide at room temperature.

The chapter 1 was focused on the elaboration of clay-fertilizer compound using kaolin as clay and urea as fertilizer. Kaolinite-urea intercalates were prepared by dry grinding kaolin KGa-1b with urea using a laboratory-scale planetary ball mill. The effect of milling conditions on the intercalation process was investigated over a wide range of urea content (25 m% - 80 m%) and milling times (up to 2 h). The purification of the complex obtained was carried out by repeated washings with isopropanol in order to remove the excess (non-intercalated) urea. For that purpose, the proportion of intercalated urea and non-intercalated urea crystals was quantified after each washing step by combining differential scanning calorimetry (DSC) and thermogravimetric analysis (TGA) results obtained simultaneously. The optimal conditions of the intercalation were realized at a 66 m% urea loading for which a relatively low-defect complex structure was obtained in a short milling time. One drawback with the use of a high urea content (> 25 m%) during grinding was the presence of a large proportion of excess urea crystals in the as ground sample. This required repeated washing with isopropanol to purify the complex. Furthermore, the results revealed that washing with water the kaolinite-urea intercalates led to the formation of 0.84 nm kaolin hydrates and that exfoliation/delamination of kaolinite was more efficient when a high concentration of urea was used in the milling process.

In chapter 2, a superabsorbent polyacrylic acid hydrogels was prepared by two routes by free radical polymerization using N,N'-methylene-bis-acrylamide MBA as a crosslinker and ammonium persulfate APS as an initiator. In the first route urea fertilizer is added to the reaction mixture and polymerized in situ within the gel matrix, PAA/urea and in the second route PAA hydrogels was prepared first and dry

gel was allowed to swell in urea solution 10 $g.L^{-1}$ to obtain urea loaded PAA. The effect of crosslinker on water absorbency Q, water retention WR, slow urea release and mechanical properties was investigated in these two types of PAA hydrogels. The result showed that in term of swelling ratio, water retention and urea release, PAA and PAA/urea gels leads to a difference for the two polymer networks.

In this part (chapter 3), poly(acrylic acid-co-acrylamide)/kaolinite-urea (p(AA-co-Am)/KU) composite hydrogel was synthetized using N,N',methylenebisacrylamide as crosslinker agent and ammonium persulfate as initiator. The kaolinite-urea (KU-m%) powder complexes were mechanochemically intercalated by ball milling with different amounts of urea, 25, 50, 66, 80 m% and were characterized by X-ray diffraction and FTIR analysis to confirm the intercalation. These complexes KU-m% where incorporated in the gel-type matrix p(AA-co-Am). The swelling ratio Q of hydrogels was 200 g/g and the retention capacity at 40°C can attained 50 hours before complete desorption of water. The interesting result in this study is the difference between the kinetic release of urea in water from hydrogel prepared by KU-m% intercalates and by K-U-m% mixture without intercalation. In p(AA-co-Am)/KU-25m%, the release of urea in water appear with significant difference in kinetics release in favor of the pre-intercalated sample.

In chapter 4, a novel organic-inorganic hybrid hydrogel material was prepared by grafting the 2-(2-dimethylaminoethoxy)ethanol (DAEE) molecule in the interlamellar kaolinite. The grafting reaction was optimized and characterized by X-ray diffraction, 13C solid NMR, thermogravimetric analysis and infrared spectroscopy. The DAEE grafts was n=0.12 mol per unit structure of kaolinite. Increasing the time of reaction from 2 hours to 17 hours led to less grafting of DAEE to interlayer of kaolinite. The amino group in this grafted molecule was used as precursor of redox polymerization of acrylamide to build hydrogel composite. The mechanical properties of hydrogel tested by dynamic mechanical analysis indicated that the storage modulus G' was 35 kPa. These types of hydrogels could be stretched to 120% and their elasticity makes it possible to return to the initial state.

A logical progression of this PhD work would consist to develop hydrogels based on biopolymers such as alginates. The lower water uptake of these polymers relative to the acrylate superabsorbent hydrogels prepared in this work should result in a slower release of urea. The initial results concerning the mechanical properties and swelling capacity of the polyacrylamide-kaolinite hydrogel composites prepared by surface initiated polymerization from the 2-(2-dimethylaminoethoxy)ethanol grafted-kaolinite are encouraging and could be optimized in the future by playing in particular on the kaolin and APS content.

**Mahamat Saleh Yacoub ELHADJ**
Laboratoire MAPIEM, Université de Toulon

## Acrylic-kaolinite composite hydrogels for controlled-release nitrogen fertilizers application

This thesis is part of the development of new granular fertilizers that can be used in agriculture and that combine a slow release of organic nitrogen fertilizer and a high water absorption and retention capacity. Urea was first incorporated into acrylic superabsorbent hydrogels by two methods, either by incorporation during polymerization or by a post-loading step with the preformed polymer. The first method leads to a more homogeneous polymer network with reduced pore sizes and leading at the same time to a slow release of the fertilizer and to excellent water retention capacity under pressure and swelling/reswelling capacity. Kaolinite-urea intercalates were prepared in a second part of this work by dry grinding kaolin KGa-1b with urea using a laboratory-scale planetary ball mill. A degree of intercalation close to 100% with very little amorphization of the kaolinite was obtained by grinding KGa-1b with a small excess of urea for only 15 minutes. The slow release of urea from composites consisting of a poly (acrylic acid-co-acrylamide) matrix and kaolinite-urea intercalates is linked to the coating of the kaolinite-urea complex in the hydrogel matrix as well as at the location of the urea in the interlayer space of the kaolinite. In a final part, polyacrylamide-kaolinite hydrogels were prepared in the absence of organic crosslinking agent and at room temperature. The polymerization of acrylamide is initiated at the surface of the kaolinite previously functionalized with 2- (2-dimethylaminoethoxy) ethanol. The grafting reaction was studied by X-ray diffraction, thermogravimetric analysis, IRTF spectrometry, $^{13}C$ NMR and elemental analysis. The XRD results revealed an expansion of the interlayer during polymerization with a low stacking order and partial exfoliation of kaolinite. Kaolin acts as a multifunctional crosslinking agent in this composite. The polyacrylamide-kaolinite composites showed good elastic recovery properties and a high swelling capacity.

**Keywords:** Hydrogels, kaolinite, urea, composite, slow release of fertilizers.

## Hydrogels composites acrylique-kaolinite pour une libération contrôlée de fertilisants azotés

Cette thèse s'inscrit dans la mise au point de nouveaux fertilisants granulaires utilisables en agriculture et combinant une libération lente de fertilisant azoté organique et une capacité d'absorption et de rétention d'eau élevée. L'urée a été intégrée dans des hydrogels superabsorbants acryliques selon deux méthodes, soit par incorporation lors de la polymérisation, soit lors d'une étape de post-chargement du polymère préformé. La 1ère méthode conduit à un réseau polymère plus homogène avec des tailles de pores réduites et conduisant à la fois à une libération lente du fertilisant à une capacité de rétention d'eau sous pression élevée et à d'excellentes propriétés de gonflement/regonflement. Dans une seconde partie de ce travail, des intercalats kaolinite-urée ont été préparés par broyage à sec de kaolin KGa-1b avec de l'urée à l'aide d'un broyeur planétaire à billes. Un degré d'intercalation proche de 100% avec très peu d'amorphisation de la kaolinite a été obtenu en broyant Kga1b avec un faible excès d'urée pendant seulement 15 minutes. La libération lente de l'urée de composites constitués d'une matrice poly(acide acrylique-co-acrylamide) et d'intercalats kaolinite-urée est liée à l'enrobage du complexe kaolinite-urée dans la matrice d'hydrogel ainsi qu'à l'emplacement de l'urée dans l'espace interfoliaire de la kaolinite. Dans une dernière partie, des hydrogels polyacrylamide-kaolinite ont été préparé en l'absence d'agent réticulant organique et à température ambiante. La polymérisation de l'acrylamide est amorcée à la surface de la kaolinite préalablement fonctionnalisée avec le 2-(2-diméthylaminoéthoxy)éthanol. La réaction de greffage a été étudiée par diffraction des rayons X, analyse thermogravimétrique, spectrométrie IRTF, RMN du $^{13}C$ et analyse élémentaire. Les résultats de diffraction des rayons X ont révélé une expansion de l'espace interfoliaire lors de la polymérisation avec un ordre d'empilement faible et une exfoliation partielle de la kaolinite. Le kaolin joue le rôle de réticulant multifonctionnel dans ce composite qui présente de bonnes propriétés élastiques et un taux de gonflement élevé.

**Mot clés:** Hydrogel, kaolinite, urée, composites, libération contrôlée de fertilisants